IN VIVO IMAGING

OF CORNEAL CONDITIONS USING

OPTICAL COHERENCE TOMOGRAPHY

By

Sameena Haque

A thesis
presented to the University of Waterloo
in fulfillment of the
thesis requirement for the degree of
Doctor of Philosophy
in
Vision Science

Waterloo, Ontario, Canada, 2006

Declaration

I hereby declare that I am the sole author of this thesis.
This is a true copy of the thesis, including any required final revisions, as required by my examiners.

I understand that my thesis may be made electronically available to the public.

Abstract

Purposes: To use optical coherence tomography (OCT) to image and quantify the effect of various corneal conditions, in terms of corneal, stromal and epithelial thickness, and light backscatter. To assess the changes caused by overnight orthokeratology (Corneal Refractive Therapy; CRT^{TM}) lens wear, keratoconus and laser in-situ keratomileusis (LASIK) refractive surgery, each of which may lead to topographical alterations in corneal thickness either by temporary moulding, degeneration, or permanent laser ablation, respectively.

Methods: Topographical thickness of the cornea was measured using OCT in all studies. The CRT^{TM} studies investigated myopic and hyperopic treatment, throughout the day. The myopic studies followed lens wear over a 4 week period, which was extended to 12 months, and investigated the thickness changes produced by two lenses of different oxygen transmissibility. CRT^{TM} for hyperopia (CRTH^{TM}) was evaluated after a single night of lens wear.

In the investigation of keratoconus, OCT corneal thickness values were compared to those obtained from Orbscan II (ORB) and ultrasound pachymetry (UP). A new fixation device was constructed to aid in the measurement of topographical corneal and epithelial thickness along 8 directions of gaze. Pachymetry maps were produced for the normal non-lens wearing cornea, and compared with the rigid gas permeable (RGP) lens wearing cornea and the keratoconic cornea.

Thickness changes prior to, and following LASIK were measured and monitored throughout six months. Myopic and hyperopic correction was investigated individually, as the laser ablation profiles differ for each type of procedure. The LASIK flap interface was also evaluated by using light backscatter data to monitor healing.

Results: Following immediate lens removal after myopic CRT™, the central cornea swelled less than the periphery, with corneal swelling recovering to baseline levels within 3 hours. The central epithelium decreased and mid-peripheral epithelium increased in thickness, with a more gradual recovery throughout the day. There also seemed to be an adaptation effect on the cornea and epithelium, showing a reduced amount of change by the end of the 4 week study period. The thickness changes did not alter dramatically during the 12 month extended study. In comparing the two lens materials used for myopic CRT™ (Dk/t 91 vs. 47), there were differences in stromal swelling, but no differences in the central epithelial thinning caused by lens wear. There was a statistically insignificant asymmetry in mid-peripheral epithelial thickening between eyes, with the lens of lower Dk causing the greater amount of thickening. Hyperopic CRT™ produced a greater increase in central stromal and central epithelial thickness than the mid-periphery. Once again, the stroma recovered faster than the epithelium, which remained significantly thicker centrally for at least six hours following lens removal.

Global pachymetry measurements of the normal cornea and epithelium found the periphery to be thicker than the centre. The superior cornea and epithelium was thicker than the inferior. In the measurement of the keratoconic cornea, OCT and ORB correlated well in

corneal thickness values. UP measured greater values of corneal thickness. The keratoconic epithelium was thinner than normal, and more so over the apex of the cone than at the centre. The location of the cone was most commonly found in the inferior temporal region. Central epithelial thickness was thinner in keratoconics than in RGP lens wearers, which in turn was thinner than in non-lens wearers.

Following LASIK surgery for both myopia and hyperopia, the topographical OCT thickness profiles showed stromal thinning in the areas of ablation. The central myopic cornea showed slight regression at 6 months. During early recovery, epithelial thickness increased centrally in hyperopes and mid-peripherally in myopes. By the end of the 6 month study, mid-peripheral epithelial thickness was greater than the centre in both groups of subjects. The light backscatter profiles after LASIK showed a greater increase in backscatter on the anterior side of the flap interface (nearer the epithelium), than the posterior side (in the mid-stroma) during healing. The flap interface was difficult to locate in the OCT images at 6 months.

Conclusion: All the CRT^{TM} lenses used in this project produced more corneal swelling than that seen normally overnight without lens wear. In order for these lenses to be worn safely for long periods of time without affecting the health of the cornea, they need to be manufactured from the highest oxygen transmissible material available. The long-term effect of thinning on the epithelium's barrier properties needs to be monitored closely.

Global topographical thickness of the cornea and epithelium was measured using OCT in normal, RGP lens wearing and keratoconic eyes. Corneal and epithelial thickness was not symmetrical across meridians. The epithelium of RGP lens wearers was slightly thinner than normal, but not as thin as in keratoconics, suggesting that the epithelial change seen in keratoconus is mainly due to the condition.

Post-LASIK corneal and epithelial thickness profiles were not the same for myopic and hyperopic subjects, since the ablation patterns vary. Epithelial thickening in the mid-periphery had not recovered by six months in myopes or hyperopes, possibly indicating epithelial hyperplasia. Light backscatter profiles were used to monitor the recovery of the LASIK flap interface, showing the band of light backscatter around the flap interface to decrease as the cornea healed.

Acknowledgements

I would like to sincerely thank Dr. Lyndon Jones for his encouragement and assistance, which has been invaluable. I appreciate the guidance of Dr. Trefford Simpson, whose words of wisdom opened doors of thought that would have otherwise remained closed. I thank Dr. Desmond Fonn for providing me the opportunity to come to Canada, and the privilege to complete my graduate education at the Centre for Contact Lens Research. I express a warm thank you to Dr. Natalie Hutchings for her ideas and advice. My deepest gratitude extends to Drs. Lyndon Jones and Trefford Simpson for their supervision, and to Drs. Desmond Fonn and Natalie Hutchings for their contribution as my research committee members. I also thank Dr. Douglas Horner for his kind presence at my thesis defence as the external examiner.

I have sincerely enjoyed my four years amongst the bright and hard-working members of the Centre for Contact Lens Research at the School of Optometry. Thank you for your daily smiles. A heartfelt thank you to Diane Bandura for her fine support, not only as a colleague but also as a friend. I appreciate the assistance of Robin Jones and Andrew Nowinski in the construction of the fixation device. I would also like to thank the Graduates in Vision Science (GIVS), for organising social events that enhanced the experience of living in Waterloo. Lastly, I owe an appreciation to all the participants who volunteered for the studies in this project.

Dedication

I dedicate this work to my parents, for all their love and support.

To my father, who taught me from a young age that *dedication is the key to success*.

To my mother, who never forced on me the traditions of my culture and

gave me the trust and freedom to be what I wanted to be.

Without the love and acceptance of my parents, I would not have reached my destination.

Having become a first time aunty during my time here in Canada,

I also dedicate this work to my two year old nephew back home in England,

who I have only met twice.

* * *

Table of Contents

List of Tables

List of Figures

List of Abbreviations

ACT	Apical Corneal Thickness
ANOVA	Analysis of Variance
BOZD	Back Optic Zone Diameter
BOZR	Back Optic Zone Radius
BSLN	Baseline
CCLR	Centre for Contact Lens Research
CCT	Central Corneal Thickness
CET	Central Epithelial Thickness
CM	Confocal Microscopy
CRT™	Corneal Refractive Therapy
CRTH™	Corneal Refractive Therapy for Hyperopia
CST	Central Stromal Thickness
D	Dioptre
Dk	Oxygen Permeability
Dk/t	Oxygen Transmissibility
DLK	Diffuse Lamellar Keratitis
DS	Dioptre Sphere
EGF	Epidermal Growth Factor
EqII	Equalens II
FDA	Food and Drug Administration (USA)
F	Female
HGF	Hepatocyte Growth Factor
HSD	Honestly Significantly Different
I	Inferior
ICC	Intraclass Coefficient of Correlation
IN	Inferior Nasal
IT	Inferior Temporal
KC	Keratoconic
KGF	Keratinocyte Growth Factor

LZA	Landing Zone Angle
LASIK	Laser in situ keratomileusis
LASEK	Laser sub-epithelial keratomileusis
LED	Light Emitting Diode
M	Male
MenZ	Menicon Z
N	Nasal
NLW	Non-lens wearer
OAD	Overall average diameter
OCT	Optical Coherence Tomography
OD	Right eye
OK	Orthokeratology
OLCR	Optical low coherence reflectometry
ORB	Orbscan II
OS	Left eye
PCI	Partial coherence interferometry
PCT	Peripheral Corneal Thickness
PET	Peripheral Epithelial Thickness
PMMA	Polymethyl methacrylate
PRK	Photorefractive keratectomy
PST	Peripheral Stromal Thickness
Re-ANOVA	Repeated measures Analysis of Variance
RGP	Rigid Gas Permeable
RLSM	Rostock Laser Scanning Microscopy
RZD	Return Zone Depth
S	Superior
SD	Standard Deviation
Sflg	Scheimpflug photography
SM	Specular Microscopy
SN	Superior Nasal
S:N	Signal to Noise ratio

ST	Superior Temporal
T	Temporal
TLC	The Laser Clinic
UBM	Ultrasound biomicroscopy
UP	Ultrasound Pachymetry
VA	Visual Acuity

Chapter 1

Introduction

1.1 Optical Coherence Tomography

Optical coherence tomography (OCT) is a non-contact technique for high-resolution cross-sectional imaging of tissue. It has been used to image many aspects of the human body, including the brain (Bizheva et al. 2005), skin (Gambichler et al. 2005; Welzel et al. 1997), blood vessels (Fujimoto et al. 1995; Meissner et al. 2006; Yabushita et al. 2002), and the eye. OCT has been used for retinal imaging, to assess macular conditions and glaucomatous damage (Hrynchak and Simpson 2000; Huang et al. 1991; Wollstein et al. 2005), and for anterior chamber imaging of the lens, iris and intra-ocular lens implants. (Leung et al. 2005; Linnola et al. 2005; Wirbelauer et al. 2005) Recently, OCT has been used to quantify the tear meniscus (Johnson and Murphy 2005; Jones et al. 2003).

This project explored corneal imaging exclusively. OCT has been used to image the cornea following refractive surgery (using laser ablation and plastic inserts), contact lens wear and corneal disorders. (Ucakhan et al. 2001; Wang et al. 2003a; Wirbelauer et al. 2000) We can quantify corneal and epithelial thickness from OCT images, and use the light backscatter profiles (discussed in detail in Chapter 3) to assess stromal changes due to surgery or contact lens induced swelling. (Thompson et al. 2003; Wang et al. 2002b) Many of these previous studies restricted their OCT measurements to the central cornea, but with the conditions above affecting the periphery also, it is important to image the corneal surface at least from

limbus to limbus across one meridian. In this project topographical imaging was taken a step further, with the construction of a specialized fixation target, enabling the measurement of the cornea along eight directions of gaze.

The technology surrounding the OCT system is constantly improving, to provide faster images, and in greater resolution. However, these advancements should not be restricted to the laboratory setting, and ideally should benefit the clinical community, aiding in the monitoring of real-world patients. This project revolved around the use of OCT to image and quantify the effect of various conditions on the cornea, all readily seen in the clinical setting. It assessed the changes created by refractive error correction, whether it was by means of temporary corneal moulding from orthokeratology, or permanent laser ablation from laser in-situ keratomileusis (LASIK) refractive surgery. This work also investigated the morphological corneal changes caused by a degenerative condition, in this case keratoconus.

If OCT is to be used in day to day practice for corneal imaging, multiple operator use is highly likely. It is therefore important that different OCT operators do not affect the outcome of measurements. This topic was also investigated in the project.

1.2 Aims of the project

Orthokeratology:

- To measure the thickness of the total cornea, epithelium and stroma after orthokeratology lens wear for myopic correction, from one month to one year.

- To compare corneal swelling differences following myopic orthokeratology, using lenses made from two different materials.
- To measure corneal changes following a single night of orthokeratology for the treatment of hyperopia.

Keratoconus:

- To compare corneal thickness readings obtained from OCT with established corneal measurement techniques, such as Orbscan II and ultrasound pachymetry.
- To produce meridional topography maps of the normal cornea and epithelium.
- To produce and compare meridional topography maps of the rigid gas permeable (RGP) contact lens wearing cornea and the keratoconic cornea.

LASIK:

- To monitor corneal, epithelial and stromal thickness changes for six months following LASIK refractive surgery, and to compare these changes following myopic and hyperopic treatment.
- To use light backscatter profiles obtained from OCT images to monitor the recovery of the LASIK flap interface, and to compare recovery between myopic and hyperopic treatment.

Chapter 2

Background and Literature Review

This chapter begins with a brief section dedicated to the many clinical instruments now available for corneal thickness measurement. It follows to review the corneal responses seen as a result of orthokeratology, keratoconus and corneal refractive surgery.

2.1 Normal thickness of the human cornea and corneal epithelium

In order to monitor and compare corneal thickness changes following contact lens wear or refractive surgery, it is important to know the range of normal corneal thickness. The same applies for epithelial thickness. Ideally, we need to be able to use OCT confidently alongside previously established corneal measurement instruments, such as ultrasound pachymetry, confocal microscopy and other optical pachymeters, including the Orbscan. The repeatability of OCT thickness values, and their reproducibility by multiple OCT operators was investigated in this project, and is discussed in Chapter 4. An experiment to test the validity of OCT thickness measures was also devised and is reported in Chapter 4.

Table 2.1 shows values of normal central corneal thickness (CCT) obtained by various corneal measuring instruments, both new and established. Since not all of these instruments automatically measure epithelial thickness, the number of studies reporting central epithelial thickness (CET) values are far fewer, seen in Table 2.2. Ultrasonic pachymetry (UP), Orbscan (ORB) and optical coherence tomography (OCT) were utilised in studies within this

project and are discussed in Chapter 3. Other instruments referred to in Table 2.1 are (in vivo) confocal microscopy (CM), Schleimpflug photography (Sflg), partial coherence interferometry (PCI), specular microscopy (SM), optical low coherence reflectometry (OLCR), ultrasonic biomicroscopy (UBM) and optical pachymetry (OP). CCT values in Table 2.1 measured by OCT range from 488µm to 696µm, averaging 537.7µm. CET values in Table 2.2 measured by OCT range from 52µm to 81µm, with an average of 62.8µm.

Peripheral corneal thickness is not often reported in corneal thickness studies, possibly due to instrument restrictions, but it is well recognized that the peripheral cornea is thicker than the centre. (Doughty and Zaman 2000; Edelhauser and Ubels 2003; Edmund 1987; Leibowitz and Waring 1998; Maurice 1957; Oyster 1999) Reports of topographical epithelial thickness measurements are uncommon. (Feng and Simpson 2005; Reinstein et al. 1993; Reinstein et al. 2000; Reinstein et al. 1994a). The investigaton of normal corneal thickness measured with OCT is reported in Chapter 7.2.

Table 2-1 A comparison of central corneal thickness (CCT) measurements of the normal cornea, from various corneal measuring devices. [Key in text].

AUTHOR (Year)	INSTRUMENT: CCT (microns)									
	OCT	**ORB**	**UP**	**CM**	**Sflg**	**PCI**	**SM**	**OLCR**	**UBM**	**OP**
Airiani (2006)			549					544		
Auffarth (2000)		490								
Barkana (2005)					512			537		
Bechmann (2001)	530		581							
Buehl (2006)		535			535	528				
Chaidaroon (2003)										581
Fam (2005)		543								
Feng (2001)	497									
Feng (2005)	507									
Gonzalez (2003)	542	555	553							
Gromacki (1994)			560							
Izatt (1994)	696									
Javaloy (2004)		551	554	553					567	
Lackner (2005)		530	552		542					
Li (1997)				532						
Li (2006)	547		553							
MacDougall (2003)		534	544							
Marsich (2000)		596	542							539
Modis L Jr (2001)		602	580				547			
Modis L Jr (2001)			570				542			
Muscat (2002)	526									
Nemeth (2006)			548			531				
O'Donnell (2005)			534		528					
Oqbuehi (2005)							532			543
Pedersen (2005)								539		
Radhakrishnan (2001)	488									
Rainer (2002)			541			518				
Sanchis-Gimeno (2006)		537					520			
Sin (2006)	536									
Tam (2003)			550				572		555	
Wang (2002)	524									
Wirbelauer (2000)	534		558							
Wirbelauer (2002)	540									
Wong (2002)	523	555	555							
Yaylali (1997)		561	527							

Table 2-2 A comparison of central epithelial thickness (CET) measurements of the normal cornea, from optical coherence tomography (OCT), confocal microscopy (CM) and optical pachymetry (OP) measurements.

AUTHOR (Year)	INSTRUMENT: CET (microns)		
	OCT	**CM**	**OP**
Alharbi (2003)			50
Cavanagh (2000)		80	
Eckard (2006)		54	
Erie (2002)		46	
Feng (2001)	61		
Feng (2005)	58		
Gauthier (1996)			54
Gauthier (1997)			57
Izatt (1994)	81		
Li (1997)		51	
Moller-Pedersen (1997)		51	
Patel (2001)		49	
Perez (2003)			48
Radhakrishnan (2001)	55		
Sin (2006)	52		
Wirbelauer (2002)	70		

2.1.1 Advancements in clinical imaging devices

While instruments such as the ultrasound pachymeter, Orbscan, optical pachymeter and even the optical coherence tomographer have been used for corneal thickness measurement for many years, there have been a few new instruments used for anterior segment imaging.

2.1.1.1 Partial coherence interferometry

One such instrument, based on a similar principle to OCT (itself discussed in Chapter 3), is the AC Master (Carl Zeiss Meditec, Jena, Germany) using partial coherence interferometry (PCI), to measure corneal thickness from anterior chamber imaging. (Buehl et al. 2006; Drexler et al. 1998; Meinhardt et al. 2006; Rainer et al. 2004; Rainer et al. 2002; Sacu et al. 2005; Vogel et al. 2001) PCI also uses a Michelson interferometer that splits a low coherence beam (of centre wavelength 855nm and 1mm beam width) into two parts, reflected on the corneal surface. (Rainer et al. 2004) The interference signals are detected once the reflected corneal images are superimposed, marking the boundaries within the structure to be measured later. Detailed operating procedures are described elsewhere. (Buehl et al. 2006; Rainer et al. 2004) The axial resolution achieved by PCI is minimally better than that achieved by a clinical retinal OCT, (Drexler et al. 1997) but there are no reports of epithelial thickness measurements to date.

2.1.1.2 Optical low coherence reflectometry

Another new optical instrument utilizing low coherence light is the optical low coherence reflectometer (OLCR), recently made commercially available by Haag-Streit ("OLCR Pachμmeter", Switzerland). (Airiani et al. 2006; Barkana et al. 2005; Gillis and Zeyen 2004) This device is available as an attachment to the traditional slit-lamp microscope for single point measures, or can be mounted to the excimer laser head during refractive surgery, enabling continuous thickness measurement throughout the laser ablation process. The

principle behind this instrument is similar to OCT, using a light source of wavelength 1310nm which is reflected back from the anterior and posterior surfaces of the cornea, and detected only when interference signals are received perpendicularly from each surface. (Barkana et al. 2005) OLCR also does not offer a much improved axial resolution compared to OCT. (Bohnke et al. 1998; Genth et al. 2002; Schmid et al. 2001) There have been no studies discussing the use of this device to measure the thickness of the corneal epithelium.

2.1.1.3 Scheimpflug photography

The Pentacam (Oculus, Lynnwood, WA) is yet another non-contact, anterior segment imaging device that became commercially available recently, marketed as a comprehensive eye scanner. Similar to the AC Master, this instrument was designed to image the anterior chamber, but also enables corneal thickness measurement. (Lackner et al. 2005b; Meinhardt et al. 2006; Rabsilber et al. 2006) The Pentacam uses Scheimpflug photography, with a 180^{o} rotating camera centred on the optical axis, obtaining up to 50 limbus to limbus cross-sectional images within two seconds. (Barkana et al. 2005; Buehl et al. 2006) The slit light source (blue LED with a wavelength of 475nm) rotates along with the camera, and each slit collects 500 points of data from the anterior and posterior surface of the cornea, from which corneal thickness is calculated. (Barkana et al. 2005; Buehl et al. 2006; Lackner et al. 2005a)

The manufacturers claim an impressive list of features for this instrument, along with corneal pachymetry and topography, also being able to measure crystalline lens opacification, corneal tomography and refractive power maps – all represented in 3-dimensional full colour

maps. The actual operation of this instrument is not greatly different from that of the Orbscan, and is reported in detail elsewhere. (Barkana et al. 2005; Buehl et al. 2006) However, there is no mention of epithelial layer measurement, most likely due to restrictions in axial resolution capability. Many studies have compared the Pentacam with more established optical pachymeters and imaging devices. (Barkana et al. 2005; Buehl et al. 2006; Lackner et al. 2005a; Lackner et al. 2005b; O'Donnell and Maldonado-Codina 2005; Ucakhan et al. 2006) Lackner et al. (Lackner et al. 2005a) reported a better inter-operator reproducibility with the Pentacam than with the Orbscan or ultrasound pachymeter. Corneal thickness values obtained by this instrument are displayed in Table 2.1 for comparison with other techniques.

2.1.1.4 Confocal microscopy

In vivo confocal microscopy has been available for many years, not only for the measurement of corneal and epithelial thickness but also for the high resolution imaging of epithelial cells and keratocytes (also called fibroblasts). (Bohnke and Masters 1999; Cavanagh et al. 1990; Hollingsworth et al. 2005a; Li et al. 1997; Masters and Bohnke 1999, 2001, 2002; Moller-Pedersen et al. 2000; Patel et al. 2002) The axial resolution of the ConfoScan3 clinical confocal microscope (Nidek, Japan) is ~10μm. Recently, this resolution has been improved ten fold, with the combination of the Heidelberg Retina Tomograph II (HRT II, Heidelberg Engineering, Germany) and the Rostock Cornea Module (RCM, Rostock University, Germany) (Eckard et al. 2006; Sharp et al. 2004), jointly being termed the confocal Rostock laser scanning microscope (RLSM). (Berlau et al. 2002; Eckard et al.

2006; Kobayashi et al. 2005; Patel and McGhee 2006; Sonigo et al. 2006; Stave and Guthoff 1998) Eckard et al. (Eckard et al. 2006) recently reported the axial resolution of this instrument as 1μm. However, RLSM remains a confocal technique, and therefore suffers from disadvantages, including requiring corneal-probe contact via a coupling gel, and eye movement.

2.1.1.5 Specular microscopy

The Topcon SP-2000P (Topcon Corporation, Tokyo, Japan) is a commercially available non-contact specular microscope that images the endothelium, and provides specular images (photographs) from which corneal thickness is calculated simultaneously. (Modis et al. 2001a, 2001b; Sanchis-Gimeno et al. 2006) This device is greatly influenced by opaque or hazy corneas, rendering image capture very difficult. (Modis et al. 2001a) The SP-2000P has been compared to other corneal measurement instruments, and was generally found to be comparable to Orbscan or ultrasound pachymetry. (Cavanagh et al. 2000; Kawana et al. 2005; Kawana et al. 2004; Sanchis-Gimeno et al. 2006; Tam and Rootman 2003; Ucakhan et al. 2006) The manufacturer highlights the measurement of peripheral corneal thickness as a feature, but epithelial thickness readings are not mentioned.

2.1.1.6 Ultrasound biomicroscopy

Ultrasound biomicroscopy (UBM) uses broadband, high frequency transducers (>50MHz) that are moved over the corneal surface to obtain B-scans, from which corneal and epithelial

thickness estimates have been made. (Foster et al. 2000; Pavlin and Foster 1998; Pavlin et al. 1991) A major disadvantage of this technique is the need for the eye to be immersed in a water-bath, used as a coupling medium for the ultrasound waves. (Ehlers and Hjortdal 2004; Reinstein et al. 1994b) This would be inconvenient and impractical in the clinical setting.

However, along with advancements in digital processing to improve the quality of images for corneal and epithelial thickness measurements, (Reinstein et al. 2005; Reinstein et al. 2000; Reinstein et al. 1999; Reinstein et al. 2001; Reinstein et al. 2006; Tam and Rootman 2003) manufacturers now boast fourth generation UBMs with self-contained water-bath probes, which may allow easier operation in the clinical setting. An advantage of UBM is the penetration depth, capable of imaging the entire anterior chamber; however the axial resolution does not yet match that of optical imaging techniques. (Foster et al. 2000; Pavlin and Foster 1998; Pavlin et al. 1991)

2.2 Normal physiological corneal and epithelial oedema

2.2.1 Anatomy

The cornea is a uniquely structured, almost entirely transparent, avascular tissue that provides refractive power and a protective barrier to the inside of the eye. The anterior corneal surface is made up of 5-7 layers of tightly packed epithelial cells that originate from stem cells in the limbus, and continually mitose to differentiate from basal to wing to superficial cells. (Edelhauser and Ubels 2003; Oyster 1999; Ruskell 1997) The well-organized stable structure of the epithelium is maintained by cell-to-cell adhesion, with support from

desmosomes, protein complexes that link cells to one another. (Edelhauser and Ubels 2003; Maatta et al. 2006; Oyster 1999; Ruskell 1997) The basal epithelial layer rests on its epithelial basement membrane, which adheres to Bowman's membrane in a similar way, with the assistance of hemidesmosomes, which are also linked to anchoring collagen fibrils that pass through Bowman's membrane and a few microns into the stroma. (Edelhauser and Ubels 2003; Kaufman et al. 1998; Maatta et al. 2006; Oyster 1999; Ruskell 1997)

Most of the cornea consists of stroma (substantia propia), consisting of many lamellae of collagen fibres and proteoglycans that are synthesized and maintained by keratocytes. These structures interact with each other to form an extracellular matrix, and are arranged in such a way to allow 99% visible light transmission, hence rendering the cornea transparent. (Edelhauser and Ubels 2003) Should this arrangement of collagen fibres be disrupted, an increase in light scatter through the stroma will occur, resulting in stromal haze. This may occur due to injury, infection, degenerative disorders, surgery or contact lens wear, dependant on severity. (Chang et al. 1998; Elliott et al. 1991; Fonn et al. 1999; Jester et al. 1999a; Kitagawa et al. 1996; Matilla et al. 1995; Meek et al. 2003b; Smith et al. 1990) Stromal oedema (swelling) is an uptake of fluid into the extracellular matrix, leading to a separation in the perfectly organized collagen lamellae. (Arffa 1997; Edelhauser and Ubels 2003; Kaufman et al. 1998; Oyster 1999; Ruskell 1997)

The endothelium is a single layer of cells that forms a leaky barrier between the posterior stroma and the aqueous, allowing an influx of fluid and nutrients. (Edelhauser and Ubels 2003; Oyster 1999; Ruskell 1997) Therefore, the posterior stroma tends to be more hydrated

(and in consequence scatters more light) than the anterior stroma. (Cristol et al. 1992; Edelhauser 2006; Edelhauser et al. 1994; Edelhauser and Ubels 2003; Komai and Ushiki 1991; Meek et al. 2003a; Meek et al. 2003b; Moezzi et al. 2004)

2.2.2 Stromal oedema

During eye closure while sleeping, the normal healthy cornea is known to swell as a result of hypoxia and osmotic imbalance. (Bonanno and Polse 1985; Brennan et al. 1987; Efron and Carney 1979; Holden and Mertz 1984; Holden et al. 1984; Meek et al. 2003b; Mertz 1980; Polse et al. 1990) The amount by which the cornea swells physiologically overnight has been measured in the range of 2-5%. (Cox et al. 1990; du Toit et al. 2003; Fonn and Bruce 2005; Graham et al. 2001; Harper et al. 1996; Kiely et al. 1982; La Hood et al. 1988; Mertz 1980; Sakamoto et al. 1991) It is also known that corneal swelling varies between subjects, exhibiting various amounts of corneal thickness change. (Efron 1986; Mertz 1980) The central cornea tends to swell more than the periphery, (Bonanno and Polse 1985; Holden et al. 1985a; Moezzi et al. 2004; Wang et al. 2002a) this being accounted to the structural scaffolding in the form of stromal collagen lamellae in the limbal region, creating a 'clamping' effect. (Bonanno and Polse 1985; Dupps and Wilson 2006; Meek et al. 1987; Meek et al. 2003a; Meek et al. 2003b; Meek and Newton 1999; Swarbrick et al. 2005)

2.2.3 Stromal recovery and overshoot

The return of corneal thickness to pre-sleep levels has been found to occur within the first three hours after eye opening on waking. (Armitage and Schoessler 1988; Bourne 1998; du Toit et al. 2003; Holden et al. 1988b; O'Neal and Polse 1985; Odenthal et al. 1999; Wang et al. 2002a) The corneal deswelling rate is also not equal in all individuals. (Johnson et al. 1985; Odenthal et al. 1999) During the course of deswelling, corneal thinning has been known to occur beyond the original (pre-oedematous) thickness levels, this event being termed 'overshoot'. The amount of overshoot measured has been as high as 11µm (~2% of total corneal thickness). (du Toit et al. 2003; Fonn et al. 1999; O'Neal and Polse 1985; Odenthal et al. 1999; Ruberti and Klyce 2003; Sakamoto et al. 1991) The reasons behind this overshoot are not confirmed, although it has been found to occur following lens-induced hypoxic stress. It has been hypothesized to be connected to an imbalance between tear evaporation from the epithelial surface and endothelial pump function. (du Toit et al. 2003; Edelhauser 2006; Kangas et al. 1990; O'Neal and Polse 1985; Odenthal et al. 1999) Another associated factor may be the loss of stromal constituents (ground substance) as a result of the oedema, including the breakdown of keratocytes. (Edelhauser 2006; Holden et al. 1983; Holden et al. 1985b; Kangas et al. 1990; Leibowitz and Waring 1998) While these cells are being restored, the cornea will be thinner than normal. (Edelhauser 2006)

2.2.4 Epithelial oedema

Epithelial oedema due to hypoxia would most likely present as an uptake of fluid in-between cells. (Caldicott and Charman 2002; Lambert and Klyce 1981; Liesegang 2002) This intercellular oedema causes an increase in light scatter, and can be detected by slit-lamp microscopy or confocal microscopy. (Caldicott and Charman 2002; Griffiths et al. 1986; Ichijima et al. 1993; Lambert and Klyce 1981; Liesegang 2002; Lohman et al. 1982b; O'Leary et al. 1981; Soni and Nguyen 2006; Wallis 1969)

An increase in epithelial thickness due to normal overnight oedema is not often reported. Some investigators have found that epithelial thickness does not change as a result of epithelial hypoxia. (Lambert and Klyce 1981; O'Leary et al. 1981; Wang et al. 2002a; Wilson and Fatt 1980) However, others have found evidence contrary to this. Feng et al. (Feng et al. 2001) measured an increase of 8% (5μm) in central epithelial thickness following overnight eye closure. Other reports of large increases in epithelial thickness (up to 20%) due to hypoxia have been shown, except with excised rabbit corneas. (Lowther and Hill 1973, 1974; Uniacke et al. 1971) As noted to occur during the recovery of stromal oedema, the epithelium has also shown an extent of overshoot. Wang et al. (Wang et al. 2002a) measured an increase in epithelial thickness of only 1.7% following a period of hypoxia, yet also reported an overshoot of 3% in epithelial thinning during recovery. Nonetheless, normal overnight corneal oedema manifests itself mainly in the stroma.

2.3 Orthokeratology

Patients are increasingly seeking alternatives to spectacles for the correction of their refractive error, venturing into the extended wear of contact lenses or refractive surgery. However, for those patients intolerant to daytime wear of contact lenses (due to the common problem of dry eye) and/or are apprehensive towards permanent surgical procedures, orthokeratology presents as an attractive option. (Hori-Komai et al. 2002)

Orthokeratology (OK) is the programmed application of rigid gas permeable (RGP) contact lenses to reduce refractive error. These lenses are worn overnight to reshape the cornea and are removed the following morning, providing a temporary but reasonable improvement in vision that regresses gradually throughout the day. (Barr et al. 2004; Binder et al. 1980; Dave and Ruston 1998; Kerns 1976, 1978; Mountford 1997b; Polse 1977; Polse et al. 1983b; Swarbrick et al. 1998) In the 1970s and 1980s, orthokeratology was conducted using flat-fitting polymethyl methacrylate (PMMA) contact lenses worn during the day, which although produced varied amounts of myopia reduction, was also deemed unpredictable with the induction of astigmatism due to poor lens centration. (Binder et al. 1980; Kerns 1978; Mountford 1997a, 1997b; Polse et al. 1983a)

The reduction in refractive error from orthokeratology is reversible, returning slowly throughout the day following removal of the lens in the morning. (Alharbi and Swarbrick 2003; Soni et al. 2004; Sorbara et al. 2005a; Wang et al. 2003c) Reversibility stands as being

the procedure's most appealing asset for those patients who do not want to commit to permanent refractive surgery such as LASIK.

2.3.1 Orthokeratology contact lenses

Advances in RGP lens materials have improved the orthokeratology procedure by enabling the lenses to be worn overnight. The degree to which oxygen may pass through a contact lens material is characterised by it's oxygen permeability (Dk) and it's thickness (t), together classified as it's oxygen transmissibility (Dk/t units x 10^{-9} (cm x ml O_2)(sec x ml x mmHg) (Harvitt and Bonanno 1999)). One indicator of the amount of oxygen reaching the corneal surface through a contact lens worn overnight is to measure the amount of corneal oedema that it produces, in comparison to the normal physiological oedema found during eye closure in sleep.

To limit overnight corneal oedema with lens wear to the 'normal' level of ~4% (Mertz 1980), the criterion for minimum acceptable oxygen transmissibility (Dk/t) of contact lenses for closed eye wear has been that set by Holden and Mertz, at 87 x 10^{-9} (cm x ml O_2)(sec x ml x mmHg). (Holden and Mertz 1984) More recently, it has been suggested that normal overnight oedema without lenses is closer to 3%. (Bruce and Brennan 1993; du Toit et al. 2003; Fonn and Bruce 2005; Graham et al. 2001; Moezzi et al. 2004) The criterion for minimal lens Dk/t for overnight lens wear was therefore re-evaluated by Harvitt and Bonanno (Harvitt and Bonanno 1999), and found to be 89 for the corneal epithelium and 125 for the total cornea. Hence, the minimum Dk/t for a contact lens to be worn overnight was

advised to be at least 125 x 10^{-9} (cm x ml O_2)(sec x ml x mmHg) to prevent additional oedema to that normally resulting from normal eye closure. (Fonn and Bruce 2005; Fonn et al. 2005; Sweeney 2003)

The renewed interest in OK was due to the new generation of reverse geometry lens designs, introduced in the late 1990's. (Dave and Ruston 1998; Mountford 1997a, 1997b) These lenses consist of four curves; the central base curve (optic zone), a steeper second curve also known as the return curve, the alignment curve providing stability and centration ('landing zone'), and the fourth curve providing edge clearance. The lenses used in this study were manufactured by Paragon Vision Sciences (Mesa, AZ), who termed their orthokeratology procedure Corneal Refractive Therapy (CRT™). Paragon CRT™ lenses (Figure 2.1) were approved for overnight wear in June 2002 by the U.S Food and Drug Administration (FDA). CRT™ uses reverse-geometry RGP contact lenses to flatten the central cornea for the treatment of myopia, or to steepen it for the treatment of hyperopia. (Choo et al. 2004a; Choo et al. 2004b; Mountford 1997a, 1997b; Swarbrick 2004, 2006; Swarbrick et al. 2004) These lenses have a Dk/t of 67, and therefore we can expect to find oedema levels slightly higher than that seen with no lens wear overnight. The near future may see further developments in lens materials that can be used for orthokeratology, to prevent excessive corneal oedema when worn overnight. (Benjamin and Cappelli 2002; Young and Benjamin 2003)

Figure 2-1 Schematic of the CRT™ lens for myopia. (OAD = overall average diameter). [Courtesy of Paragon Vision Sciences teaching material].

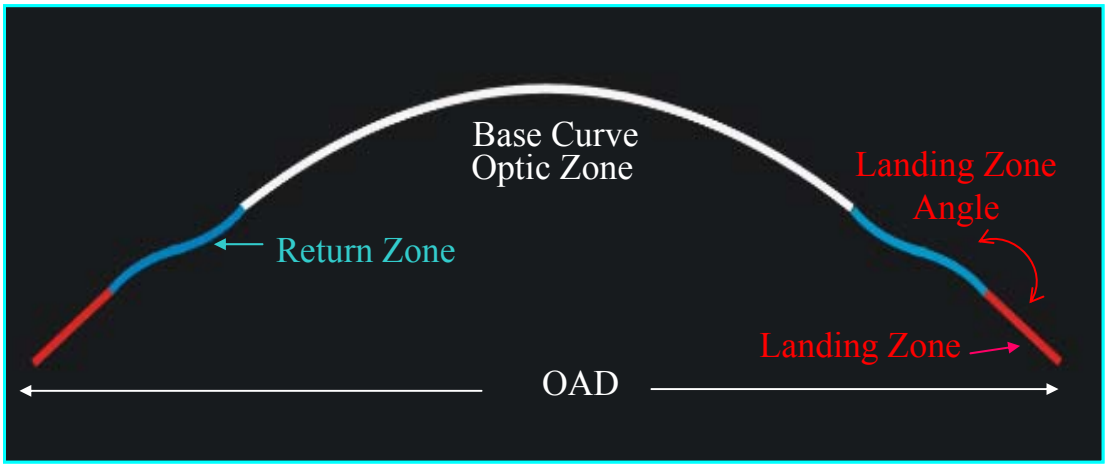

For myopic treatment, the base curve of the lens was designed to be flatter than the central corneal curvature. The lens design, together with eyelid pressure during sleep, aimed to cause central corneal flattening. (Mountford 1997a, 1997b) Figure 2.2 shows a myopic CRT™ lens on eye, which shows the return curve having clearance from the cornea, producing a tear reservoir seen by the mid-peripheral fluorescein pooling. The central area is seen as a dark circle where there is minimal clearance (and hence minimal fluorescein).

Figure 2-2 Fluorescein 'bulls-eye' pattern of a reverse geometry Paragon CRT™ lens, in the myopic design. The central dark ring indicates apical touch, with mid-peripheral fluorescein pooling under the return curve.

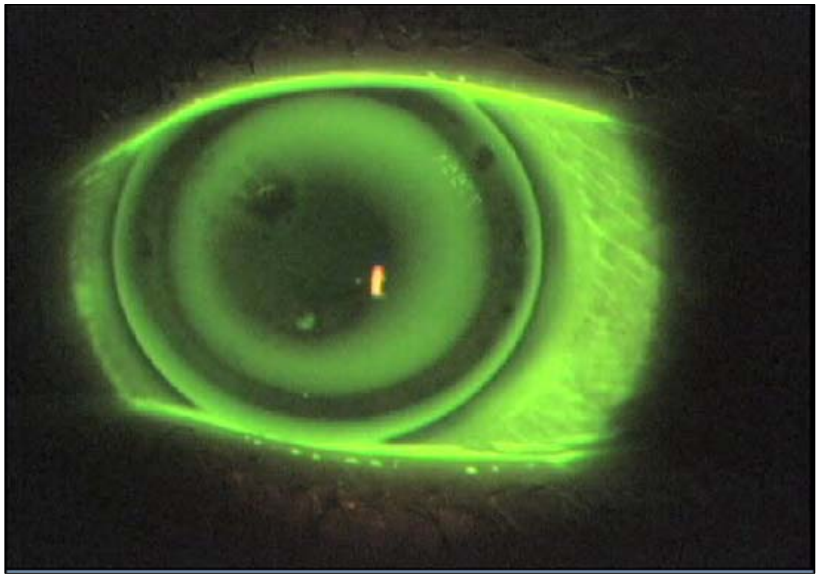

To date, orthokeratology has focussed on the treatment of myopia. The principle of a lens design opposite to that used to correct myopia may allow the treatment of hyperopia. (Swarbrick et al. 2004) This lens would need to steepen the cornea centrally. (Choo et al. 2004b; Mountford 1997b; Swarbrick et al. 2004) Figure 2.3 shows a Paragon CRTH™ lens on eye for the treatment of hyperopia, displaying a fluorescein pattern opposite to that seen in Figure 2.2. The hyperopic fluorescein pattern shows a central button of tear pooling, with an adjacent dark band indicating corneal alignment, with subsequent landing/return and peripheral zones. The change in corneal shape is expected to be a result of mechanical pressure from contact of the transition region, between the steepened central optic zone and the concentric return zone.

Figure 2-3 The fluorescein pattern of a Paragon CRT^{TM} lens on-eye, designed to reduce hyperopia.

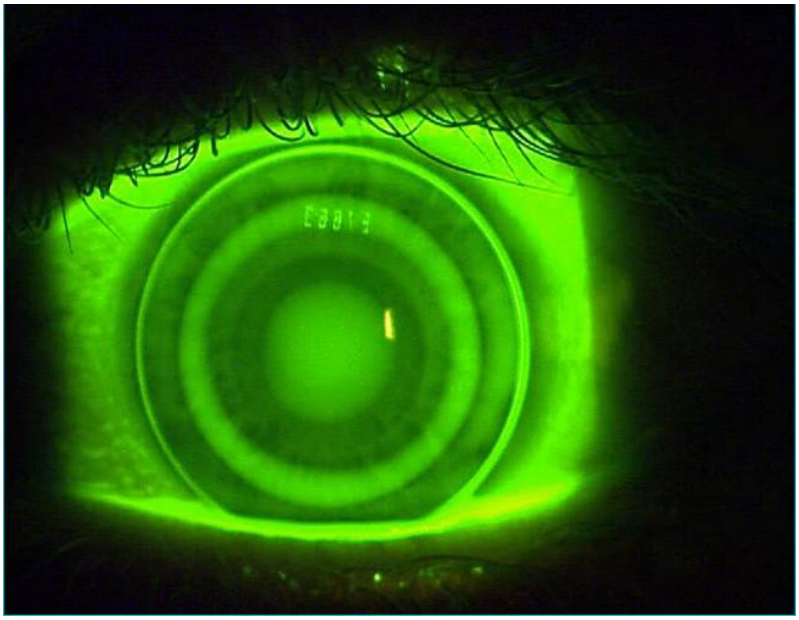

2.3.2 Stromal changes

Specific quantities of stromal swelling found after overnight wear of various OK lenses will be discussed in experimental chapters to follow. Stromal oedema caused by hypoxia from traditional contact lenses follows a similar pattern to that seen following normal overnight oedema, with greater swelling centrally than peripherally. (Bonanno and Polse 1985; Fonn et al. 1999; Fonn et al. 1984; Holden et al. 1985a; Lu et al. 2006b; Moezzi et al. 2004; Wang et al. 2002a) The topographical pattern of stromal change with OK lenses has been found to be opposite to that found after traditional RGP or soft contact lens wear.

The majority of studies reporting corneal changes following myopic OK, have found the central stroma to swell less than the mid-periphery. (Alharbi and Swarbrick 2003; Soni et al. 2003; Sorbara et al. 2005a; Swarbrick et al. 2005; Wang et al. 2003c) Some studies have measured no central stromal swelling at all. (Alharbi and Swarbrick 2003; Nichols et al. 2000) Recently, it has been hypothesized that this reduced amount of central swelling may be due to a 'clamping' effect, created by a joint effort from the OK lens and lid closure, with intraocular pressure (IOP) forces contributing from the opposite side of the cornea. (Alharbi et al. 2005; Holden et al. 1988a; Swarbrick et al. 2005) Swarbrick and colleagues (Alharbi et al. 2005; Swarbrick et al. 2005) have used this theory to explain the mid-peripheral corneal thickening found in their studies, in the absence of mid-peripheral epithelial thickening.

There are only a few studies that have reported stromal changes following hyperopic orthokeratology. (Choo et al. 2004b; Lu et al. 2006b; Swarbrick et al. 2004) Light microscopy images of the cat stroma after 14 days of OK showed an increase in central stromal thickness, more so after hyperopic treatment than for myopic. (Choo et al. 2004b) Lu et al. (Lu et al. 2006b) recently measured greater corneal swelling centrally than peripherally after CRT^{TM} lens wear for hyperopia, with the opposite after correction for myopia. Swarbrick et al. (Swarbrick et al. 2004) reported no central stromal swelling following an experiment to reduce hyperopia using RGP lenses, but this study did not use speciality OK lenses.

2.3.3 Epithelial changes

Initially thought to have been due to an overall bending of the cornea, it is now thought that the initial response to orthokeratology is due to alterations in the epithelial layer. (Greenberg and Hill 1973; Mountford 1997a, 1997b; Sridharan and Swarbrick 2003; Swarbrick et al. 1998) The epithelium has been pronounced to be remarkably mouldable, transforming under an OK lens in as little as ten minutes. (Jayakumar and Swarbrick 2005; Lu et al. 2006b; Sridharan and Swarbrick 2003) However, Matsubara et al. have stated that extensive epithelial re-distribution is unlikely to occur during short-term orthokeratology, and that epithelial oedema may have an influence on epithelial thickness. (Matsubara et al. 2004)

Current theories behind the mechanism of epithelial change include cell re-distribution, cell compression with fluid transfer, cell retention, increased cell mitosis, or a combination of all of these factors. (Choo et al. 2004a; Choo et al. 2004b; Ladage 2004) Epithelial cell re-distribution would be encouraged by the tear film forces beneath the pressure of the OK lens, moulding the epithelium to take the shape of the lens profile. Positive pressures would represent a 'push' force, leading to a thinning in the epithelium, with negative pressures creating a 'pull' force, leading to a thickening of the epithelium. (Choo et al. 2004a; Swarbrick 2004, 2006) Epithelial cell re-distribution, including cell compression following OK, has been shown in histological images. (Choo et al. 2004b; Matsubara et al. 2004) Although these experiments were not performed in humans, these studies reported a reduction in the number of cell layers and a flattening of cells centrally, after myopic OK. (Choo et al. 2004b; Matsubara et al. 2004) In the same studies, mid-peripheral regions of

epithelial thickening consisted of an increase in cell layers, and an elongation of epithelial basal cells. (Choo et al. 2004b; Matsubara et al. 2004) The opposite was found in eyes that underwent hyperopic OK. (Choo et al. 2004b; Matsubara et al. 2004) Swarbrick et al. did not report any epithelial changes in their study using steeply fitted RGP lenses to treat hyperopia, but did report an increase in central corneal curvature (steepening) in the absence of corneal oedema. (Swarbrick et al. 2004)

One aspect of epithelial re-distribution involves the actual migration of cells from an area of flattening (thinning) to an area of thickening. The possibility of this occurring has been questioned, due to the presence of desmosomes adhering epithelial cells to each other. These inter-cellular links would need to be broken in order for individual cells to migrate, but it has been suggested that the pressure from an OK contact lens may be enough of a stimulus to enable this to occur. (Choo et al. 2004a)

Considering the above mechanisms explaining epithelial change following OK, increased cell mitosis seems the least likely, as many studies have discovered that contact lenses actually suppress epithelial metabolism. (Cavanagh 2003; Hamano et al. 1983; Holden et al. 1985b; Ladage 2004; Ladage et al. 2003a; Ladage et al. 2002a, 2002b; Ladage et al. 2001a; Liesegang 2002; Lin et al. 2002)

2.4 Keratoconus

Keratoconus is a non-inflammatory ectasia of the cornea, in which gradual thinning of the stroma and epithelium lead to the cornea developing a cone-like appearance. (Leibowitz and Waring 1998; Rabinowitz 1998; Zadnik et al. 1996) Refractive error changes include an increase in myopia and astigmatism, with clinical signs consisting of epithelial iron deposition (Fleischer's ring), stromal stress lines (Vogt's striae), and Munson's sign (cone protrusion on down-gaze). (Edrington et al. 1995; Leibowitz and Waring 1998; Rabinowitz 1998; Rah et al. 2002a; Zadnik et al. 1996) The condition can advance to hydrops (corneal oedema caused by Descemet's membrane rupture) and eventually corneal scarring. (Barr et al. 2000; Edrington et al. 1995; Leibowitz and Waring 1998; Nakagawa et al. 2006; Rabinowitz 1998; Thota et al. 2006)

2.4.1 Aetiology

The cause of keratoconus remains unknown. The aetiology still cannot be defined by a single specific aspect. Current theories regarding the cause and progression of keratoconus include biochemical factors, heredity, contact lens wear, and allergies with associated eye rubbing. (Andreassen et al. 1980; Arffa 1997; Comaish and Lawless 2002; Hollingsworth et al. 2005a; Hollingsworth et al. 2005b; Kaufman et al. 1998; Leibowitz and Waring 1998; McMonnies 2005; McMonnies and Boneham 2003; Moon et al. 2006; Phillips 1990; Rabinowitz 1998; Wilson et al. 2003a; Wilson et al. 2001b; Wilson et al. 2003c) Although keratoconus usually presents bilaterally, the disorder has been found to occur in one eye only

(Diniz et al. 2005; Ioannidis et al. 2005; Phillips 2003; Weed and McGhee 1998), which has raised some doubt regarding keratoconus being purely a genetic disorder. Phillips (Phillips 2003) declared that if keratoconus was entirely inherited, it would express as a binocular condition. Owens and Watters (Owens and Watters 1996), using family history questionnaires, discovered that 92% of keratoconic patients rubbed their eyes throughout their life. They also concluded that inheritance played just as great a role in the cause of keratoconus as the influence of asthma, hayfever or eczema. (Owens and Watters 1996)

2.4.1.1 Micro-trauma and epithelial-stromal interactions

One factor that connects the proposed theories above, is that of epithelial-stromal interactions and immune cell responses. Both contact lens wear (mainly rigid lenses) and eye rubbing (due to allergies) can be considered to produce a chronic form of micro-trauma to the corneal surface. (Kim et al. 1999; Maatta et al. 2006; Wilson et al. 2001b; Wilson et al. 2003c) The tears and epithelium contain cytokines and growth factors (both secreted proteins) that respond to corneal injury by initiating a wound-healing response. (Dayhaw-Barker 1995a, 1995b; Lu et al. 2001; Wilson 1998; Wilson et al. 2003a; Wilson et al. 2003c) This response is initiated with a release of cytokines due to the damaged epithelium, which begins a cascade of events starting with the removal of the injured epithelial cells. (Dayhaw-Barker 1995b; Dupps and Wilson 2006; Netto et al. 2005b; Wilson 1998; Wilson et al. 2003a; Wilson et al. 2001b; Wilson et al. 2003c) An important wound-healing response that occurs early after the initial injury is the stimulation of stromal keratocyte apoptosis (programmed cell death with minimal damage to neighbouring cells). (Wilson 2000; Wilson et al. 1999a;

Wilson et al. 2002; Wilson et al. 2001b) These events would ultimately lead to epithelial degeneration and stromal disintegration, representative of a wound-healing process gone wrong.

Knowledge of this wound-healing activity raises the question of whether contact lens wear and/or eye rubbing influences the occurrence of keratoconus. These two factors have a cause-and-effect relationship with keratoconus, and the question remains as to whether lens wear or eye rubbing causes keratoconus, or whether lens wear is prescribed for the treatment of keratoconus. (Andreassen et al. 1980; Kallinikos and Efron 2004; Kallinikos et al. 2006; McMonnies 2005; McMonnies and Boneham 2003; Moon et al. 2006; Nauheim and Perry 1985; Owens and Watters 1996; Rabinowitz 1998; Wilson et al. 2001b; Wilson et al. 2003c) Recently, Barr et al. (Barr et al. 2006), as a result of their long-term keratoconic study, found a two-fold increase in corneal scarring in subjects who wore contact lenses than those who did not. The influence of RGP lens wear on corneal and epithelial thickness is discussed in Chapter 7.3.

2.4.1.2 Biochemical factors

Keratoconus may be caused by specific biochemical factors residing in the epithelial cells and the stroma. These may include abnormal enzyme (e.g. matrix metalloproteinases) and protein activity, creating an imbalance in normal corneal homeostasis, resulting in an over-active digestion of collagen. (Brookes et al. 2003; Comaish and Lawless 2002; Leibowitz and Waring 1998; Nielsen et al. 2006; Rumelt et al. 2001) There may also be a reduction in

collagen and keratocyte production, resulting in stromal thinning which leads to corneal ectasia. (Andreassen et al. 1980; Arffa 1997; Doughty and Zaman 2000; Hollingsworth et al. 2005a; Hollingsworth et al. 2005b; Kaufman et al. 1998; Leibowitz and Waring 1998; Meek et al. 2005; Rabinowitz 1998; Wilson et al. 2001b) Previous studies have reported a lower keratocyte density in keratoconic eyes compared to normal, more so in the anterior stroma than the posterior, with a greater decrease still being found in contact lens wearing keratoconic eyes. (Erie et al. 2002a; Hollingsworth et al. 2005a; Hollingsworth et al. 2005b) This strengthens the proposition of keratoconus being affected by biochemical factors primarily in the epithelial layer.

2.4.1.3 Corneal nerves

Corneal nerves have been found to be affected by keratoconus, by appearance and function. (Patel and McGhee 2006; Simo Mannion et al. 2005) However, a reasonably new interest has arisen regarding the influence of corneal nerves in the mechanism and progression of keratoconus. (Brookes et al. 2003) This area of research focuses on the corneal nerves that pass between the stroma and epithelium at the sites of early keratoconic change, and the role of these nerves in facilitating certain degradative enzymes in the stromal keratocyte-epithelial interactions in keratoconus. (Brookes et al. 2003)

2.4.2 Corneal changes

Although all layers of the keratoconic cornea are ultimately affected, early changes occur in the epithelial layer. (Leibowitz and Waring 1998; Rabinowitz 1998) Specifically, the basal cells become pale and oedematous due to intracellular disorganisation, which leads to the breakdown of the cell membranes. (Aktekin et al. 1998; Leibowitz and Waring 1998; Lohman et al. 1982a; Pfister and Burstein 1977) The epithelial basal cells eventually disintegrate, leaving a few layers of superficial cells. (Aktekin et al. 1998; Leibowitz and Waring 1998; Rabinowitz 1998) Some investigators have found these superficial cells to be elongated. (Hollingsworth et al. 2005a; Tsubota et al. 1995) Histological images and thickness measurements would represent the above activity in the form of epithelial thinning.

This destructive process continues onto the Bowman's layer, altering the basement membrane by fibrillar degeneration and fragmentation. (Aktekin et al. 1998; Brookes et al. 2003; Hollingsworth et al. 2005a; Maatta et al. 2006; Rabinowitz 1998; Somodi et al. 1996) Bowman's layer is gradually destroyed, along with the superficial stroma, where a reduction in the number of collagen lamellae occurs. (Aktekin et al. 1998; Hollingsworth et al. 2005b; Leibowitz and Waring 1998; Somodi et al. 1996) These stromal lamellae in turn are replaced with newly formed, irregularly arranged fibres, which create a more opaque stroma. (Aktekin et al. 1998; Leibowitz and Waring 1998; Meek et al. 2005; Somodi et al. 1996) The degeneration of stromal tissue leads to an area of stromal thinning, ultimately creating an ectatic cornea (being cone-like in shape). The area most affected by this thinning would

form the apex of the cone, and is often measured as the thinnest part of the keratoconic cornea.

The endothelium is not affected in the early stages of keratoconus, but as the disease progresses, endothelial cells may also disintegrate, leaving behind the remaining cells to maintain this essential barrier. (Edelhauser and Ubels 2003; Hollingsworth et al. 2005a; Hollingsworth et al. 2005b; Leibowitz and Waring 1998) Following extreme polymegathism and pleomorphism, the endothelium will fail and the cornea will immediately swell, resulting in hydrops. (Leibowitz and Waring 1998; Nakagawa et al. 2006; Thota et al. 2006)

2.5 Laser in-situ keratomileusis (LASIK)

In lay terms, LASIK is referred to as the 'flap and zap' technique of corneal refractive surgery. The procedure initially involves using a microkeratome to create a flap of corneal tissue consisting of the epithelium, Bowman's membrane and anterior stroma, cut to a precise depth. The exposed stromal bed is ablated with an excimer laser, by an amount associated with the patient's refractive error, and the flap is re-positioned. LASIK has been used to correct myopia, hyperopia and astigmatism.

LASIK has major advantages over other laser refractive procedures such as photorefractive keratectomy (PRK), where there is no flap created, and the laser is occasionally directed onto the epithelial surface for corneal ablation. LASIK offers a hastier visual recovery, with less post-operative haze (discussed below), compared to PRK. (Bansal and Veenashree 2001;

Dupps and Wilson 2006; Erie et al. 2002b; Rumelt et al. 2001; Wilson 2002) It is also the procedure of choice for correcting higher amounts of myopia (>4.00DS). (Amm et al. 1996; Bansal and Veenashree 2001; Chayet et al. 1998a; Kato et al. 1999; Kim et al. 2004; Magallanes et al. 2001; Montes et al. 1999; Pallikaris and Siganos 1994, 1997) The quality of residual vision and refractive change however, are influenced by how well the cornea heals after photoablation. (Bansal and Veenashree 2001)

2.5.1 Ablation profiles

The LASIK ablation patterns for myopic and hyperopic correction are different, and the aims of LASIK correction are not different from those discussed earlier in orthokeratology treatment. To reduce myopia, the laser ablation attempts to flatten the central cornea by permanently reducing thickness. The opposite is true for hyperopic correction, where the ablation is restricted to the mid-peripheral cornea, in an attempt to steepen the central cornea.

The diameter of the corneal flap usually created for myopic treatment is ~8mm, (Pallikaris and Siganos 1994) where the flap diameter for hyperopic treatment is slightly larger at ~9mm. (Qazi et al. 2005; Rosa and Febbraro 1999; Vesaluoma et al. 2000) The latter is due to the more peripheral ablation in the correction of hyperopia. The actual ablation zone is smaller than the flap diameter, with the margins of ablation being blended towards the flap boundary. (Maldonado et al. 2000) The ablation zone diameter for both types of refractive error treatment is ~6mm, centred for myopic correction, while arranged in a 'doughnut-shape' for hyperopic correction. (Buzard and Fundingsland 1999; Davidorf et al. 2001;

Lafond et al. 2004; Qazi et al. 2005) For myopic treatment, it has been found that a larger ablation zone benefits the post-operative outcome, by reducing night-time haloes perceived as a consequence of large pupil size. (Carones et al. 2003; Miller et al. 2001; Tahzib et al. 2005; Tuan 2006)

2.5.2 Wound healing

PRK involves the removal of the epithelium, basement membrane and Bowman's layer, with the anterior stroma being laser ablated, whereas apart from at the flap margins, LASIK leaves these areas intact. (Dupps and Wilson 2006) For this reason, LASIK produces a much reduced cascade of wound healing events. (Wilson et al. 2001a) Introduced earlier in Chapter 2.4.1.1, epithelial-stromal interactions are vital to the wound healing response, and of utmost importance is the preservation of the epithelium and the epithelial basement membrane.

The disruption of the epithelial layer is a stimulus for the wound healing response, which begins immediately with keratocyte apoptosis in the anterior stroma. (Dupps and Wilson 2006; Wilson et al. 1996; Wilson and Kim 1998; Wilson et al. 2001a; Wilson et al. 2001b; Wilson et al. 2003c) This is thought to occur for the protection of the cornea, and the death of keratocytes would avoid passing on any infective organisms. (Wilson et al. 2001a) The initial 12-24 hours after epithelial insult is an active period, with cytokine release and growth factor production (particularly hepatocyte growth factor (HGF), keratinocyte growth factor (KGF), and epidermal growth factor (EGF)), which regulate epithelial cell differentiation and

proliferation for accelerated wound closure. (Dayhaw-Barker 1995a; Imanishi et al. 2000; Lu et al. 2001; Nakamura et al. 2001b; Wilson et al. 1999a; Wilson et al. 1999b; Wilson et al. 2003a) This activity leads to epithelial mitosis and migration to the site of the wound, with cells occasionally travelling as a 'sheet' due to their desmosome attachments. (Dayhaw-Barker 1995b)

Over the next few days in the wound healing process, keratocyte activity is initiated, also consisting of cell mitosis and migration to the wounded region. (Wilson et al. 2001a) Keratocytes communicate with each other via long processes, extending through collagen lamellae and the ground substance. (Dayhaw-Barker 1995b; Jester et al. 1999b) At this point, some keratocytes are likely to undergo a transformation into myofibroblasts, due to the release of another growth factor. These larger cells exhibit muscular characteristics (hence the term 'myo'), assisting in the contraction of wound margins, and the deposition of new keratocytes and collagen. (Gatlin et al. 2003; Jester et al. 1999b; Kuo et al. 2001; Nakamura et al. 2001a; Netto et al. 2005b) However, this newly placed material is disorganised. Maurice (Maurice 1987) described the healing of the stromal incision at the macroscopic and cellular level. He described that new collagen does not simply re-unite fibres that have been severed, but form a new network of collagen fibres that connect the severed lamellae, albeit in an irregular fashion. This leads to an increase in light scatter in the region, thus resulting in the reported corneal haze. (Dawson et al. 2005a; Dawson et al. 2005b; Dawson et al. 2005c; Ivarsen et al. 2003; Kato et al. 1999; Maurice 1987; Netto et al. 2005b; Tervo and Moilanen 2003)

The process of wound healing concludes weeks to months later, with the myofibroblasts differentiating back into quiescent keratocytes, and the epithelial defect being repaired. (Dayhaw-Barker 1995b; Jester et al. 1999b; Wilson et al. 2001a) With time, the areas of disorganised (scarred) tissue may become transparent again. (Dawson et al. 2005a; Dawson et al. 2005b; Maurice 1987) Despite this cascade of wound healing events, the recovery following LASIK is more reduced than following PRK, especially in terms of post-operative corneal haze. Animal experiments have found that after LASIK, compared to after PRK, there tends to be less stromal irregularity with minimal deposition of newly secreted substances (e.g. striated collagen and re-population of keratocytes), which resulted in a clearer interface, reduced scarring and haze. (Amm et al. 1996; Park and Kim 1999; Perez-Santonja et al. 1998; Rumelt et al. 2001) Histological images of the LASIK cornea have found greater healing activity at the flap margin, where scarring and epithelial ingrowth was seen. (Amm et al. 1996; May et al. 2004; Pallikaris et al. 1990; Park and Kim 1999; Perez-Santonja et al. 1998; Ustundag et al. 2000)

2.5.3 Post-LASIK stromal change

Chapter 8 is dedicated to the investigation of post-LASIK changes, in terms of corneal thickness and light backscatter changes, comparing myopic and hyperopic correction. Briefly, the myopic cornea is expected to thin centrally, with the hyperopic cornea expected to thin mid-peripherally. The non-ablated areas of stroma are not expected to change in thickness. However, the reduction in collagen lamellae due to ablation may lead to a similar occurrence as seen in keratoconus. If the residual stromal bed is less than 250μm, corneal

ectasia may occur. (Chayet et al. 1998b; Pallikaris and Siganos 1997; Price et al. 1999; Seiler et al. 1998)

2.5.4 Post-LASIK epithelial change

Following the initial surface ablation after PRK, the central epithelium has been found to thicken and become hyperplasic. (Bansal and Veenashree 2001; Dierick and Missotten 1992; Erie et al. 2002b; Gauthier et al. 1997; Park and Kim 1999) Wilson and colleagues (Wilson 2000, 2002; Wilson and Kim 1998; Wilson et al. 2003a; Wilson et al. 2001a) describe how the cornea has a tendency to smooth out it's surface, following an event that has lead to tissue loss. As well as the regeneration of the stroma, the epithelium is thought to play a role in the re-modelling of the corneal surface, by attempting to compensate for the loss of stromal tissue, resulting in epithelial hyperplasia. (Chayet et al. 1998a; Dierick and Missotten 1992; Dillon et al. 1992; Erie et al. 2002b; Gauthier et al. 1996; Guell et al. 1999; Lohmann and Guell 1998; Lohmann et al. 1997; Lohmann et al. 1999; Reinstein et al. 2005; Reinstein et al. 1999) After hyperopic LASIK, the occurrence of epithelial hyperplasia has the potential to mask the majority of the refractive effect (Figure 2.4). (Wilson et al. 2001a)

Figure 2-4 The simulated effect of epithelial hyperplasia (B) following hyperopic PRK (A), which may also occur after hyperopic LASIK. Diagram courtesy of Dr. Steven E. Wilson. ('The wound healing response after LASIK and PRK: elusive control of biological variability and effect on custom laser vision correction.' 2001. 119; 890).

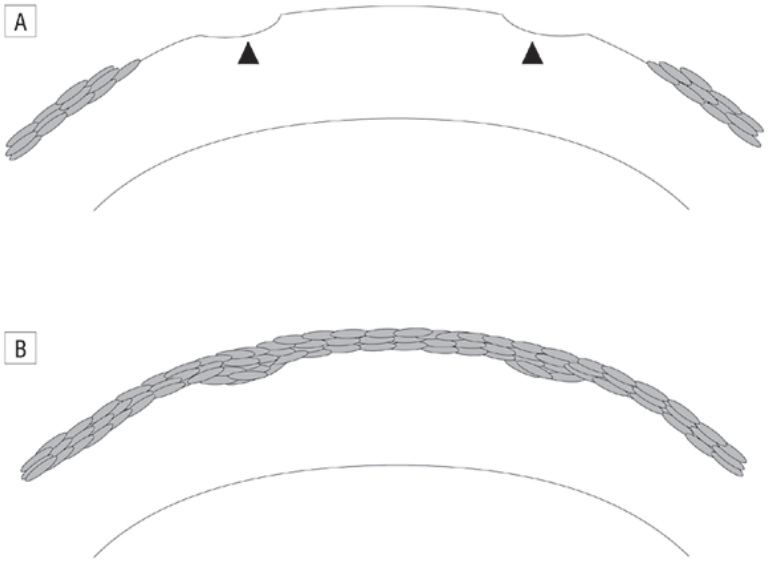

During routine LASIK, the central epithelium remains intact and only the epithelium at the borders of the flap is disturbed. This epithelium at the edge of the ablated zone has been found to become 8-10 layers thicker following LASIK, forming a hyperplasic epithelial 'plug', which reduces in size during recovery. (Amm et al. 1996; Anderson et al. 2002b; Crawford et al. 2003; Erie et al. 2002b; Kato et al. 1999; Pallikaris et al. 1990; Park and Kim 1999; Perez-Santonja et al. 1998). Nonetheless, many studies have found an increase in epithelial thickness in the central ablation zone also, presumably due to epithelial hyperplasia, with an ultimate influence on myopic regression. (Barker et al. 1999; Erie et al.

2002b; Naoumidi et al. 2003; Oliva et al. 2004; Rajan et al. 2005; Reinstein et al. 2000; Spadea et al. 2000)

Another major concern following LASIK is the development of diffuse lamellar keratitis (DLK). This inflammatory condition occurs following the accidental implantation of epithelium within the flap interface during the surgical procedure. The epithelial cells would create a type of wound healing response, and stimulate cytokines, leading to widespread haze. (Asano-Kato et al. 2003; Dupps and Wilson 2006; Netto et al. 2005b; Noda-Tsuruya et al. 2004; Sachdev et al. 2002; Wilson and Ambrosio 2002)

2.5.5 Reducing the healing response

Current research is concentrating on improving the wound healing response, specifically, reducing post-operative complications such as haze and regression. Wilson et al. (Wilson et al. 2001a) question whether attempts to cease the initial keratocyte apoptosis, would cease (or reduce) the wound healing cascade that follows. One step of the LASIK procedure being investigated is the creation of the flap. Femtosecond lasers have been used to produce the flap, in place of mechanical microkeratomes. While many studies have found laser microkeratomes to create smoother and more reproducible flaps, others have found the energy emitted from the laser to cause a cytokine response from the damaged cells. (Dhaliwal and Mather 2003; Dupps and Wilson 2006; Durrie and Kezirian 2005; Holzer et al. 2006; Kezirian and Stonecipher 2004; Kim et al. 2006; Krueger et al. 1998; Lim et al. 2006; Netto et al. 2005a; Nordan et al. 2003; Ratkay-Traub et al. 2001; Sonigo et al. 2006;

Stonecipher et al. 2006; Sugar 2002; Touboul et al. 2005; Tran et al. 2005) Therefore, reports are conflicted on whether laser microkeratomes improve the post-operative outcome of LASIK.

Another deviation to the traditional LASIK procedure is the creation of an epithelial flap instead of an epithelial-stromal one. This technique is called laser sub-epithelial keratomileusis (LASEK) or Epi-LASIK, where solely the epithelium is removed, either by mechanical or chemical (alcohol) means. (Ambrosio and Wilson 2003; Anderson et al. 2002a; Dupps and Wilson 2006; Lee et al. 2005; Netto et al. 2005a; Netto et al. 2005b; Taneri et al. 2004; Wilson et al. 2001a) Initially, it was hoped that LASEK would reduce the post-operative wound healing response as Bowman's layer remained intact, but this proved optimistic, as the epithelial basement membrane is still interrupted.

Non-surgical methods of controlling the wound healing response include the topical application of various corticosteroids, growth factors and other pharmacological therapies. (Nakamura et al. 2001b; Nejima et al. 2005) This topic is outside the immediate interest of this project.

Chapter 3

Methods

3.1 Instrumentation

3.1.1 Optical Coherence Tomography

A Zeiss-Humphrey retinal OCT2 (model 2010, Zeiss Humphrey Systems, Dublin, CA; now Carl Zeiss Meditec) was used in all studies. Initially designed to capture images of the retina, (Hee et al. 1995; Hrynchak and Simpson 2000; Huang et al. 1991; Voo et al. 2004) this computer-assisted optical instrument can be easily adapted to measure the anterior segment. In order to focus the light beam on the cornea, the subject's head needed to be placed slightly further away from the headrest than that required for retinal imaging. This was achieved by attaching a slice of high density plastic foam (approximately 15mm wide) to the headrest, creating a cushion to place the subjects head away from the machine, while maintaining a steady position. (Muscat et al. 2002; Wang et al. 2002a) Figure 3.1 shows the OCT instrument with the forehead attachment (seen in blue).

OCT uses low coherence Michelson interferometry. The near infrared (~820nm) light beam and fibre-optic based interferometer was used to identify boundaries within the tissue sample, by comparing the echo time delay of light that was backscattered from within the tissue, to that reflected from a reference mirror at a known distance. (Fujimoto 2001; Fujimoto et al. 1995; Huang et al. 1991; Izatt et al. 1994) The reflected light from both the sample and

reference mirror returned through the fibre-optic splitter to the detector and the interference was measured. Figure 3.2 displays a schematic diagram showing these pathways. The distance between reflective structures within the eye can be determined with OCT. (Fujimoto 2001; Fujimoto 2003; Fujimoto et al. 1995; Huang et al. 1991; Puliafito et al. 1995; Wirbelauer et al. 2001)

Figure 3-1 The optical coherence tomographer (OCT), with the forehead attachment, new fixation device and control box.

Figure 3-2 Schematic of optical coherence tomography.
Diagram courtesy of the National Research Council, Canada.
[http://ibd.nrc-cnrc.gc.ca/ibd_external/research/spectroscopy/2_oct_e.html].

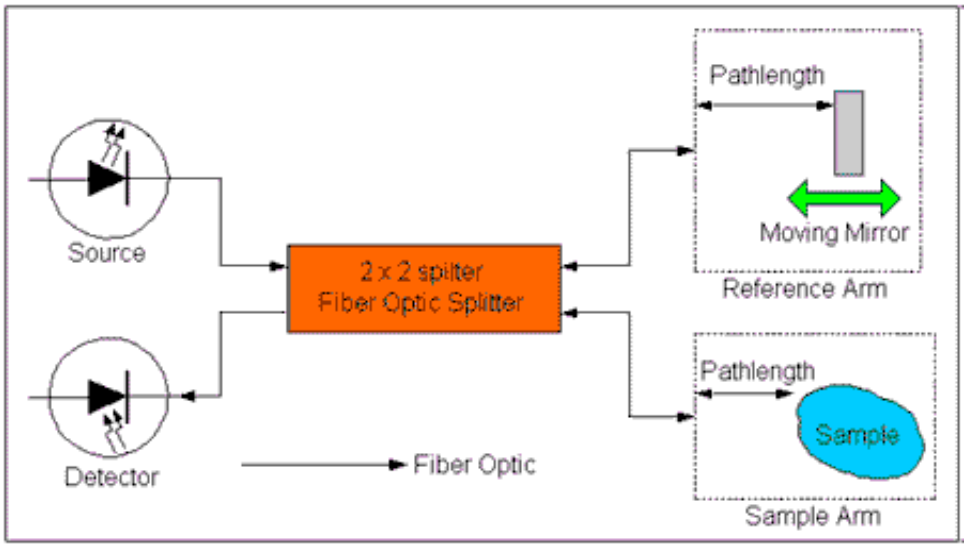

Similar to an axial (longitudinal) scan produced in ultrasound pachymetry, the resultant OCT image is a depiction of the degree of backscattered light measured at a range of depths within the tissue. The OCT image was shown as a pseudo-colour representation of backscatter intensity, in an arrangement of multi-coloured pixels (Figure 3.3). A greater intensity of backscatter is represented by red and white pixels, while black and blue pixels represented areas of less intensity. (Hirano et al. 2001; Wirbelauer et al. 2002c)

Each OCT image consisted of a set of 100 axial scans (analogous to ultrasonic B-scan), captured per second. Each column of pixels in the image represented a single axial scan. The transverse or lateral resolution (scan length of the light beam) was determined by the focussing power of the condensing lens of the instrument, and was kept to a minimum at

1.13mm. While this resulted in a small section of the cornea being imaged at a time, it also enhanced the details of the image. Figure 3.4 shows an OCT image obtained with a larger scan length of 5mm (but still 100 axial pixels), and can be compared in terms of detail with Figure 3.3.

Figure 3-3 Typical OCT image of the normal central cornea. Actual scan length was 1.13mm, consisting of 100 axial scans (100 columns of pixels).

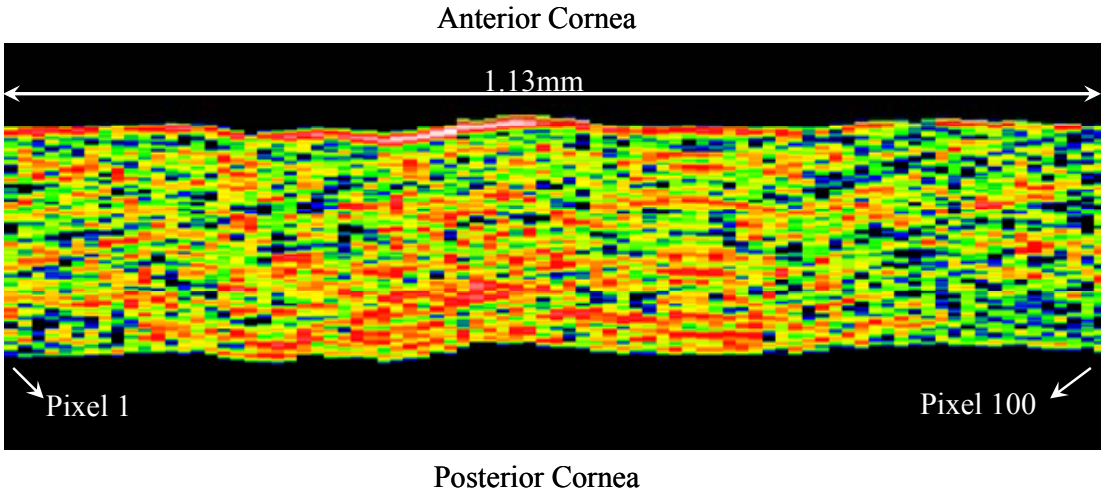

Figure 3-4 The normal cornea imaged using a wide OCT scan beam of 5mm.

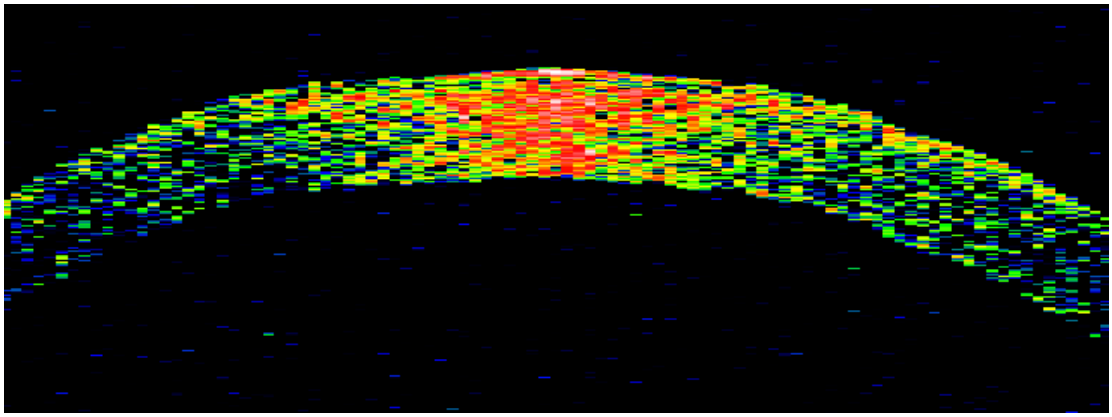

The OCT2 uses a super luminescent diode (SLD) near infrared light source operating at a wavelength of 820nm (Humphrey 2001). The bandwidth of the light source governs the axial resolution available for imaging, in this case being 10-20µm, which is inadequate to image the cornea at the cellular level, but can distinguish the epithelial layer from the stroma. (Fujimoto 2003; Fujimoto et al. 2000a; Fujimoto et al. 2000b; Hirano et al. 2001; Humphrey 2001; Puliafito et al. 1995) Axial resolution holds an inversely proportional relationship with the bandwidth of a particular light source; i.e. the larger the bandwidth, the better the axial resolution.

Recent experimental (lab-based) OCT instruments have achieved impressive axial resolutions as small as 1-3µm, using state-of-the-art broadband lasers (such as $Ti:Al_2O_3$) as a light source. (Bizheva et al. 2003; Chan et al. 2006b; Drexler 2004; Drexler et al. 2001; Fujimoto et al. 1998; Fujimoto et al. 2000a; Lim et al. 2005; Unterhuber et al. 2004; Unterhuber et al. 2003; Wojtkowski et al. 2005) However, many of these lasers are often costly and difficult to maintain, but have the potential to be used in clinical OCT systems in the near future. (Drexler et al. 2001; Schuman et al. 2004; Unterhuber et al. 2003) Other improvements to OCT imaging include using a light source of a longer wavelength (~1310nm) which allows a higher scan acquisition rate (up to 4000 axial scans per second), and a greater penetration depth (advantageous in retinal-choroid imaging), but axial resolution does not vastly improve. (Drexler 2004; Radhakrishnan et al. 2001; Schuman et al. 2004; Wirbelauer and Pham 2004) With images being acquired at a higher speed, artefacts

caused by eye motion during scanning are reduced. (Radhakrishnan et al. 2001; Schuman et al. 2004)

Recently, a new OCT instrument was FDA approved (October 2005) and made commercially available for anterior segment imaging and biometry – the Visante^{TM} OCT (model 1000, Carl Zeiss Meditec, Jena, Germany). Images of the entire anterior chamber are possible, with a scan width of 1 to 16mm and scan depth of 1 to 8mm (www.meditec.zeiss.com). The Visante^{TM} OCT uses a SLD light source at 1310nm, enabling faster scanning but the axial resolution of 15μm is not an improvement from that provided by the OCT2.

3.1.1.1 Determination of corneal and epithelial thickness

The high resolution imaging capability of OCT enabled the differentiation of anatomical layers within the cornea. A boundary was detected when there was a change in refractive index through the cornea, and was displayed with a peak in the backscattered light profile. Figure 3.5 shows a cropped OCT image of the normal central cornea, with associated axial light backscatter profile. Peak A indicates the interface between the air and the anterior surface of the cornea (including the tear film). Peak E indicates a change in intensity of the backscattered light, representing the basal epithelial-stromal barrier, designating the distance between peaks A and E as epithelial thickness (A-E). The distance between the first (A) and last peak (P) would be measured as total corneal thickness (A-P). (Muscat et al. 2002; Wang et al. 2002a; Wirbelauer et al. 2002c; Wong et al. 2002) Automated, multiple OCT scan analysis is discussed later.

3.1.1.2 Determination of corneal light backscatter

The light backscatter profile seen in Figure 3.5 shows the varying degrees of light intensity through the associated OCT corneal scan. Red and white pixels indicated a greater magnitude of backscatter, whereas black and blue pixels represented areas of lower reflectivity. Custom OCT scan analysing software was used to quantify corneal backscatter alongside corneal and epithelial thickness. Light backscatter analysis through the cornea involved treating the epithelial layer as a separate entity and dividing the remaining stroma into ten equal sections. (Wang et al. 2003d) The software provided a backscatter value for each band of stroma (1 to 10), normalized over the whole ten stromal bands, and an additional backscatter value for the epithelium.

Figure 3-5 OCT scan of the cornea (right) and the axial reflectivity profile (left). Corneal thickness was calculated from the distance between peak 'A' (representative of the anterior corneal surface) and peak 'P' (posterior corneal surface). Epithelial thickness was obtained as the distance between peak 'A' and 'E'.

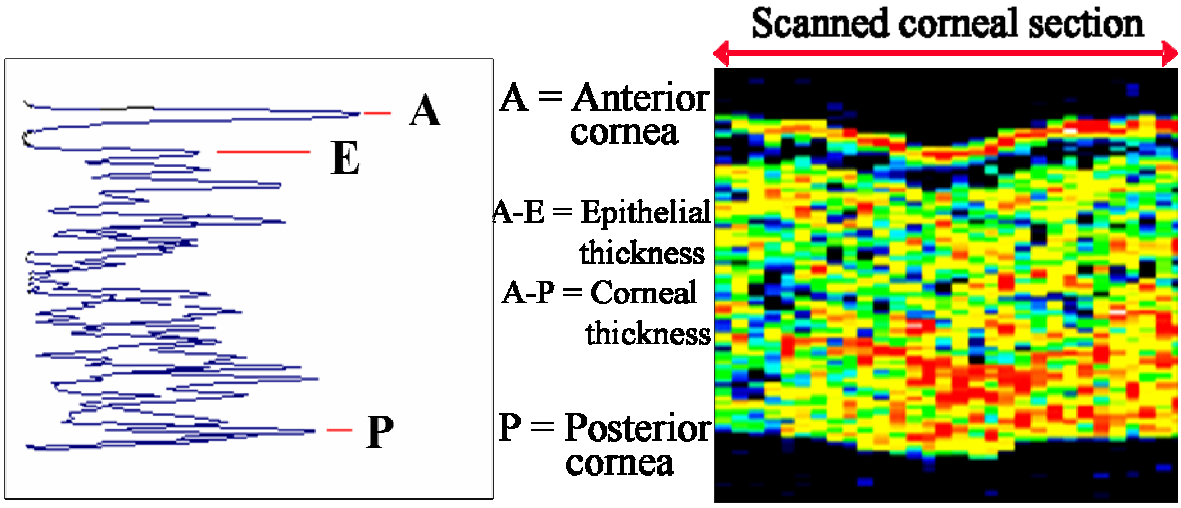

3.1.1.3 OCT scanning procedure

Study participants were seated comfortably at the OCT instrument, with their chin and forehead settled on the headrest. A video monitor connected to the OCT instrument enabled the observation of the cornea. In order for the corneal surface to be in focus on the monitor, the condensing lens of the OCT needed to be fully turned towards the 'plus' position, in effect defocusing the image away from the original retinal setting, towards the cornea.

The transverse length of the scan beam was minimized to 1.13mm (as mentioned earlier). Initially, the subject was asked to fixate on the flashing target within the OCT eyepiece, to obtain a central corneal reading. They would later be asked to fixate on peripheral fixation lights, with the aid of custom built devices (discussed later), to obtain mid- and far-peripheral corneal readings. The incident beam was aligned with the reflection of the fixation target on the corneal surface, and a specular reflection was sought to confirm the incident beam was perpendicular to the cornea (Figure 3.6). The corneal surface was scanned every second, producing a false-coloured image on the monitor. Once the specular reflection was obtained at the required corneal location, an optimal image and accompanying raw data was captured. Typically, an image was captured within 1-3 seconds, presuming minimal eye and head movement on the subject's behalf. The image along with the raw data was saved on the OCT hard drive for future retrieval and analysis (discussed later).

Figure 3-6 Operator view of the video monitor attached to the OCT, displaying the scan beam of 1.13mm (horizontal line) and the specular reflection (seen as a shimmer), produced when the scan beam was aligned with the reflection of the fixation light (circular reflection in centre of beam) on the corneal surface.

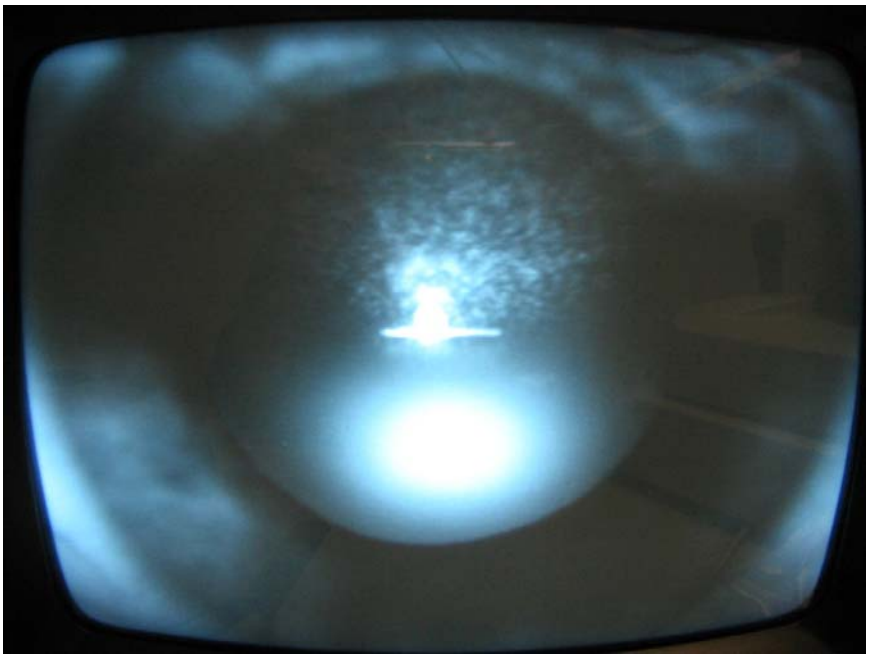

3.1.1.4 External fixation devices

The fixation target in Figure 3.7 was used in the majority of studies discussed in this project. This target was designed to aid in the measurement of the horizontal cornea only, at four points either side of the centre (Figure 3.8). To obtain a measurement of the temporal cornea, the subject fixated a nasal light, and vice versa. Unfortunately, the construction of this device was such, that the row of light emitting diodes (LEDs) was not in the central plane, but was fixed slightly higher than the centre of the ring in which it was held. Turning

the row of lights to stand vertically did not enable corneal readings along the central vertical meridian, as the eye was forced into a temporal / nasal gaze.

Figure 3-7 Subject view of the OCT, with the original fixation target (showing the first position lit). In addition to the internal central fixation light of the OCT, the target illuminates at four positions either side, enabling the measurement of the temporal and nasal cornea. Nine readings in total are obtained along the horizontal meridian.

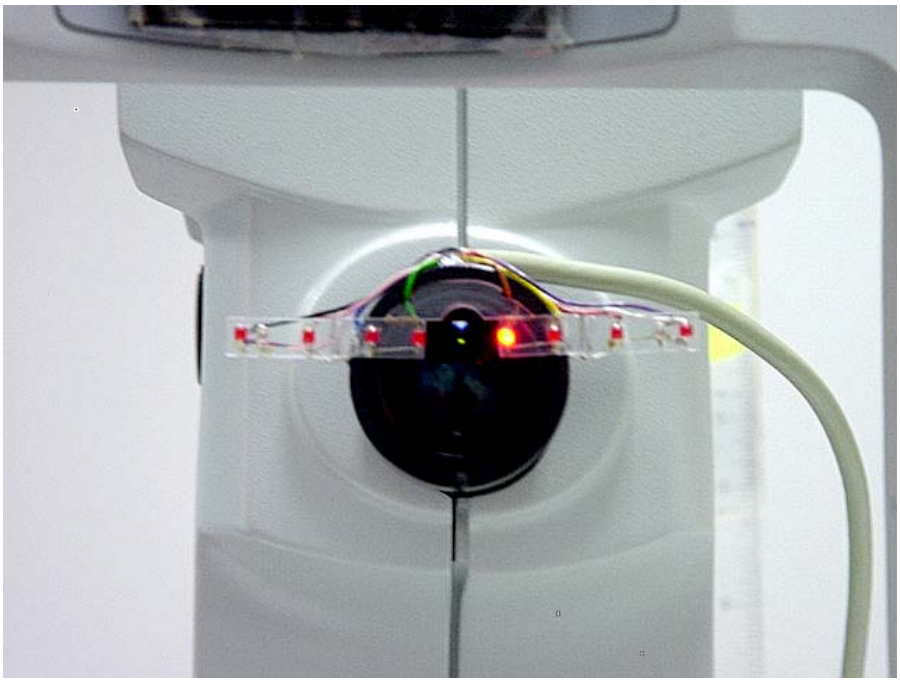

Figure 3-8 Locations of the OCT beam on the cornea, using the fixation target in Figure 3.7. The distance of each measured location was taken from the central corneal scan (white line), and each location in 'mm' represents the centre of each scan beam. The actual scan length of the OCT beam for each location was 1.13mm. The temporal (T) corneal measurements were obtained by fixating on a nasal (N) light, and vice versa.

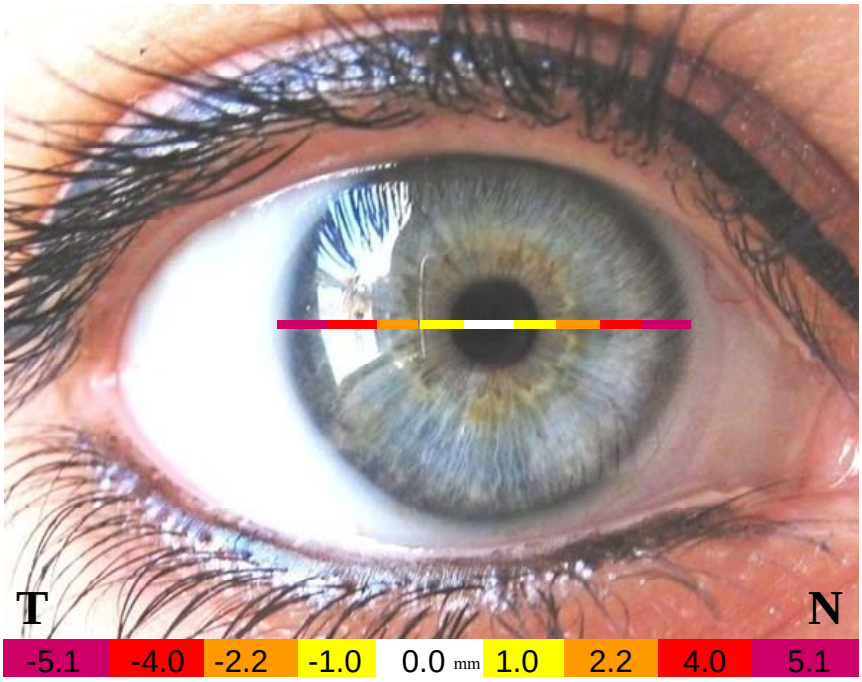

To aid in the measurement of the cornea aside from along the horizontal meridian, another device was designed and constructed, for readings along the vertical and along two oblique meridians (Figure 3.9). The new fixation target consisted of eight arms in a 'star-like' formation, each representing a different direction of gaze – temporal (T), nasal (N), superior (S), inferior (I), superior temporal (ST), superior nasal (SN), inferior temporal (IT) and inferior nasal (IN). Each arm held six lights 1mm apart, in three different colours (red, green and yellow) and could be illuminated in turn via a control box (seen in Figure 3.1). The

purpose of using coloured lights was to aid fixation, since the subject's view of the LEDs would be out of focus, making lights of the same colour difficult to track. The original prototype of this fixation target consisted of six LEDs on each arm, but it was necessary to remove two lights from each of the two inferior oblique arms, because the nose was an obstruction.

In the same manner as for the fixation target in Figure 3.7, the location of corneal measurement was opposite to the light fixated; i.e. fixating on the third superior temporal light with the right eye would enable the measurement of the inferior nasal mid-peripheral cornea. Due to the number of LEDs (44) on the new fixation target (and therefore number of individual measurements), for the sake of time efficiency and subject comfort, the OCT scanning beam was kept in the horizontal position for all measurements. Preliminary testing of the new fixation device revealed that the outer most light on each arm (position 6) was rarely utilised, since at this position the reflection of the LED was located outside of the limbus on the sclera, not of use for the corneal imaging in this project.

Although subjects were asked to fixate on the LEDs, a small amount of eye movement would have been present in the form of micro-saccades (0.25-0.50^{o} with the head being voluntarily held against the head rest. (Skavenski et al. 1979) This may have introduced some variability to the corneal location scanned during fixation.

Figure 3-9 Subject view of the new fixation target attached to the OCT eyepiece, aiding corneal measurement not only in the horizontal, but in the vertical and oblique meridians. The LEDs were multi-coloured to improved subject fixation, and are displayed here in the superior oblique position as red, green and yellow.

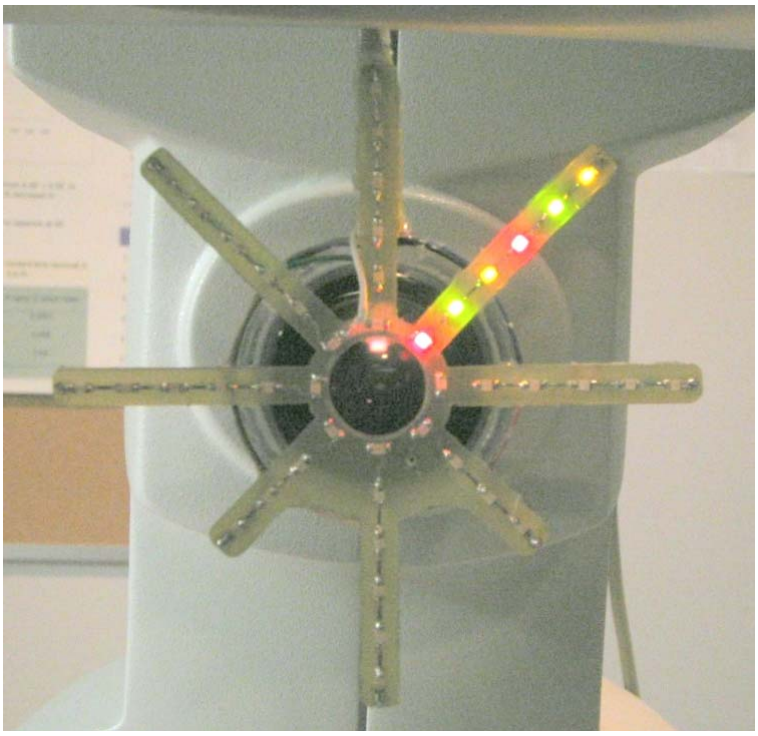

3.1.2 Orbscan optical pachymetry

The Orbscan II (Bausch & Lomb, Rochester, NY) is a non-contact optical topographer that uses a calibrated video and scanning slit system to measure corneal thickness (Figure 3.10). Hundreds of data points are collected along the cornea by 20 slit-beams scanning the temporal side and 20 scanning the nasal side of the cornea. The Orbscan II automatically analysed the data captured by the 40 slit-beam edge reflections, calculating the difference

between the anterior and posterior surface reflections to produce corneal thickness values. An acoustic factor of 0.92 was recommended by the manufacturer. This factor originated soon after it was found that the Orbscan was producing corneal thickness values greater than the gold standard of ultrasound pachymetry. (Boscia et al. 2002; Iskander et al. 2001; Yaylali et al. 1997) The acoustic factor was therefore used to calibrate Orbscan readings with ultrasound pachymetry. (Boscia et al. 2002; Fakhry et al. 2002; Gherghel et al. 2004; Iskander et al. 2001; Kawana et al. 2004; McLaren et al. 2004) This instrument created colour-coded maps by default, of corneal thickness, anterior and posterior corneal curvature and radius of curvature.

Figure 3-10 The Orbscan II topographer.

3.1.3 Ultrasonic Pachymetry

The DGH 550 (Pachette 2) ultrasonic pachymeter (UP) (DGH Technology Inc, Exton, PA) was used in one study in this project. This instrument operates using ultrasound at a frequency of 20 MHz and a velocity of 1640m/sec. The principle behind this technique was parallel to that of OCT, except with sound waves being transmitted through a tissue and being reflected back to the probe. The distance between boundaries was calculated in a similar way, using the echo time delay of sound and constructing an axial scan (a-scan). (Ehlers and Hjortdal 2004) This early model of UP does not measure epithelial thickness, but next generation versions such as the CorneoGage Plus™ (Sonogage, Cleveland, OH) with transducers of 50MHz have claimed epithelial measurements. (Young et al. 2004)

Figure 3-11 The DGH 550 (Pachette 2) ultrasonic pachymeter.

Each reading with the Pachette 2 automatically captured and averaged five measurements simultaneously. As recommended by Realini and Lovelace (Realini and Lovelace 2003), a series of three individual readings was obtained from eyes in this study. The operation of this instrument was limited by only measuring one region at a time, restrained by the diameter of the applanation probe (1.5mm). An advantage was being able to measure any corneal location, but measurement at the exact same location was difficult to replicate. It was very important to position the probe head perpendicular to the cornea, as misalignment leads to an over-estimation of corneal thickness. (Haun et al. 2004) This made UP very operator dependent. The issue of probe placement may be associated with the lower inter-observer reproducibility found with contact ultrasonic pachymetry. (Miglior et al. 2004)

3.2 Data Analysis

3.2.1 OCT Raw data analysis

Corneal and epithelial thickness values were not available at a glance from the OCT. Manual analysis could be performed using the instrument's on-board software, however only single pixel (axial) analysis was permitted. Custom software designed by the CCLR enabled multiple pixel analysis per scan, and multiple scan analysis per subject, in an automated fashion. A screenshot of the OCT scan analysis software (MK4) is shown in Figure 3.12. Raw data files, each with a three figure code were stored on the OCT computer. Spreadsheets were used to log these raw files, labelling each with an identity consisting of subject identification, corneal location and other pertinent information such as the study visit. Raw data files were imported to a personal computer, and analysed to yield values for

corneal and epithelial thickness or light backscatter. Scan settings could be set to analyse any number of the 100 pixels. For all images in this project, the central 51 pixels were analysed and the average value displayed in the data table on screen.

3.2.2 Image Processing

For the construction of colour-coded maps in the studies discussed in Chapter 7, MATLAB software (Version 7.0, The Mathworks, Natick, MA) was used. This software required a set of codes to be written, to instruct the program to construct the desired maps following input of raw data. The raw thickness data (for either the cornea or epithelium) were organized in a matrix, shown in Figure 3.13. The individual points were interpolated to produce a smooth map, with each square representing the average of neighbouring squares (taken from the centre).

Figure 3-12 A screenshot of the custom OCT analysis software. The selected number of pixels to be included in the analysis was highlighted in the image (top left corner), and the associated backscatter profile was displayed (top right corner). Columns of data were listed in the table.

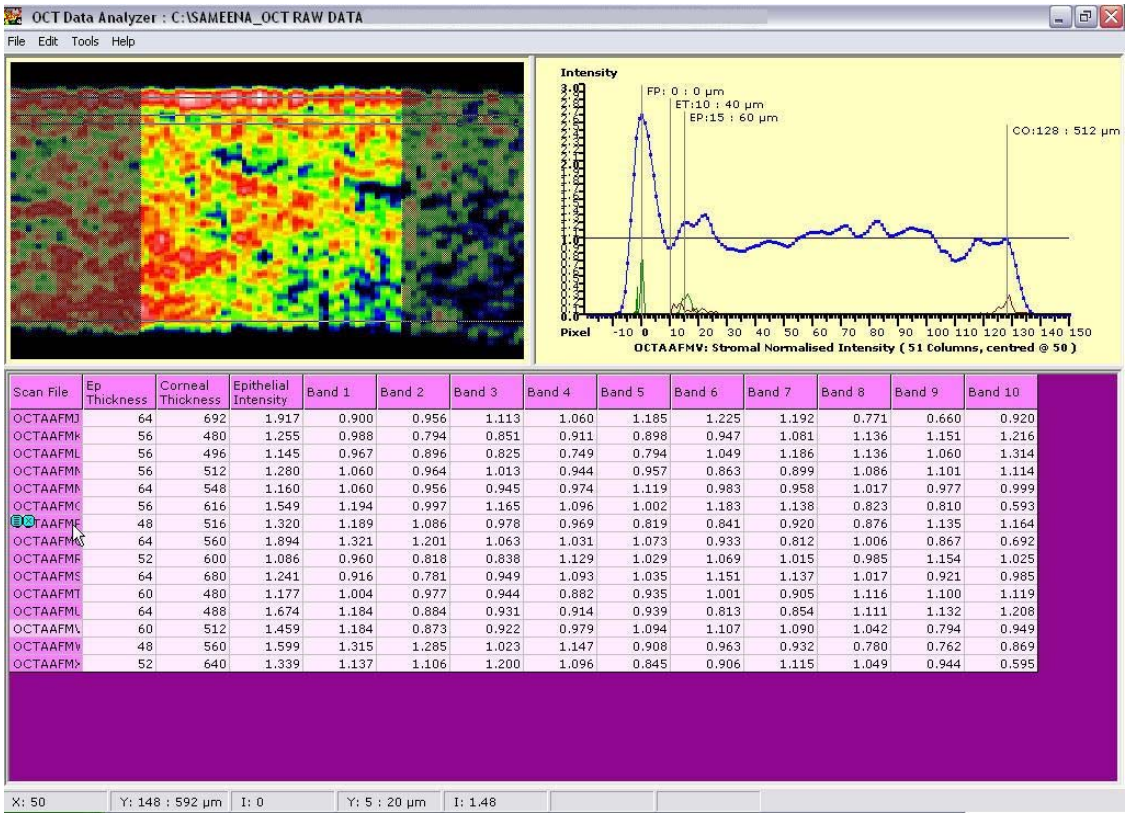

Scan File	Ep Thickness	Corneal Thickness	Epithelial Intensity	Band 1	Band 2	Band 3	Band 4	Band 5	Band 6	Band 7	Band 8	Band 9	Band 10
OCTAAFMJ	64	692	1.917	0.900	0.956	1.113	1.060	1.185	1.225	1.192	0.771	0.660	0.920
OCTAAFMk	56	480	1.255	0.988	0.794	0.851	0.911	0.898	0.947	1.081	1.136	1.151	1.216
OCTAAFML	56	496	1.145	0.967	0.896	0.825	0.749	0.794	1.049	1.186	1.136	1.060	1.314
OCTAAFMM	56	512	1.280	1.060	0.964	1.013	0.944	0.957	0.863	0.899	1.086	1.101	1.114
OCTAAFMN	64	548	1.160	1.060	0.956	0.945	0.974	1.119	0.983	0.958	1.017	0.977	0.999
OCTAAFMO	56	616	1.549	1.194	0.997	1.165	1.096	1.002	1.183	1.138	0.823	0.810	0.593
OCTAAFMP	48	516	1.320	1.189	1.086	0.978	0.969	0.819	0.841	0.920	0.876	1.135	1.164
OCTAAFMQ	64	560	1.894	1.321	1.201	1.063	1.031	1.073	0.933	0.812	1.006	0.867	0.692
OCTAAFMR	52	600	1.086	0.960	0.818	0.838	1.129	1.029	1.069	1.015	0.985	1.154	1.025
OCTAAFMS	64	680	1.241	0.916	0.781	0.949	1.093	1.035	1.151	1.137	1.017	0.921	0.985
OCTAAFMT	60	480	1.177	1.004	0.977	0.944	0.882	0.935	1.001	0.905	1.116	1.100	1.119
OCTAAFMU	64	488	1.674	1.184	0.884	0.931	0.914	0.939	0.813	0.854	1.111	1.132	1.208
OCTAAFMV	60	512	1.459	1.184	0.873	0.922	0.979	1.094	1.107	1.090	1.042	0.794	0.949
OCTAAFMW	48	560	1.599	1.315	1.285	1.023	1.147	0.908	0.963	0.932	0.780	0.762	0.869
OCTAAFMX	52	640	1.339	1.137	1.106	1.200	1.096	0.845	0.906	1.115	1.049	0.944	0.595

Figure 3-13 Arrangement of thickness values as a data matrix, for input into the imaging software used to construct topographical maps. Each point referred to the corneal location (example for right eye), hence the two superior oblique arms had only four possible measures, to correspond with the fixation target. [T = temporal, N = nasal, S = superior, I = inferior].

						S						
						5						
		4				4				4		
			3			3			3			
				2		2		2				
					1	1	1					
T	5	4	3	2	1	C	1	2	3	4	5	**N**
					1	1	1					
				2		2		2				
			3			3			3			
		4				4				4		
	5					5					5	
						I						

3.2.3 Statistical analysis

Study cohort information including age (mean, standard deviation and range) and gender were obtained. Statistical analysis was performed using Statistica 6.0 (Statsoft Inc, Tulsa, OK). Repeated measures analysis of variance (Re-ANOVA) and Tukey Honestly Significantly Different (HSD) post-hoc testing were used to signify differences between variables. The tests were used to identify significant differences between time, between corneal location, between instruments and between subjects, for corneal and epithelial thickness or light scatter, in their respective studies. Paired t-tests were used to determine pair-wise differences and Pearson's correlation coefficient was used to determine the association between two variables. Statistical significance was set at a value of $p<0.05$.

3.3 Participants

3.3.1 General inclusion and exclusion criteria

Informed consent was obtained from each individual and ethics clearance was obtained from the Office of Research Ethics at the University of Waterloo prior to commencement of all studies. Participant eligibility was determined at a screening appointment using the guidelines for inclusion and exclusion criteria. Specific requirements for each study such as refractive error limits are discussed within each sub-chapter but in general, all participants were required to be a minimum age of 18, willing to volunteer and follow study instructions. Each was recommended to have a full eye examination every two years. Subjects were not enrolled into a study if they had been diagnosed with a systemic disease affecting ocular

health or an active ocular infection. Any person who had undergone recent ocular injury or surgery (that was not part of the protocol) was also not enrolled into a study. All participant records and data were securely stored within the CCLR.

Chapter 4

Multiple operator use of OCT

As OCT technology improves and becomes more readily available in the clinical setting, it is likely to be operated by many individuals, even within a single study. Hence, it is important to know the degree to which these measurements differ between investigators, and whether it would confound the results of a particular study. Recently, Sin and Simpson (Sin and Simpson 2006) reported on the repeatability of OCT readings in the measurement of corneal and epithelial thickness. Repeatability is defined as the similarity between test and re-test measures, which in an ideal situation would be perfect. The terms 'reliability' and 'reproducibility' are synonyms for repeatability. (Essex-Sorlie 1995) The study examined within-session, between-day and between-eye repeatability of thickness measures, but with all OCT readings being obtained by a single operator.

An experiment was devised to test the repeatability of corneal and epithelial thickness measures between three investigators (SH, AM and YF), all proficient in the operation of OCT. A group of ten subjects were enrolled, and two OCT readings of the central cornea were obtained from each individual, by each operator. Each pair of readings was obtained a few minutes apart, with the subject removing their head from the chin-rest to force re-focusing of the OCT beam on the corneal surface. Between-operator and within-operator repeatability were assessed. Intraclass correlation (ICC) can be used to evaluate the level of agreement in the measurements between operators. The ICC coefficient represents concordance, where '1' indicates perfect agreement and '0' indicates no agreement at all.

However, an instrument can be repeatable, but not necessarily valid. Validity refers to how well a device actually measures what it is intended to measure. Since we cannot test the validity of in vivo measurements of the human cornea, a series of ten polymethyl methacrylate (PMMA) lenses were used. Each lens was measured twice with OCT by each of the three operators, and with digital callipers (by AM) to obtain values of real thickness. All thickness values are displayed in Appendix A. Each operator measured the lenses to be significantly thicker than their real thickness ($p<0.05$). However, a major source of error leading to this difference was probably due to the refractive index (n) of the lenses (1.485), while the refractive index assumed in OCT measurement is that of the retina (1.36). (Puliafito et al. 1995) Hence, the OCT values were multiplied by a conversion factor of 1.092 (n1.485/n1.36), but they remained significantly different from the real lens thickness values ($p<0.05$). There was no difference in the two measures obtained by each operator ($p>0.05$), and neither was there any difference between operators in the measurement of each lens ($p>0.05$). The ICC for this latter relationship was 1.00 (0.9998).

4.1 Intra-operator repeatability

The values of corneal thickness obtained by each investigator for each corneal reading per subject are shown in Appendix B, with epithelial thickness values shown in Appendix C. Intra-operator or within-operator repeatability assessed the degree by which the two values of corneal thickness differed per subject. For corneal thickness, the ICC for operators SH, AM and YF were 0.990, 0.973 and 0.980 respectively, in the comparison of the first with the

second corneal measurement. These values indicated very good repeatability and matched the results found by Sin and Simpson. (Sin and Simpson 2006) However, for epithelial thickness, ICC for SH, AM and YF were 0.594, 0.410 and 0.337 respectively. These lower values strengthened the notion of obtaining more readings for epithelial thickness within a study, i.e. taking an average of five measurements rather than two.

4.2 Inter-operator reproducibility

Inter-operator or between-operator reproducibility assessed how well the average of the two corneal measurements (for each subject) compared between investigators. The ICC for the three operators was 0.975 for corneal values and 0.412 for epithelial values. The first ICC value indicated very good repeatability; however the second indicated that epithelial values were more variable between investigators. Sin and Simpson (Sin and Simpson 2006) also found a much lower ICC for epithelial values at 0.38. It can be concluded that for corneal thickness measurement, more than one OCT operator can be used in a single study without jeopardizing results, however for epithelial thickness measurement greater caution should be applied. Where possible, the use of a single OCT operator may be advised.

Chapter 5

Corneal, Stromal and Epithelial thickness changes following Corneal Refractive Therapy for the treatment of Myopia

5.1 Overnight myopic CRT™ lens wear for a four week period

5.1.1 Abstract

Purpose: To investigate thickness changes of the total cornea and epithelium across the horizontal corneal meridian following four weeks of overnight CRT™ rigid contact lens wear.

Methods: Thirty subjects were fitted with CRT™ contact lenses (Dk/t = 67) and worn overnight for 4 weeks. Baseline corneal thickness was measured at 9 locations along the horizontal meridian using OCT before lens insertion the evening prior to sleeping at the CCLR. The same thickness measurements were obtained the next morning immediately following lens removal and at 1, 3, 7 and 14 hours later. These were repeated on days 4, 10 and 28 of the study, followed by a recovery measurement 3 days after discontinuing lens wear.

Results: Twenty three subjects completed the study. At lens removal on Day 1, the central and mid-peripheral cornea increased in thickness (mean ± SD, compared to baseline) by 4.9 ± 2.0% and 6.2 ± 2.2% respectively (both $p<0.001$). The central epithelium thinned -7.3 ±

3.2% and mid-peripheral epithelium thickened 13.0 ± 1.7% (both $p<0.001$). Corneal swelling recovered throughout the day, with the majority of deswelling taking place within the first 3 hours following lens removal ($p>0.05$). Maximum central epithelial thinning reached -13.5 ± 2.0% by Day 4. After three days of no lens wear, corneal thickness had recovered towards baseline more so than the epithelium, which remained -4.1 ± 2.5% thinner centrally and 2.4 ± 1.5% thicker mid-peripherally ($p<0.05$ compared to baseline).

Conclusion: This study demonstrated that overnight wear of CRT^{TM} lenses for myopia induce different amounts of swelling across the cornea, with rapid deswelling during the day. Central epithelial thinning and mid-peripheral epithelial thickening occurred, with 96% recovery after 3 days discontinuation of lens wear.

5.1.2 Introduction

Several investigators have examined the degree to which the cornea and epithelium respond to modern orthokeratology (OK) lenses. Wang et al. (Wang et al. 2003c), who also used Paragon Corneal Refractive Therapy (CRT^{TM}) lenses measured thickness using OCT, and found central corneal swelling of 4.9% and central epithelial thinning of -5.1% following a single night of CRT^{TM} lens wear. The central cornea was found to swell less than the periphery – opposite to that seen following extended wear of traditional rigid and soft contact lenses. (Wang et al. 2003a) The mid-peripheral epithelium was found to thicken by ~2%. (Wang et al. 2003a)

Soni et al. (Soni et al. 2003) used Airperm lenses manufactured by Contex (Sherman Oaks, CA) with a Dk/t of 81. Following three months of lens wear, Orbscan topography (Bausch & Lomb Surgical, Salt Lake City, UT) showed a 3% increase in central corneal thickness on lens removal that recovered to baseline within four hours. However, epithelial thickness measured by confocal microscopy was reported in only four subjects, and revealed a thinning of -32.5% at lens removal after three months of lens wear that did not recover to baseline throughout the day.

This is not the only study that has found such a great amount of central epithelial thinning, with Alharbi and Swarbrick (Alharbi and Swarbrick 2003) (using BE lenses, Ultra Vision Pty.Ltd., Brisbane, Australia) also finding a marked -33% calculated by subtraction of stromal from total corneal thickness values measured by optical pachymetry. This study

however, found no significant epithelial changes in the mid-periphery, but an increase in corneal thickness that was accounted for by stromal thickening. The two month overnight study by Nichols et al. (Nichols et al. 2000) (using Contex lenses) reported corneal thickness data measured using Orbscan and stated a decrease in central corneal thickness but no mid-peripheral changes. As the Orbscan cannot differentiate between layers of the cornea, it cannot be determined whether these changes were stromal or epithelial.

The three studies described above differed experimentally, using different lens designs and equipment to measure corneal and epithelial thickness. Although there was a similar amount of central epithelial thinning found in the Alharbi and Swarbrick (Alharbi and Swarbrick 2003) and Soni et al. (Soni et al. 2003) studies, there is a scarcity of information on the diurnal and temporal effects of overnight wear of reverse geometry and CRT^{TM} lenses. Further work is also required to monitor the recovery of the cornea following CRT^{TM}.

The purpose of this study was to measure corneal and epithelial thickness changes using OCT across the horizontal corneal meridian, following overnight wear of myopic CRT^{TM} lenses for a period of four weeks.

5.1.3 Study procedure

Subjects

Thirty healthy subjects were enrolled (20 females and 10 males; mean age 25.8 ± 6.9 years; ranging from 21 to 51 years). Refractive error of participants was restricted to a spherical

range of -1.00 to -6.00, with no more than -1.75D cylinder. Table 5.1 summarizes the corneal parameters of the cohort. Current RGP lens wearers were excluded and soft lens wearers had to discontinue lens wear two weeks prior to the start of the study.

Table 5-1 Summary of baseline corneal parameters.

Baseline Corneal Parameters (Mean ± SD)		
	OD	**OS**
Refractive error – sphere (D)	-2.77 ± 1.19	-2.54 ± 1.11
Refractive error – cylinder (D)	-0.49 ± 0.39	-0.53 ± 0.41
Keratometry – flat K (D)	43.73 ± 1.57	43.71 ± 1.54
Keratometry – cyl (D)	-0.64 ± 0.40	-0.67 ± 0.43
Central corneal thickness (μm)	508 ± 28.3	506 ± 26.2
Central epithelial thickness (μm)	52 ± 2.6	52 ± 3.1

Instrumentation and Lenses

The CRT™ lenses used (Paragon Vision Sciences Proximity Control Design™) were manufactured from fluorosilicone acrylate with oxygen permeability (Dk) of $100x10^{-11}$ units and transmissibility (Dk/t) of $67x10^{-9}$ units. The lenses were fit using software provided by the manufacturer. The computer program uses the flat keratometry reading, sphere and over-refraction values to calculate the back optic zone radius (BOZR), return zone depth (RZD) and landing zone angle (LZA) for the 10.5mm diameter lens. The lenses selected by the program were assessed on eye to ensure that there was appropriate apical touch (4mm), mid-

peripheral clearance, adequate edge lift and proper centration. The lens parameters for the 23 subjects are listed in Table 5.2.

Table 5-2 CRT™ lens parameters.

Lens Parameters	
Total Diameter (mm)	10.5
BOZR (mm)	8.4 ± 0.38
BOZD (mm)	6.0
Power (D)	+0.50
Centre Thickness (mm)	0.15
Dk / t (x 10^{-9} units)	67
Return Zone Depth (μm)	526 ± 0.03
Landing Zone Angle (deg)	33.08 ± 1.09

In the evening prior to the first night of the study, baseline corneal thickness was measured using OCT. The fixation target shown in Figure 3.7 aided in the capture of the nine measurements across the horizontal meridian of the cornea. The CRT™ lenses were placed on each eye and the fit was assessed for adequate movement, centration and fluorescein pattern prior to sleep. Participants slept at the Centre for Contact Lens Research, retiring at 10pm and waking at 7am the next morning for the Day 1 measurements. On waking, the subjects kept their eyes closed until lenses were removed for corneal measurements. The measurements were repeated 1, 3, 7 and 14 hours after lens removal. The entire procedure was repeated on days 4, 10 and 28 of the study. At the end of the 4 week study period, lens

wear was discontinued and corneal thickness measurements were repeated 3 days (72 hours) later.

Raw data files captured by the OCT were processed using custom software as described in Chapter 3. Repeated measures analysis of variance (Re-ANOVA) and Tukey HSD post-hoc testing was used to analyse changes in corneal and epithelial thickness from baseline levels over the study period. The chosen level for significance was 0.05. Corneal and epithelial thickness changes were expressed as percentage change based on the following:

$$([thickness_{time} - thickness_{baseline}] / [thickness_{baseline}]) \times 100.$$

5.1.4 Results

Twenty-three subjects completed the study. Two subjects withdrew due to lens discomfort, three due to poor vision, one due to conjunctivitis and one due to a corneal abrasion. The mid-peripheral values are represented as the mean of the first two nasal and temporal positions from the centre. Mean (±SD) baseline refraction (spherical equivalent) improved from –3.00 ± 1.03DS to –1.70 ± 0.53DS after the first night of lens wear ($p<0.05$). Following lens removal on Day 28, refractive error had improved to –0.41 ± 0.77DS ($p<0.05$ from baseline, but $p>0.05$ from Day 10). After the 72 hour recovery period, the refraction was still –1.91 ± 1.01DS ($p<0.05$ from baseline), which represented a 60% recovery. (Sorbara et al. 2005a)

The cornea exhibited maximum swelling immediately on lens removal, reducing rapidly, as seen in Figure 5.1. Immediately after lens removal, central corneal swelling was 4.9 ± 2.0% ($p<0.001$ compared to baseline), and 6.2 ± 2.2% in the mid-peripheral region ($p<0.001$ compared to baseline). Figure 5.2 illustrates the central and mid-peripheral corneal swelling from the time of lens removal to the 14 hour measurement, following the first night of CRT™ lens wear. These results show that the mid-peripheral swelling was significantly greater than the central swelling ($p<0.001$). The corneal swelling pattern was similar for Days 4, 10 and 28 as illustrated in Figure 5.1, but the amount of central corneal swelling decreased to ~3% compared to Day 1 (~5%; $p<0.05$). Central deswelling increased from Day 1 to Day 28, showing greatest overshoot at hour 14 on Day 10 (-2.5 ± 1.2%). The values for corneal thickness change (mean % ± SD) throughout the study are displayed in Appendix D.

Figure 5-1 Corneal swelling and deswelling following 4 weeks of CRT™ lens wear, with measurements obtained on four separate study days.

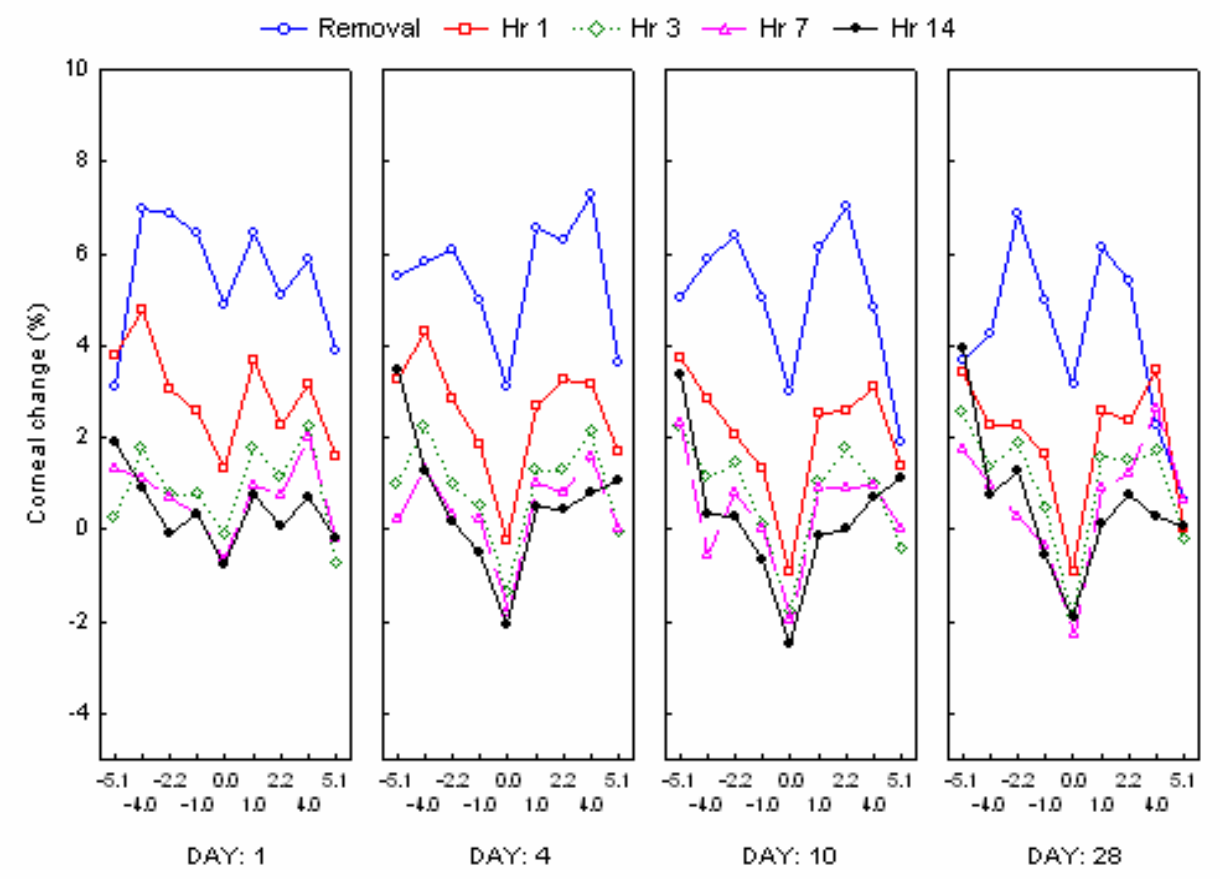

Figure 5-2 Mean central and mid-peripheral corneal swelling and deswelling following the first night of CRT™ lens wear. (Vertical bars denote 0.95 confidence intervals).

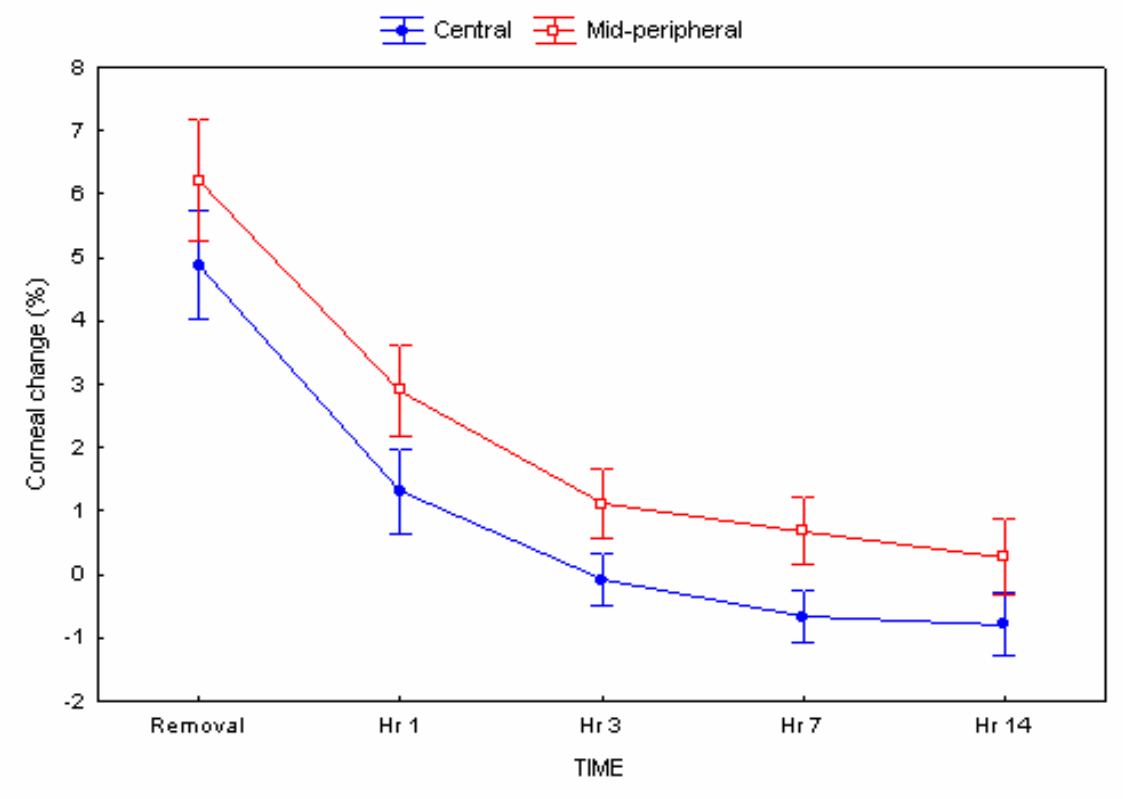

Figure 5.3 illustrates the change in epithelial thickness from lens removal to the end of the day, measured on the 4 study days over 4 weeks. The central epithelium thinned by -7.3 ± 3.2% immediately following lens removal on Day 1, compared to the mid-peripheral epithelium which thickened by 13.0 ± 1.7% (both $p<0.001$ compared to baseline). The pattern of epithelial thickness change was consistent for the remaining study days, however the extent of central epithelial thinning increased ($p<0.05$ for Days 4, 10 and 28 compared to Day 1). The extent of mid-peripheral thickening decreased after Day 4. Maximum epithelial

thinning after lens removal (-13.5 ± 2.0%) occurred on Day 4, progressing to -15.0 ± 2.7% thinning by hour 14. The absence of recovery to baseline was evident on all 4 measurement days. The values for epithelial thickness change (mean % ± SD) throughout the study are displayed in Appendix E.

Figure 5-3 Epithelial changes during 4 weeks of CRT™ lens wear measured over 4 study days. Data points for hours 3 and 7 have been omitted for clarity.

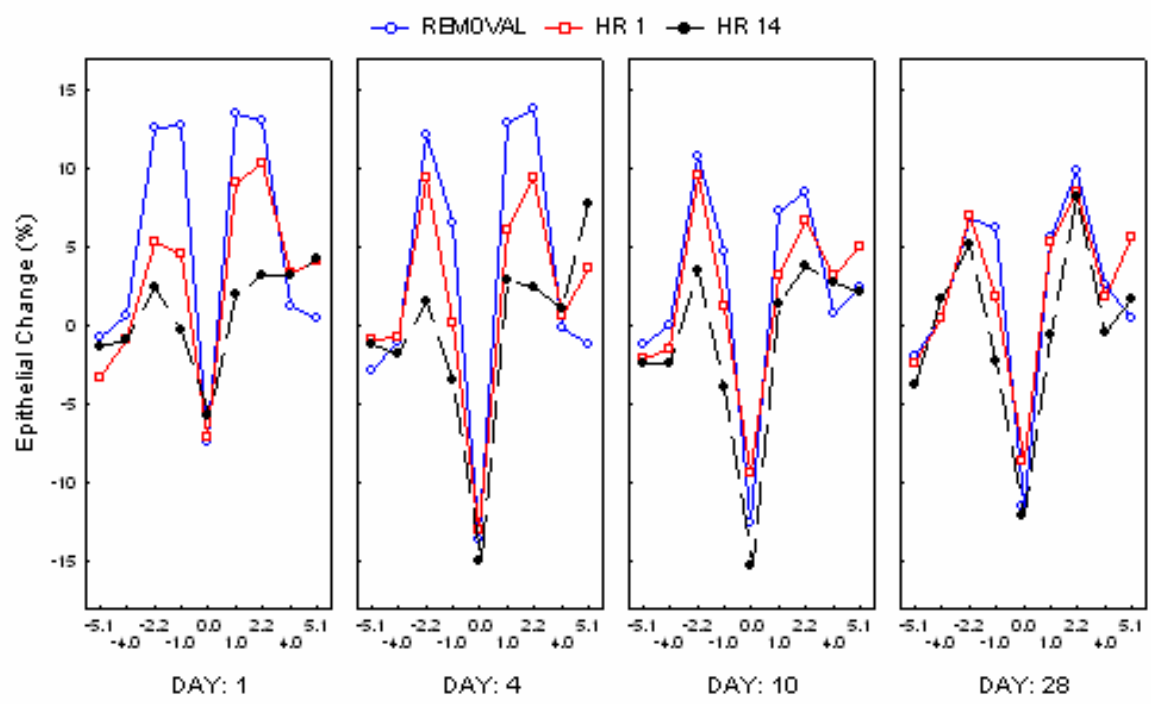

Following 72 hours without lens wear after Day 28 (Figure 5.4), the cornea had recovered to baseline, with 99.7% recovery at the centre ($p>0.05$) and 98.5% recovery mid-peripherally ($p<0.05$). Epithelial thickness did not fully recover to original values (Figure 5.5). The

centre was still approximately -3.8% thinner and the mid-periphery remained 3.5% thicker than baseline (both $p<0.05$ compared to baseline).

Figure 5-4 Corneal thickness at baseline and after 72 hours of non-lens wear.

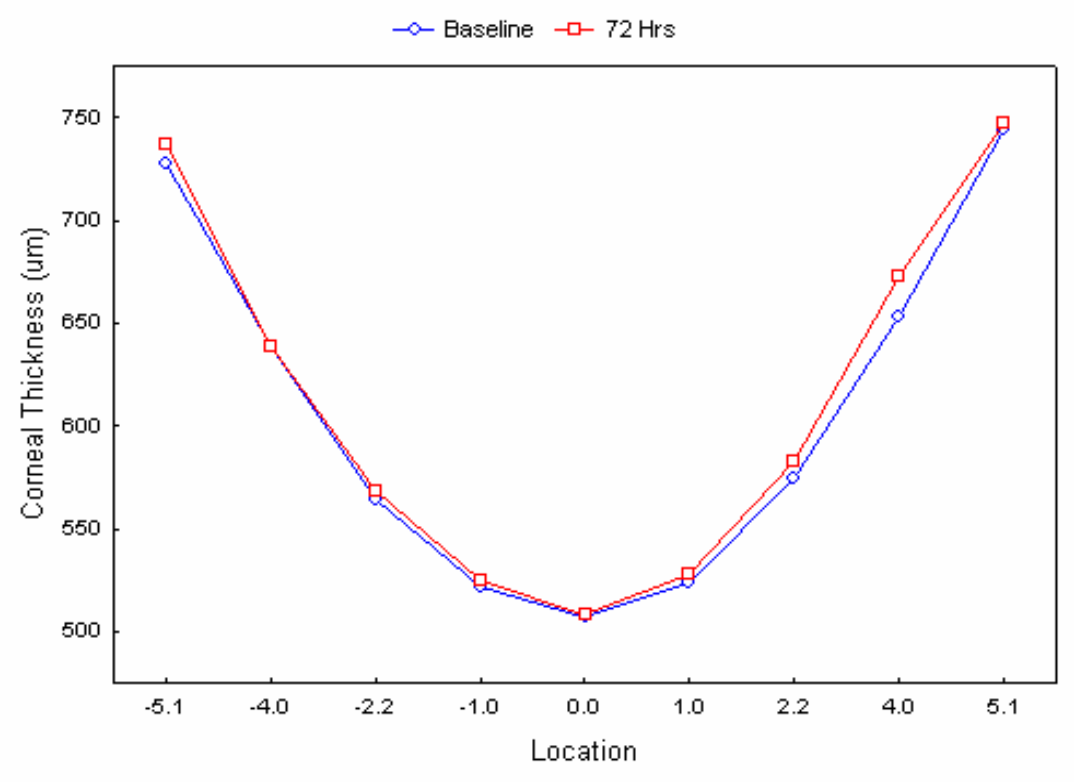

Figure 5-5 Epithelial thickness at baseline and after 72 hours of non-lens wear.

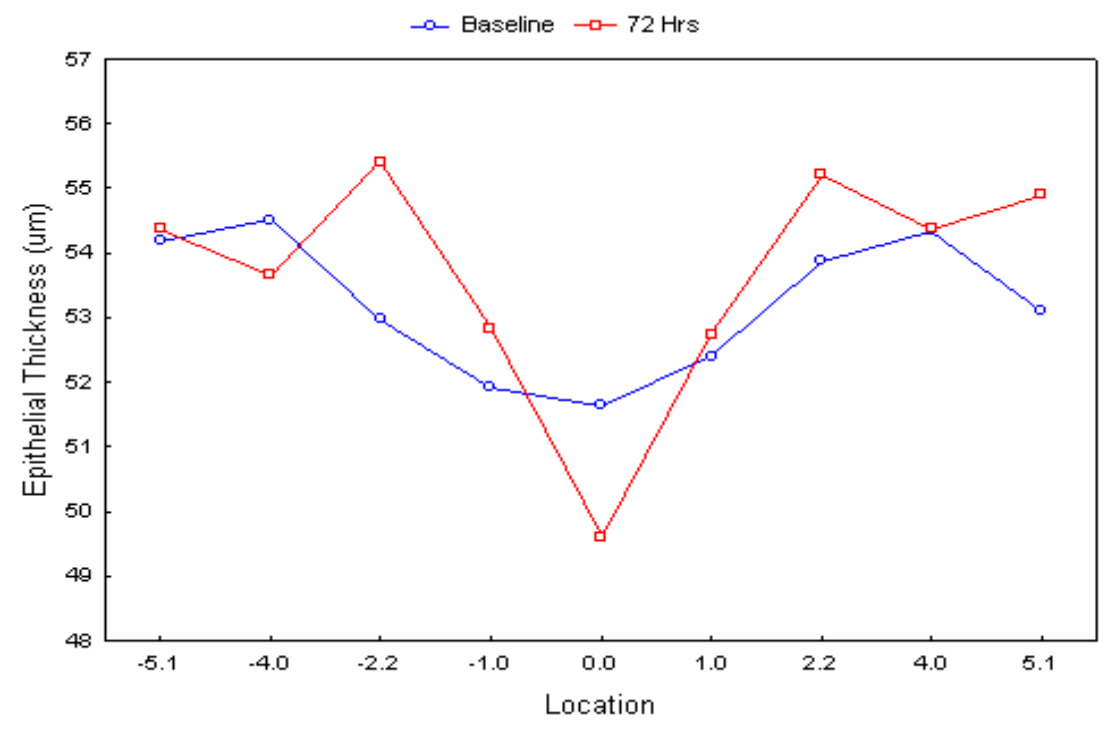

5.1.5 Discussion

In this study, there were significant amounts of corneal swelling and epithelial thickness changes following overnight CRT™ lens wear. The meridional corneal swelling pattern showing greater mid-peripheral over central swelling immediately following lens removal was similar to that reported by Wang et al. (Wang et al. 2003c) The swelling patterns induced by CRT™ lenses in these studies are different to that induced by conventional rigid designs (Fonn et al. 1984; Wang et al. 2003a) and soft lenses, (Fonn et al. 1999; Holden et al. 1985a; Wang et al. 2003a) in which the reverse is true, where swelling is greater centrally than peripherally. The aetiology of the swelling differences between the central and mid-

peripheral cornea may be influenced by the central mechanical pressure induced by the CRT™ lenses.

The degree of central corneal swelling reported in this study differs from the results of Alharbi and Swarbrick (Alharbi and Swarbrick 2003), who showed no central stromal thickness changes. It has been estimated that to prevent lens induced corneal swelling following overnight lens wear the oxygen transmissibility of a contact lens needs to be at least 87 x 10^{-9} (cm x ml O_2) / (sec x ml x mmHg) (Holden and Mertz 1984). In this study the central Dk/t was 67 x 10^{-9} (cm x ml O_2) / (sec x ml x mmHg) which explains the 4.9% central and 6.2% mid-peripheral corneal swelling compared to the 2-5% typically seen centrally following overnight eye closure without lens wear. (Cox et al. 1990; du Toit et al. 2003; Fonn and Bruce 2005; Graham et al. 2001; Harper et al. 1996; Kiely et al. 1982; La Hood et al. 1988; Mertz 1980; Sakamoto et al. 1991)

Three hours after lens removal, full return to baseline central corneal thickness occurred. The speed at which the cornea deswelled strengthens the notion of measuring thickness as soon as possible following lens removal after eye opening, which was the procedure in this study. The central cornea continued to deswell beyond baseline ('overshoot') towards the end of the day as shown in Figure 5.1. 'Overshoot' and has been reported after contact lens wear previously. (du Toit et al. 2003; O'Neal and Polse 1985; Odenthal et al. 1999)

Following the first night of CRT™ lens wear, central epithelial thinning and mid-peripheral epithelial thickening was observed immediately after lens removal. The central epithelium,

which had thinned by -7.3% showed very little recovery after 14 hours yet most of the mid-peripheral thickening decreased with time. The epithelial thickness changes followed a consistent pattern for the duration of the study, although there was greater central thinning and less mid-peripheral thickening from Day 4 onwards. We found approximately -12% thinning after 1 month but this is substantially less than the -30% reported by others. (Alharbi and Swarbrick 2003; Soni et al. 2003) Possible explanations for these differences include lens design variations and the difference in technique of epithelial measurement. We used Paragon CRT^{TM} lenses and OCT for corneal and epithelial measurements. The Alharbi (Alharbi and Swarbrick 2003) and Soni (Soni et al. 2003) studies used lenses from two other manufacturers (BE and Contex designs respectively) and the use of optical pachymetry and confocal microscopy respectively to measure epithelial thickness.

Central corneal swelling decreased from 4.9% after the first night of CRT^{TM} lens wear to 3% on subsequent study days. This indicated a possible adaptation effect. New contact lens wearers have shown to possess a higher initial swelling response than adapted lens wearers, (Armitage and Schoessler 1988; Cox et al. 1990; Ichikawa et al. 1989) hence the greater central corneal swelling seen on Day 1. Adaptation to contact lens wear is thought to down-regulate the overnight corneal swelling response. (Alharbi et al. 2005; Ichikawa et al. 1989; Mertz 1980)

Reversibility has been touted as an advantage of corneal refractive therapy. Although the duration of this study was relatively short (28 days), Figures 5.4 and 5.5 are good examples of how the cornea was able to recover from four weeks of overnight CRT^{TM} lens wear. Barr

et al. (Barr et al. 2004) followed the recovery of refractive error over 72 hours, after 9 months of CRT™ lens wear, and also found the cornea to return rapidly to baseline. Soni et al. (Soni et al. 2004) measured corneal recovery after CRT™ lens wear for 1 month. Central corneal thickness was thinner at the end of the month, but following one day of no lens wear, fully recovered.

In summary, overnight CRT™ lens wear induced corneal and epithelial thickness changes. As mentioned in Chapter 2, the central epithelial thinning was likely due to the compression induced by the eyelid onto the relatively flat fitting CRT™ lenses. The mid-peripheral thickening may be due to the negative pressure of the tear film induced by localized lens clearance, with re-distribution of the epithelial tissue and fluid being partly responsible for the thickness changes. Central corneal swelling recovered rapidly following lens removal and it appeared that there was adaptation to overnight lens wear.

5.2 Overnight myopic CRT™ lens wear over a one year period

5.2.1 Abstract

Purpose: To measure and monitor corneal and epithelial thickness changes following CRT™ lens wear for myopia, over a one year period.

Methods: This study was a continuation of the 4 week study discussed in the last chapter, with fourteen subjects volunteering to continue lens wear after the 4 week initial study, for up to 12 months. Following the 3 day non-lens wear period at the end of the last study, daily wear of the same CRT™ lenses was resumed. A single visit was arranged after 10am, when OCT measurements of corneal thickness were obtained at the same 9 locations across the horizontal meridian. The measurements were taken at 3, 6, 9 and 12 months. The three month measurement included the 4 weeks from the previous study.

Results: Eight participants completed the study. At 1 month, CCT was significantly thinner than baseline ($p<0.05$). From the 1st to the 12th month measurement, mean central corneal thickness (CCT) did not change significantly ($p>0.05$). Central epithelial thickness (CET) after 1 month of lens wear was -5.7 ± 7.0% thinner than baseline ($p<0.05$). Mid-peripheral epithelial thickening at 1 month was 4.0 ± 3.2% ($p<0.05$ compared to baseline). Maximum thinning of CET occurred at 9 months (-16.5 ± 8.8%, $p<0.05$ compared to baseline).

Conclusion: Extended wear of CRT™ lenses for myopia produces corneal and epithelial thickness changes, which seem to maintain over many months. Following the initial month of lens wear, the cornea and epithelium do not change significantly in thickness.

5.2.2 Introduction

To date, the majority of orthokeratology studies have reported corneal and/or refractive changes over short periods of time. Some studies report single night lens wear, (Ladage et al. 2004; Sridharan and Swarbrick 2003; Wang et al. 2003c) while others report lens wear over many weeks and months. (Alharbi and Swarbrick 2003; Choo et al. 2004b; Matsubara et al. 2004; Rah et al. 2002b; Soni et al. 2003; Swarbrick et al. 1998; Tahhan et al. 2003) It is important to monitor corneal changes due to CRT^{TM} lens wear over a longer period of time, not only to assess when the optimal refractive effect occurs, but also to monitor any adverse reactions long-term lens wear may cause.

A recent study by Soni and Nguyen (Soni and Nguyen 2006) evaluated the safety and effectiveness of OK lens wear for a period of 12 months, using refractive error, unaided VA and slit-lamp biomicroscopy findings. The study did not report any measure of corneal thickness. The Boston XO material (Dk = 100) was used in three different lens designs (DreamLens, BE Retainer and Contex OK), however since previous studies had found these lenses to be clinically equivalent, (Soni et al. 2004; Tahhan et al. 2003) the data from all three lens designs were pooled in this study. At the 1 month measurement, haloes were found to be a common symptom following lens wear, while at 12 months, ~80% of the subjects were asymptomatic.

Of increasing concern, has been the topic of epithelial proliferation, or the lack thereof, in orthokeratology lens wear. The pressures of lens wear on the corneal surface are thought to

reduce the normal turnover rate of the epithelium, (Ladage et al. 2003b; Ladage et al. 2003c; Ladage et al. 2002a; Ladage et al. 2003d; Ren et al. 1999a; Shin et al. 2005) which in turn increases the adherence and presence of bacteria such as Pseudomonas aeruginosa (PA), due to the more 'stagnant' ocular surface (Cavanagh et al. 2002; Fleiszig et al. 1992; Imayasu et al. 1994; Ladage et al. 2001b; Ladage et al. 2004; Ren et al. 1999b; Ren et al. 2002; Ren et al. 1997). The pseudomonas organisms potentially cause severe infection (keratitis), which can lead to scarring and extreme loss of vision (Asbell 2004; Lang and Rah 2004).

At present, there have been no published studies that have monitored corneal and epithelial thickness throughout 12 months of CRT^{TM} lens wear for myopia. This study used OCT to measure corneal and epithelial thickness at regular intervals in a one year period of lens wear. Of particular interest was when or if central epithelial thinning would stabilize and whether there would be an adaptation effect to the lenses.

5.2.3 Study procedure

Subjects

This study was a continuation of the 4 week study discussed in Chapter 5.1. From the original 23 participants, 14 volunteered to continue with CRT^{TM} therapy for myopia (mean age 28.0 ± 9.2 years, range 19 to 51 years) and were enrolled into the one year study.

The study visit consisted of a single appointment, scheduled after 10am to discount any residual oedema present as a result of sleep. The primary interest in this study was the

monitoring of long-term effects caused by CRT™ lenses, and therefore did not want the presence of overnight oedema influencing the results of corneal morphology. The study visits were scheduled for 3, 6, 9 and 12 months, with the 3 month visit including the 4 weeks from the original study.

Instrumentation and Lenses

Subjects were asked to continue lens wear in the same regime as the previous study, after the 72 hour no lens wear period ended. Subjects removed the lenses in their home and OCT measurements were obtained at the CCLR. The same nine measurements of corneal thickness were taken across the horizontal meridian, as in the original study. Corneal and epithelial changes were expressed in real thickness values and as a percentage change from baseline levels (as in Chapter 5.1).

5.2.4 Results

Eight participants completed the 12 month study. The remainder were not available for follow-up visits due to relocation away from the area. Baseline myopia for this cohort was –2.57 ± 1.23DS. At one month, myopia had decreased to -0.27 ± 0.47DS, and was not different after twelve months of lens wear (-0.29 ± 0.56DS, $p<0.05$).

Baseline (BSLN) central corneal thickness (CCT) for the 8 subjects who completed the study was 511.2 ± 18.9μm and baseline central epithelial thickness (CET) was 51.5 ± 1.4μm. Figure 5.6 shows topographical corneal thickness during the year of CRT™ lens wear, with

Figure 5.7 showing the percentage change in corneal thickness throughout the year. Figure 5.8 highlights the changes in CCT throughout the year.

Figure 5-6 Topographical corneal thickness at baseline, and at 1, 3, 6, 9 and 12 months of CRT™ lens wear.

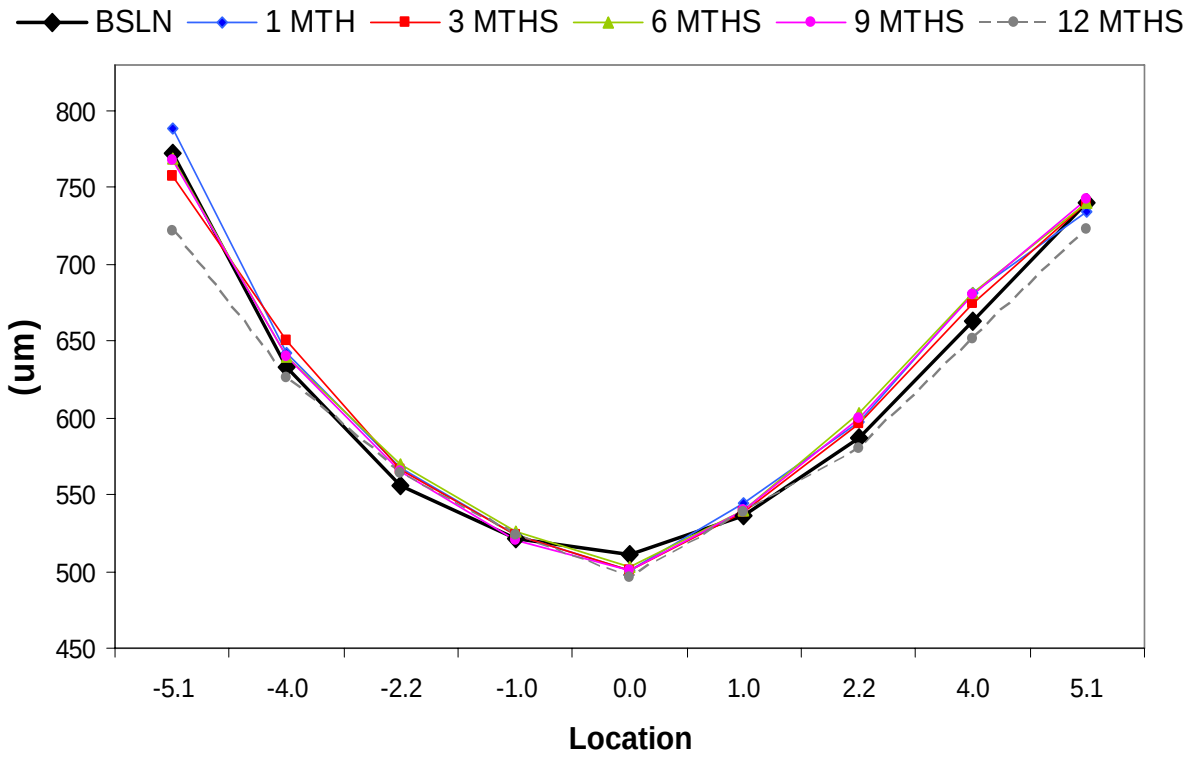

Figure 5-7 Percentage change in topographical corneal thickness from baseline, at 1, 3, 6, 9 and 12 months of CRT™ lens wear.

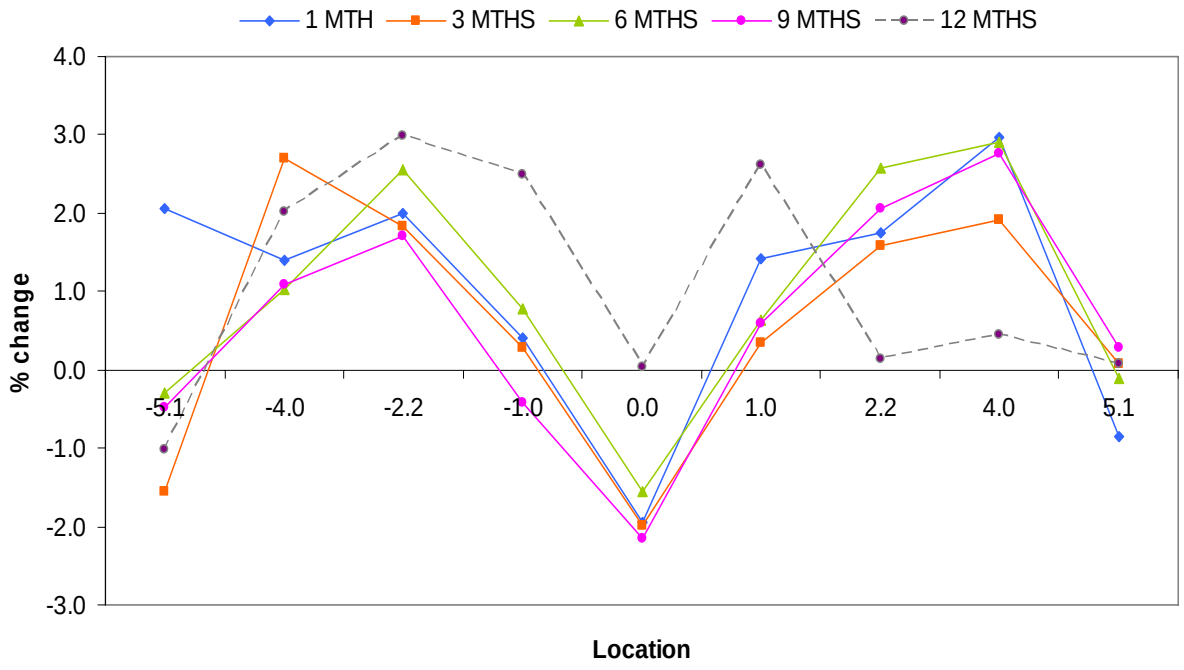

Compared to baseline, topographical corneal thickness maintained a steady pattern from the first up to the twelve month (Figure 5.6). The mid-peripheral cornea (as an average of positions T1, T2, N1 and N2) showed an increase in thickness at one month of 1.4 ± 1.5% ($p<0.05$ compared to baseline), and showed thinning at twelve months of -1.8 ± 4.1% ($p>0.05$ compared to one month). The '12 month' line in Figure 5.7 represented only three subject's data (the remainder being lost to technical difficulties), and therefore deviated from the general pattern. Topographical corneal thickness change (mean % ± SD) throughout the 12 months is displayed in Appendix F.

At 1 month, CCT was significantly thinner than baseline by -10.1 ± 8.6µm (-2.0 ± 1.7%, $p<0.05$). Up to 12 months, mean CCT did not change significantly from the one month measurement (-3.6 ± 5.0%, $p>0.05$). The greater increase in central corneal thinning at 12 months was not different statistically from the CCT measured at 9 months ($p>0.05$).

Figure 5-8 Central corneal thickness throughout 12 months of CRT™ lens wear.

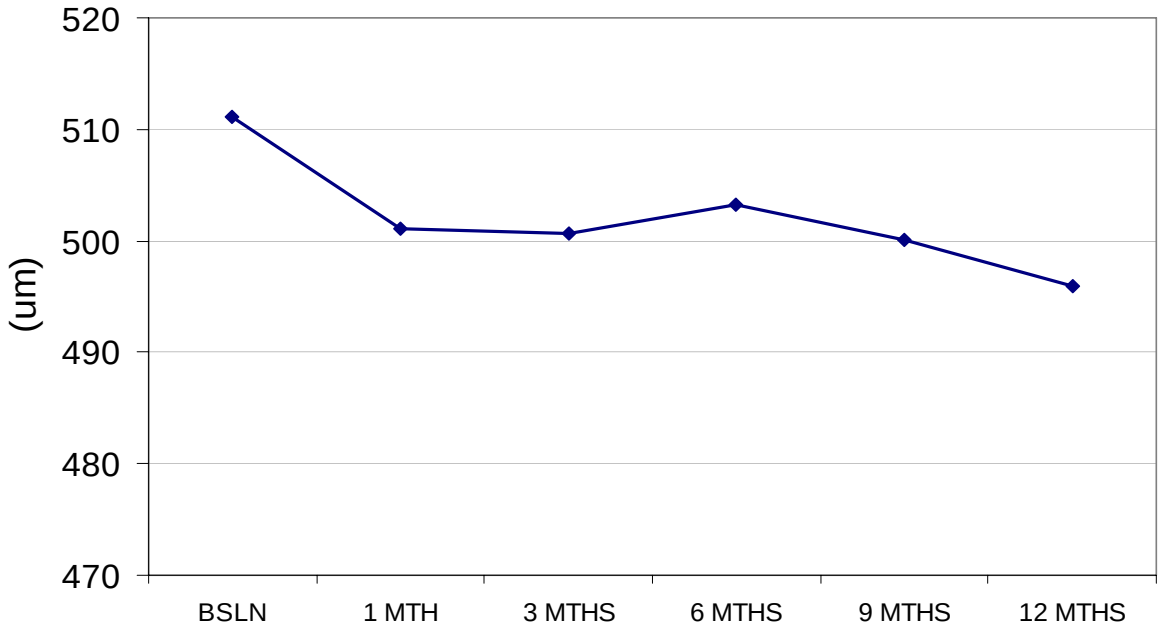

Figure 5.9 shows topographical epithelial thickness over the 12 month period and Figure 5.10 displays the percentage changes (values are displayed in Appendix G). Figure 5.11 shows the CCT changes throughout the year of CRT™ lens wear. Compared to baseline, CET after 1 month of lens wear was -5.7 ± 7.0% thinner (-3.0 ± 3.6µm, $p<0.05$). Mid-peripheral epithelial thickening at 1 month was 4.0 ± 3.2% ($p<0.05$ compared to baseline). Maximum

thinning of CET occurred at 9 months, at -16.5 ± 8.8% (-8.5 ± 4.5µm, $p<0.05$ compared to baseline). In comparison to baseline, at twelve months the central epithelium was -15.7 ± 4.6% thinner (-8.1 ± 2.5µm, $p<0.05$) and the mid-periphery was 1.3 ± 3.5% thicker ($p>0.05$).

Figure 5-9 Topographical epithelial thickness throughout 12 months of CRT™ lens wear.

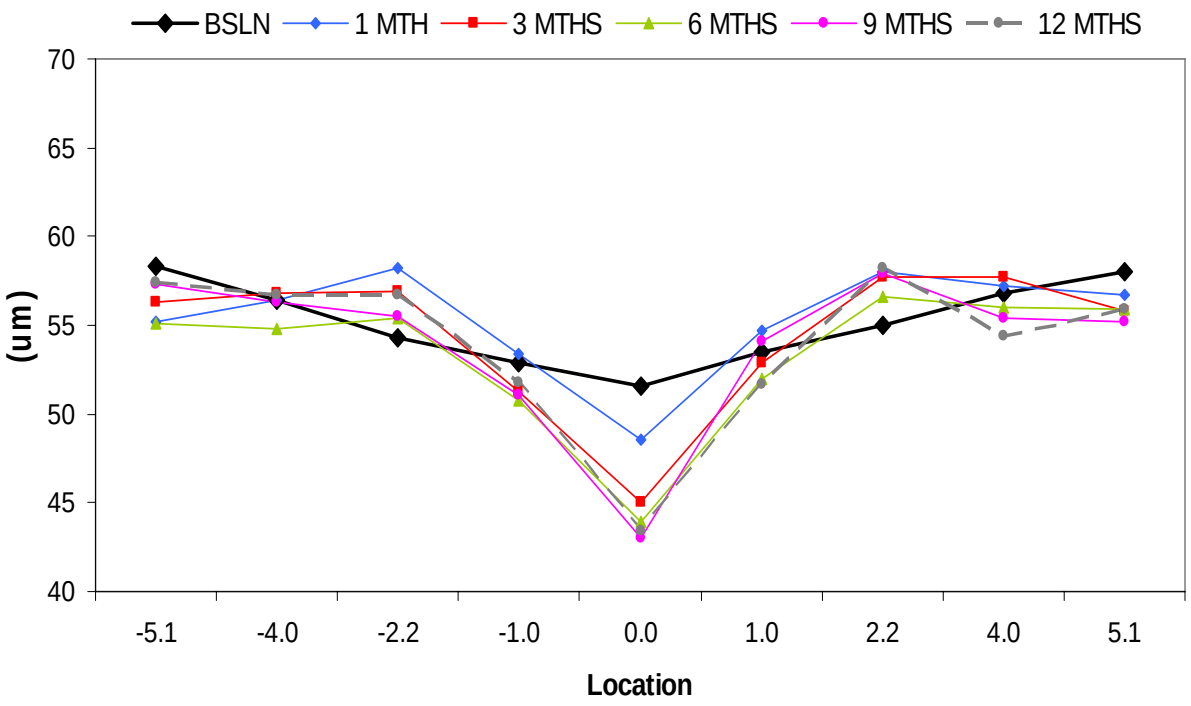

Figure 5-10 Percentage changes in topographical epithelial thickness throughout 12 months of CRT™ lens wear.

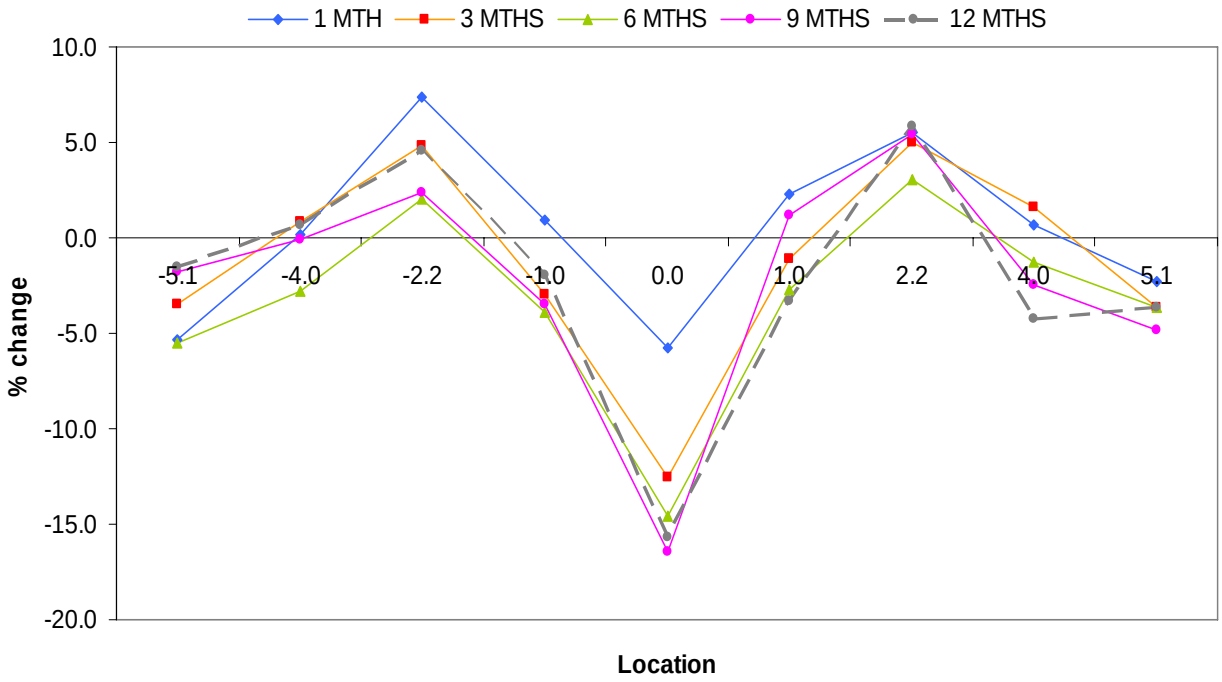

Figure 5-11 Central epithelial thickness following CRT™ lens wear over a 12 month period.

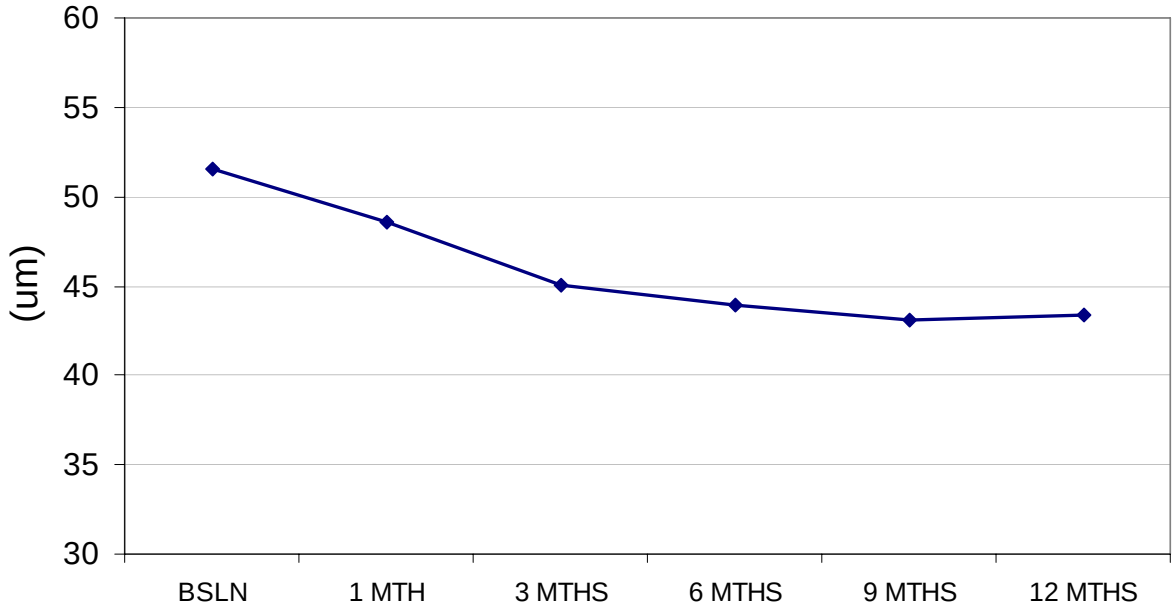

5.2.5 Discussion

This study monitored the changes in corneal and epithelial thickness throughout a year of CRT™ lens wear for myopia. The study was a continuation of the experiment described in Chapter 5.1.

Since there are no published studies reporting on corneal and/or epithelial thickness changes following myopic CRT™ lens wear for as long as a year, it is not possible to directly compare the results found in this present study. Alharbi et al. (Alharbi and Swarbrick 2003) monitored CRT™ changes over 3 months, measuring corneal and epithelial thickness using

optical pachymetry. This group found the central cornea to thin and stabilize by the 10th day of the study, with no significant changes occurring after this time. At 3 months, central corneal thinning had reached -19μm and was accounted entirely to the epithelium. Mid-peripheral corneal thickening had also stabilized by day 10, and measured ~11μm at 3 months, which was accounted entirely to the stroma.

A study by Soni et al. (Soni et al. 2003) also followed subjects for 3 months, wearing Contex OK lenses, and using confocal microscopy for the measurement of the cornea and epithelium. After 3 months of overnight lens wear, the central cornea showed a thinning of 24.3μm (4.2%), most of this change being located in the epithelial layer. By 3 months, the epithelium had thinned by 32% on lens removal and was maintained throughout the day. Nichols et al. (Nichols et al. 2000) measured corneal thickness using the Orbscan topographer, in ten subjects wearing Contex OK lenses over a period of 2 months. The authors reported a significant decrease in CCT of -12μm by the end of the study period, but did not find any mid-peripheral corneal thickness changes. Epithelial thickness changes were not investigated.

After the first month of lens wear, the cornea and epithelium did not change significantly in thickness. The thickness changes caused by CRT™ lens wear were maintained for the long-term and did not return to baseline levels after lens removal each day. The study in Chapter 5.1 showed that the longer the lenses were worn, the more the daily effect was maintained. However, in hindsight, a measurement obtained following a period of no lens wear after the

12 month study (of 3-5 days), may have been useful to assess how rapidly the cornea and epithelium recover following long-term CRT™ lens wear.

In summary, long-term CRT™ lens wear for myopia reduction produces corneal and epithelial thickness changes, which seem to maintain over many months. It would be necessary to continue to monitor these subjects, longer than the first year of lens wear, to assess the changes to the cornea after extended CRT™ lens wear.

5.3 Single night myopic CRT™ comparing different lens transmissibility

5.3.1 Abstract

Purpose: To assess the corneal swelling response to two CRT™ lenses for myopia, with different oxygen transmissibility (Dk/t), worn for 1 night. Change in thickness of the total cornea, stroma and epithelium was measured across the horizontal meridian using optical coherence tomography (OCT).

Methods: In this double-masked, randomized contralateral eye study, twenty subjects wore a CRT™ design lens in each eye, manufactured from Menicon Z™ (MenZ, Dk/t=91) and Equalens II™ (EqII, Dk/t=47) materials. Baseline corneal thickness was measured centrally and at four points either side of the centre using OCT, the night prior to sleeping at the CCLR. The next morning, lenses were removed and thickness measurements were immediately taken, and then repeated 1, 3, 6 and 12 hours later.

Results: On lens removal, the MenZ eye had central and paracentral corneal swelling (mean ± SD) of 4.1 ± 2.0% and 5.6 ± 2.4%, while the EqII eye had 5.8 ± 2.6% and 7.0 ± 2.6%. These values were significantly different from baseline (ReANOVA; $p<0.001$) and were different between lens materials ($p<0.001$). The central epithelium thinned by -10.0 ± 4.5% in the MenZ eye and by -10.2 ± 8.5% in the EqII eye, with the mid-peripheral epithelium thickening by 13.4 ± 7.9% in the MenZ eye and 18.3 ± 9.8% in the EqII eye (all changes different from baseline $p<0.001$). These epithelial values were not statistically different between materials ($p>0.05$). Stromal swelling values on lens removal were 5.7 ± 2.2%

centrally and 5.5 ± 3.0% mid-peripherally (MenZ) and 7.7 ± 3.1% centrally and 6.6 ± 2.9% mid-peripherally (EqII) (all $p<0.001$ from baseline). Central stromal swelling was different between eyes at lens removal ($p<0.001$). Stromal thickness in both eyes returned to baseline values within 3 hours.

Conclusion: The higher Dk/t MenZ material caused significantly less overnight corneal and stromal swelling than the EqII material, which reinforces the need to prescribe lenses with high Dk/t for overnight wear. Neither central epithelial thinning nor mid-peripheral thickening was significantly affected by Dk/t.

5.3.2 Introduction

CRT™ lenses are currently approved for overnight wear, being typically worn during the night and removed every morning. Individuals may wear the lenses in this modality for many years. Overnight wear of lenses clearly places an extra physiological burden upon the cornea, which makes oxygen transmissibility all the more critical to minimise corneal swelling. The degree to which oxygen may pass through a contact lens is governed by it's oxygen transmissibility (Dk/t units x 10^{-9} (cm x ml O_2)(sec x ml x mmHg) (Harvitt and Bonanno 1999)). One method of assessing the effect of oxygen transmissibility of a contact lens is measuring the amount of corneal swelling that occurs following overnight lens wear, in addition to the normal physiological oedema that results from eye closure following sleep. The latter is classically accepted as ~4%. (Holden and Mertz 1984; Mertz 1980) However, more recent data has suggested that this value is closer to 3%. (Bruce and Brennan 1993; du Toit et al. 2003; Fonn and Bruce 2005; Graham et al. 2001; Moezzi et al. 2004)

The CRT™ lenses used in this project had a central Dk/t of only 67, falling below the guidelines suggested for providing oedema-free overnight wear. Previous studies investigating the clinical performance of the Paragon CRT™ design have reported that the central cornea swells by ~5% upon eye-opening, (Wang et al. 2003c) supporting the notion that they provide insufficient oxygen to the cornea to produce no additional overnight corneal swelling. To-date, few studies have been reported that investigate the impact of increased oxygen transmissibility on corneal swelling during overnight orthokeratology lens wear. (Lum and Swarbrick 2006; Swarbrick et al. 2005; Swarbrick 2006)

The purpose of this study was to measure corneal, stromal and epithelial thickness changes after a single night of CRT™ lens wear for the treatment of myopia. Two different lenses were used, consisting of the same design but manufactured from two different materials, one with a higher Dk/t than the other. Optical coherence tomography (OCT) was used to measure the corneal thickness changes, as described in previous chapters.

5.3.3 Study procedure

Subjects

Twenty subjects were enrolled (13 females and 7 males; mean age 24.2 ± 3.6 years; ranging from 19 to 35 years). Non-lens wearers and soft lens wearers were recruited but current RGP lens wearers were excluded. Each subject presented without history of ocular disease or surgery. Refractive error of participants was restricted to a spherical range of -1.00 to -6.00, with no more than -1.75D cylinder. Mean baseline corneal parameters for the cohort are displayed in Table 5.3.

Table 5-3 Baseline corneal parameters for the study cohort.

Baseline Corneal Parameters (Mean ± SD)		
	Menicon Z	**Equalens II**
Refractive error – sphere (D)	-2.85 ± 1.55	-2.80 ± 1.51
Refractive error – cylinder (D)	-0.49 ± 0.44	-0.41 ± 0.35
Keratometry – flat K (D)	43.3 ± 1.24	43.4 ± 1.37
Keratometry – cyl (D)	-0.62 ± 0.44	-0.62 ± 0.42
Central corneal thickness (μm)	512 ± 17.5	510 ± 18.7
Central epithelial thickness (μm)	54.0 ± 2.1	53.7 ± 2.9

Instrumentation and Lenses

OCT was used to measure corneal thickness across the horizontal meridian at nine points, with the aid of an external fixation device, similar to the procedure described in Chapter 5.1. Each cross-sectional scan of the cornea was kept at 1.13mm in length.

Each eye of all subjects was fitted with a CRT™ lens of the Paragon design (Paragon Vision Sciences, Mesa, AZ) and randomly chosen to wear either a lens manufactured from the Equalens II™ (Bausch & Lomb, Rochester, NY) or the Menicon Z™ (Menicon, Nagoya, Japan) material. The Equalens II (EqII) lens material (fluorosilicone acrylate) had a Dk of 85 x 10^{-11} and the Menicon Z (MenZ) lens material (fluorosiloxanylstyrene) had a Dk of 165 x 10^{-11}. Both lenses had a centre thickness of 0.18mm. The lenses were fit using software provided by the manufacturer and assessed on eye for appropriate apical touch (4mm), mid-

peripheral clearance, adequate edge lift and proper centration. The lens parameters are listed in Table 5.4.

Table 5-4 CRT^{TM} lens parameters for the two study lenses.

	Menicon Z	**Equalens II**
BOZR (±SD mm)	8.48 ± 0.47	8.48 ± 0.46
Return Zone Depth (±SD μm)	525 ± 0.19	525 ± 0.18
Landing Zone Angle (±SD deg)	33 ± 1.08	33.1 ± 1.12
Total Diameter (mm)	10.5	10.5
Centre thickness (mm)	0.18	0.18
Power (D)	+0.50	+0.50
Dk/t (x 10^{-9} units)	**91**	**47**

In the evening prior to sleeping at the CCLR, baseline measurements for corneal thickness were obtained. The CRT^{TM} lenses were inserted and the participants slept at 10pm, to be woken at 7am the next morning. On waking, the subjects were asked to keep their eyes closed until the lenses were removed one at a time at the OCT instrument and corneal measurements taken. These were repeated 1, 3, 6 and 12 hours after lens removal.

Raw data files captured by the OCT were processed in the same manner as described previously (Chapter 3). Corneal and epithelial thickness changes were expressed as a percentage change, compared to baseline levels, as in Chapter 5.1. Repeated measures

analysis of variance (Re-ANOVA), Tukey HSD post-hoc testing and paired t-tests were used to analyse the changes in thickness from baseline levels over the study period.

5.3.4 Results

All 20 subjects completed the study. After initial lens removal, myopia was reduced by 0.69 ± 1.04DS and 0.69 ± 1.15DS in the MenZ and EqII eyes respectively ($p<0.05$ from baseline). There was no difference between eyes ($p>0.05$) and refractive error had not returned to baseline after 12 hours ($p<0.05$).

At lens removal, the central and mid-peripheral corneal swelling of the MenZ lens wearing eye was 4.1 ± 2.0% and 5.6 ± 2.4% (mean ± SD) respectively, (ReANOVA; both $p<0.001$ from baseline). Corneal swelling in response to the EqII lens was 5.8 ± 2.6% and 7.0 ± 2.6% respectively (both $p<0.001$ from baseline) (Figure 5.12). Mid-peripheral values were the average of two nasal and two temporal points closest to the centre]. These values were different between lens materials ($p<0.01$). Corneal swelling of both eyes had returned to baseline levels within 3 hours of lens removal ($p>0.05$). Values of corneal thickness change (mean % ± SD) in both eyes are displayed in Appendix H.

Figure 5-12 Change in total corneal thickness after CRT™ lens wear using two different lens materials.

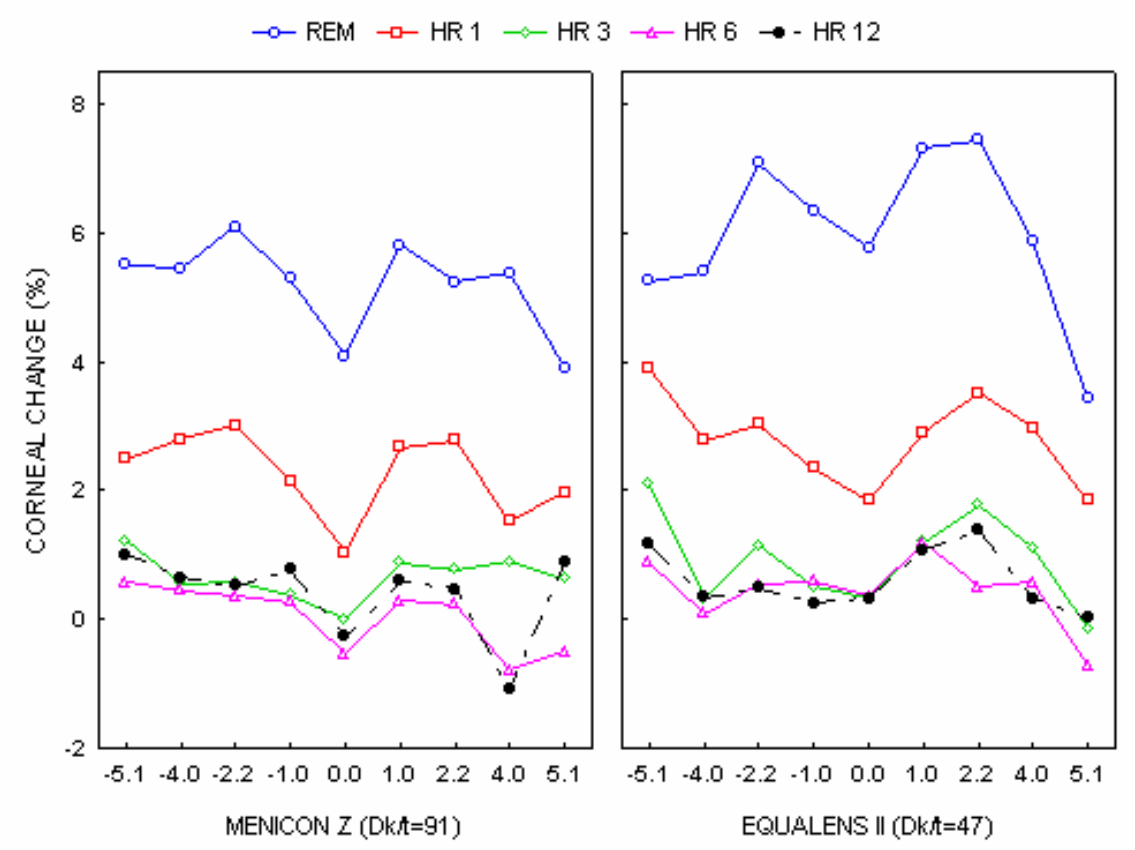

Stromal swelling in the MenZ wearing eye was 5.7 ± 2.2% centrally and 5.5 ± 3.0% mid-peripherally, while in the EqII wearing eye the stroma swelled by 7.7 ± 3.1% centrally and 6.6 ± 2.9% mid-peripherally after lens removal (all $p<0.001$) (Figure 5.13). In comparing both eyes, the central stromal swelling caused by the EqII lens was significantly greater than that caused by the MenZ lens ($p<0.001$). Stromal swelling of both eyes had returned to baseline levels within 3 hours following lens removal ($p>0.05$). Stromal thickness change (mean % ± SD) for both eyes is listed in Appendix I.

Figure 5-13 Stromal swelling and recovery following CRT™ lens wear using two different lens materials.

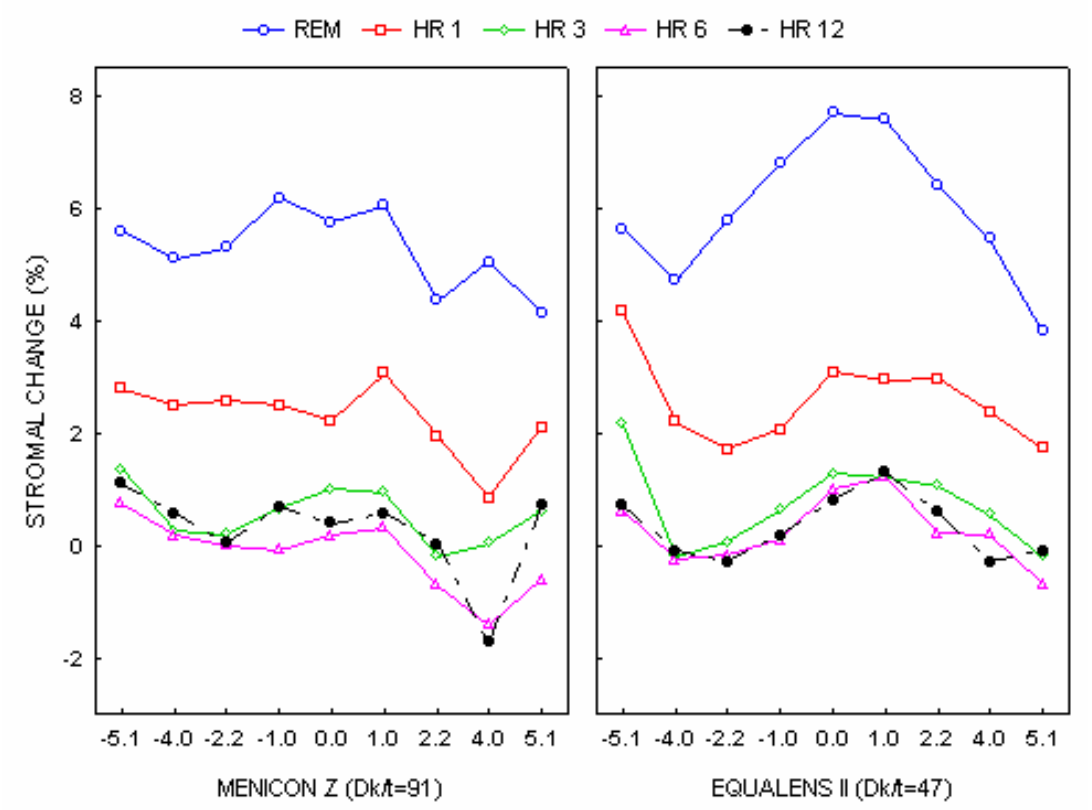

On lens removal, the central epithelium had thinned by -10.0 ± 4.5% in the MenZ wearing eye and similarly by -10.2 ± 8.5% in the EqII wearing eye (both $p<0.001$, compared to baseline) (Figure 5.14). There was no difference in the epithelial thinning measured between eyes ($p>0.05$). The epithelial mid-periphery thickened by 13.4 ± 7.9% in the MenZ wearing eye and 18.3 ± 9.8% in the EqII wearing eye (both $p<0.001$ from baseline). This epithelial thickening when compared between eyes, was statistically insignificant ($p>0.05$). After 12

hours, the central epithelium had not completely returned to baseline levels, being still -5.7 ± 6.5% thinner in the MenZ eye ($p<0.05$) and -3.3 ± 9.2% thinner in the EqII eye ($p>0.05$). The paracentral epithelium in the MenZ eye had recovered to baseline levels after 12 hours (3.2 ± 6.7%, $p>0.05$), but in the EqII eye, it remained significantly thicker than baseline (4.4 ± 6.1%, $p<0.05$). Changes in epithelial thickness (mean % ± SD) in both eyes are displayed in Appendix J.

Figure 5-14 Change in epithelial thickness following CRT™ lens wear using two different lens materials.

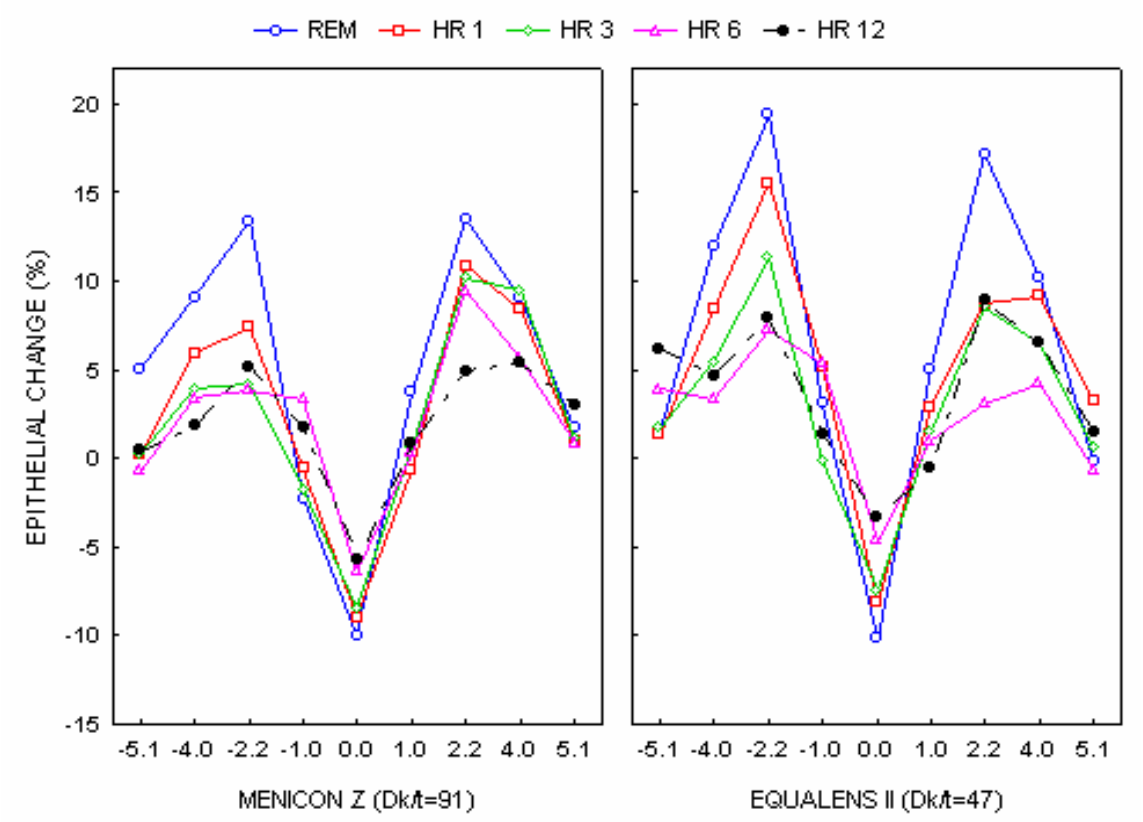

5.3.5 Discussion

This single night study compared two identically designed CRT^{TM} lenses for the reduction of myopia, manufactured from two lens materials of differing oxygen transmissibility (Dk/t).

The work of Holden and Mertz (Holden and Mertz 1984; Mertz 1980) and Harvitt and Bonanno (Harvitt and Bonanno 1999) suggested that a minimum oxygen transmissibility of 87 and 125 respectively, is necessary to prevent overnight hypoxia and subsequent corneal swelling. The degree of stromal and total corneal swelling measured in this study showed that both lenses caused greater swelling than that reported overnight (2-5%) without lens wear. (Bruce and Brennan 1993; du Toit et al. 2003; Graham et al. 2001; Moezzi et al. 2004) These results show that oxygen transmissibility has a significant effect on corneal swelling after overnight wear of contact lenses.

The amount of stromal swelling seen on lens removal was significantly different between the two lenses (5.7% versus 7.7%) with the Menicon Z (Dk/t = 91) lens causing less swelling than the Equalens II lens (Dk/t = 47) (Figure 4.13). The latest suggested value for the critical Dk/t for no additional oedema over that seen on eye-opening without lens wear value is 125. (Fonn and Bruce 2005; Fonn et al. 2005; Harvitt and Bonanno 1999) In this study, the lens with the higher Dk/t (91) still fell below the criterion recommended, which would suggest that some degree of corneal swelling would be expected, which was the case in this study. On eye-opening, the range of stromal swelling seen with the Menicon Z lens was 0 to 9.3%, as compared with 2.5 to 14.7% for the EqualensII lens-wearing eyes.

The change in central epithelial thickness did not differ between lenses, with each producing ~10% epithelial thinning after lens removal. This amount of central epithelial thinning was slightly higher than that reported in Chapter 5.1. However, other investigators, albeit having used different lenses and instrumentation, (Alharbi and Swarbrick 2003; Choo et al. 2004b; Soni et al. 2003) have found as much as -33% (Alharbi and Swarbrick 2003) central epithelial thinning. Many lenses currently available are manufactured from the Boston XO material (Bausch & Lomb, NY) with a Dk of 100 (e.g. Contex OK, DreamLens, BE Retainer) and thus a Dk/t of approximately 67. Tahhan et al. (Tahhan et al. 2003) and Soni et al. (Soni and Nguyen 2006) have compared these different lens designs and found little difference in the effectiveness of the procedure for myopic correction. Identical lens designs are not expected to lead to differences in refractive effects.

Mid-peripheral epithelial changes were greater from EqII lens wear (18%) than from MenZ lens wear (13%), although this difference did not reach statistical significance. Some investigators have found epithelial thickness to increase as a result of epithelial oedema (in ex vitro studies), (Lowther and Hill 1973, 1974; Uniacke et al. 1971) but the majority of in-vivo studies have shown that the epithelium does not thicken in response to hypoxia. (O'Leary et al. 1981; Wang et al. 2002a; Wilson and Fatt 1980)

A major concern of lower Dk/t lens wear in the overnight modality is that of infection and corneal ulceration. Previous studies have found correlations between low oxygen transmission and increased bacterial (pseudomonas) binding to the epithelium. (Fleiszig et al.

1992; Imayasu et al. 1994; Ladage et al. 2004; Ren et al. 2002; Ren et al. 1997) Although rigid gas permeable (RGP) lens materials have shown to lead to less bacterial adherence to human corneal epithelial cells than silicone hydrogel lens materials, (Ren et al. 2002) this difference was associated with increased tear exchange characteristic of RGP lenses. Since overnight lens wear does not allow adequate tear exchange, and therefore flushing of metabolic debris, the advantage of RGP lens use in the overnight modality may be minimized. (Sakamoto and Sugimoto 2004)

Recovery of the total cornea and stroma occurred within three hours following lens removal, which has been reported in previous studies. (Wang et al. 2003c) Data from this study showed that epithelial recovery was more gradual and incomplete, which was in agreement to that reported in other studies. (Barr et al. 2004; Nichols et al. 2000; Soni et al. 2003)

In conclusion, this study showed effects of CRT^{TM} lens wear on corneal and epithelial thickness after a single night of wear, comparing two different Dk lens materials. There were differences in central stromal swelling between the two lenses but no differences in central epithelial thinning. The results of this study reinforce the need to prescribe lenses with higher oxygen transmissibility if they are to be worn overnight. Epithelial change after CRT^{TM} was not as affected by the Dk of the lens material as stromal change.

Chapter 6

Corneal, Stromal and Epithelial thickness changes following Corneal Refractive Therapy for the treatment of Hyperopia

6.1 Abstract

Purpose: To investigate thickness changes of the cornea, epithelium and stroma across the horizontal corneal meridian following a single night of CRT™ rigid contact lens wear for hyperopia.

Methods: Twenty subjects wore a CRTH™ contact lens on one eye for a single night. The untreated eye served as a control. The lenses are designed to temporarily reduce hyperopia through corneal steepening. Corneal and epithelial thickness was measured at nine points across the horizontal meridian using optical coherence tomography (OCT). Readings were obtained the evening prior to sleep (baseline), immediately following lens removal on eye opening the next morning and at 1, 3, 6 and 12 hours later. An additional measurement was taken 28 hours later to observe recovery.

Results: All values were compared to baseline. At lens removal, the treated eye showed central and mid-peripheral corneal swelling (mean ± SD) of 8.8 ± 2.2% and 8.1 ± 2.5% respectively (both $p<0.001$), with central and mid-peripheral epithelial thickening of 21.5 ± 8.6% and 18.1 ± 6.0% respectively, ($p<0.001$). The central stroma swelled 7.3 ± 2.6% with the mid-peripheral stroma swelling by 7.0 ± 3.0% (both $p<0.001$). In the control eye, central

corneal swelling was 3.1 ± 1.6% and central epithelial thickness increased by 7.1 ± 6.0% (both $p<0.05$). The stroma in the control eye swelled by 2.7 ± 1.7% centrally ($p<0.001$). Stromal swelling of both eyes had returned to baseline levels within 3 hours ($p>0.05$).

Conclusion: CRTH^{TM} lenses for hyperopic correction as worn overnight caused a greater increase in the central stroma and epithelium than the mid-peripheral area. A reduced response was seen in the control eye. Both eyes recovered rapidly from the thickness changes induced.

6.2 Introduction

The studies discussed in Chapter 5 related to orthokeratology for myopia reduction, but Corneal Refractive Therapy (CRT^{TM}) lenses can also be modified to reduce hyperopia, designed and fitted in the 'opposite' manner to allow the cornea to steepen centrally. There are many published studies discussing myopic CRT^{TM} (Alharbi and Swarbrick 2003; Dave and Ruston 1998; Mountford 1997a; Nichols et al. 2000; Rah et al. 2002b; Soni et al. 2003; Sridharan and Swarbrick 2003; Swarbrick et al. 1998; Wang et al. 2003c) but until very recently (Lu et al. 2006b), there have been no reports on hyperopic CRT^{TM} treatment (in humans).

Swarbrick et al. (Swarbrick et al. 2004) recently used steeply fitted rigid lenses with apical clearance to induce corneal steepening and hence a myopic shift. In the study, two sets of Conoid lenses (PMMA and Boston XO) were worn in the open eye for four hours, inducing corneal oedema of 8.2% and 0.4% in the PMMA and Boston XO eyes respectively (measuring corneal thickness with ultrasonic pachymetry). Both lenses steepened the cornea, albeit more mid-peripherally than centrally, but the resultant decrease in hyperopia was slight (0.32D) and failed to reach statistical significance. The study however, did not report any epithelial changes.

One study reporting on hyperopic CRT^{TM} is that by Choo and colleagues, (Choo et al. 2004b) who examined histological changes in the cat epithelium. Light microscopy images (where epithelial thickness was calculated using image measurement software), showed thickening

of the central epithelium with a subsequent thinning of the mid-peripheral epithelium, opposite to the changes seen following myopic CRT™. In the five cats used in the study, the central epithelium had on average thickened by 146% (54um) after wearing the lenses continuously for two weeks. The report displayed images that indicated a large degree of central stromal thickening after 14 days of CRTH™ lens wear.

Recently, Lu et al. (Lu et al. 2006b) measured in vivo corneal and epithelial changes in human subjects, and found the pattern of central and mid-peripheral thickness change to be opposite for CRTH™ compared to CRT™ treatment. After 60 minutes of closed-eye hyperopic correction, the central cornea swelled by ~3% and the mid-periphery thinned by ~1.7%. Epithelial thickness changes were ~1.7% for both the central and mid-peripheral regions.

The purpose of this current study was to measure thickness changes of the cornea, stroma and epithelium following a single night's wear of CRTH™ lenses for hyperopia reduction. OCT was used to measure these thickness changes across the horizontal meridian.

6.3 Study procedure

Twenty healthy subjects were enrolled (15 females and 5 males; mean age 20.1 ± 7.5 years; ranging from 22 to 48 years). There were no restrictions on the type of refractive error to be enrolled, but emmetropic or hyperopic participants were preferred. Low myopes (<1.50DS) were permitted into the study, only with the understanding that they may become more short-

sighted (for which spectacles were available for temporary use until the cornea recovered). Spherical error was limited to +3.00D, with no more than -1.50D cylinder. Table 6.1 summarizes the baseline corneal parameters of the cohort. Current RGP lens wearers were excluded and soft lens wearers had to discontinue lens wear two weeks prior to the start of the study.

Table 6-1 Summary of corneal parameters prior to study commencement.

Baseline Corneal Parameters (Mean ± SD)		
	Experimental eye	Control eye
Refractive error – sphere (D)	-1.86 ± 2.64	-1.99 ± 2.62
Refractive error – cylinder (D)	-0.56 ± 0.42	-0.58 ± 0.43
Keratometry – flat K (D)	43.14 ± 1.78	43.02 ± 1.70
Keratometry – cyl (D)	-0.71 ± 0.42	-0.79 ± 0.39
Central corneal thickness (μm)	508.8 ± 27.0	508.6 ± 27.1
Central stromal thickness (μm)	456.3 ± 26.0	456.6 ± 26.7
Central epithelial thickness (μm)	52.5 ± 2.6	52.0 ± 2.8

CRTH^{TM} lenses (Paragon Vision Sciences, Meza, AZ) have a reverse geometry design and are manufactured from fluorosilicone acrylate, with oxygen permeability (Dk) of 100 and transmissibility (Dk/t) of 67. The lenses were fitted using software provided by the manufacturer, utilizing the flat keratometry, vertexed sphere and over-refraction values to compute the resultant BOZR, RZD and LZA. The BOZR was then steepened by subtracting

0.7mm from the flat keratometry reading and adding 175μm to the RZD. The lenses selected by the program were assessed on eye using slit-lamp biomicroscopy, to ensure that there was appropriate apical clearance (up to 4mm wide), mid-peripheral touch, adequate edge lift and proper centration. The lens parameters are listed in Table 6.2. For each subject, the eye to wear the CRTH^{TM} lens was assigned at random. The other eye did not wear a lens to act as a control.

Table 6-2 CRTH^{TM} lens parameters.

CRTH^{TM} Lens Parameters	
Total Diameter (mm)	10.5
BOZR (mm)	7.19 ± 0.32
BOZD (mm)	2.5 – 3.5
Power (D)	-0.50
Centre Thickness (mm)	0.17
Dk / t (x 10^{-9} units)	67
Return Zone Depth (μm)	656 ± 38.0
Landing Zone Angle (deg)	34.0 ± 1.0

In the evening prior to sleeping in the lenses, baseline corneal thickness was measured with OCT. Both eyes were measured, at nine locations along the horizontal corneal meridian. The CRTH^{TM} lenses were inserted into one eye and the fit was assessed for adequate movement, centration and fluorescein pattern prior to sleep. Participants slept at the CCLR, retiring at 10pm and waking at 7am the next morning. On waking, the subjects kept their

eyes closed until lenses were removed for corneal measurements. The measurements were repeated 1, 3, 6 and 12 hours after lens removal. An additional set of readings were obtained the next day (28 hours after initial lens removal) to monitor recovery. Previous OK studies have shown that the cornea demonstrates no residual swelling three hours after lens removal, hence the recovery measurement was taken after 10am the next day. (Wang et al. 2003c)

6.4 Results

All twenty subjects completed the study. All values were compared to baseline, unless otherwise stated. Refractive data from this study, reported in detail by Sorbara et al. (Sorbara et al. 2004; Sorbara et al. 2005b), showed a myopic shift (or decrease in hyperopia) of 1.03 ± 0.89DS, with a range of 0.00 to 2.25DS. The correction had regressed by 48% by the 12th hour, and at the recovery measurement 28 hours later, refractive error had still not recovered to baseline, and was 0.19DS myopic (representing 98% recovery).

Figure 6.1 shows the changes in corneal thickness in both the experimental and control eyes following a single night of CRTH^{TM} lens wear. Corneal swelling (mean ± SD) in the experimental eye was greatest immediately on lens removal, measuring 8.8 ± 2.2% centrally and 8.1 ± 2.5% mid-peripherally ($p<0.001$). Mid-peripheral values are represented by the mean of two points either side of the centre (four points in total). At lens removal the control eye swelled by 3.1 ± 1.6% centrally and 2.6 ± 1.3% mid-peripherally, (both $p<0.05$). The difference in central corneal swelling at lens removal between eyes was statistically significant ($p<0.001$). Both eyes demonstrated rapid corneal deswelling and had recovered to

baseline levels within three hours ($p>0.05$). Values for corneal thickness change (mean % ± SD) are displayed in Appendix K.

Figure 6-1 Corneal thickness changes across the horizontal meridian following a single night of CRTH™ lens wear for hyperopia. The experimental eye is shown on the left and the control eye (no lens worn) shown on the right.

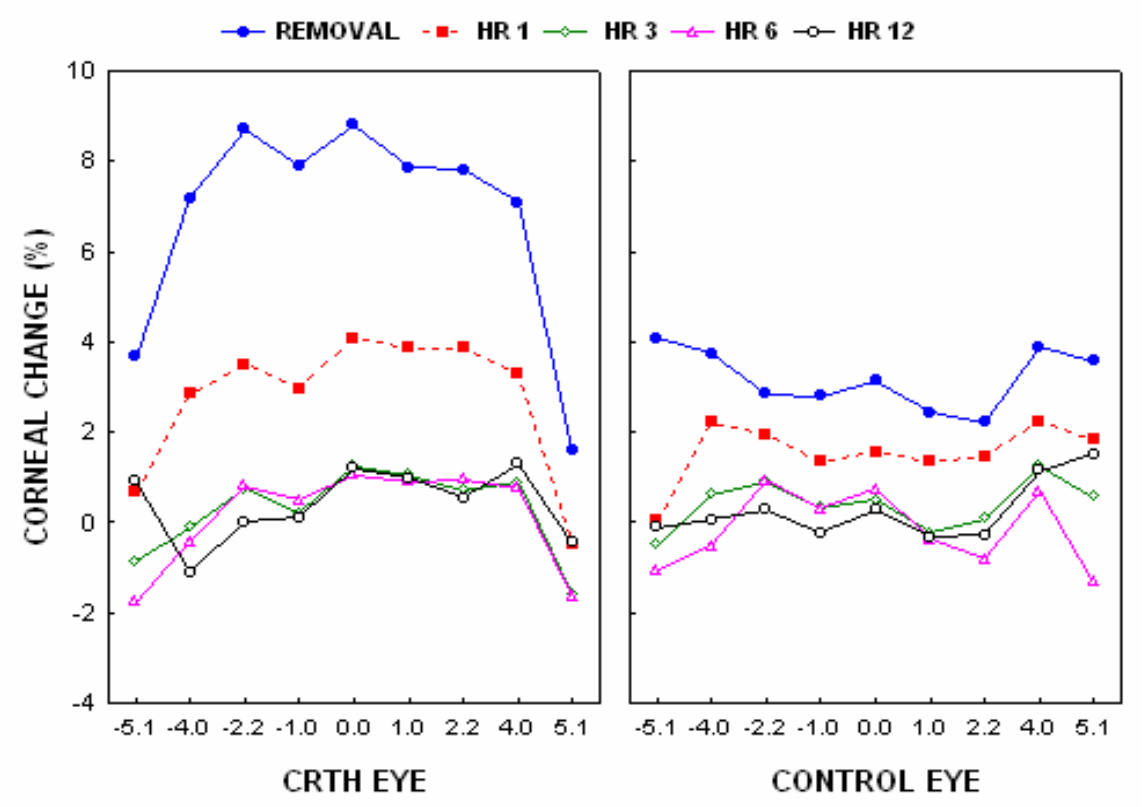

Changes to stromal thickness in both eyes are shown in Figure 6.2. Stromal swelling (mean ± SD) in the CRTH™ eye was greatest immediately on lens removal, measuring 7.3 ± 2.6% centrally and 7.0 ± 3.0% mid-peripherally (both $p<0.001$). Also at lens removal, the control eye swelled by 2.7 ± 1.7% centrally and 2.1 ± 1.4% mid-peripherally (both $p<0.001$).

Central stromal swelling in the control eyes ranged from 0 to 5.7%. The between-eye difference in stromal swelling on lens removal, centrally and mid-peripherally was significant ($p<0.001$). Stromal swelling in the experimental eye rapidly deswelled to baseline levels by hour 3 ($p>0.05$). Stromal thickness change (mean % ± SD) for both eyes is displayed in Appendix L.

Figure 6-2 Stromal thickness changes throughout the day, following a single night of CRTH^{TM} lens wear for hyperopia, comparing the experimental and control eyes.

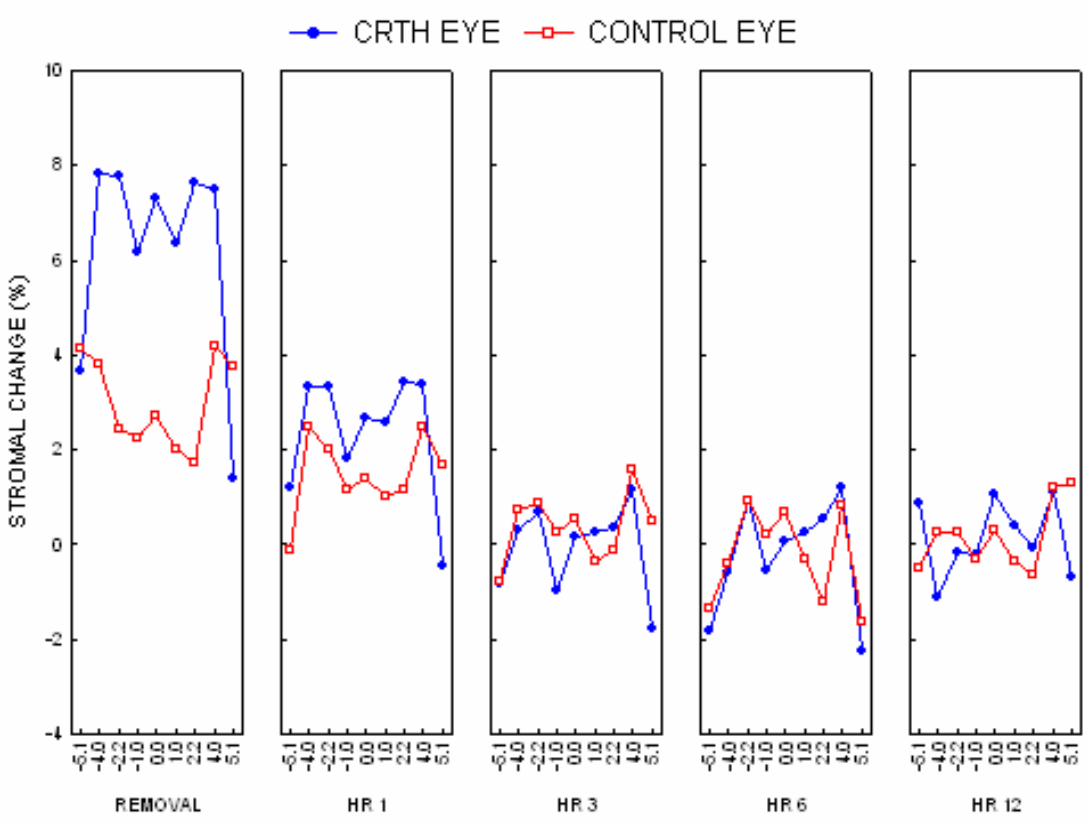

Figure 6.3 shows the changes in epithelial thickness in both the experimental and control eyes following a single night of CRTH^{TM} lens wear. At lens removal, the epithelium (mean ± SD) of the lens wearing eye had thickened by 21.5 ± 8.6% centrally and 18.1 ± 6.0% mid-peripherally (both $p<0.001$). At the same time in the control eye the epithelium thickened by 7.1 ± 6.0% centrally, and 7.0 ± 5.1% mid-peripherally (both $p<0.05$). These changes were significantly different, comparing eyes ($p<0.001$). The epithelium recovered gradually throughout the day, the centre remaining insignificantly thicker by 2.6 ± 5.6% at hour 12 ($p>0.05$). Changes in epithelial thickness (mean % ± SD) for both eyes are listed in Appendix M.

Figure 6-3 Epithelial thickness changes across the horizontal corneal meridian following a single night of CRTH^{TM} lens wear for hyperopia.

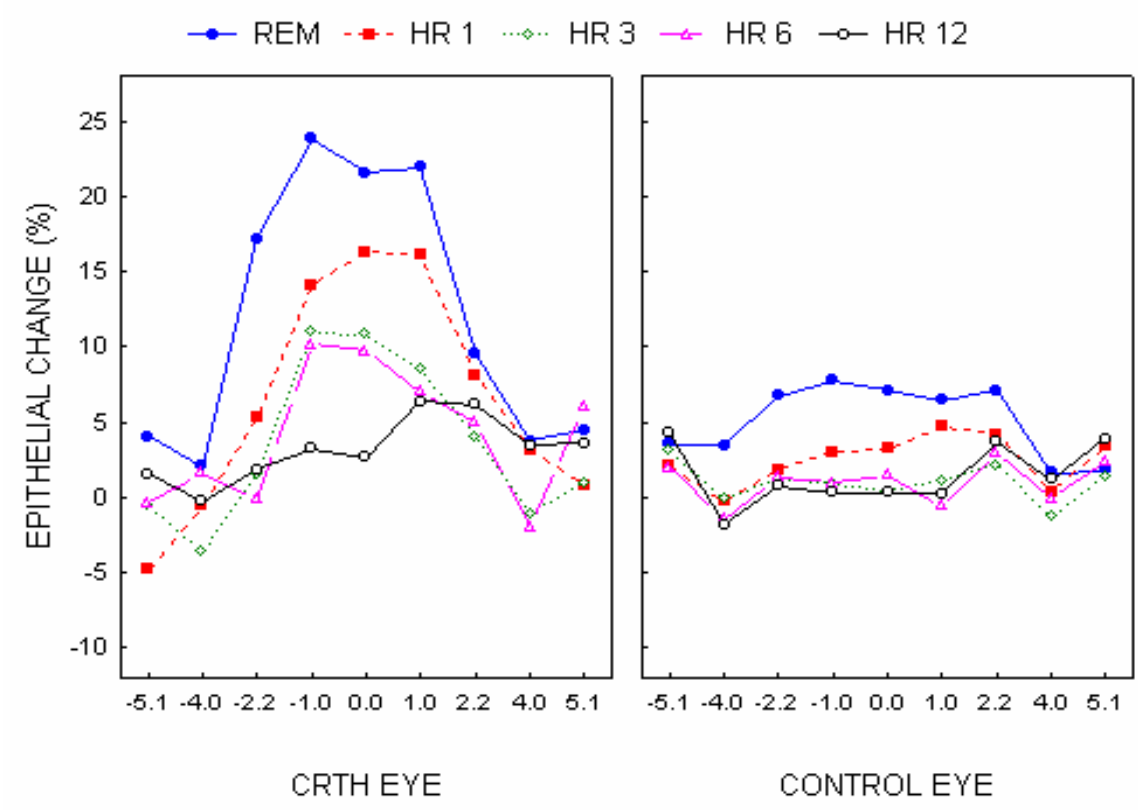

Following 28 hours without lens wear, stromal thickness in the CRTH^{TM} eye had recovered by 99% in the centre and 98.9% mid-peripherally (Figure 6.4, $p>0.05$). Epithelial thickness in the CRTH^{TM} eye recovered by 98.5% in the centre and 97.2% mid-peripherally (Figure 6.5, $p>0.05$).

Figure 6-4 Recovery of stromal thickness after 28 hours of no lens wear, comparing experimental and control eyes.

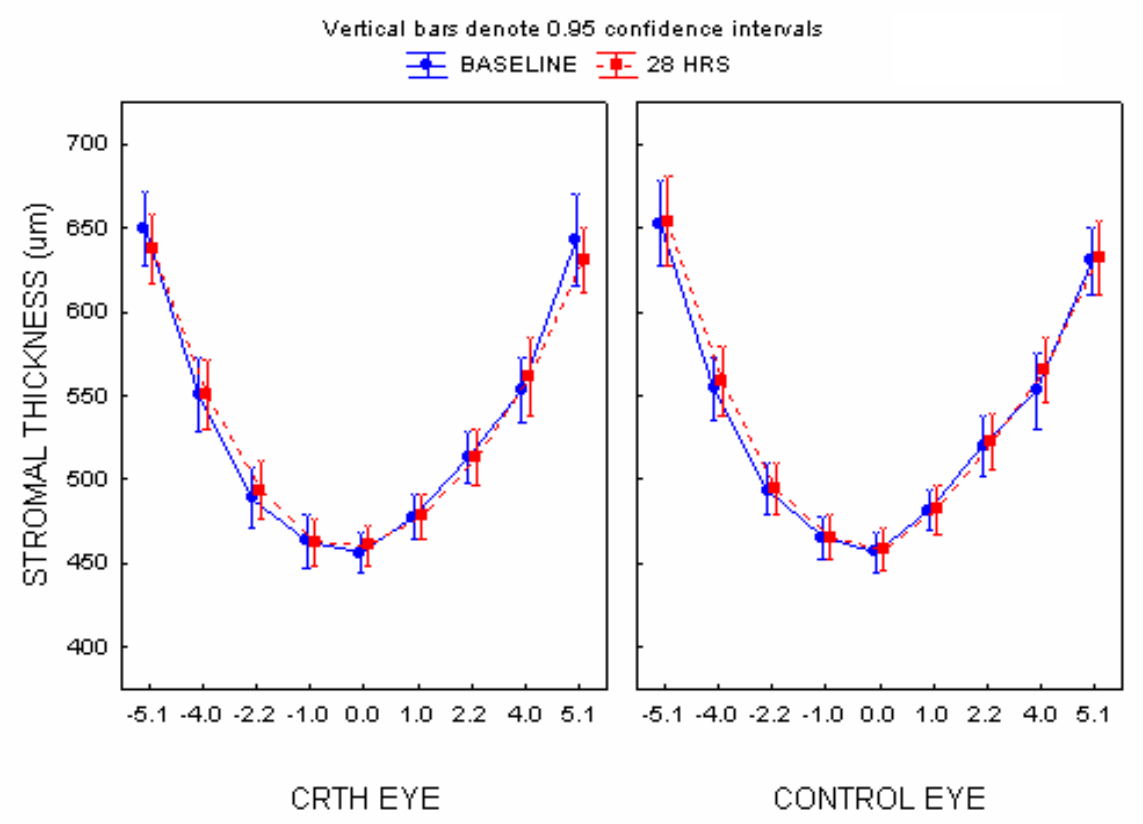

Figure 6-5 Recovery of epithelial thickness in the experimental eye after 28 hours of no lens wear.

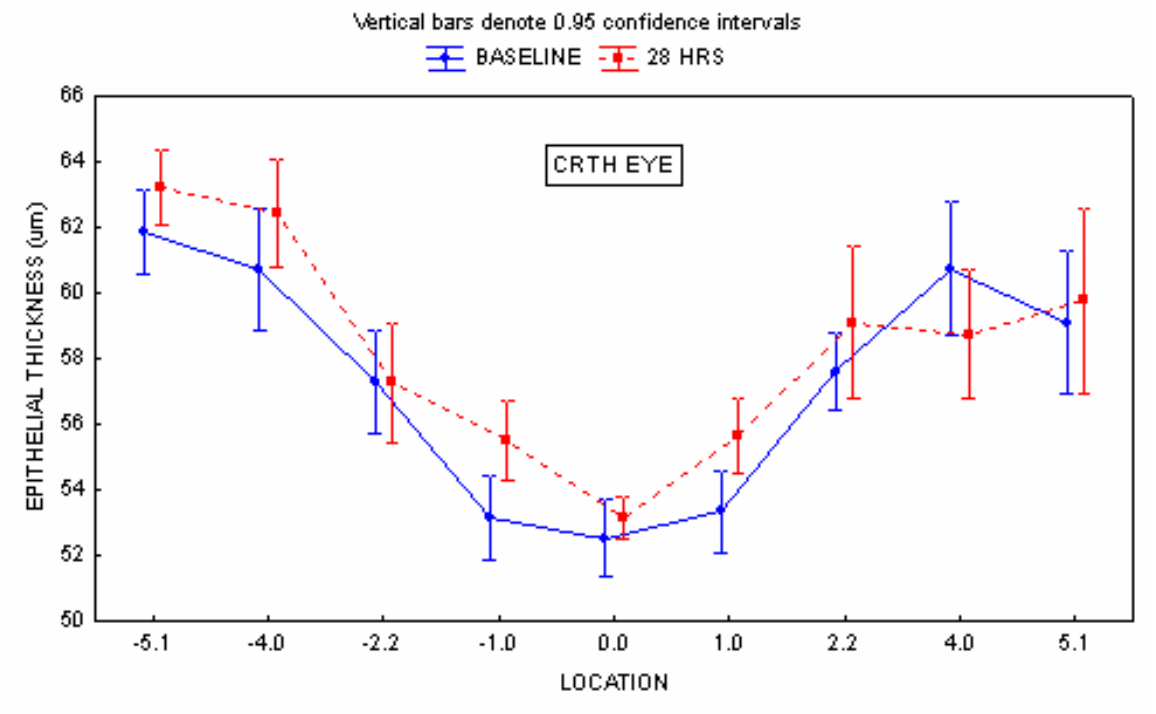

6.5 Discussion

This study showed a significant increase in stromal swelling and epithelial thickening following a single night of CRTH^{TM} lens wear. The degree of stromal swelling can be accounted for by the Dk/t of the lens material used (67), which was lower than the Holden and Mertz criterion of 87. (Holden and Mertz 1984) The central corneal swelling results found in this study were understandably greater than those found by Lu et al. (Lu et al. 2006b) (who used the same design of lenses and also obtained corneal and epithelial

thickness measurements using OCT), as in the present study the lenses were worn overnight, compared to only 60 minutes in the Lu study.

The study by Swarbrick et al. (Swarbrick et al. 2004) used apical clearance lenses made by Conoid, while those used in the present study were specifically designed for hyperopic orthokeratology by Paragon Vision Sciences. The corneal measurements were also obtained using different instruments (OCT versus ultrasonic pachymetry). The amount of central corneal swelling seen in both studies was similar (~8%), despite one lens having a Dk/t of 67 and the other a Dk/t of zero (PMMA material). The differences in study method may account for the similar amount of corneal swelling measured.

The control eye in this study also showed a swelling response, albeit reduced. Many studies have shown that corneal swelling in the control eye appears to be influenced by swelling of the fellow lens wearing eye. (Fonn et al. 1999; Guzey et al. 2002; Lu et al. 2006b; Wang et al. 2002b) This is thought to be a type of sympathetic physiological response. The epithelium of the control eye also showed a response, to the lens being worn in the contralateral eye. Ladage et al. (Ladage et al. 2003b) have found the proliferation rate of corneal epithelium to reduce in the control eye of a subject, when it was reduced in the experimental eye. They also mentioned that a corneal wound in one eye would lead to an increase in wound healing activity in the control eye. (Ladage et al. 2003b) The same authors reported that sympathetic responses could be responsible for changing the osmolarity of tears in the contralateral eye when the other wears a contact lens. (Ladage et al. 2003b)

It also appears that some subject's corneas are more susceptible to change than others. Previous studies have shown that new contact lens wearers have a higher initial swelling response than adapted lens wearers, (Armitage and Schoessler 1988; Cox et al. 1990; Ichikawa et al. 1989; Schoessler and Barr 1980). In this study we found that some control eyes did not show any sympathetic stromal swelling response, while others swelled to levels approaching that of the lens wearing eye (range 0 to 5.7%).

The topographical pattern of epithelial change was opposite to that seen following CRT™ treatment for myopia, where the central epithelium thins and mid-periphery thickens. (Rah et al. 2002b; Soni et al. 2003; Swarbrick et al. 1998; Wang et al. 2003c) The increase in central epithelium created a myopic shift, ultimately leading to a reduction in hyperopia. The underlying concepts leading to these results are still unclear, but a joint theory of post-lens tear film pressures and mechanical forces from the contact lens are favoured (discussed in Chapter 2). (Choo et al. 2004a; Mountford 1997b; Swarbrick et al. 2004)

The amount of central epithelial thickening found in this study was far greater than that measured by Lu et al. (Lu et al. 2006b), which can be attributed to the lens wearing modality. The most noticeable difference between the epithelial results in this study compared with Choo et al. (Choo et al. 2004b) and Lu et al. (Lu et al. 2006b), was the lack of mid-peripheral epithelial thinning measured. While there was a large increase in central epithelial thickness, the mid-peripheral epithelium did not highlight the thinning that was expected after lens removal. Unforeseen findings such as this have been found in other previous studies investigating changes following myopic OK, where central epithelial thinning was

accompanied by an absence of mid-peripheral epithelial thickening. (Alharbi and Swarbrick 2003; Jayakumar and Swarbrick 2005)

With regards to the reversibility of the CRTH™ procedure, stromal swelling of both eyes had returned to baseline levels within three hours of initial lens removal. This was similar to the stromal recovery time found in the myopic CRT™ studies (Chapter 5). Also as found in the myopic studies, the epithelium did not recover as fully, even after 28 hours of no lens wear.

In summary, overnight CRTH™ lens wear induced corneal and epithelial thickness changes. The central epithelial thickening may be due to the negative pressure induced by the tear film under the central lens clearance region, ultimately re-distributing the epithelial tissue and fluid. Stromal swelling recovered rapidly following lens removal. Further studies are required to investigate the corneal changes produced by CRTH™ lens wear over a longer time period.

Chapter 7

Measurement of Corneal, Stromal and Epithelial Thickness in Keratoconus

7.1 A Comparison of Ultrasonic Pachymetry, Orbscan II and Optical Coherence Tomography

7.1.1 Abstract

Purpose: To compare corneal thickness measurements in normal and keratoconic subjects using Optical Coherence Tomography (OCT), Orbscan II (ORB) and ultrasonic pachymetry (UP) and measure epithelial and stromal thickness in keratoconics using OCT.

Methods: Twenty keratoconic and twenty control subjects were enrolled. The Orbscan II was used to locate the steepest area of the cornea, which was taken to represent the cone apex. Each instrument was used to obtain four total corneal thickness measurements; from the cone apex, corneal centre, mid-nasal and mid-temporal cornea. OCT scans were analysed to provide epithelial and stromal thickness readings for the keratoconic cornea.

Results: In keratoconic subjects, mean (± SD) central corneal thickness (CCT) measured by UP, ORB and OCT was 494.2 ± 50.0µm, 438.6 ± 47.7µm and 433.5 ± 39.7µm respectively. Regardless of measurement technique, the central keratoconic cornea was 57.7µm thinner than the normal cornea ($p<0.001$). The cone apex was thinner than the central cornea ($p<0.001$). Keratoconic epithelium was 48.2 ± 5.5µm centrally and 42.1 ± 4.5µm at the

apex. Central keratoconic epithelium was 4.7μm thinner and central keratoconic stroma was 57.8μm thinner than the normal cornea (both $p<0.001$). Comparing instruments, ORB and OCT were most correlated in CCT measurement ($r = 0.890$) and apical thickness ($r = 0.846$). All instruments produced similar readings for mid-nasal and mid-temporal corneal thickness in keratoconics ($p>0.05$).

Conclusion: Ultrasonic pachymetry produced the highest corneal thickness readings in the centre and apex, compared to Orbscan II and OCT. Centrally, the total cornea, epithelium and stroma were thinner in the keratoconic patient than in normal subjects.

7.1.2 Introduction

There is an abundance of studies discussing the measurement of central corneal thickness (CCT) in normal subjects using ultrasonic pachymetry (UP), (Bechmann et al. 2001; Boscia et al. 2002; Doughty and Zaman 2000; Fakhry et al. 2002; Gherghel et al. 2004; Giraldez Fernandez et al. 2002; Gonzalez-Meijome et al. 2003; Gromacki and Barr 1994; Iskander et al. 2001; Marsich and Bullimore 2000; Modis et al. 2001b; Prisant et al. 2003; Rainer et al. 2004; Rainer et al. 2002; Wong et al. 2002; Yaylali et al. 1997) the Orbscan II (ORB), (Auffarth et al. 2000; Boscia et al. 2002; Fakhry et al. 2002; Gherghel et al. 2004; Giraldez Fernandez et al. 2002; Gonzalez-Meijome et al. 2003; Iskander et al. 2001; Liu et al. 1999; Marsich and Bullimore 2000; Modis et al. 2001b; Prisant et al. 2003; Rainer et al. 2004; Wong et al. 2002; Yaylali et al. 1997) and optical coherence tomography (OCT). (Bechmann et al. 2001; Muscat et al. 2002; Wirbelauer et al. 2002b; Wirbelauer et al. 2002c; Wong et al. 2002)

CCT and thickness of the cone apex in keratoconics has previously been reported using ORB and UP, (Auffarth et al. 2000; Gherghel et al. 2004; Gromacki and Barr 1994; Liu et al. 2002; Owens and Watters 1996) but rarely using OCT. (Bechmann et al. 2001; Wirbelauer et al. 2002c) OCT is relatively new to anterior segment research and no studies have yet been published discussing the use of OCT to simultaneously measure the thickness of the cornea, epithelium and stroma in keratoconus.

This study examined corneal thickness in keratoconics, as measured by OCT, ultrasonic pachymetry and the Orbscan II. These thickness measurements were compared between techniques and also to readings taken from the 'normal' (non-keratoconic) cornea, at approximated equivalent locations. Since OCT was the only instrument capable of measuring epithelial and stromal thickness in this experiment, there could not be a comparison with the other two techniques. Therefore epithelial and stromal thickness was measured in keratoconic and normal subjects using OCT, at the same locations as total corneal thickness measurements.

7.1.3 Study procedure

Subjects

Twenty keratoconic (7 females and 13 males, mean age (± SD) 34.9 ± 11.7 years, range 17 to 59 years) and twenty control participants (14 females and 6 males, mean age (± SD) 31.1 ± 8.1 years, range 22 to 47 years) were enrolled. Control subjects had no history of ocular disease or surgery and were non-contact lens wearers. Keratoconic subjects were recruited from a database maintained by the School of Optometry contact lens clinic at the University of Waterloo and were all confirmed as being keratoconic using topography plots, and had been keratoconic for at least one year. All keratoconic subjects were rigid gas permeable (RGP) contact lens wearers and presented with the condition bilaterally. Both eyes of each subject were used in this study.

Instrumentation

The single visit commenced with an ocular case history (including the length of time since keratoconus had been diagnosed), visual acuity (VA) and slit-lamp assessment; the latter was performed after contact lenses were removed in keratoconic subjects. Each of the three instruments was used to obtain four corneal thickness measurements; from the cone 'apex', corneal centre, mid-nasal and mid-temporal cornea (~3.5mm from centre) along the horizontal meridian.

In this study, the Orbscan II was used initially to locate the thinnest point of the cornea, taken to be the apex of the cone in keratoconic subjects. Corneal thickness values for the central, nasal and temporal locations were collected from colour-coded maps produced by the instrument (Figure 7.1).

Figure 7-1 Screenshot of the Orbscan II after measurement of a keratoconic cornea.

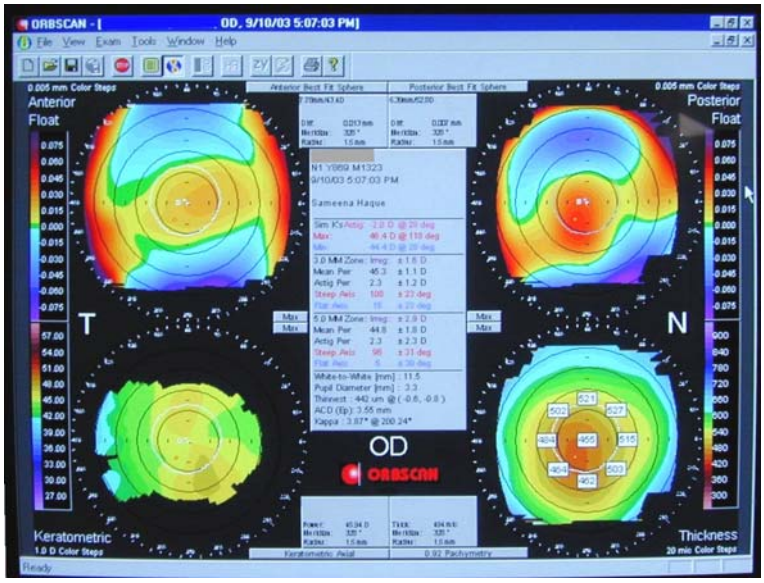

OCT was used next to measure corneal thickness at the same four points across the cornea. Figure 7.2 shows a central OCT scan of a keratoconic cornea from a single subject, illustrating the change in thickness from the centre (left side of image) to the cone apex region (right side of image). Regions of increased light scatter (seen as red and white pixels), represent scarring and disorganization of tissue due to keratoconus.

Figure 7-2 An OCT scan of the central keratoconic cornea.

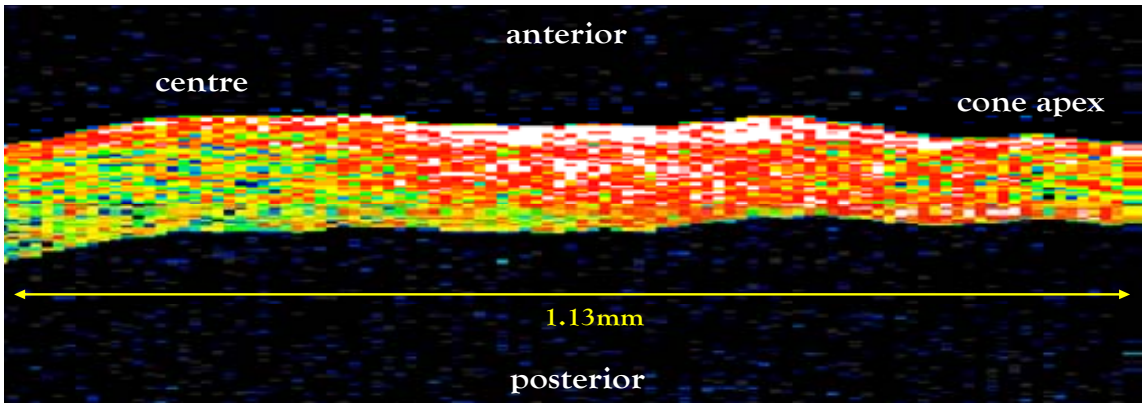

Ultrasonic pachymetry was performed at the end to prevent any possible alteration to thickness measurements, due to mechanical effects caused on contact. Initially, the subject's cornea was anaesthetized with 1-2 drops of Alcaine® (Proparacaine Hydrochloride 0.5%; Alcon, Mississauga, Canada) and the pachymeter probe sterilized with an alcohol swab, and let to air dry. The surface of the probe (1.5mm in diameter) needed to contact the corneal surface perpendicularly for correct measurement, which was taken automatically by the

instrument once achieved. Central readings were obtained using the centre of the pupil as a guide and peripheral readings were taken at approximately 2-3mm from the limbus. UP readings for the corneal apex in keratoconics were obtained using Orbscan II data to locate the thinnest point of the cornea. A series of 3 to 5 readings were obtained in succession and averaged automatically by the instrument, and displayed on the screen to be recorded manually. Data was not saved on the instrument.

Re-ANOVA and Tukey HSD post-hoc testing was used to signify differences between instruments, between corneal location and between keratoconic and control subjects, for corneal, epithelial and stromal thickness. Pearson's correlation coefficient (r) was used to correlate measurements of total corneal thickness between techniques.

7.1.4 Results

Keratoconic Subjects

Figure 7.3 illustrates the corneal thickness measurements obtained by each of the three instruments in keratoconic subjects (values are displayed in Appendix N). Mean CCT (± SD) measured by UP, ORB and OCT was 494.2 ± 50.0 µm, 438.6 ± 47.7µm and 433.5 ± 39.7µm respectively. Mean apical corneal thickness (ACT) (± SD) measured by UP, ORB and OCT was 439.8 ± 44.8µm, 401.7 ± 47.9µm and 398.1 ± 43.5µm respectively. There was no significant difference between techniques in measuring the peripheral cornea ($p>0.05$).

UP measured higher thickness values than ORB and OCT in the central and apical locations (all $p<0.001$). For central (Figure 7.4) and apical locations, ORB and OCT showed the highest correlation (Pearson's coefficient $r = 0.890$ and $r = 0.846$ respectively), followed by OCT with UP ($r = 0.765$ and $r = 0.750$ respectively).

Figure 7-3 Corneal thickness in keratoconics measured by ultrasonic pachymetry (UP), Orbscan II (ORB) and optical coherence topography (OCT) (vertical bar represents 95% confidence level).

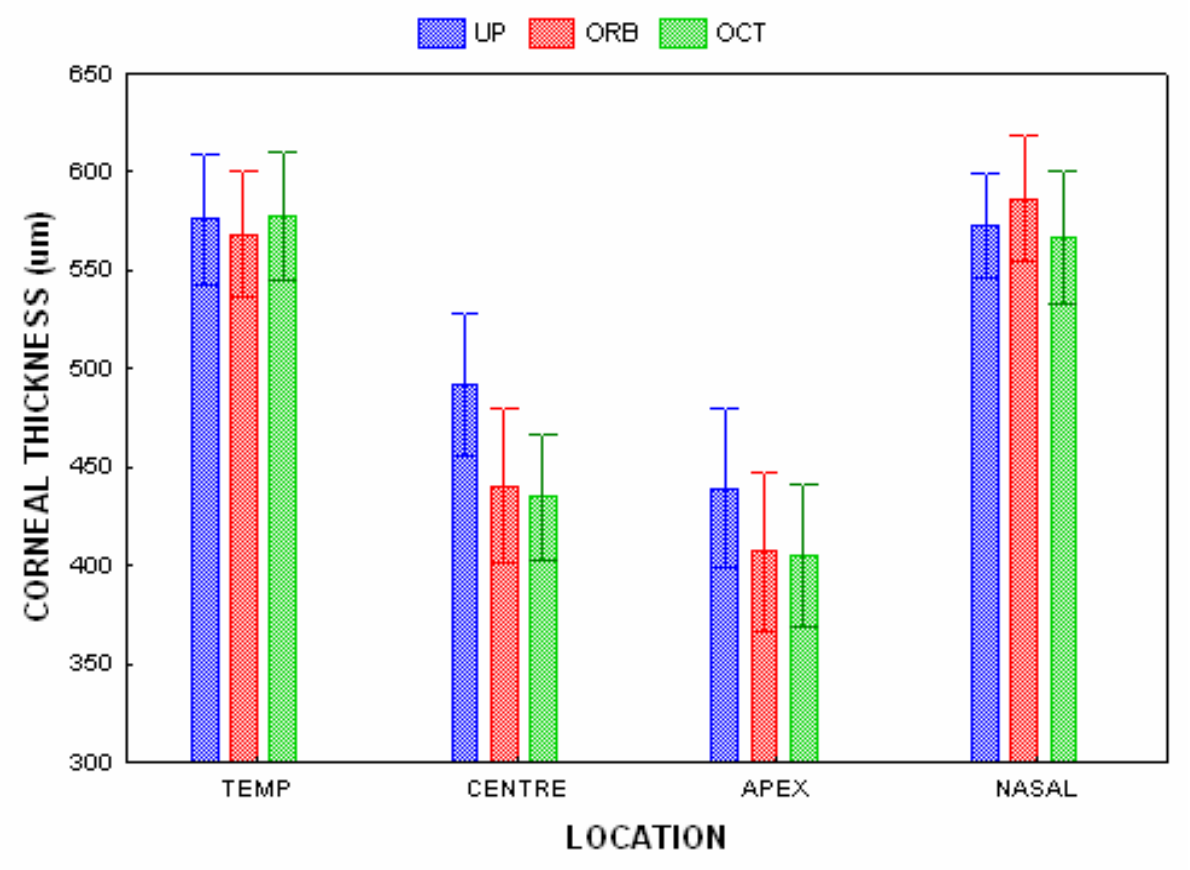

Figure 7-4 Scatterplot showing correlation of central corneal thickness measurements taken by ORB and OCT. (Pearson's correlation coefficient r = 0.890, p<0.001).

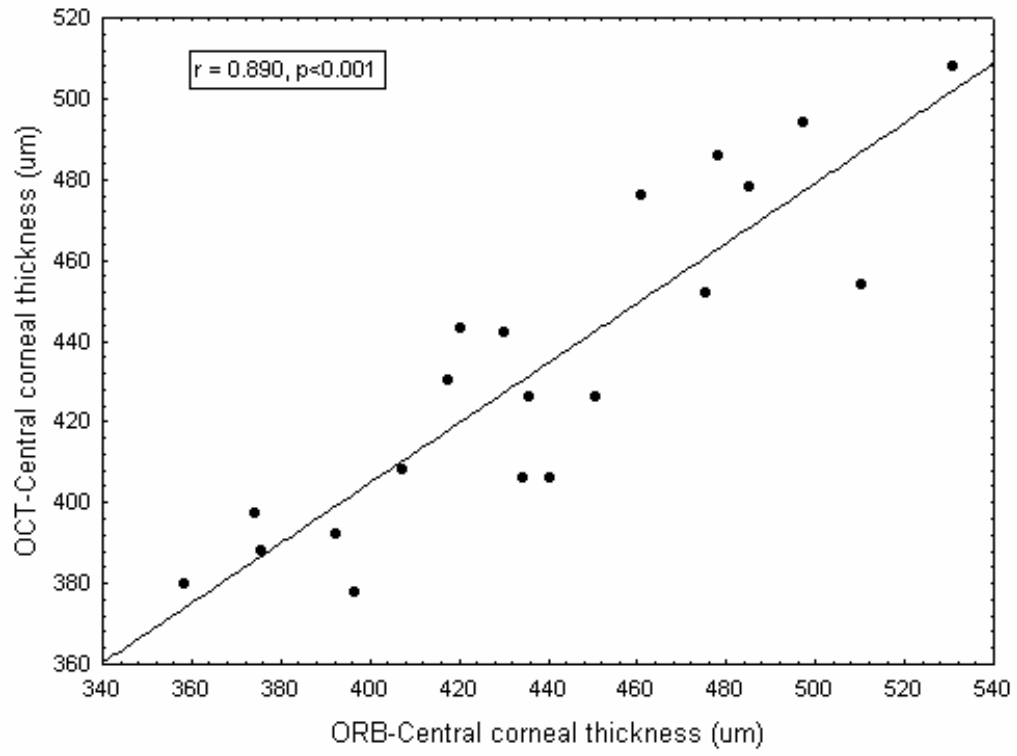

Corneal epithelial thickness in keratoconic subjects measured by OCT was compared to the length of time since diagnosis. Subjects were placed in two categories – those who had been diagnosed with keratoconus within the last five years and those diagnosed over five years ago. This division resulted in an equal ten subjects being placed in each category. Mean epithelial thickness (± SD) for all keratoconic subjects was 48.2 ± 5.5µm in the centre and 42.1 ± 4.5µm at the cone apex, the difference being statistically significant (p<0.001). Central and apical epithelium was 2.7µm (5.4%) and 2.6µm (6.0%) thinner respectively, in keratoconics who had been diagnosed with the condition for over five years. However, this

difference was not statistically significant (p>0.05). Figure 7.5 plots the VA of each eye for all keratoconic subjects against the length of time since their diagnosis of the condition. There was no association between the two measures (p>0.05), with some subjects having keratoconus for over 20 years and still presenting with excellent VA.

Figure 7-5 The visual acuity (logMAR VA) of each keratoconic eye plotted against the length each subject was diagnosed with the condition (years).

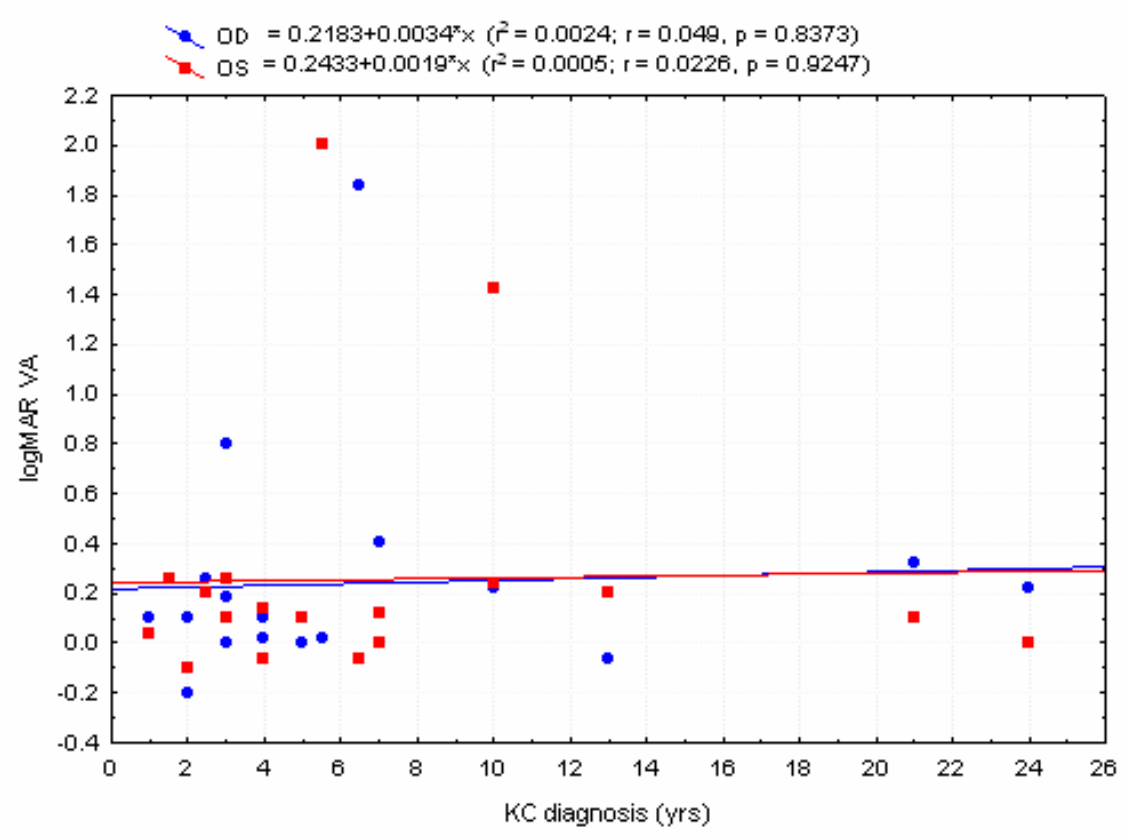

Keratoconics compared with controls

Figure 7.6 shows the comparison of corneal thickness in keratoconics and controls, measured by UP, ORB and OCT, at the temporal, central and nasal locations (the cone apex was assumed absent in normal subjects). Each instrument measured the keratoconic cornea as being significantly thinner than controls at all three locations; (all $p<0.001$). Keratoconic CCT was 36.3µm (6.8%), 74.2µm (14.5%) and 62.5µm (12.6%) thinner than control, measured by UP, ORB and OCT respectively. On average, this made the total keratoconic cornea 57.7µm (11.2%) thinner than the normal cornea ($p<0.001$). In control subjects, CCT (mean ± SD) measured by UP, ORB and OCT was 530.5 ± 30.1µm, 512.9 ± 44.0µm and 496.0 ± 29.1µm, respectively. Only the difference between the CCT_{UP} and CCT_{OCT} measurements reached statistical significance ($p<0.001$). There was no difference between instruments in the measurement of the temporal cornea in control subjects (all $p>0.05$), but ORB measured the nasal cornea significantly thicker than UP and OCT ($p<0.001$). Corneal thickness values for the control subjects are listed alongside those for the keratoconic subjects in Appendix N.

Figure 7-6 Corneal thickness comparison between keratoconic and control subjects, measured by UP, ORB and OCT; (vertical bar represents 95% confidence level).

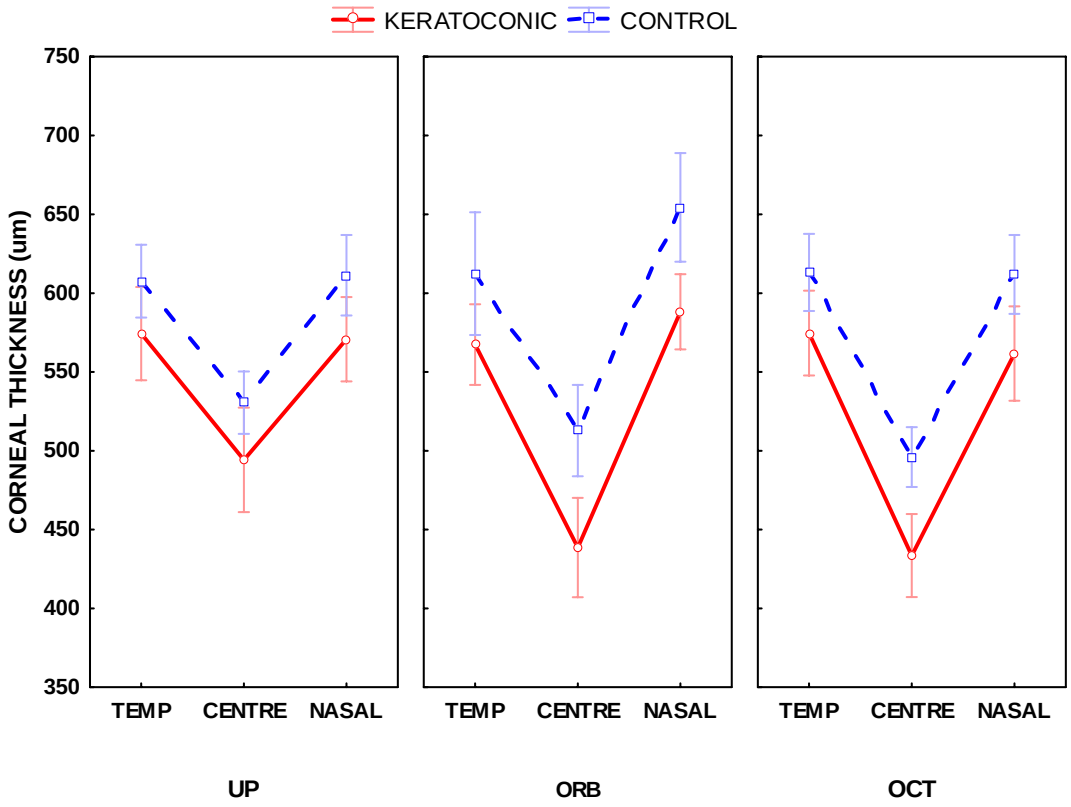

Differences in epithelial and stromal thickness between keratoconic and control subjects are represented in Table 7.1. Central epithelial thickness in the keratoconic subjects was 4.7µm (8.9%) thinner than control thickness ($p<0.001$). There was no significant difference in epithelial thickness temporally or nasally, in keratoconics compared with controls ($p>0.05$). However, stromal thickness in keratoconics was significantly thinner than controls temporally, centrally and nasally by 36.5µm (6.6%), 57.8µm (13.0%) and 49.0µm (8.9%) respectively (all $p<0.001$).

Table 7-1 Epithelial and stromal thickness in microns (mean ± SD), comparing keratoconic and control subjects, measured by OCT.

Subjects	**Stromal Thickness** (μm)			**Epithelial Thickness** (μm)		
	Temp	Centre	Nasal	Temp	Centre	Nasal
Keratoconic	517.3 ± 42.3	385.4 ± 43.3	504.2 ± 46.6	57.4 ± 4.1	48.2 ± 5.5	57.4 ± 4.6
Control	553.8 ± 39.6	443.1 ± 28.1	553.3 ± 39.4	59.4 ± 4.6	52.9 ± 4.1	58.6 ± 4.4

7.1.5 Discussion

Corneal thickness values obtained by the Orbscan II are dependent on the use of the acoustic factor, applied to calibrate thickness with ultrasound pachymetry. (Boscia et al. 2002; Iskander et al. 2001; Yaylali et al. 1997) In this study, the factor of 0.92 was applied as default. Without applying this factor, ORB would yield thickness values greater than UP, as found in previous studies. (Fakhry et al. 2002; Gherghel et al. 2004; Gonzalez-Meijome et al. 2003; Iskander et al. 2001; Prisant et al. 2003; Yaylali et al. 1997) For example, if we divide the CCT for normal subjects by the acoustic factor, ORB would have measured CCT 27μm greater than UP. Wong and colleagues (Wong et al. 2002) found OCT to measure normal central corneal thickness lower than UP, and ultimately applied a correction factor of 32μm to OCT measurements to calibrate the two sets of readings.

Thickness readings were more difficult to obtain using UP for scarred keratoconic corneas, whereas ORB and OCT captured images regardless of scarred tissue. A similar occurrence was encountered by Bechmann et al. (Bechmann et al. 2001) Although the Orbscan II was successful in producing thickness maps, the thickness values may not necessarily be accurate for the keratoconic cornea. It has been stated that ORB may not be calibrated suitably for measuring thin corneas. (Kawana et al. 2004) The presence of corneal haze following laser refractive surgery affects the transmittance of light through the cornea, and therefore may affect the scanning ability of the instrument. This seems to lead to lower thickness readings. (Boscia et al. 2002; Fakhry et al. 2002; Gherghel et al. 2004; Iskander et al. 2001; Kawana et al. 2004; Prisant et al. 2003) The same reason may be responsible for ORB producing lower thickness values than UP in keratoconic eyes. As in this study and one by Gherghel et al. (Gherghel et al. 2004) it was shown that in keratoconic eyes, the Orbscan II (acoustic factor applied) produced significantly lower measurements than ultrasound pachymetry. In agreement, ultrasound velocity is believed to decrease with increasing corneal oedema, causing artificially high UP readings in cases of keratoconus, when measurements were indeed successfully obtained. (Bechmann et al. 2001)

Although OCT has no difficulty in capturing images of atypical corneas, the question arises as to whether oedema and/or stromal disorganization affects the actual corneal thickness values in the same way as it does Orbscan II values. (Wirbelauer et al. 2002c) It has been shown previously that OCT measures thickness greater than optical pachymetry (with an apparatus of design similar to the Holden-Payor optical pachymeter) in normal and even more so in oedematous eyes. (Wang et al. 2002b) The same report stated that oedema does

impact the measurements of both OCT and optical pachymetry, through changes in refractive index and the shape of the cornea. (Wang et al. 2002b) Bechmann et al. (Bechmann et al. 2001) found OCT to read consistently lower than UP by 50µm in normal eyes, and this difference in measurements increased as corneal oedema increased.

In contrast to ORB and OCT, UP had obvious disadvantages. The probe required corneal contact, and therefore the need for topical anaesthesia, which can cause ocular irritation. UP also lacked control of fixation, probe placement could not be repeated with precision, and it was difficult to ensure that the probe was perpendicular to the corneal surface. (Avitabile et al. 1997; Pflugfelder et al. 2002; Rabinowitz et al. 1998) But in contrast to ORB, it has been found that corneal thickness measurements obtained by UP are not affected by the degree of corneal haze found after refractive surgery. (Boscia et al. 2002; Fakhry et al. 2002; Iskander et al. 2001; Prisant et al. 2003) It has been stated that thickness measurements of the keratoconic cornea by UP may be more accurate, because ultrasound waves are less affected by haze caused by tissue disorganization. (Fakhry et al. 2002; Iskander et al. 2001)

A few studies have suggested the tear film (of up to 40µm thickness) having an influence on the differences in thickness measurements by UP and ORB. (Gonzalez-Meijome et al. 2003; Kawana et al. 2004; Liu et al. 1999; Prisant et al. 2003) Where ORB had produced higher values, corneal indentation by the ultrasound probe displacing the tear layer was suggested as an explanation to the underestimation of thickness by UP. (Kawana et al. 2004; Liu et al. 1999; Prisant et al. 2003) However, if the tear film was in fact ~40µm thick, the OCT would have likely detected this as a separate layer in the light backscatter scans. This strengthens

the notion that the pre-corneal tear film is closer to 3 – 7μm thick, (King-Smith et al. 2000; King-Smith et al. 2004; Nichols and King-Smith 2003; Wang et al. 2003b) and therefore cannot be distinguished by our OCT.

As expected, the keratoconic cornea was thinner than normal, regardless of measurement technique. The reduction in thickness was seen in the stroma and also the epithelium, where the basal layer is involved at an early stage. The keratoconic epithelium was thinner at the cone apex than in the centre, which was thinner than the mid-periphery, partly due to the cone being more centrally located in some subjects. However, the exact apex of the cone was difficult to locate with UP and OCT so measurement position was estimated, unlike with ORB where colour maps determine the region of the cone clearly.

With time, the epithelium is expected to thin further, as basal cells disintegrate leaving only the superficial layers. (Leibowitz and Waring 1998; Rabinowitz 1998) This was supported by results found in this study, where the apical epithelium was 6% thinner in subjects who had been diagnosed with keratoconus for over five years. However, these subjects were more likely to have worn their rigid contact lenses for a longer period of time, which raised the question of how much influence the contact lenses had on the thinning of the epithelium. (Ladage et al. 2001b) This topic was investigated and is reported in Chapter 7.3.

ORB and OCT showed the greatest correlation for the measurement of keratoconic corneal thickness. However, when comparing ease of data analysis, the particular set-up of OCT used in this study proved to be the most inconvenient, as thickness readings were not

immediately available and raw data needed to be analyzed at a later date. This would be a hindrance if using OCT shortly before a surgical procedure and an OCT program producing immediate thickness information would be essential.

With all these differences in mind, caution should perhaps be applied regarding patient suitability for corneal refractive surgery, if corneal thickness is only measured using one method. Underestimation of thickness may lead to the exclusion of otherwise suitable candidates; while on the other hand, overestimation of thickness may ultimately lead to excessive thinning of the stromal bed. (Gonzalez-Meijome et al. 2003; Iskander et al. 2001)

In summary, ultrasonic pachymetry produced higher central corneal thickness values than Orbscan II and optical coherence tomography for the measurement of the normal and keratoconic cornea. The corneal apex and associated corneal epithelium were thinner than the centre in keratoconic subjects. OCT is a valuable tool to corneal research and is able to provide information regarding epithelial thickness – an advantage over the other two techniques used in this study.

7.2 Mapping normal thickness using OCT

7.2.1 Abstract

Purpose: To measure and compare the thickness of the normal cornea, stroma and epithelium, along a 10mm diameter section in 4 meridians (8 directions of gaze), using OCT.

Methods: Twenty healthy non contact lens wearers were enrolled. A fixation target employing LEDs in 4 meridians was attached to the OCT and corneal images obtained from centre to periphery. Raw OCT scans were analysed to yield values for corneal and epithelial thickness and interpolated colour-coded plots were compiled using MATLAB software.

Results: Mean (± SD) central corneal thickness of the 20 subjects was 516.9 ± 21.3μm and central stromal thickness was 463.4 ± 21.1μm, both significantly thinner than the periphery in all meridians ($p<0.001$). Peripheral corneal thickness was significantly thicker in the superior temporal region (719.4 ± 43.0μm) and thinnest in the inferior region (629.7 ± 40.7μm; $p<0.001$ compared to each other). Mean (± SD) central epithelial thickness was 53.6 ± 2.2μm. Peripheral epithelial thickness averaged across meridians (62.9 ± 2.6μm) was significantly thicker than central ($p<0.001$). The superior peripheral epithelium was thickest (68.0 ± 8.5μm) and inferior epithelium was thinnest (58.0 ± 4.3μm; $p<0.001$ compared to each other).

Conclusion: The normal cornea and epithelium was thicker in the periphery than in the centre. The superior region was thickest and inferior the thinnest. For the first time, this study used OCT to measure and plot meridional topographical epithelial thickness in vivo.

7.2.2 Introduction

In order to monitor corneal changes due to disease, surgery or contact lens wear, it is vital to know the parameters of the normal cornea and its epithelium, in particular corneal thickness. Most studies investigating corneal thickness only report on central measurements. (Bechmann et al. 2001; Chakrabarti et al. 2001; Gurdal et al. 2003; Kawana et al. 2004; Prisant et al. 2003; Radford et al. 2004; Rainer et al. 2004; Realini and Lovelace 2003; Sallet 2001; Tam and Rootman 2003) However, corneal refractive surgery and contact lenses infringe upon the peripheral cornea, (Dumbleton 2002; Ivarsen et al. 2003) and the importance of monitoring the peripheral morphology is clear. Recently, a series of articles was published that compared new instruments, such as the OCULUS Pentacam, (Barkana et al. 2005; Buehl et al. 2006; Lackner et al. 2005a; O'Donnell and Maldonado-Codina 2005), partial coherence interferometry (Buehl et al. 2006) and optical low coherence reflectometry (Barkana et al. 2005) with the more established techniques of ultrasound pachymetry and Orbscan. These studies only measured central corneal thickness, and while a few studies have reported peripheral thickness along the horizontal meridian (Feng and Simpson 2005), very few studies have reported on vertical corneal thickness. (Erickson et al. 2002)

Ultrasonic pachymetry is considered the gold standard for the measurement of corneal thickness, (Miglior et al. 2004; Rapuano et al. 1993) and has been compared to various instruments, including Orbscan, confocal and specular microscopy and OCT. (Avitabile et al. 1997; Fakhry et al. 2002; Giraldez Fernandez et al. 2002; Gokmen et al. 2002; Gonzalez-Meijome et al. 2003; Hrynchak and Simpson 2000; Javaloy et al. 2004; Modis et al. 2001a,

2001b; Rainer et al. 2004; Reinstein et al. 1994a; Sanchis-Gimeno et al. 2006; Tam and Rootman 2003; Yaylali et al. 1997) Orbscan routinely produces maps of thickness for the total corneal surface; however the other instruments mentioned above are not always used to measure the periphery along with the central cornea, unless adapted to do so. Additionally, few instruments have the ability to measure epithelial thickness with ease, hence an advantage of OCT.

Reports of epithelial thickness measurement are scarce, particularly for the corneal periphery. Reinstein et al. (Reinstein et al. 1993; Reinstein et al. 2000; Reinstein et al. 1994a) used high frequency ultrasound to produce topographical plots of epithelial thickness over the entire corneal surface. However, although this technique was possible in vivo, the procedure was not user-friendly, as the eye needed to be submerged in a water bath while the subject assumed a supine position. Recently, Feng and Simpson (Feng and Simpson 2005) compared central with limbal epithelium using OCT and found the latter to be significantly thicker.

In this study, OCT was used to capture images across several meridians of the normal cornea, in order to more fully characterise its geographical variation.

7.2.3 Study Procedure

Subjects

Twenty healthy non contact lens wearers (9 females and 11 males, mean age (± SD) 27.6 ± 5.9 years, range 21 to 45 years) were enrolled. All subjects had no history of ocular disease or surgery and had never worn contact lenses. Both eyes of each subject were used in the study (n = 40 eyes) and all readings were taken in the afternoon (between 1 and 5 pm) to ensure no residual corneal oedema following sleep.

Instrumentation

OCT was used to obtain corneal thickness measurements, with the aid of a fixation device designed and constructed for this study (Figure 3.9). The device consisted of up to six coloured LEDs (1mm apart) along each of the eight arms, representing eight directions of gaze. The measured point on the cornea was opposite to the location of the light fixated (i.e. fixating on the third superior light would enable the measurement of the inferior mid-peripheral cornea). Following the central measurement, subjects were asked to fixate each illuminated point on the device, working from the centre to the periphery. Once the raw OCT data were analysed to yield values for corneal and epithelial thickness, the values were imported into imaging software ('MATLAB', The Mathworks, Natick, MA) to construct colour-coded plots of the entire corneal and epithelial surface (Figure 7.7).

Figure 7-7 A plot showing the thickness of the normal cornea, highlighting the location and thickness of each point measured, according to the coloured legend.

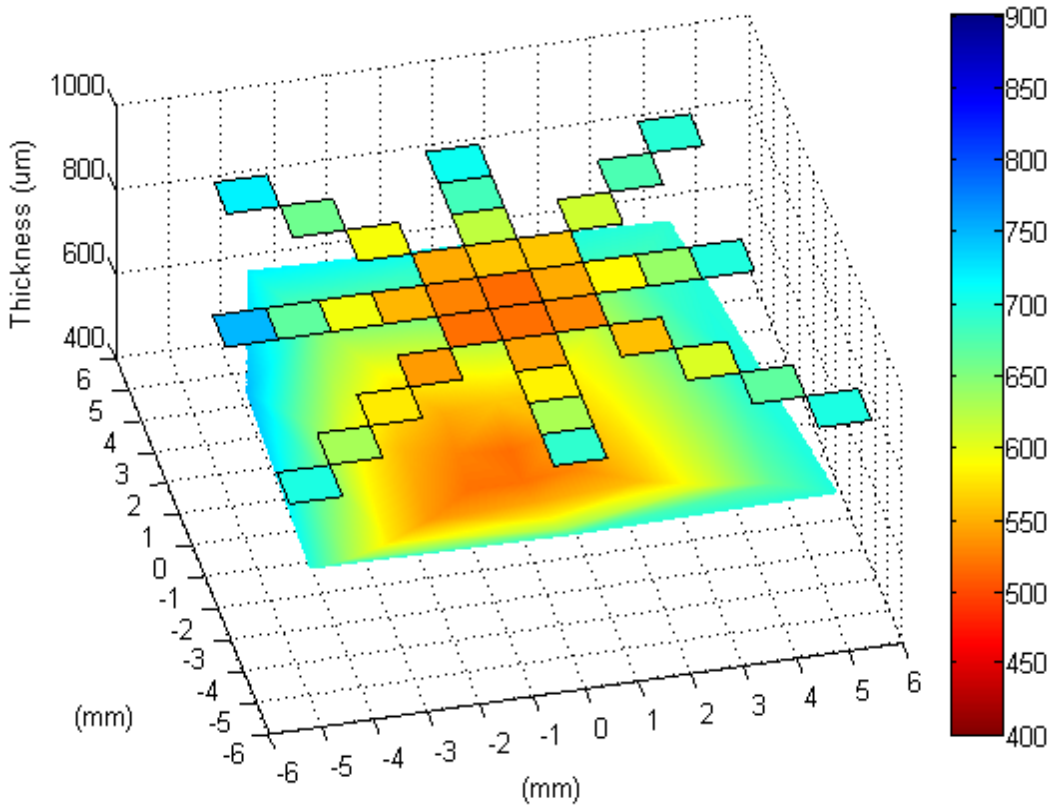

Analysis of variance (ANOVA) and Tukey HSD post-hoc tests were used to signify differences between thickness values for all locations, comparing the central cornea to the periphery and the superior / inferior / temporal and nasal regions to each other.

7.2.4 Results

Data from both eyes of all subjects were included in the data analysis. Since a fifth measurement point was not possible along all meridians in some subjects (due to the fixation light reflecting on the sclera or the nose causing an obstruction), statistical analysis was restricted to four points each side of the centre along all meridians. All values of peripheral thickness reported below, regard the fourth corneal location (point 4) measured, unless otherwise stated. However, additional points were used to construct the thickness plots.

Corneal Thickness

Table 7.2 shows the thickness of the central and peripheral cornea (at the limbus), displayed in order of thickest to thinnest regions. Mean (± SD) central corneal thickness (CCT) of the 20 subjects was 516.9 ± 21.3μm, and was significantly thinner than the periphery in all meridians ($p<0.001$). Peripheral corneal thickness (PCT) was thickest in the superior temporal (ST; 719.4 ± 43.0μm) region and thinnest in the inferior (I; 629.7 ± 40.7μm) region – this difference being significantly different ($p<0.001$). There was also a significant difference between the temporal (T; 666.1 ± 47.6μm) and nasal (N; 698.2 ± 35.8μm) peripheral cornea ($p<0.001$). Average thickness of the periphery across meridians was 676.4 ± 31.1μm.

Table 7-2 Central and peripheral thickness (mean ± SD, averaged between eyes) of the normal human cornea. Peripheral thickness measurement shown was obtained adjacent to the limbus (4th fixation light) and is displayed from thickest to thinnest. (T=temporal, N=nasal, S=superior, I=inferior).

	Centre	ST	S	N	SN	IN	T	IT	I
CORNEA (mean)	516.9	719.4	706.7	698.2	693.5	666.4	666.1	631.2	629.7
(SD)	± 21.3	± 43.0	± 40.1	± 35.8	± 40.4	± 42.5	± 47.6	± 37.4	± 40.7

Figure 7.8 illustrates the mean thickness of the normal cornea at 4 points along each of the 8 directions of gaze. From left to right, each set of bars represents the cornea from limbus to limbus along the four meridians: temporal (T) to nasal (N) (0^o to 180^o), superior temporal (ST) to inferior nasal (IN) (45^o to 225^o), superior (S) to inferior (I) (90^o to 270^o) and superior nasal (SN) to inferior temporal (IT) (135^o to 315^o). The fourth measurement in each direction ('-4' and '4') was obtained at or within 1mm of the limbus. This graph shows that at this peripheral region, the superior temporal cornea was the thickest and the inferior cornea was the thinnest. There was no significant difference in corneal thickness between eyes across all data points ($p>0.05$). Corneal thickness at each measured location is listed in Appendix O.

Figure 7-8 Mean thickness of the normal cornea at 4 points either side of the centre, along each of the 8 directions of gaze. Each set of bars represents the cornea from limbus to limbus along the four meridians: temporal to nasal (T to N), superior temporal to inferior nasal (ST to IN), superior to inferior (S to I) and superior nasal to inferior temporal (SN to IT).

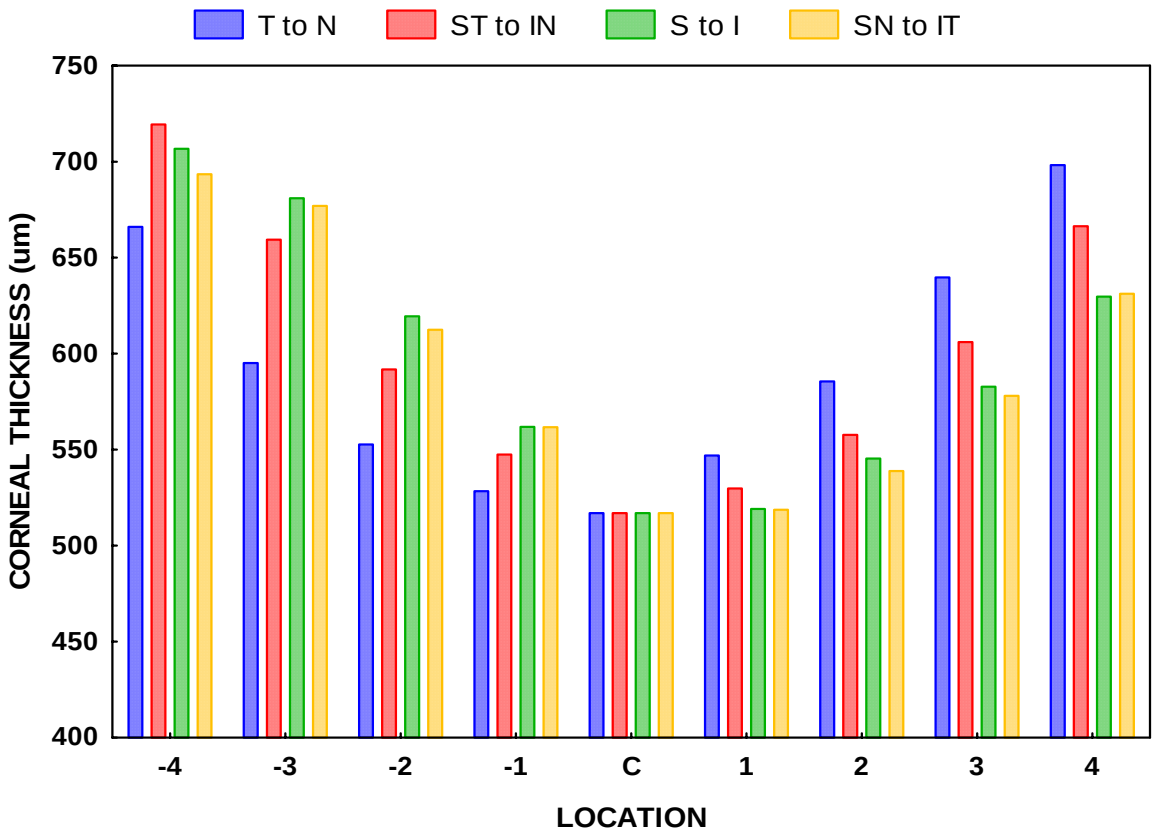

Figure 7.9 shows a colour-coded plot of corneal thickness, with data points interpolated between adjacent values using MATLAB. It shows the the variation in corneal thickness from the centre (shown in red hues) to the periphery (blue hues).

Figure 7-9 A plot showing the mean thickness of the normal cornea. The colour-coded legend (right) reads in microns and represents thinner areas of the cornea in red hues and thicker areas in blue.

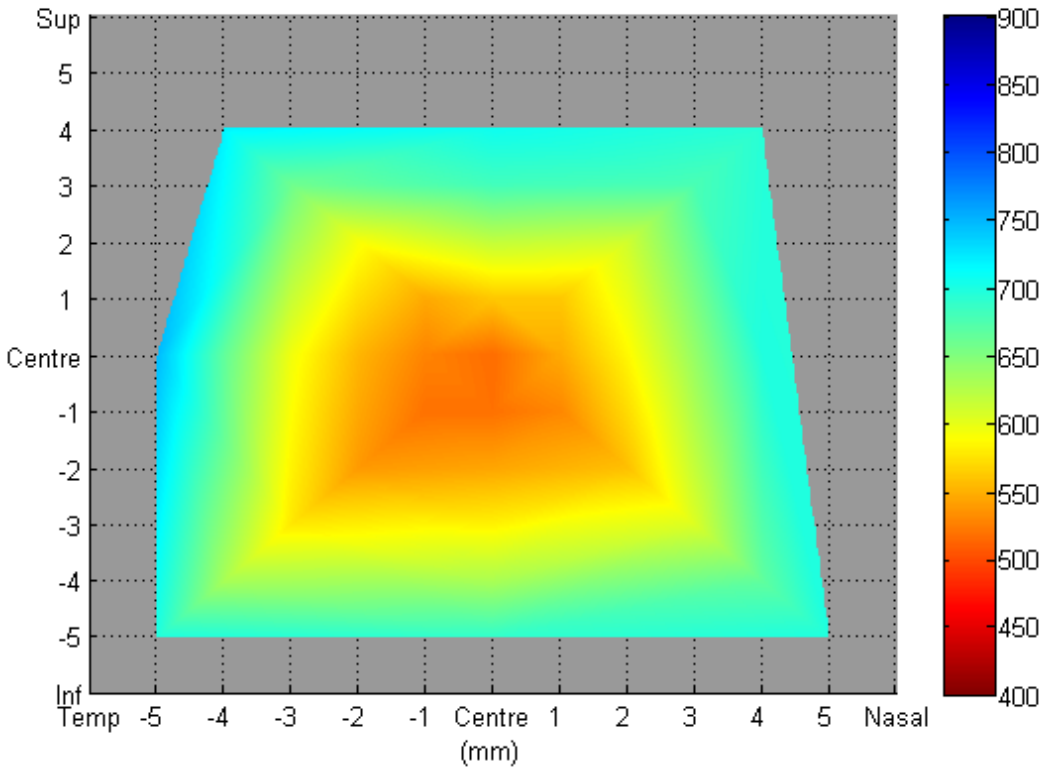

Stromal Thickness

Central stromal thickness (CST) (mean ± SD) was 463.4 ± 21.1µm, and was significantly thinner than the averaged peripheral stromal thickness (PST) across meridians (613.5 ± 30.1µm; $p<0.05$). Similar to the cornea, PST was thickest in the superior temporal region (ST; 653.6 ± 44.8µm) and thinnest in the inferior temporal region (IT; 571.5 ± 35.8µm; $p<0.001$). The temporal (T; 606.0 ± 46.2µm) and nasal (N; 633.3 ± 34.7µm) PST was

significantly different ($p<0.001$). The thickness of the stroma at each measured corneal location is displayed in Appendix P.

Epithelial Thickness

Table 7.3 shows the thickness of the central and peripheral epithelium, displayed in order of thickest to thinnest regions. Mean (± SD) central epithelial thickness (CET) of all subjects was 53.6 ± 2.2μm. Peripheral epithelial thickness (PET) followed a similar pattern to PCT and was thickest in the superior (S; 68.0 ± 8.5μm) region and thinnest in the inferior region (I; 58.0 ± 4.3μm; $p<0.001$ compared to each other). Temporal PET (T; 60.1 ± 3.5μm) was also significantly different from nasal PET (N; 64.9 ± 4.7μm; $p<0.001$). Averaged PET across all meridians (62.9 ± 2.6μm) was significantly thicker than CET ($p<0.001$). Epithelial thickness values at each measured corneal location are listed in Appendix Q.

Table 7-3 Central and peripheral thickness (mean ± SD, averaged between eyes) of the normal human corneal epithelium. Peripheral thickness measurement shown was obtained adjacent to the limbus (4^{th} fixation light) and is displayed from thickest to thinnest. (T=temporal, N=nasal, S=superior, I=inferior).

	Centre	S	SN	ST	N	IN	T	IT	I
EPITHELIUM (mean)	53.6	68.0	65.8	65.8	64.9	60.9	60.1	59.7	58.0
(SD)	± 2.2	± 8.5	± 6.5	± 6.1	± 4.7	± 3.8	± 3.5	± 3.3	± 4.3

Figure 7.10 shows the mean thickness of the epithelium at 4 points along each of the 8 directions of gaze. There was no significant difference in epithelial thickness between eyes across all locations ($p>0.05$). Figure 7.11 shows a colour-coded plot of mean epithelial thickness from all 20 subjects. The plot shows thinner epithelium located in the centre (red) with the peripheral epithelium being thicker (green).

Figure 7-10 Mean thickness of the epithelium at 4 points either side of the centre, along 8 directions of gaze. The cornea was measured from limbus to limbus along four meridians: temporal to nasal (T to N), superior temporal to inferior nasal (ST to IN), superior to inferior (S to I) and superior nasal to inferior temporal (SN to IT).

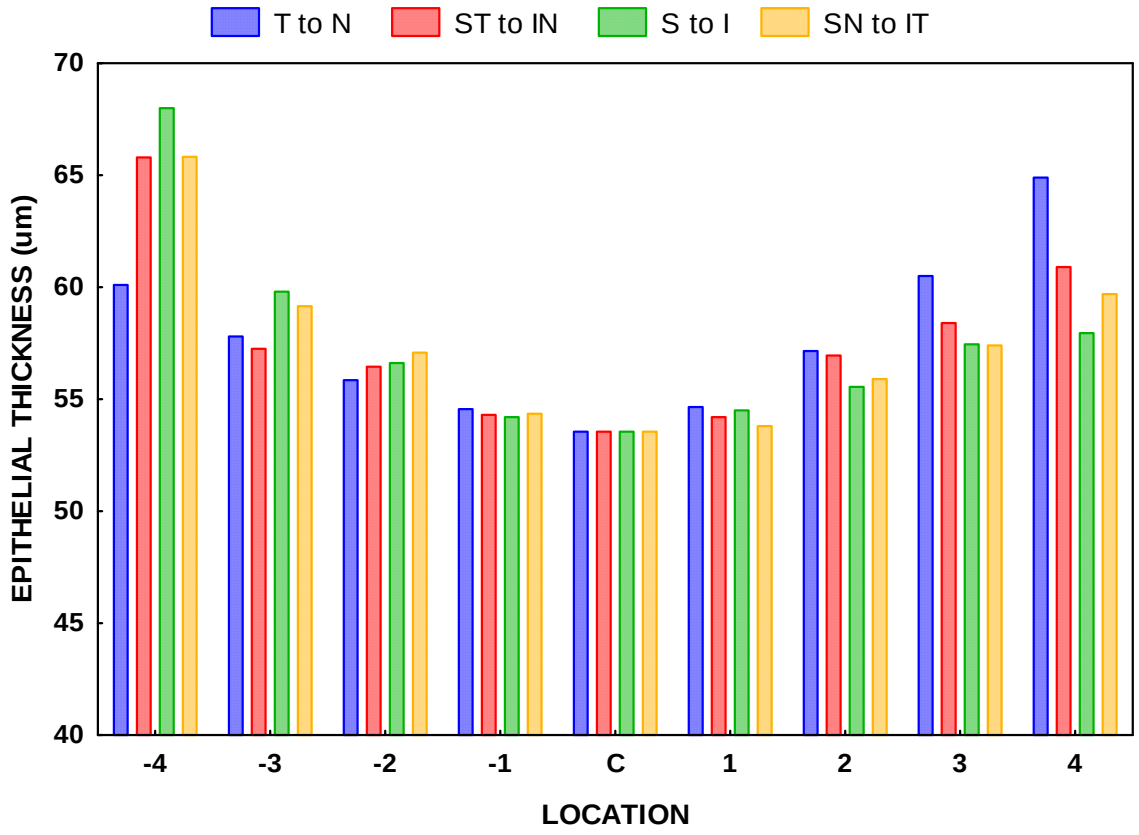

Figure 7-11 A plot showing the mean thickness of the epithelium. The colour-coded legend (right) reads in microns. The plot represents areas of thinner epithelium in red and thicker areas in green.

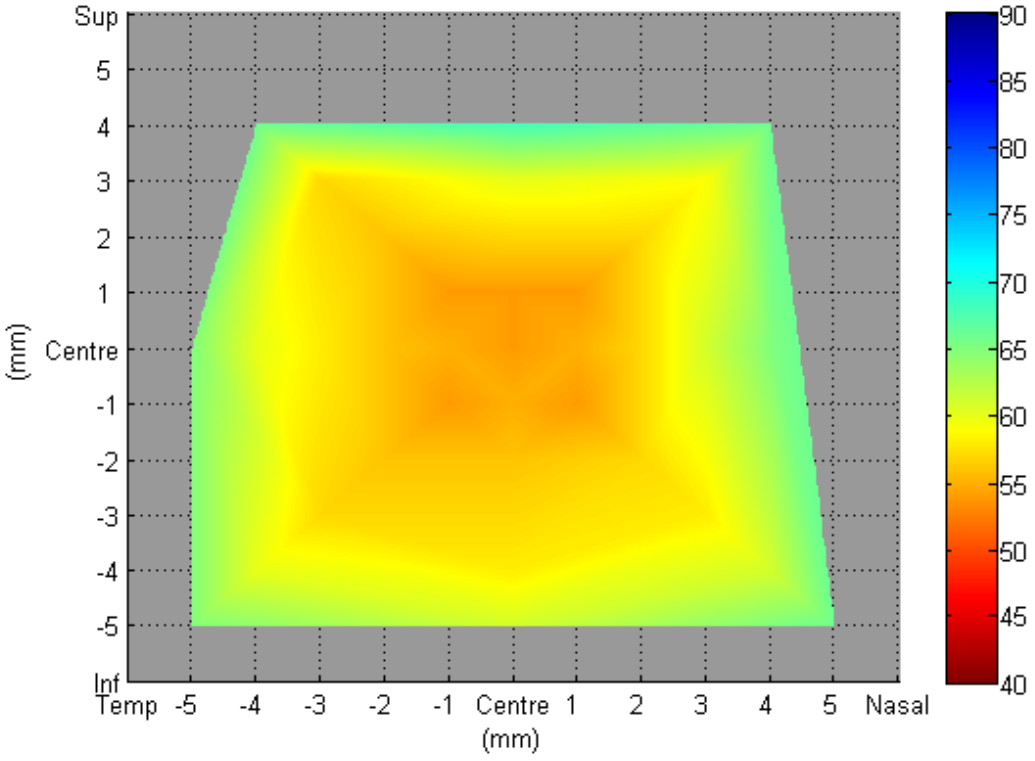

Although the analysis consisted of averaged data from all subjects, there were a few occurrences where PET values greatly exceeded the mean. Figure 7.12 is an example of such a case, showing an OCT scan of the peripheral cornea of a single subject, obtained close to the lower limbus. PCT in this image was 732µm and PET was 96µm.

Figure 7-12 An OCT image of the inferior cornea of a single subject. The scan was obtained in the periphery, close to the lower limbus. Total corneal thickness was measured as 732µm and epithelial thickness as 96µm. Actual scan length was 1.13mm. Total corneal thickness was measured as 732µm (A-P) and epithelial thickness as 96µm (A-E). [A = anterior cornea, E = epithelial-stromal boundary, P = posterior cornea].

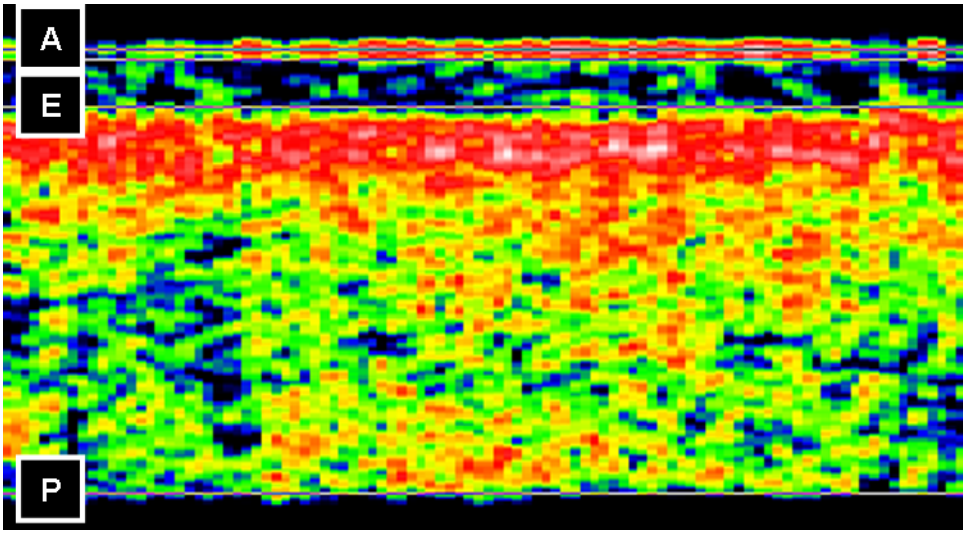

7.2.5 Discussion

This study investigated the thickness of the normal cornea and epithelium, measured with optical coherence tomography. Data were obtained at various points across the entire cornea, and later interpolated by imaging software to produce plots of thickness. Until very recently, this had not been accomplished previously using the OCT technique. (Li et al. 2006)

The average value for central corneal thickness in this study was 517μm, which was slightly lower than that found by other investigators that have used OCT to measure the normal cornea (Table 2.1). Although the values in Table 2.1 appear somewhat varied, most are within a similar range, apart from that by Izatt et al. (Izatt et al. 1994). All were obtained by different versions of OCT in various experimental settings and used a variety of methods to analyse the raw OCT scans for corneal thickness values.

Peripheral corneal thickness (PCT) is rarely reported in studies discussing corneal thickness measurement, particularly those using OCT. While it is established that the peripheral cornea is thicker than the centre, (Doughty and Zaman 2000; Edelhauser and Ubels 2003; Edmund 1987; Leibowitz and Waring 1998; Maurice 1957; Oyster 1999) few studies have been published describing which areas of the periphery are thicker. Using OCT to compare the superior, inferior, nasal and temporal areas, including points along the oblique meridians was a unique aspect of this study. The present study found the superior (S) region of the cornea to measure 77μm thicker than the inferior (I). Erickson et al. (Erickson et al. 2002) measured the vertical corneal meridian using optical pachymetry and found the superior periphery to be 31μm thicker than the inferior. It was concluded that this difference was due to the chronic hypoxic effect caused by the upper eyelid.

Most studies measuring normal corneal thickness have used the Orbscan topography system, where superior and inferior measurements are captured by default. (Gonzalez-Meijome et al. 2003; Liu and Pflugfelder 2000; Marsich and Bullimore 2000) Marsich et al. (Marsich and Bullimore 2000) found the superior region of the cornea to be 33μm thicker than the inferior

region. Liu et al. (Liu and Pflugfelder 2000) found only a difference of 20μm between the superior and inferior periphery. Gonzalez-Meijome and colleagues (Gonzalez-Meijome et al. 2003) however, found the superior peripheral cornea (at only 3mm from the centre) to be thicker than the inferior cornea by 102μm. The latter investigators stated that the thickness of one corneal meridian can be extended to any other, and so only used vertical thickness for their analysis. The present study has found evidence contrary to this statement, with marked differences between meridians. Corneal thickness measured by OCT in comparison with ultrasound pachymetry and Orbscan II has been discussed previously in Chapter 7.1.

OCT has gained renewed interest in recent years since it's adaptation from a retinal imaging device to a corneal one, (Bechmann et al. 2001; Muscat et al. 2002; Wang et al. 2002a; Wirbelauer et al. 2001) and it's ability to measure epithelial thickness in vivo is a major advantage over traditional instruments designed to measure corneal thickness alone, such as Orbscan. However, there seems to be a large variation in epithelial thickness values measured with OCT in its various designs (Table 2.2). While CET was found to be 54μm in this study, other studies have reported much higher values. Recently, Feng and Simpson (Feng and Simpson 2005) compared central to limbal epithelial thickness across the horizontal meridian using the same OCT instrument as that used in this study. They reported CET as reading 58μm and peripheral thickness as reading approximately 77μm, compared to PET of 63μm found in the present study. A possible explanation for this dissimilarity may be due to different inter-operator methods of data processing of the raw data scans (i.e. manual analysis versus using automated software) and the use of differing versions of the

OCT analysis software. However, the general findings were that PET was greater than CET in normal subjects.

Wirbelauer et al. (Wirbelauer et al. 2002a) used a slit-lamp adapted OCT to measure CET as 70μm, while early work by Izatt et al. (Izatt et al. 1994) quantified CET at 81μm and PET at 97μm. A hand-held real time OCT used by Radhakrishnan et al. (Radhakrishnan et al. 2001) measured a CET value closer to this study at 55μm. The only other work that has compared superior to inferior epithelial thickness in normal individuals and produced topographical maps of global epithelial thickness is that by Reinstein's group, (Reinstein et al. 2000) using arc-scanning digital ultrasound. However, their study found the opposite to that of the current study, reporting that epithelium increases in thickness from the superior (~55μm) to inferior cornea (~60μm), with the centre being as thick as the superior.

In summary, the normal cornea and epithelium was thinner centrally and thickened towards the periphery. The superior region was thickest and inferior region the thinnest. For the first time, this study measured meridional corneal and epithelial using OCT. We found inter-meridional differences in thickness, and with this in mind, caution should be applied when measuring corneal or epithelial thickness only along a single meridian.

7.3 Mapping thickness in keratoconus with comparison to rigid gas permeable lens wearers and non-lens wearers

7.3.1 Abstract

Purposes: To measure corneal, stromal and epithelial thickness along a 10mm diameter section along 4 meridians using OCT, in RGP lens wearers (RGP) and RGP-wearing keratoconics (KC) and to compare these measurements with healthy non-lens wearers (NLW) from the previous study.

Methods: Both eyes of 40 subjects were measured (20 RGP – 20F; mean age ± SD 23.9 ± 7.6yrs, and 20 KC – 7F:13M; 32.4 ± 8.1yrs). A fixation target employing LEDs in 8 directions of gaze was attached to the OCT and corneal images were obtained. Raw OCT scans were analysed to yield values for corneal and epithelial thickness and colour-coded maps were compiled. The results from this study were compared with those obtained for normal non-lens wearers (NLW) from the Chapter 7.2.

Results: Central corneal thickness (CCT) (mean ± SD) was thinner in the KC group (446.8 ± 68.1μm) than the RGP group (517.8 ± 31.5μm; $p<0.001$), and the NLW group (516.9 ± 21.3μm; $p<0.001$). The central cornea and stroma in the RGP group was not significantly different from the NLW group ($p>0.05$). Averaged peripheral corneal and stromal thickness was thinner in the KC subjects than in the NLW and RGP subjects (both $p<0.05$). Central epithelial thickness (CET) (mean ± SD) in the KC group (43.7 ± 6.5μm) was significantly thinner than the RGP group (50.0 ± 3.9μm) ($p<0.001$). CET of the RGP

subjects was significantly different from the NLW subjects (53.6 ± 2.2μm) ($p>0.001$). Peripheral epithelial thickness (PET) was thicker than central in the RGP (64.2 ± 3.7μm; $p<0.001$) and KC groups (59.6 ± 3.3μm; $p<0.001$).

Conclusion: In all groups, the inferior cornea and epithelium was thinnest, to a greater extent in the keratoconic group. The central epithelium in RGP wearers was a significant 4μm thinner than normal, suggesting that the epithelial thinning seen in keratoconus may be exacerbated by RGP lens-wear, and may encourage the progression of the condition.

7.3.2 Introduction

One consequence of keratoconus is irregular astigmatism and increased myopia, (Rabinowitz 1998; Zadnik et al. 1996) and once spectacles and soft contact lenses cease to improve visual acuity, rigid gas permeable (RGP) contact lenses are usually prescribed. These individuals with keratoconus often wear their RGP lenses on an extended wear basis. Therefore it is of the utmost importance that these lenses do not interfere with the integrity of the already compromised cornea, in particular the epithelium. A review by McMonnies (McMonnies 2005) stated that a decrease in corneal thickness may increase the risk of keratoconus development.

It is well known that keratoconus causes a thinning of the cornea and epithelium. (Aktekin et al. 1998; Hollingsworth et al. 2005a; Leibowitz and Waring 1998; Rabinowitz 1998; Somodi et al. 1996; Tsubota et al. 1995) However, there are conflicting reports on whether rigid contact lens wear encourages the morphology of the keratoconic cornea. It has been found that prolonged wear of RGP lenses can lead to epithelial thinning, by inhibiting the normal homeostatic turnover rate of the epithelium. (Ladage et al. 2003a, 2003b; Ladage et al. 2002b; Ladage et al. 2001b; Ren et al. 2002; Yamamoto et al. 2002) Ladage and colleagues (Ladage et al. 2002b; Ladage et al. 2001b) have shown that in normal subjects, extended RGP lens wear significantly decreases epithelial thickness by up to 10%, with an associated 10.5% increase in epithelial cell surface area, which was concluded to have been caused by the mechanical effect from the lenses. The reduced amount of epithelial thinning found in their studies following extended soft lens wear, may have had a physiological cause.

Moon et al. (Moon et al. 2006) investigated epithelial and conjunctival morphology in keratoconus, incorporating the effects of contact lens wear. They reported that the ocular surface shows changes in subjects with keratoconus wearing RGP lenses compared to those who do not. The authors concluded that contact lens wear may be directly related to the corneal changes in keratoconus. Hollingsworth et al. (Hollingsworth et al. 2005a) using slit scanning confocal microscopy, failed to observe any differences in the corneal morphology of keratoconic eyes, between those that wore RGP lenses and those that did not. The same author has previously reported that corneal morphology is no different between healthy RGP lens wearers and non-lens wearers. (Hollingsworth and Efron 2004) A similar conclusion was reached by Tsubota et al. (Tsubota et al. 1995) who stated that the epithelium of chronic wearers of hard contact lenses (with no corneal pathology) revealed no abnormalities and that the histological changes observed in keratoconus are due to the disease and not due to the wearing of contact lenses. The latter study did not report thickness changes. So the issue of whether epithelial thinning in keratoconus is partly caused by the wearing of RGP lenses requires further investigation.

This study attempted to answer the question; does RGP lens wear encourage the epithelial thinning seen in keratoconus? The study methodology was a continuation from the previous experiment, discussed in Chapter 7.2. In this study, topographical corneal and epithelial thickness was compared between RGP lens wearers and keratoconics. Both groups were also compared with results from Chapter 7.2 regarding normal corneal and epithelial thickness.

7.3.3 Study procedure

Subjects

Twenty RGP lens wearers (20 females, mean age (± SD) 23.9 ± 7.6 years, range 18 to 53 years) and twenty keratoconics (7 females and 13 males, mean age (± SD) 32.4 ± 8.1 years, range 21 to 48 years) were enrolled. All subjects in the RGP group had worn their lenses for a minimum of one year and had otherwise no history of ocular disease, including keratoconus. All subjects with keratoconus had been diagnosed with the condition bilaterally, for over a year, and were current RGP lens wearers. Each subject was asked to remove their contact lenses minutes before the start of measurement, and was permitted to re-insert them following the study visit. Both eyes of each subject were measured in the study (n = 80 eyes) and all readings were taken in the afternoon (between 1 and 5 pm) to ensure no residual corneal oedema following sleep.

Instrumentation

OCT was used in an identical method to that described in Chapter 7.2.3 to obtain corneal thickness measurements. The raw data were analysed in the same way, to yield values for corneal and epithelial thickness, and imported into the MATLAB program to construct similar colour-coded plots. The same statistical tests were applied to signify differences between the two groups of subjects, in terms of location for corneal and epithelial thickness.

7.3.4 Results

Data from both eyes from all 20 subjects within each group of subjects were included in the analysis. All data were averaged between eyes, and values for peripheral thickness refer to the fourth measured corneal location (point 4) along each meridian, unless otherwise stated. The average duration (± SD) of lens wear in the RGP lens wearing group was 9.1 ± 4.6years (range 1 to 20 years). The average duration since diagnosis (± SD) in the keratoconic group was 8.4 ± 7.6years (range 1 to 26 years).

Corneal Thickness

Tables 7.4 and 7.5 show the thickness of the central and peripheral cornea (at the limbus), displayed in order of thickest to thinnest regions, for the RGP lens wearing group and the keratoconic group, respectively. Mean (± SD) CCT of the 20 RGP lens wearing subjects was 517.8 ± 31.5μm and was significantly thinner than the periphery in all meridians ($p<0.001$). Mean CCT of the RGP lens wearing group was not significantly different from the non-lens wearing group ($p>0.05$) (Chapter 7.2). In the RGP group, the average thickness of the peripheral cornea nearest the limbus, across meridians was 678.6 ± 20.6μm. Peripheral corneal thickness (PCT) was thickest in the nasal region (N; 712.2 ± 28.0μm) and thinnest in the inferior region (I; 643.8 ± 28.9μm) – the difference between the two locations was significantly different ($p<0.001$). Corneal thickness values for the RGP lens wearing group are displayed in Appendix R.

In the keratoconic group, mean (± SD) CCT was 446.8 ± 68.1μm and was also significantly thinner than the periphery in all meridians ($p<0.001$). Average thickness of the overall periphery was 635.5 ± 37.7μm. PCT in the keratoconic subjects was thickest in the nasal (N; 677.4 ± 57.0μm) and thinnest in the inferior temporal regions (IT; 577.7 ± 51.0μm) ($p<0.001$ compared to each other). Corneal thickness values for the keratoconic group are displayed in Appendix S.

Table 7-4 Central and peripheral corneal thickness (mean ± SD, averaged between eyes) of the RGP lens wearing group. Peripheral thickness measurement shown was obtained adjacent to the limbus (4th fixation light) and is displayed from thickest to thinnest. (T=temporal, N=nasal, S=superior, I=inferior).

	Centre	N	ST	T	SN	IN	S	IT	I
CORNEA (mean)	517.8	712.2	703.9	689.8	678.6	676.2	675.8	648.9	643.8
(SD)	± 31.5	± 28.0	± 31.2	± 48.7	± 24.3	± 36.8	± 27.1	± 30.4	± 28.9

Table 7-5 Central and peripheral corneal thickness (mean ± SD, averaged between eyes) for the keratoconic group.

	Centre	N	ST	S	SN	IN	T	I	IT
CORNEA (mean)	446.8	677.4	674.9	664.1	664.1	630.6	616.6	578.9	577.7
(SD)	± 68.1	± 57.0	± 40.9	± 43.2	± 43.0	± 40.2	± 62.4	± 46.8	± 51.0

Figure 7.13 illustrates the mean thickness of the RGP lens wearing cornea at 4 points along each of the 8 directions of gaze. Each set of bars represents the cornea from limbus to limbus across the four meridians, as in Figure 7.8. This graph shows that in the periphery, the nasal cornea was the thickest and the inferior cornea was the thinnest.

Figure 7-13 Mean thickness of the RGP lens wearing cornea, at 4 points either side of the centre, along each of the 8 directions of gaze. Each set of bars represents the cornea from limbus to limbus along the four meridians: temporal to nasal (T to N), superior temporal to inferior nasal (ST to IN), superior to inferior (S to I) and superior nasal to inferior temporal (SN to IT).

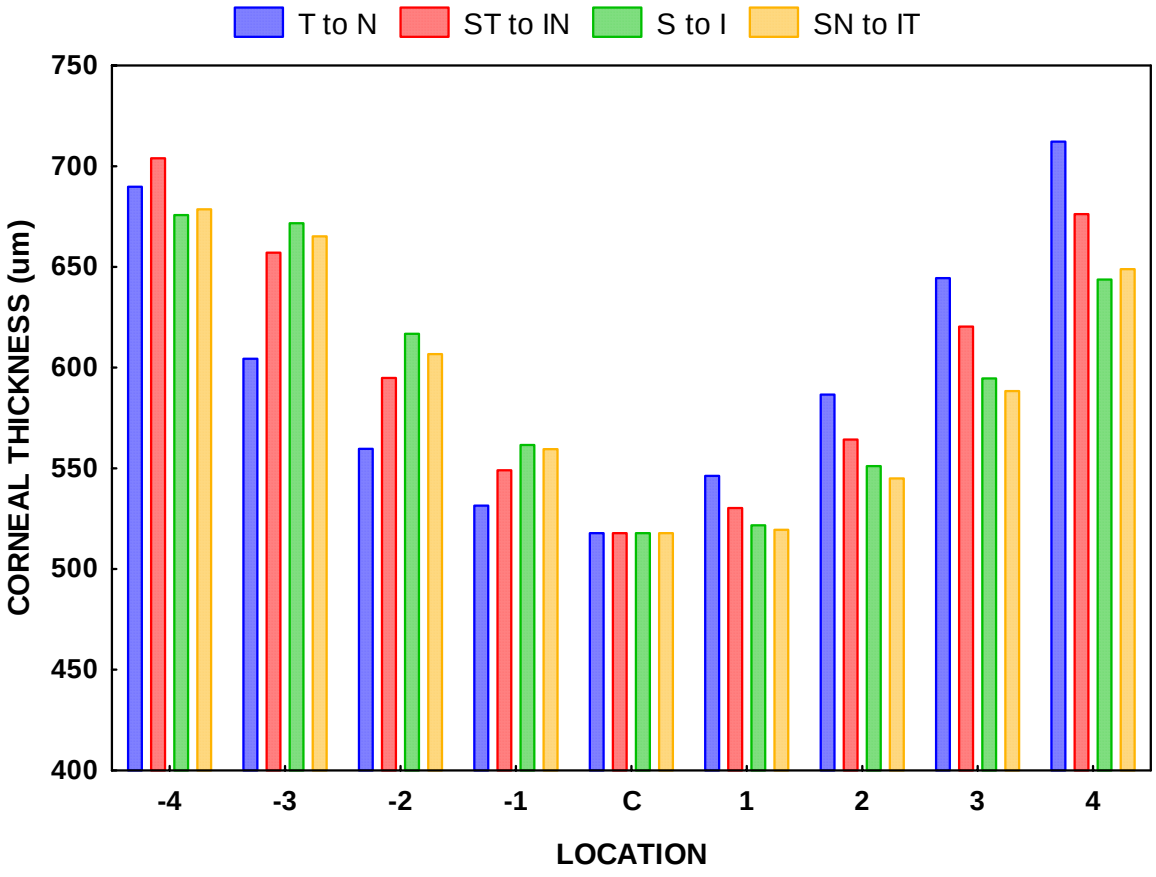

Figure 7.14 illustrates the mean thickness of the keratoconic cornea, comparing the centre to 4 points either side, along each of the 8 directions of gaze. This graph highlights that in the periphery, the nasal cornea was the thickest and the inferior temporal cornea was the thinnest.

Figure 7-14 Mean thickness of the cornea for the keratoconic group, centrally and at 4 points either side of the centre, along each of the 8 directions of gaze.

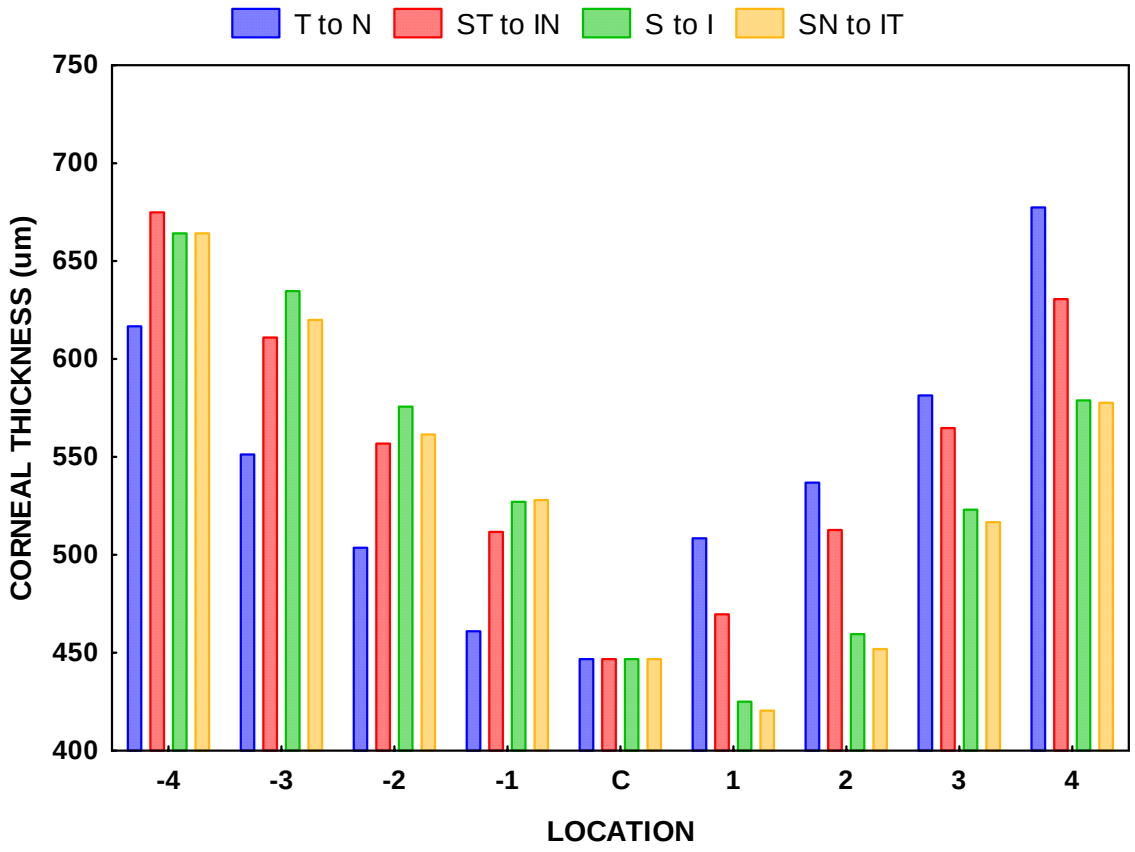

Figure 7.15 shows a colour-coded plot of corneal thickness for the RGP lens wearing group (mean of all subjects) and Figure 7.16 shows the plot for the keratoconic group. It can be

seen that the keratoconic cornea shows overall thinner values, by the greater distribution of red hues within the plot.

Figure 7-15 A plot showing mean thickness of the total corneal surface measured, for the RGP lens wearing group. The colour-coded legend (right) reads in microns and represents thinner areas of the cornea in red hues and thicker areas in blue.

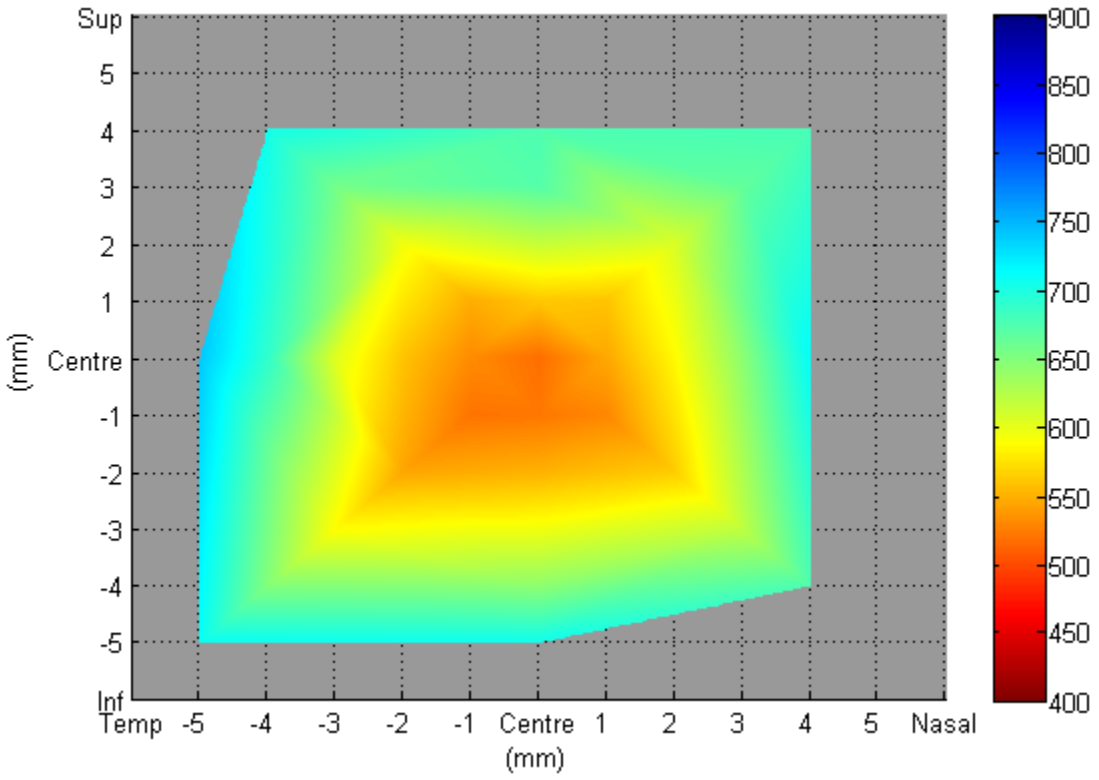

Figure 7-16 A plot showing mean corneal thickness for the keratoconic group. The colour-coded legend (right) reads in microns and represents thinner areas of the cornea in red hues and thicker areas in blue.

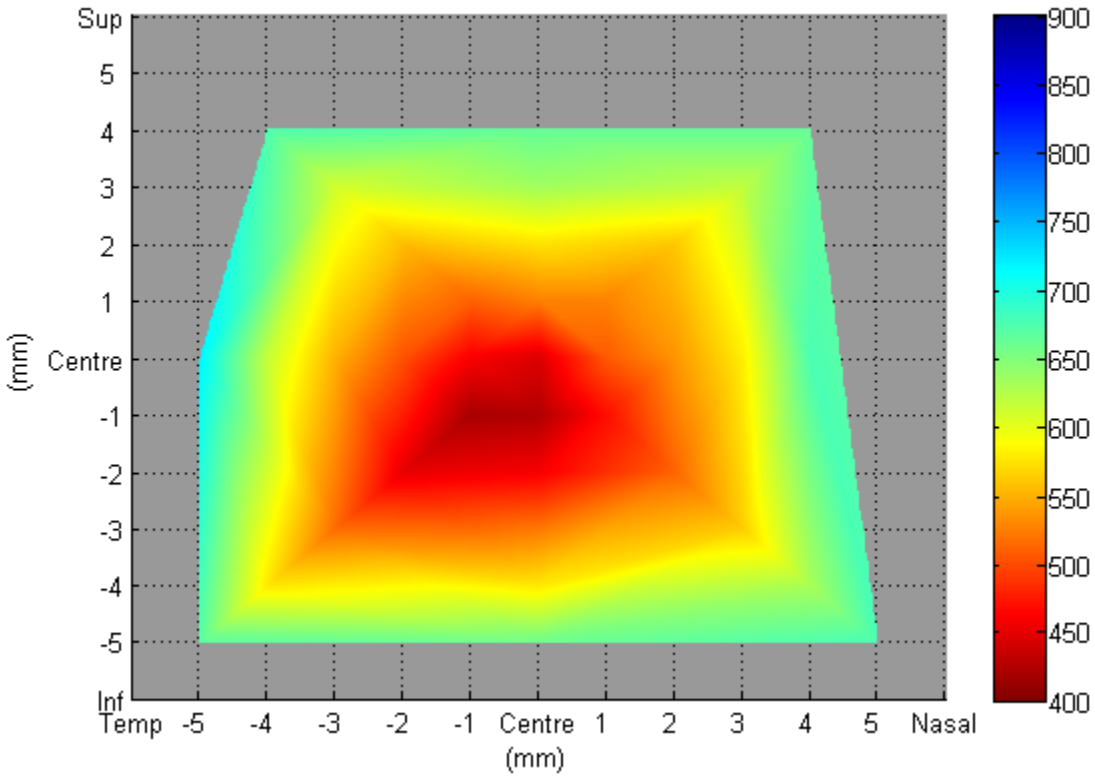

Stromal Thickness

Mean (± SD) central stromal thickness (CST) was 467.9 ± 31.5µm for the RGP lens wearing eyes, and 403.1 ± 63.7µm for the keratoconic eyes ($p<0.001$). CST was not significantly different between the non-lens wearing and the RGP lens wearing groups ($p>0.05$). The area of thinnest stroma in the keratoconic eyes was located at the first measured point in the inferior temporal direction (378.2 ± 68.9µm). Averaged peripheral stromal thickness (PST) in the RGP lens wearing group was 614.4 ± 20.7µm, and was significantly thicker than

averaged PST in the keratoconic group (575.9 ± 38.0μm; $p<0.05$). In the RGP lens wearing group, PST was thickest in the nasal periphery (645.4 ± 29.0μm) and thinnest in the inferior periphery (585.0 ± 28.3μm; $p<0.001$). A similar pattern was seen in the keratoconic group, with the thickest PST being in the nasal region (614.7 ± 56.6μm) and the thinnest PST being in the inferior temporal region (522.2 ± 52.0μm; $p<0.001$). Stromal thickness values for each measured corneal location for the RGP lens wearing, and keratoconic groups are displayed in Appendices T and U, respectively.

Epithelial Thickness

Tables 7.6 and 7.7 show the mean (± SD) thickness of the central and peripheral epithelium, in the RGP lens wearing subjects and the keratoconic subjects. Mean (± SD) central epithelial thickness (CET) of the RGP lens wearing group was 50.0 ± 3.9μm. Averaged PET across all meridians (64.2 ± 3.7μm) was significantly thicker than CET ($p<0.001$). In the RGP lens wearing group, peripheral epithelial thickness (PET) was thickest in the superior temporal region (ST; 67.9 ± 7.8μm) and thinnest in the inferior region (I; 58.7 ± 3.7μm) ($p<0.001$ compared to each other). Topographical epithelial thickness values for this group are listed in Appendix V.

In the keratoconic group, CET was 43.7 ± 6.5μm which was significantly thinner than the periphery in all meridians ($p<0.001$). CET in this group was thinner than in both the non-lens and the RGP lens wearing groups ($p<0.001$). The thinnest epithelium was located paracentrally in the inferior temporal region, and measured 42.3 ± 5.2μm ($p>0.05$ compared to CET). Averaged PET across all meridians was 59.6 ± 3.3μm. PET in the keratoconic

subjects followed a similar pattern to PET in the RGP lens wearing group, and was thickest in the superior region (63.8 ± 7.7μm) and thinnest in the inferior region (55.1 ± 5.0μm), the difference being significantly different ($p<0.001$). Topographical epithelial thickness values for this group are listed in Appendix W.

Table 7-6 Central and peripheral epithelial thickness (mean ± SD, averaged between eyes) of the RGP lens wearing group, displayed in order from thickest to thinnest regions. Peripheral thickness measurement shown was obtained adjacent to the limbus (4th fixation light) and is displayed from thickest to thinnest. (T=temporal, N=nasal, S=superior, I=inferior).

	Centre	ST	S	N	SN	IN	T	IT	I
EPITHELIUM (mean)	50.0	67.9	67.7	66.8	66.4	63.4	62.2	60.6	58.7
(SD)	± 3.9	± 7.8	± 8.5	± 5.7	± 7.3	± 5.0	± 5.8	± 3.9	± 3.7

Table 7-7 Central and peripheral epithelial thickness (mean ± SD, averaged between eyes) of the keratoconic subjects, displayed in order from thickest to thinnest regions.

	Centre	S	N	SN	ST	IN	T	IT	I
EPITHELIUM (mean)	43.7	63.8	62.7	61.6	61.3	59.2	57.6	55.5	55.1
(SD)	± 6.5	± 7.7	± 6.2	± 7.2	± 5.1	± 4.5	± 4.0	± 4.9	± 5.0

Figure 7.17 shows the mean thickness of the epithelium in the RGP lens wearing group, at 4 points along each of the 8 directions of gaze. Figure 7.18 shows the same for the keratoconic

group. These graphs highlight the mean epithelial thickness values for each location measured, respective of corneal meridian.

Figure 7-17 Mean thickness of the epithelium at 4 points either side of the centre, along 8 directions of gaze, in the RGP lens wearing group.

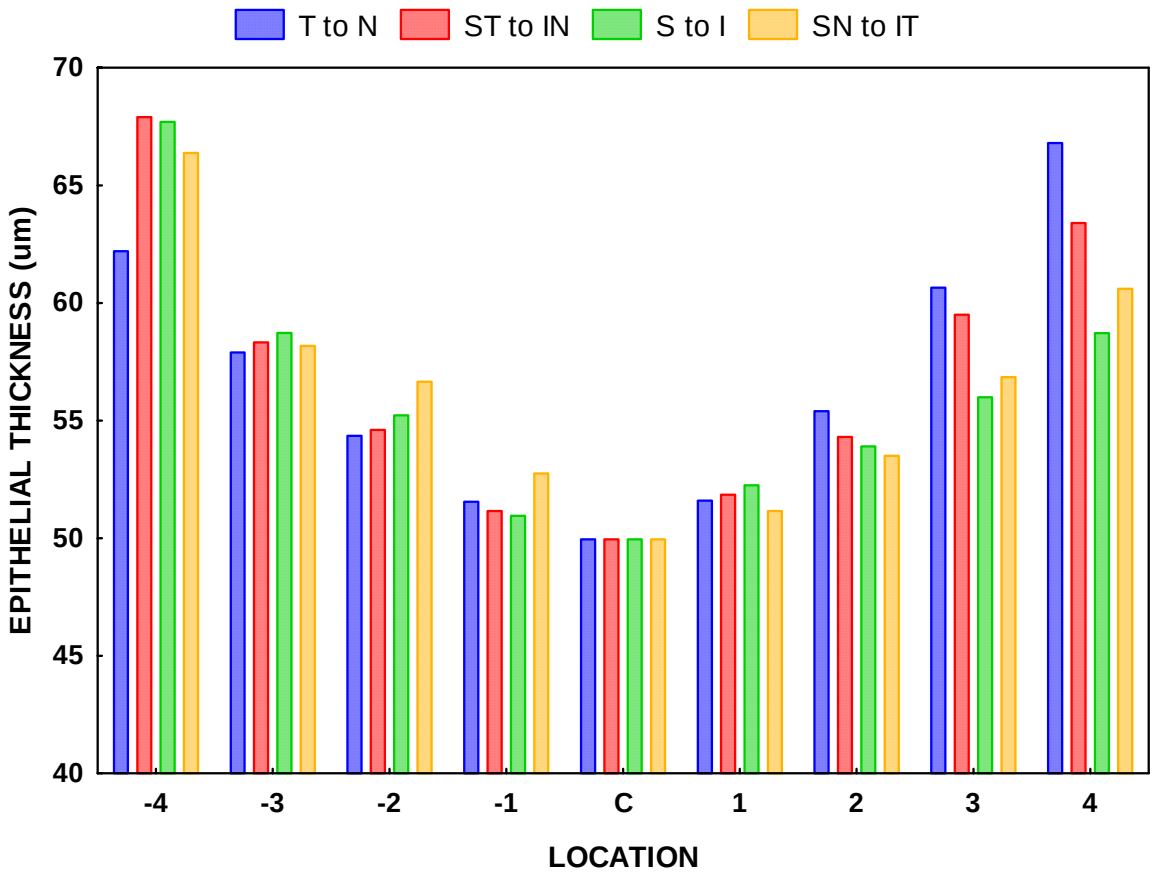

Figure 7-18 Mean thickness of the epithelium at 4 points either side of the centre, along 8 directions of gaze, in the keratoconic group.

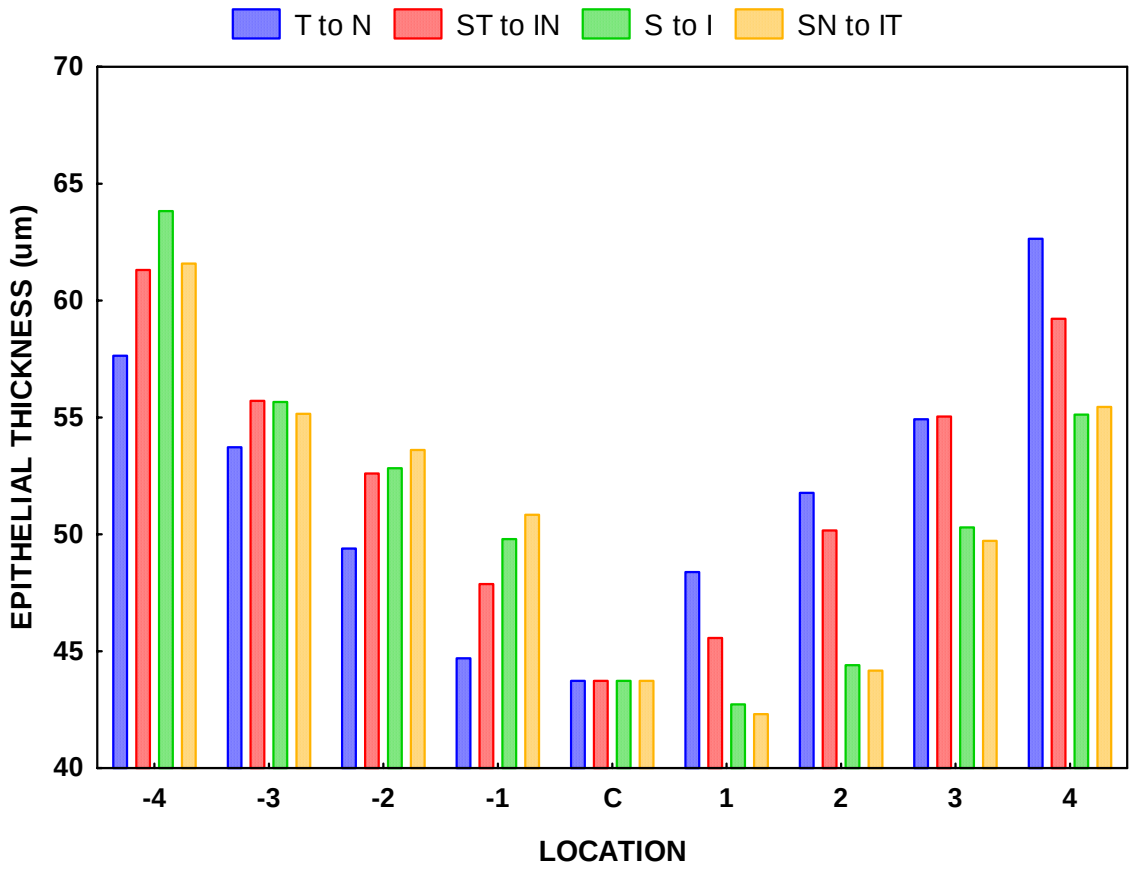

Figure 7.19 shows a colour-coded plot of mean epithelial thickness from all 20 RGP lens wearing subjects. The plot shows thinner epithelium located in the centre (red) with the peripheral epithelium being thicker (green). Figure 7.20 shows the same type of plot for the keratoconic group.

Figure 7-19 A plot showing mean thickness of the epithelium for the RGP lens wearing subjects. The colour-coded legend (right) reads in microns. The plot represents areas of thinner epithelium in red and thicker areas in green.

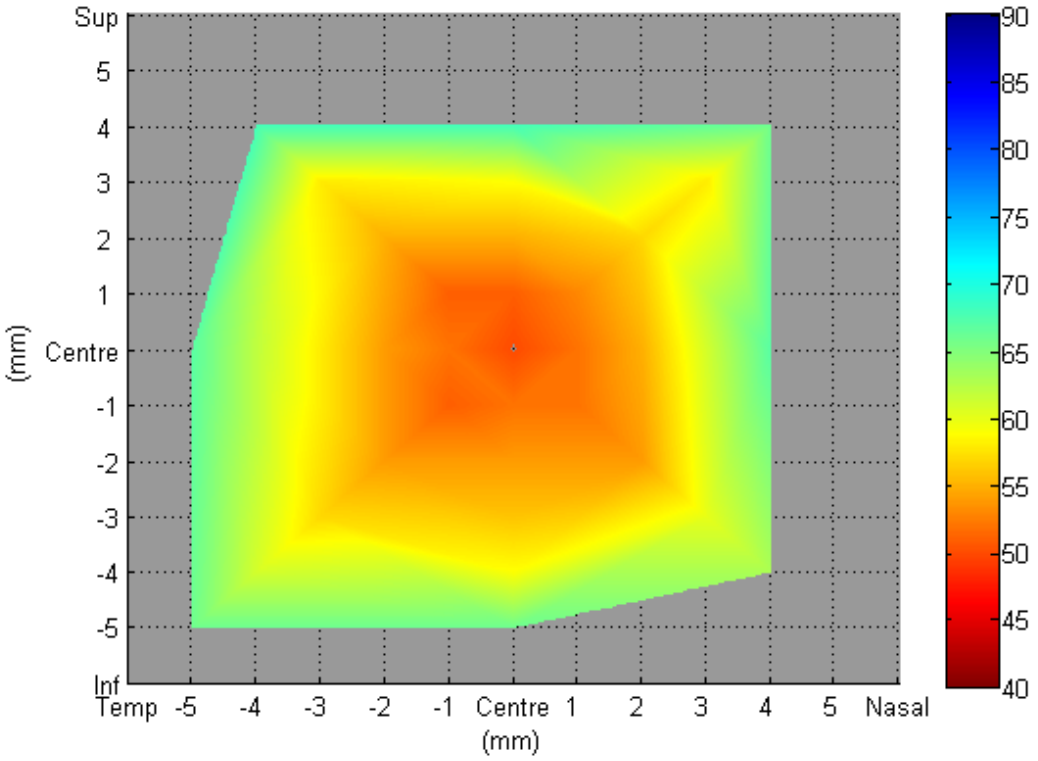

Figure 7-20 A plot showing mean thickness of the epithelium for the keratoconic subjects. The colour-coded legend (right) reads in microns.

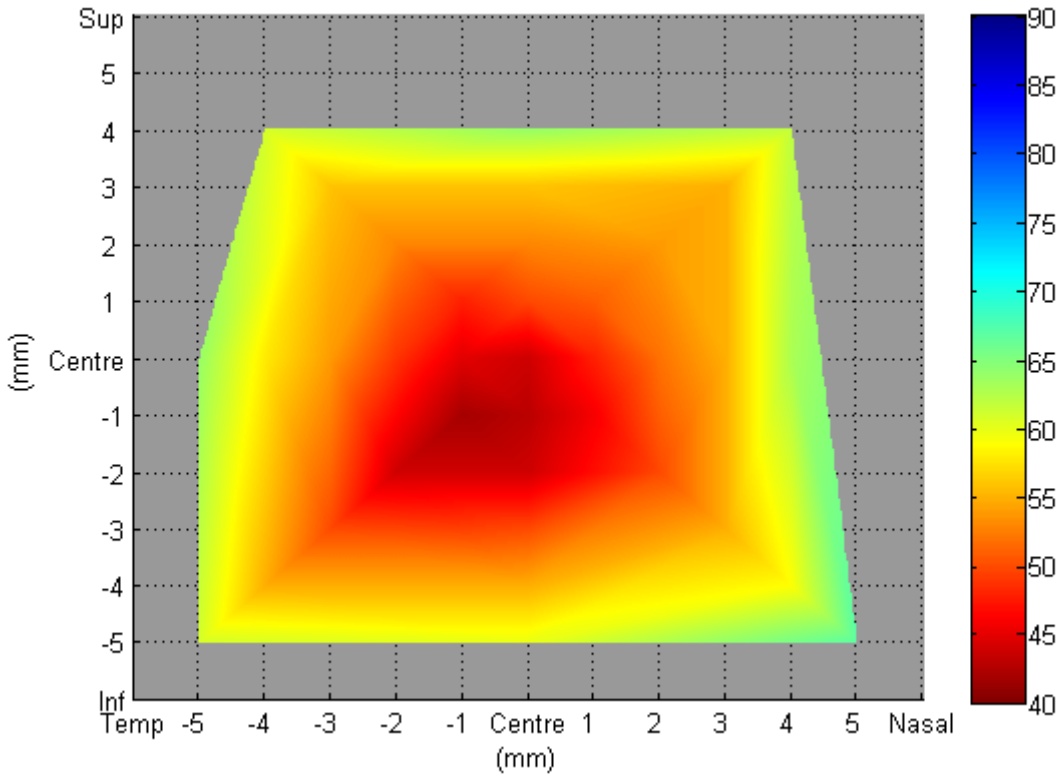

As a group, CET in the RGP lens wearing subjects was significantly thinner than in the non-lens wearing subjects (53.6 ± 2.2µm) from Chapter 7.2 ($p<0.001$). In addition, the RGP data were separated into two categories; to represent one group having worn their RGP lenses for less than ten years and the other group having worn their lenses for over 10 years (mean ± SD values are listed in Appendix X). CET in the 11 subjects who had worn their lenses for less than 10 years (length of lens wear 6.0 ± 2.9 years) was 50.2 ± 2.4µm and in the remaining 9 subjects (12.9 ± 3.3 years), CET was 49.7 ± 3.7µm. These two values were not significantly different to each other ($p>0.05$).

7.3.5 Discussion

This study used OCT to measure topographical corneal and epithelial thickness of the keratoconic cornea, and compared it with that of RGP contact lens wearers and the healthy non-lens wearing cornea discussed in Chapter 7.2. For the first time, topographical maps of corneal and epithelial thickness were constructed using OCT data for the keratoconic and RGP lens wearing subjects.

Many previous studies have restricted their measurement of the keratoconic cornea to the centre only, regardless of instrument capability. (Erie et al. 2002a; Hollingsworth et al. 2005a; Hollingsworth et al. 2005b; Kawana et al. 2005) However, it has been found that the majority of cones or areas of greatest corneal thinning in keratoconus, are located in the inferior and temporal regions of the mid-peripheral cornea, (Auffarth et al. 2000; Liu et al. 2002; Owens and Watters 1996; Pflugfelder et al. 2002) and therefore it is essential to measure and monitor the whole cornea. In the keratoconic subjects from the present study, the far periphery of the inferior temporal cornea was found to be 100μm thinner than its nasal counterpart. The cornea and stroma were found to be thinner in the inferior temporal region in this cohort. This reinforced the common finding of the keratoconic cone being located in the inferior temporal cornea.

Although it is well known that the cornea in keratoconus undergoes thinning due to stromal degeneration, (Auffarth et al. 2000; Leibowitz and Waring 1998; Li et al. 2002; Rabinowitz

1998; Zadnik et al. 1996), it is not expected for RGP lenses to have such a dramatic effect on the cornea and be significantly thinner than normal. In the present study, we found no difference in central corneal thickness between the RGP lens wearing cornea and the non-lens wearing cornea. However, previous investigators have found otherwise. (Braun and Anderson Penno 2003; Hirji and Larke 1979; Liu and Pflugfelder 2000; Nauheim and Perry 1985; Pflugfelder et al. 2002; Schoessler and Barr 1980)

Liu et al. (Liu and Pflugfelder 2000) reported that the entire thickness of the cornea was 30 – 50μm thinner than normal, as a result of long-term contact lens wear. CCT was significantly thinner in the 16% of subjects wearing hard contact lenses than the 84% wearing soft lenses. Holden et al. (Holden et al. 1985b) reported a significant 2.3% reduction in stromal thickness and a 5.6% decrease in epithelial thickness, after the extended wear of soft contact lenses. However, Myrowitz et al. (Myrowitz et al. 2002) found that soft contact lens wear did not alter central corneal thickness, but RGP lens wear reduced CCT by 37μm compared to non-lens wear.

One possible theory for corneal thinning as a result of long-term RGP lens wear, relates to epithelial-stromal interactions. (Kallinikos and Efron 2004; Kallinikos et al. 2006; Wilson et al. 2001b; Wilson et al. 2003c) It is hypothesized that contact lens wear could take the form of chronic epithelial microtrauma. This may trigger a chronic release of cytokines (in the tears, epithelium and stroma), which would stimulate keratocyte apoptosis (programmed cell death), and ultimately lead to stromal thinning. This loss of keratocytes due to mechanical stimulation from the lens is thought to occur to a greater extent in RGP lens wear than soft

lens wear. (Kallinikos and Efron 2004; Kallinikos et al. 2006) A similar process of apoptosis may also occur in the epithelium, leading a reduction in epithelial cells and therefore epithelial thinning. (Ladage et al. 2003d; Wilson et al. 2001b; Wilson et al. 2003c)

The main purpose of this study was to determine whether the long-term wear of RGP lenses in RGP lens wearing keratoconics has an exaggerated effect on the epithelial thinning. From this cohort of 20 RGP lens wearing subjects, there was no difference in the mean central epithelial thickness related to length of lens wear. There was no difference in CET in the group of subjects that had worn their RGP lenses for an average of 6 years, compared to those who had worn their lenses for 13 years. The average central epithelial thickness found in the RGP lens wearing group was a statistically significant 4μm (8%) thinner than the non-lens wearing group, from Chapter 7.2.

We may speculate from these results that RGP contact lens wear has an influence on the epithelial thinning seen in keratoconus, and may add to the progression of the condition. It may also be that this cohort of RGP subjects simply presented with a lower value for mean CET compared to non-lens wearers, since length of lens wear did not affect CET. Without measuring epithelial thickness in a cohort of keratoconic subjects who did not wear RGP lenses, we cannot conclude that epithelial thinning is greatly exacerbated by RGP lens wear; i.e. epithelial thickness may be just as thin in those who do not wear lenses as those who do. However, these findings emphasize the need for caution in the fitting of rigid contact lenses in keratoconic patients, ensuring the lens does not cause excessive bearing onto the corneal surface.

To date, few studies have discussed the effect of RGP lens wear on epithelial morphology in keratoconus. (Erie et al. 2002a; McMonnies 2005; Moon et al. 2006; Pflugfelder et al. 2002; Tsubota et al. 1995) Hollingsworth et al. (Hollingsworth et al. 2005a) stated that rigid lens wear had no effect on the keratoconic cornea. Tsubota et al. (Tsubota et al. 1995) analysed the epithelium of normal subjects who were chronic wearers of hard lenses, and found no abnormalities compared to those found in keratoconic eyes. However, some studies have found the opposite.

A recent study by Moon et al. (Moon et al. 2006) investigated the effects of contact lens wear on the ocular surface in keratoconus. They assessed tear film break-up time, conjunctival cell density and epithelial cell morphology in four groups of subjects: RGP lens wearing and non-RGP lens wearing keratoconics, healthy RGP lens wearers and healthy controls. The study reported that all the measures above were reduced in subjects wearing RGP lenses, and concluded that contact lens wear may be directly related to the ocular surface changes in keratoconus. Pflugfelder et al. (Pflugfelder et al. 2002) also compared subjects with keratoconus to contact lens wearers (80% soft lens wearers and 20% RGP lens wearers) and normal non-lens wearing subjects. Using the Orbscan, these authors found that central corneal thickness in the contact lens wearing eyes was a significant 42μm thinner than in the normal eyes. CCT in the keratoconic subjects was thinner than both other groups, but the authors failed to mention whether the keratoconic subjects were contact lens wearers or not.

Erie et al. (Erie et al. 2002a) measured keratocyte density using confocal microscopy, and in subjects with keratoconus who wore contact lenses, the keratocyte density was lower compared with those who did not. They also reported that among the non-lens wearers, there was no difference in keratocyte density between keratoconics and controls, which does not agree with the majority of studies discussing keratoconic change. These authors concluded that the changes seen in keratoconus are more related to contact lens wear, than to a biochemical effect due to the condition. However, Ladage et al. (Ladage et al. 2002a) found the extreme result of a 17% decrease in central epithelial thickness following 30 nights of hyper Dk/t RGP lens wear.

In summary, this study found that the total cornea and epithelium in subjects with keratoconus was thinner than in RGP contact lens wearers and non-lens wearers. In comparing the RGP lens wearing cornea to the non-lens wearing cornea, there was no difference in total corneal thickness, but central epithelial thickness was slightly reduced in the RGP lens wearing group. However, since there seemed to be no effect of length of lens wear on the epithelium in the RGP lens wearing subjects, we may still conclude that the epithelial thinning seen in keratoconus is mainly due to the condition and may only be slightly influenced by contact lens wear.

Chapter 8

Monitoring corneal change after Laser In-Situ Keratomileusis (LASIK)

8.1 Corneal, Stromal and Epithelial thickness changes throughout six months, after LASIK for myopia and hyperopia

8.1.1 Abstract

Purpose: To measure corneal, stromal and epithelial thickness along the horizontal meridian, following LASIK refractive surgery for myopia and hyperopia, using OCT.

Methods: Both eyes of twenty six subjects were monitored for six months, divided into two groups of 17 myopes (mean age ± SD 32.6 ± 8.9 years, range 21 – 48 years), and 9 hyperopes (mean age ± SD 47.0 ± 12.6 years, range 23 – 63 years). Baseline OCT measurements were taken prior to surgery, and repeated at one day, one week, one month and six months after surgery. OCT data were analysed to yield values for total corneal, stromal and epithelial thickness.

Results: In the myopic subjects one day after LASIK, the central cornea (mean ± SD) was -69.9 ± 20.2μm (-13.3 ± 3.7%) thinner than pre-operative levels, which comprised a central stromal change of -71.7 ± 21.7μm (-15.1 ± 4.3%; both $p<0.001$). The central epithelium in this group increased to a maximum of 55.6 ± 5.3μm (5.5 ± 10.0%) by the one month visit ($p<0.05$), and recovered by six months to be 1.0 ± 4.9μm thicker than baseline

($p>0.05$). The mid-peripheral epithelium increased by 4.6 ± 2.5µm (8.6 ± 4.7%) after one month, and was 4.2 ± 2.7µm (8.0 ± 5.1%) thicker than baseline at the end of the study ($p<0.001$).

Central corneal thickness in hyperopes did not change the day following LASIK, being 0.2 ± 9.6µm (0.0 ± 1.9%) thinner than baseline ($p>0.05$). The mid-peripheral stroma decreased by -16.6 ± 11.7µm (-3.2 ± 2.2%) at 1 day ($p<0.05$). At six months, this change had increased to -21.9 ± 14.7µm (-4.2 ± 2.7%; from pre-operative levels), but was not significantly different from the change found at Day 1 ($p>0.05$). The central hyperopic epithelium increased on Day 1 by 4.9 ± 5.5µm (9.7 ± 10.6%; $p<0.05$), but recovered towards baseline at six months ($p>0.05$). The mid-peripheral epithelium increased by a maximum of 4.7 ± 4.2µm (8.7 ± 7.6%) at one week ($p<0.05$) and was still thicker than baseline at six months ($p<0.05$).

Conclusion: Post-LASIK corneal and epithelial thickness profiles were different for myopic and hyperopic subjects. Corneal thickness decreased in the centre for myopes and in the mid-periphery for hyperopes, in accordance with laser ablation. Early epithelial thickening was seen centrally in hyperopes, whereas myopes showed greater epithelial response in the mid-periphery. Increased epithelial thickness in the mid-periphery had not recovered by six months in myopes or hyperopes, possibly indicating epithelial hyperplasia.

8.1.2 Introduction

Since the development of optical coherence tomography (OCT) for anterior segment imaging, an interest has arisen in the assessment of the cornea following laser in-situ keratomileusis (LASIK). Accurate pachymetry is essential in refractive surgery, and more so in procedures such as LASIK, where a minimum residual stromal thickness of 250µm is required post-operatively to maintain corneal integrity. (Chayet et al. 1998b; Pallikaris and Siganos 1997; Price et al. 1999; Seiler et al. 1998) Prior to anterior segment imaging with OCT, confocal microscopy was often used to evaluate corneal and epithelial changes following LASIK. (Erie et al. 2004; Erie et al. 2002b; Spadea et al. 2000)

One of the earlier studies to use OCT for imaging the post-LASIK cornea was by Ustundag et al. (Ustundag et al. 2000). These authors were interested in the detection of the flap interface and any flap dislocation / misalignment present, which was clearly resolved. The OCT detected flap striae and displacement that was otherwise missed by slit-lamp microscopy. They also quantified epithelial ingrowth, seen as a highly reflective area in the OCT image, and measured flap and stromal thickness. It was concluded from this study that OCT performed superiorly to biomicroscopy in the detection of flap interface complications.

Maldonado et al. (Maldonado et al. 2000) used OCT to measure stromal and flap thickness after LASIK for high myopia. Only central corneal measurements were obtained, at one day, one month and three months post-operatively. The day after surgery, central corneal thickness (CCT) was 420µm. This value increased by ~6µm at the one month visit and by

~9µm at the three month visit, indicating corneal regression. It was concluded that the source of the regression was likely located in the stroma and not the corneal 'cap', since this did not change in thickness during the study period.

In a similar study to that above, Thompson et al. (Thompson et al. 2003) also measured stromal and flap thickness after myopic LASIK using OCT. This group also restricted their measurements to the central cornea, but they monitored subjects for a shorter time, obtaining readings on the first and seventh post-operative day. Corneal flap thickness was an insignificant 4µm thicker at day 7 than at day 1, and the residual stromal bed was 9µm thinner. This latter finding suggests an opposite conclusion to that by Maldonado et al. (Maldonado et al. 2000), regarding corneal regression. Instead, Thompson et al. (Thompson et al. 2003) proposed the resolution of stromal oedema to be responsible for the decrease in stromal bed thickness.

The measurement of epithelial thickness after LASIK using OCT, was recently reported by Wang et al. (Wang et al. 2004). Central epithelial thickness (CET) was measured in myopic subjects, and monitored at one day, one week and one month post-operatively. This study found the pre-operative epithelium to measure ~60µm, which thinned insignificantly the day following surgery. At one week, CET remained at baseline levels, but significantly thickened at one month to ~65µm. The authors suggested epithelial hyperplasia as a possible cause for the thickening.

To date, there are few studies reporting epithelial thickness changes following LASIK for hyperopia (Reinstein et al. 1999), and no studies using OCT to measure epithelial thickness after hyperopic LASIK. In this study, OCT was used to measure and monitor corneal, stromal and epithelial thickness, following LASIK for both myopia and hyperopia. Thickness measurements were obtained across the horizontal corneal meridian to assess central, as well as peripheral changes, and subjects were monitored over a six month period.

8.1.3 Study procedure

This study was performed in conjunction with The Laser Clinic (TLC) at the School of Optometry at the University of Waterloo. A target cohort of 50 subjects was intended, to undergo LASIK refractive surgery and follow-up within a reasonable timeline for the study. All subjects had consented to undergo CustomCornea® wavefront-assisted LASIK. Wavefront results from the LADARWave™ (Alcon, Fort Worth, Texas) have been reported elsewhere (MacDougall et al. 2002, 2003). The LASIK flap was created by the Hansatome microkeratome (Bausch and Lomb, Rochester, NY).

Prior to the day of surgery, baseline OCT measurements were obtained at nine locations across the horizontal cornea, centrally and at four points either side of the centre, in the same manner as in previous studies using the fixation target in Figure 3.7. One day after the LASIK procedure, subjects attended for follow-up OCT measurements. The measurements were repeated one week following surgery, and again at one month and six months. All

study visits were conducted at the CCLR, with subjects attending TLC for ophthalmic attention only if medically necessary.

Since the myopic ablation profile differed from the hyperopic ablation profile in LASIK (discussed in Chapter 2), the subjects were divided into separate groups according to refractive error. In all subjects however, the LASIK flap was created with a superior hinge. The raw OCT data were analysed as described previously (Chapter 3) to yield thickness values, and compared to pre-operative values. Statistical analysis involved repeated measures ANOVA and Tukey HSD post-hoc testing to signify differences between pre- and post-operative thickness.

8.1.4 Results

Twenty six subjects were successfully monitored for six months, divided into two groups of 17 myopes (mean age ± SD 32.6 ± 8.9 years, range 21 – 48 years), and 9 hyperopes (mean age 47.0 ± 12.6 years, range 23 – 63 years). The mean ± SD pre-operative refractive error (spherical equivalent) for the 17 myopes was -2.94 ± 1.27D (range -0.75 to -5.13D), and for the 9 hyperopes was +1.67 ± 1.03D (range +0.13 to +3.38D).

Many subjects who were originally enrolled into the study were discontinued post-operatively, because they underwent conventional LASIK and not the CustomCornea® procedure. Subjects who did not complete the full six month follow-up were excluded from

the data analysis. There was no significant difference between eyes pre- or post-operatively at any time during the study, and so all results are reported as the average of both eyes.

Corneal Thickness:

Pre-operative central corneal thickness (CCT) (mean ± SD) for the myopic group was 525.6 ± 30.8μm. Figure 8.1 shows corneal thickness following LASIK in the myopic subjects. In these subjects one day after LASIK, the central cornea was -69.9 ± 20.2μm (-13.3 ± 3.7%) thinner than pre-operative levels ($p<0.001$). After a maximum thinning of -79.8 ± 19.1μm (-15.1 ± 3.5%) at one week, the central myopic cornea regressed by 14.3μm and was -65.5 ± 22.7μm (-12.4 ± 4.1%) thinner than baseline at the 6 month visit ($p<0.001$). Comparing CCT at 1 week to that at 6 months, the change was statistically significant ($p<0.05$).

Figure 8-1 Corneal thickness (in microns) throughout six months following LASIK, for myopic subjects.

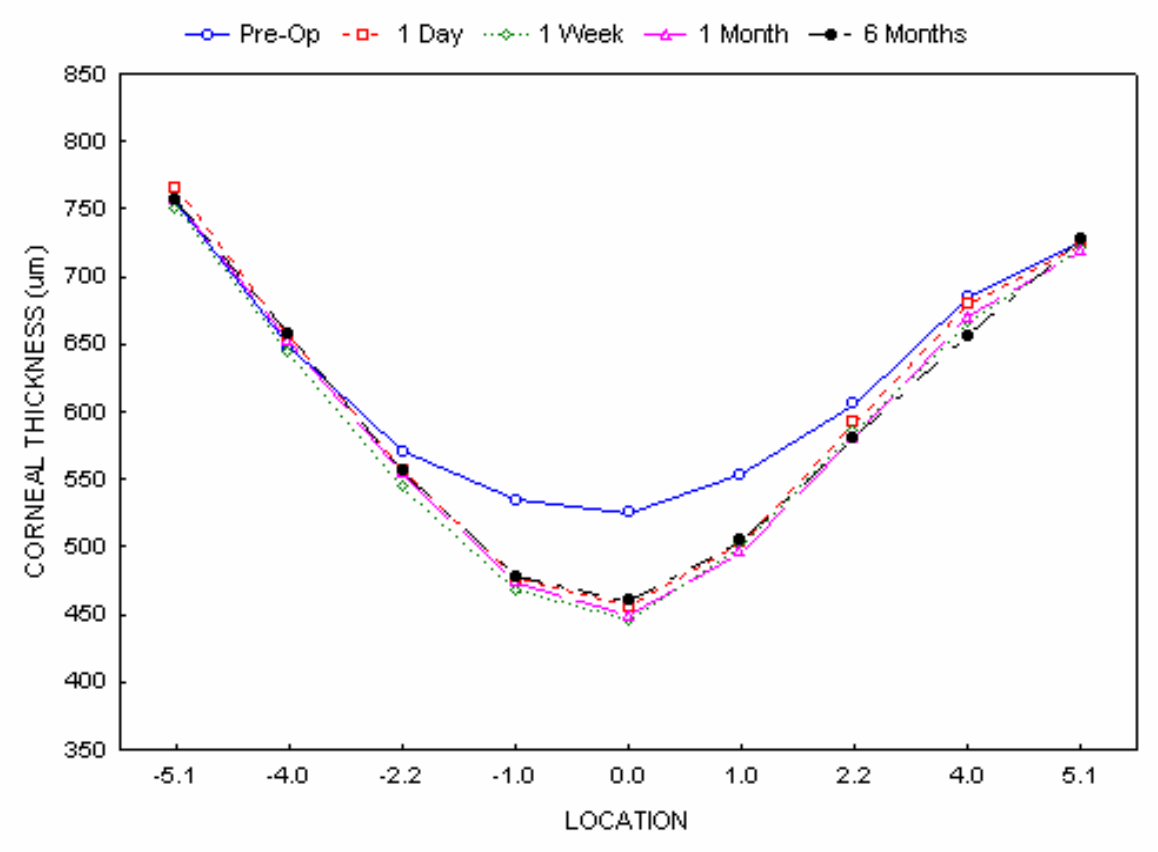

Figure 8.2 shows the thickness of the hyperopic cornea, followed through six months after LASIK. Pre-operative CCT (mean ± SD) for the hyperopic group was 532.7 ± 26.9µm. The central hyperopic cornea did not change in thickness the day after LASIK, being 0.2 ± 9.6µm (0.0 ± 1.9%) thinner than baseline ($p>0.05$). CCT decreased and stabilized by the one month visit, and was -7.3 ± 7.2µm (-1.4 ± 1.2%) at six months ($p>0.05$ from baseline). The mid-peripheral cornea decreased by -15.4 ± 11.2µm (-2.7 ± 1.9%) at 1 day ($p<0.05$). At six

months, this change had increased to -19.7 ± 14.3µm (-3.4 ± 2.3%) but was not significantly different from the one day measurement ($p>0.05$).

Figure 8-2 Corneal thickness (in microns) of the hyperopic group, monitored for six months after LASIK.

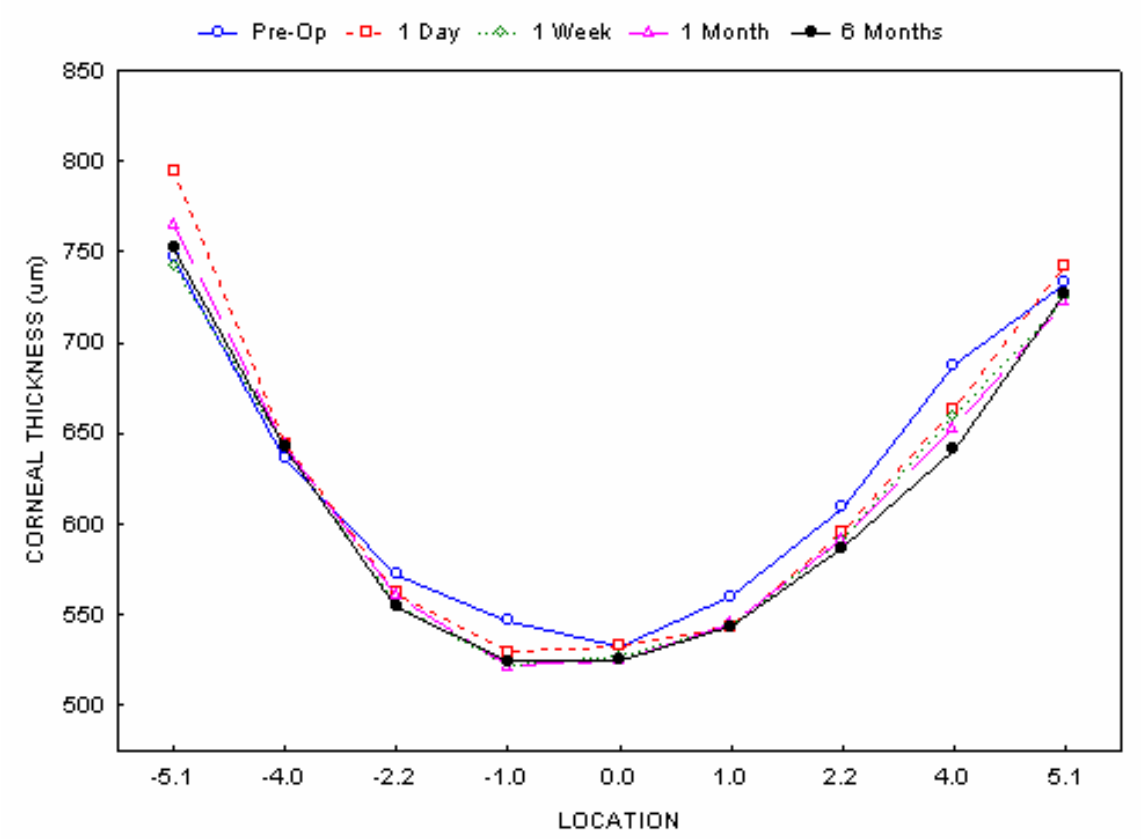

Stromal thickness:

Figures 8.3 and 8.4 show the real thickness and percentage changes in stromal thickness respectively, after LASIK for myopia. Baseline central stromal thickness (mean ± SD) for the myopic group was 472.9 ± 30.6µm. One day after LASIK, the central stroma was -71.7 ±

21.7µm (-15.1 ± 4.3%) thinner than pre-operative levels ($p<0.001$). After a maximum thinning of -82.0 ± 21.5µm (-17.3 ± 4.2%) at one week, the central stroma had thickened by the 6 month visit and was -66.5 ± 24.5µm (-13.9 ± 4.8%) thinner than baseline ($p<0.001$).

Figure 8-3 Stromal thickness (in microns) of the myopic cornea, during six months after LASIK.

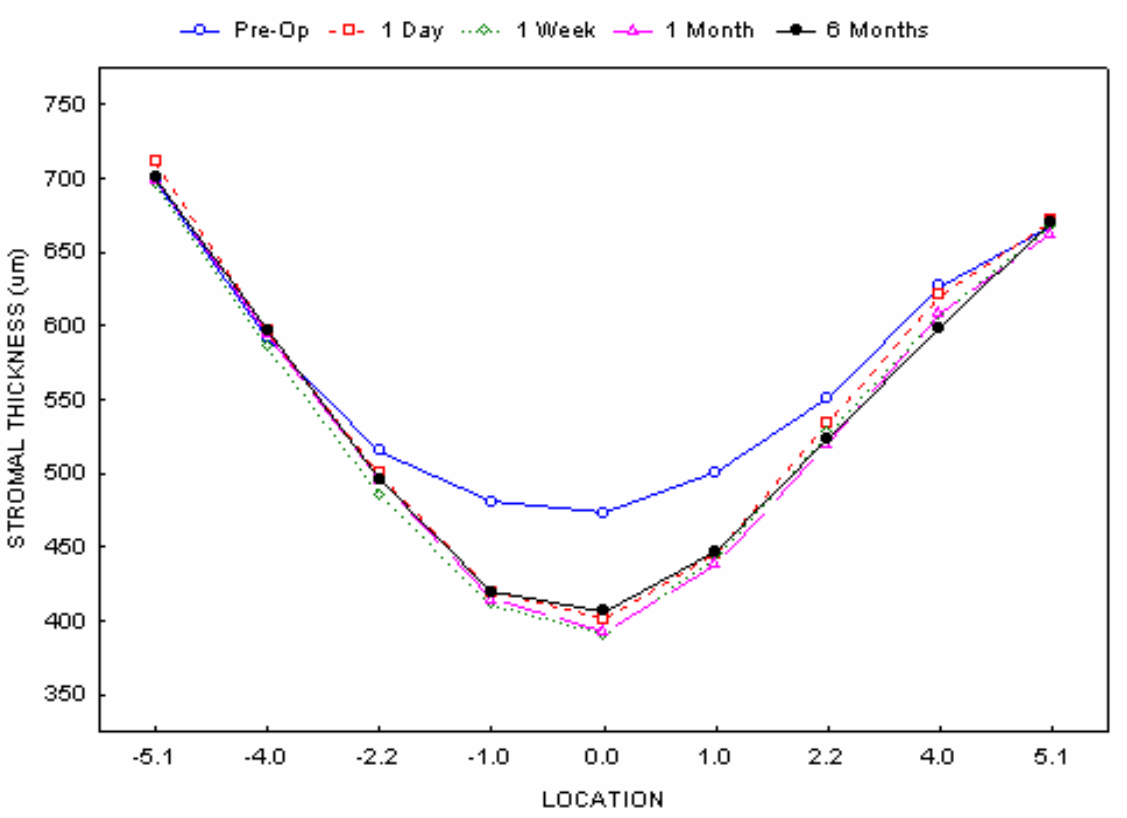

Figure 8-4 Change in stromal thickness from pre-operative levels, following LASIK for myopia.

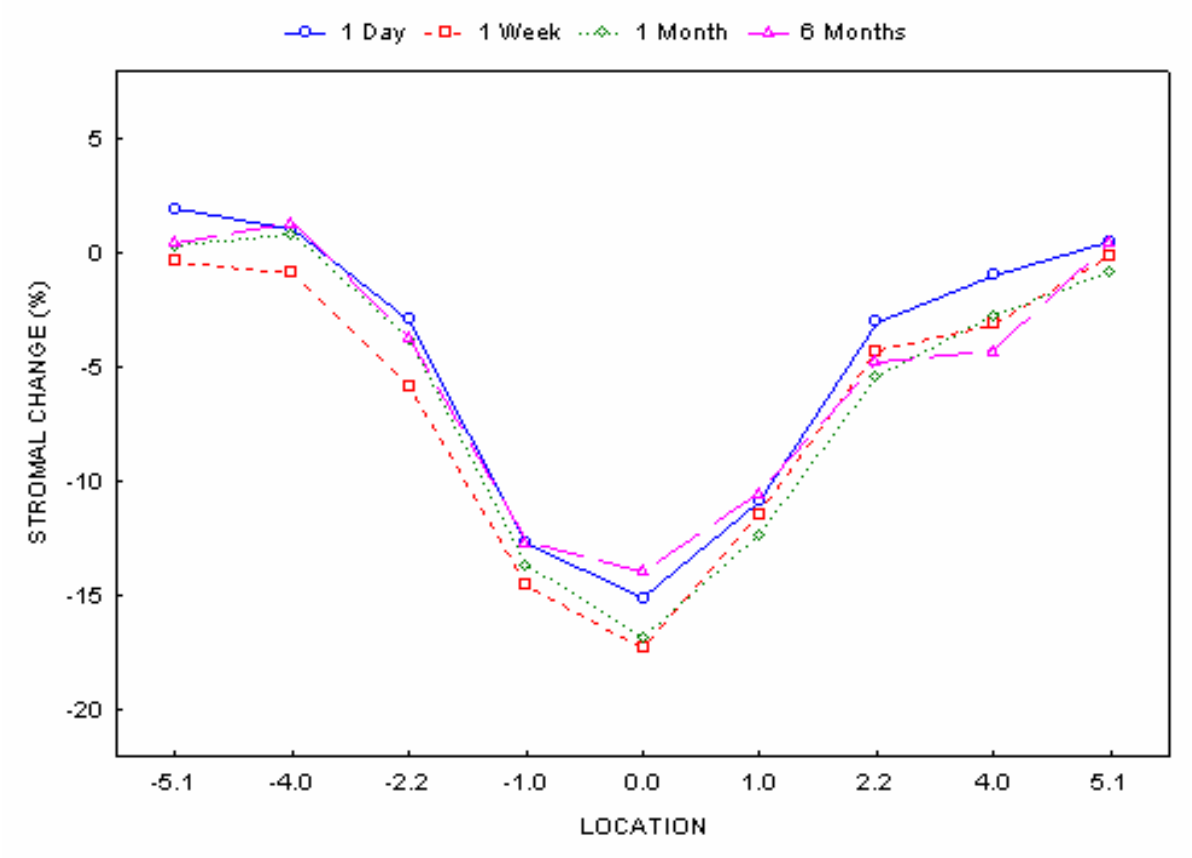

Figures 8.5 and 8.6 show the real thickness and percentage changes in stromal thickness respectively, for the hyperopic subjects. Pre-operative central stromal thickness (mean ± SD) in this group was 481.8 ± 27.3µm. Central stromal thickness decreased by -5.1 ± 9.3µm (-1.0 ± 1.9%) the day after LASIK ($p>0.05$). Greatest central stromal change occurred at one week (-2.4 ± 1.2%), but was not significantly different from baseline ($p>0.05$). The mid-peripheral stroma showed more change, decreasing by -16.6 ± 11.7µm (-3.2 ± 2.2%) at 1 day ($p<0.05$). At six months, this change had increased to -21.9 ± 14.7µm (-4.2 ± 2.7%, from

pre-operative levels), but the additional thinning was not significantly different from the amount seen at Day 1 ($p>0.05$). The topographical stromal thickness changes (mean % ± SD) after LASIK for myopia and hyperopia are listed in Appendices Y and Z, respectively.

Figure 8-5 Stromal thickness (in microns) after LASIK in the hyperopic group.

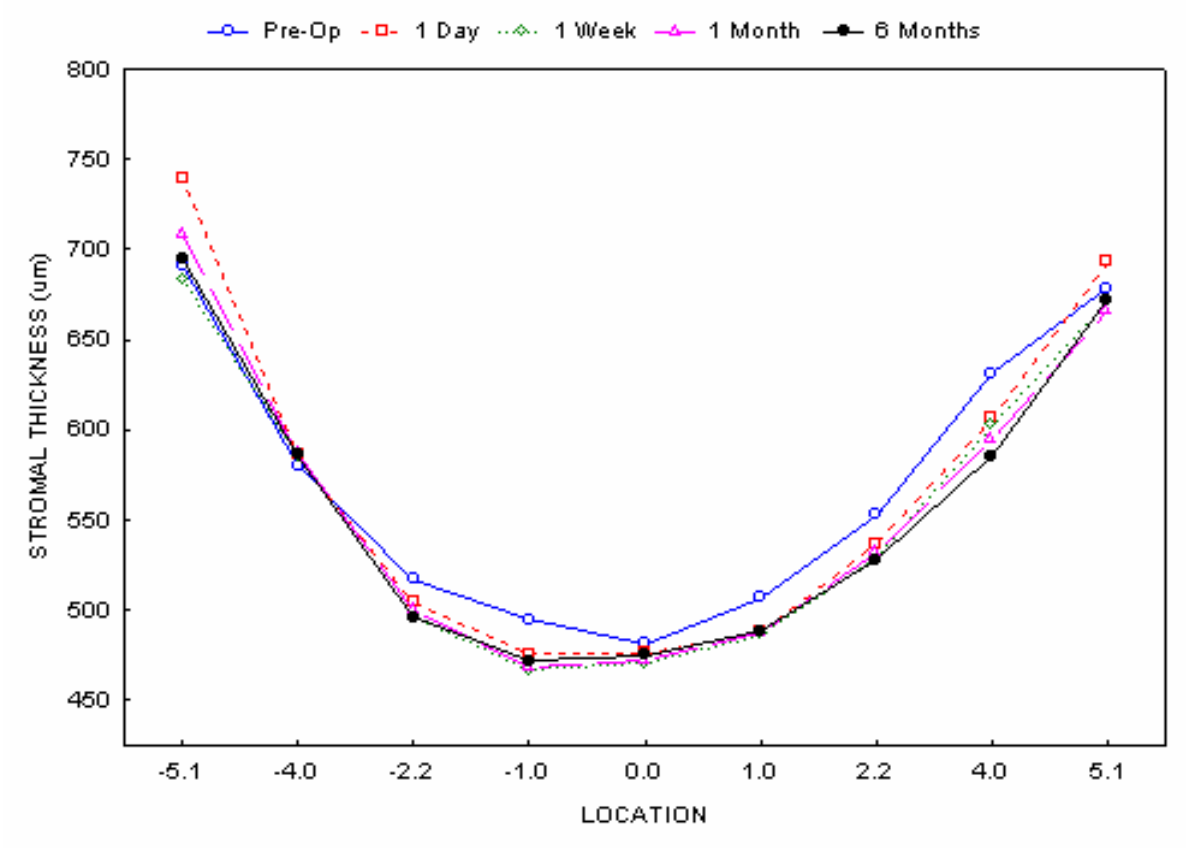

Figure 8-6 Percentage change (%) in stromal thickness after hyperopic LASIK.

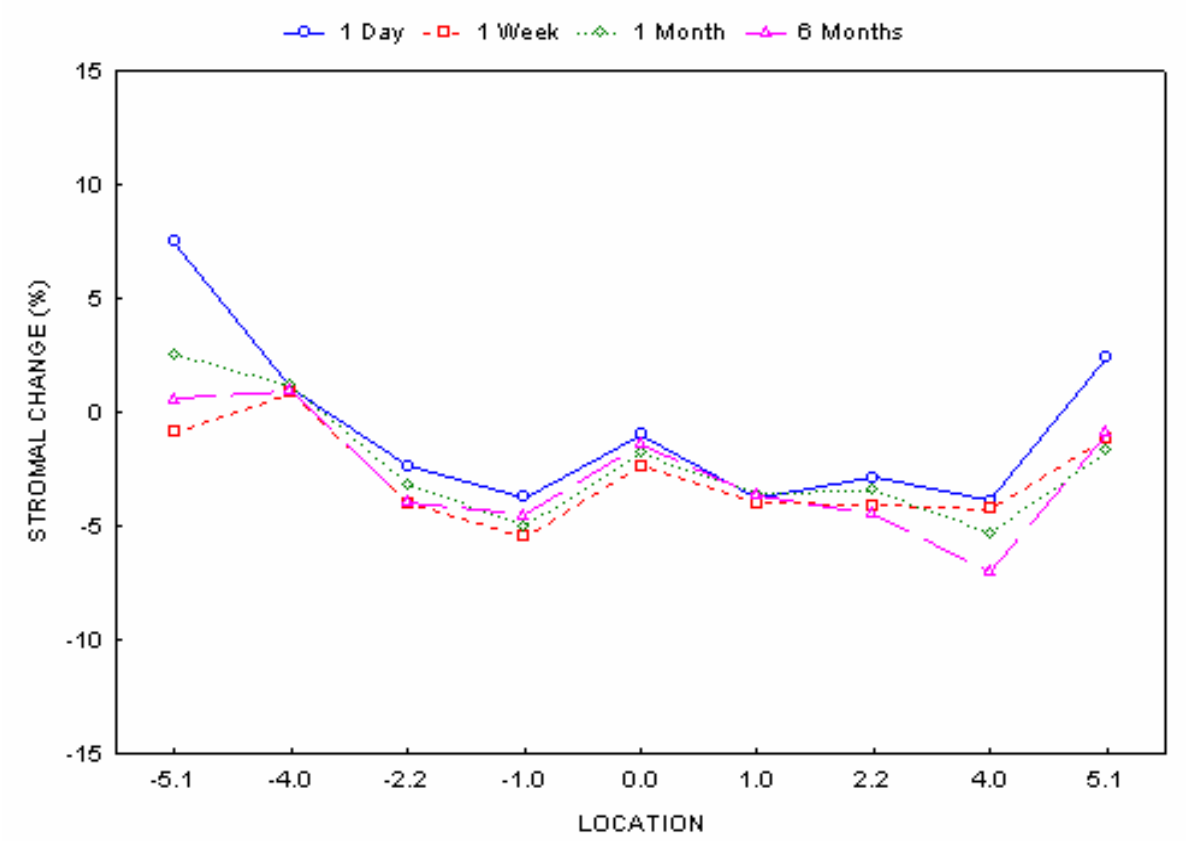

Epithelial thickness:

Figure 8.7 shows epithelial changes following myopic LASIK. Pre-operative central epithelial thickness (CET) (mean ± SD) for these subjects was 52.7 ± 2.2µm. CET increased to a maximum of 55.6 ± 5.3µm (5.5 ± 10.0%) by the one month visit ($p<0.05$), but had recovered by six months to be only 1.0 ± 4.9µm thicker than baseline ($p>0.05$). The mid-peripheral epithelium increased by 3.3 ± 3.1µm (5.8 ± 6.0%) on Day 1 ($p<0.05$), and increased further throughout the six months, to be 4.2 ± 2.7µm (8.0 ± 5.1%) thicker than baseline at the end of the study ($p<0.001$).

Figure 8-7 Epithelial change (%) from pre-operative values, following myopic LASIK.

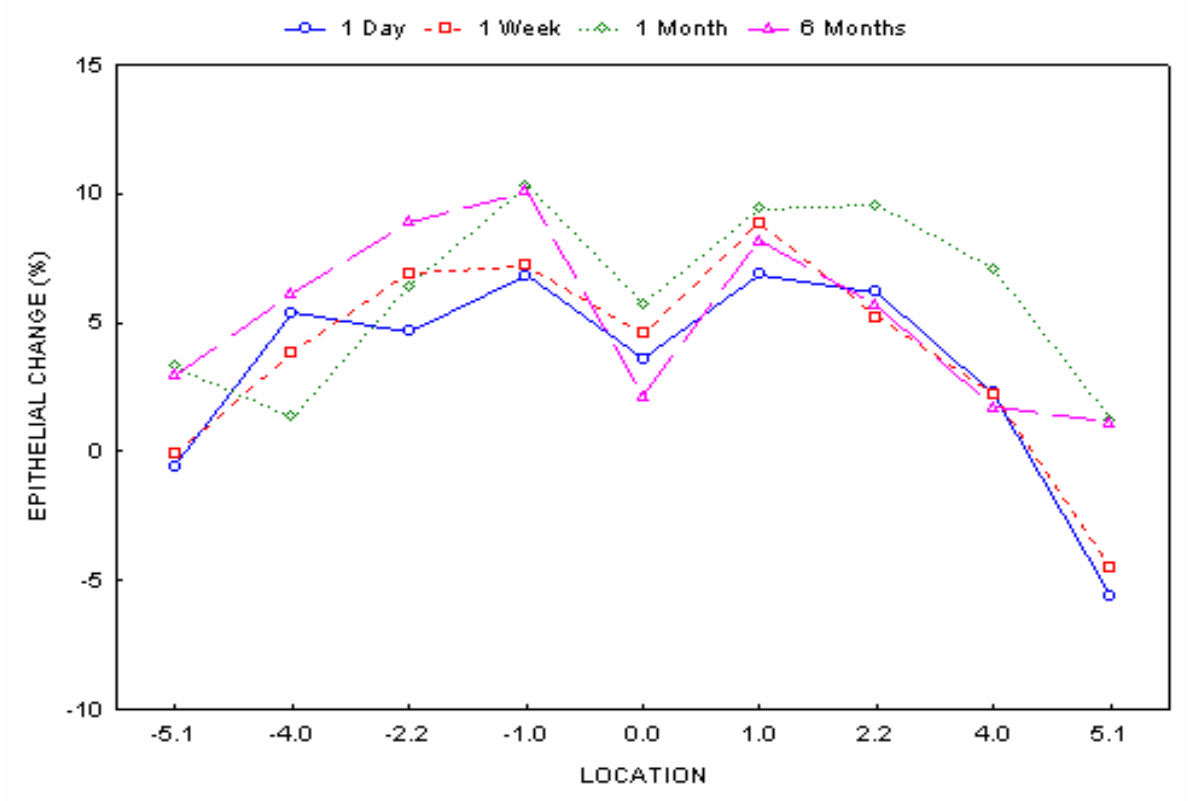

Figure 8.8 shows the percentage change in epithelial thickness in the hyperopic subjects. Pre-operative CET for this group was 50.9 ± 2.3µm. The central hyperopic epithelium increased on Day 1 by 4.9 ± 5.5µm (9.7 ± 10.6%; $p<0.05$). The one month visit showed recovery of CET towards baseline and at six months, was not different from pre-operative values ($p>0.05$). The mid-peripheral epithelium followed a similar pattern to CET, and increased by a maximum of 4.7 ± 4.2µm (8.7 ± 7.6%) at one week ($p<0.05$). At six months, the mid-peripheral epithelium was still 2.2 ± 2.5µm (4.1 ± 4.6%) thicker than baseline

($p<0.05$). The topographical changes in epithelial thickness (mean % ± SD) after LASIK for myopia and hyperopia are listed in Appendices AA and BB, respectively.

Figure 8-8 Percentage epithelial change following hyperopic LASIK.

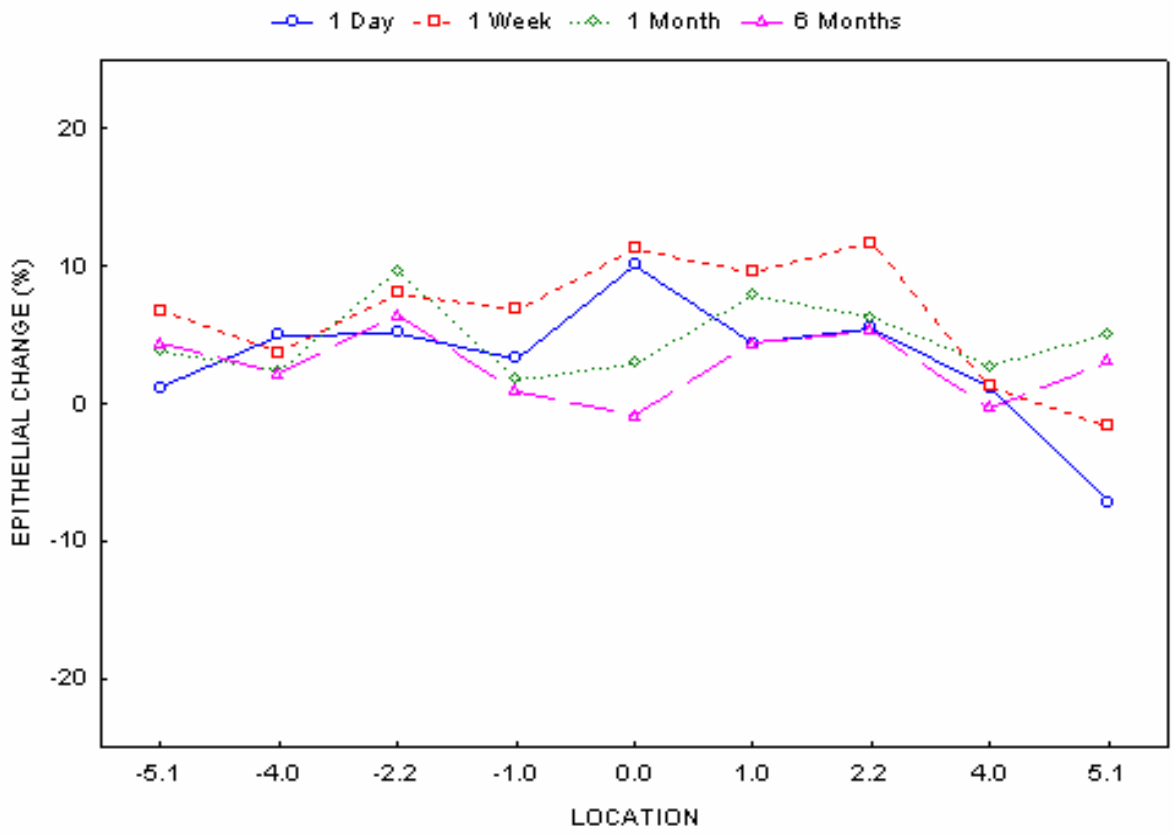

8.1.5 Discussion

This study measured total corneal, stromal and epithelial thickness after LASIK for myopia, and for the first time hyperopia, using optical coherence tomography. The use of OCT to measure these changes across the horizontal meridian, and not solely the centre, was a novel

aspect of this study. While there are many studies discussing corneal thickness changes following myopic LASIK (Avunduk et al. 2004; Erie et al. 2004; Hjortdal et al. 2005; Javaloy et al. 2004; Kawana et al. 2004; Kozak et al. 2003; Magallanes et al. 2001; Price et al. 1999; Ustundag et al. 2000), there are only a few that have reported post-operative thickness changes after hyperopic treatment (Huang et al. 2003; Muallem et al. 2004; Philipp et al. 2003).

In terms of stromal thickness change following LASIK, the results found in this study were not unexpected. The topographical pattern of change for the myopic stroma showed greatest thinning in the centre, with less mid-peripherally, since the laser ablation for myopic treatment was intended centrally. The pattern of thickness change was the opposite for the hyperopic stroma, showing a thinner mid-periphery than centre. However, this mid-peripheral stromal thinning (~4%) was not as marked as the central thinning seen after myopic treatment (~14%).

Regression of the cornea following LASIK is a well documented occurrence, and was noted in this study. (Chayet et al. 1998a; Dawson et al. 2005b; Huang et al. 2003; Lohmann and Guell 1998; Magallanes et al. 2001; Maldonado et al. 2000; Netto et al. 2005b; Reinstein et al. 2005; Wilson et al. 2001a) Through stromal regeneration, the cornea attempts to replace the tissue that has been lost through laser ablation. (Chayet et al. 1998a; Moller-Pedersen et al. 2000; Netto et al. 2005b; Wilson et al. 2001a) A study by Avunduk et al. (Avunduk et al. 2004) did not find any changes in flap or epithelial thickness, but reported an increase of 30μm in the stromal bed, at one month following myopic LASIK. These authors proposed a

regression of approximately 10μm in stromal thickness being accountable for approximately 1D of refractive regression. Ivarsen et al. (Ivarsen et al. 2004) reported a regression of 13μm, once stromal thickness had stabilized after eight weeks. Erie et al. (Erie et al. 2002b) found a similar amount of stromal thickening after LASIK for myopia, reporting a 10μm regression at 12 months.

There are many studies that have reported on LASIK for hyperopia, but these do not often include measurements of corneal or epithelial thickness. (Argento and Cosentino 1998; Buzard and Fundingsland 1999; Cobo-Soriano et al. 2002; Jaycock et al. 2005; Jin et al. 2005; Nanba et al. 2005; Nepomuceno et al. 2004; Rosa and Febbraro 1999; Spadea et al. 2006; Zadok et al. 2000; Zadok et al. 2003; Zaldivar et al. 2005) A few of these studies do mention the occurrence of refractive regression, but do not discuss the possible causes. (Jaycock et al. 2005; Roman Guindo et al. 2005; Zadok et al. 2000) Philipp et al. (Philipp et al. 2003) reported histological changes after hyperopic LASIK, and found the areas of mid-peripheral stromal thinning to be partially obscured by epithelial hyperplasia.

The concern of practitioners however, is the affect of regression on the fine surface changes created by custom ablation LASIK. Through epithelial hyperplasia, the subtle effects of custom LASIK may be masked, especially following hyperopic treatment. (Netto et al. 2005b)

Epithelial hyperplasia has been detected by Ivarsen et al. (Ivarsen et al. 2004) one week after myopic LASIK measuring 4μm, while Nau et al. (Nau et al. 2005) found epithelial thickness

to increase by 9μm at one month and 12μm at five years. Erie et al. (Erie et al. 2002b) found a large increase of 22% in central epithelial thickness at one month after myopic LASIK, which did not change over a year. A study by Spadea et al. (Spadea et al. 2000), also found epithelial hyperplasia (6μm) at 12 months following myopic LASIK. These authors proposed a 10% increase in epithelial thickness being equivalent to approximately 1D of refractive regression.

Following LASIK for hyperopia, Zadok et al. (Zadok et al. 2000) concluded that regression tended to occur more often after the treatment of low and moderate amounts of hyperopia. This may be due to the masking effects of epithelial hyperplasia on the delicately ablated zones from hyperopic LASIK. Reinstein et al. (Reinstein et al. 1999) and Philipp et al. (Philipp et al. 2003) have made similar statements, observing that epithelial hyperplasia was restricted to the ablated regions after hyperopic LASIK, and possibly accounting for refractive regression.

Regarding the topographical pattern of epithelial thickness changes, throughout the study, the mid-periphery showed greater changes than the centre, in the myopic subjects. There are few studies reporting topographical epithelial thickness changes following LASIK. (Philipp et al. 2003; Reinstein et al. 2005; Reinstein et al. 2000) Reinstein et al. (Reinstein et al. 2000) constructed maps of corneal and epithelial thickness from data obtained by digital ultrasound pachymetry, following LASIK for myopia. After six months, the maps illustrated a central zone of epithelial thickening, spanning the ablation area. Central epithelial thickness increased from 54μm pre-operatively to 67μm after LASIK. This epithelial hyperplasia

gradually decreased towards the flap margin to 60μm. The hyperopic results matched closely to those from Philipp et al. (Philipp et al. 2003), who also found the mid-peripheral epithelium to be thicker than the centre.

This study used OCT to measure topographical thickness after LASIK, in both myopes and hyperopes. Earlier LASIK studies have often reported only central measurements, using OCT (Maldonado et al. 2000; Thompson et al. 2003; Ustundag et al. 2000; Wang et al. 2004), or commonly confocal microscopy. (Avunduk et al. 2004; Erie et al. 2004; Erie et al. 2002b; Ivarsen et al. 2004). OCT is a useful instrument for imaging the post-LASIK cornea, and would be an extremely beneficial tool in surgical practice.

8.2 Light Backscatter Analysis of the Incision Interface throughout six months following LASIK

8.2.1 Abstract

Purposes: To measure recovery of the stromal incision (flap interface) after LASIK, using light backscatter profiles to quantify scatter intensity and width of the incision interface, using OCT.

Methods: Both eyes of twenty six LASIK subjects are reported in this study, divided into groups based on pre-operative refractive error, as in Chapter 8.1. Central corneal OCT measurements were obtained pre-operatively, at one day, one week, one month and six months following surgery. Raw OCT scans were analysed using custom built software to yield values for pre-incision and post-incision light scatter intensity, as well as for the width of the incision (the interface was defined by the band of increased scatter either side of the incision). Intensity values were represented in signal-to-noise ratios.

Results: One day after LASIK, the flap interface could be clearly seen on the OCT image, represented by a large peak on the respective scan profile. Signal-to-noise ratio of the incision peak significantly increased pre- and post-incision, on day one from baseline ($p<0.001$). Pre-incision S:N ratio was significantly greater than post-incision, for myopic subjects ($p<0.001$) and for hyperopic subjects ($p<0.05$). Only the post-incision intensity had recovered to baseline at six months, in both groups (both $p<0.05$). However, the flap interface was not always visible in the OCT images at the six month measurement. The

width of the incision interface (mean ± SD) was greatest at one week post-LASIK, in myopes being 57.8 ± 10.6μm, and in hyperopes being 64.2 ± 7.8μm ($p>0.05$ compared to each other). There was no difference in incision width between groups at any time during the study ($p>0.05$).

Conclusion: There was a greater increase in light backscatter on the anterior side of the incision (nearer the epithelium) than the posterior side (in the mid-stroma) during healing after LASIK. The band of interface backscatter decreased with time, suggesting a reduced area of healing at six months. These results suggest that both interface signal-to-noise ratio and width may be used as indices of healing following LASIK.

8.2.2 Introduction

The previous study used OCT to measure and monitor corneal, stromal and epithelial thickness, following Laser In-Situ Keratomileusis (LASIK). While these parameters assessed corneal surface change after LASIK, analysing the light backscatter of the OCT image may improve our understanding of wound healing after LASIK.

Previous wound healing studies have found increases in keratocyte activity at the site of injury. (Bansal and Veenashree 2001; Helena et al. 1998; Ichijima et al. 1994; Netto et al. 2005b; Wilson 2000; Wilson et al. 2003c) After LASIK, the site of interest is often the flap interface and the flap margins. Many investigators have imaged this region of disorganised stromal tissue, representing the flap interface, often using confocal microscopy to compare a micro-cellular view with histological samples. (Dawson et al. 2005a; Dawson et al. 2005b; Dawson et al. 2005c; Ivarsen et al. 2003; Kato et al. 1999; May et al. 2004; Netto et al. 2005b; Philipp et al. 2003; Tanaka 2000; Tervo and Moilanen 2003; Vesaluoma et al. 2000) Histological images show the flap interface as a region of disordered collagen fibres, while confocal images display keratocyte density, and can measure light scatter through the tissue.

Ivarsen et al. (Ivarsen et al. 2003; Ivarsen et al. 2004) assessed healing of the flap interface using light intensity profiles from confocal microscopy images, and found that keratocyte activity was limited to a narrow circumferential band around the incision, which increased in reflectivity within the first weeks following LASIK. Keratocytes below this band, in the stromal bed, remained quiet. After six months, the band of reflectivity had narrowed and

decreased in intensity, and no peak was visible in the scatter profile. (Ivarsen et al. 2003; Ivarsen et al. 2004)

Avunduk et al. (Avunduk et al. 2004) also used confocal microscopy to monitor keratocyte morphology after LASIK, and measured the thickness of the activated keratocyte zone around the flap interface. This study found the opposite to that reported by Ivarsen et al. (Ivarsen et al. 2003; Ivarsen et al. 2004) above, in that only cells posterior to the incision were found to be activated, with no keratocyte activity anterior to the incision. Avunduk et al. (Avunduk et al. 2004) recorded the thickness of the activated keratocyte zone around the flap interface as 22µm at one week after LASIK, with no detectable band of activated cells at six months.

Keratocyte apoptosis is a well-documented event, thought to be influenced by epithelial injury. (Helena et al. 1998; Kallinikos and Efron 2004; Mohan et al. 2003; Wilson 2002; Wilson et al. 1996; Wilson et al. 2001a; Wilson et al. 2003b; Wilson et al. 2001b) Following LASIK, Wilson and colleagues (Wilson et al. 2001a) have found a higher keratocyte apoptosis response closer to the epithelium, and therefore hypothesise that the cascade of wound healing events are likely to also occur on the epithelial side of the incision after LASIK.

To date, a number of studies have used light backscatter profiles from OCT images to evaluate wound healing of the cornea following LASIK. (Maldonado et al. 2000; Thomas et al. 2003; Thompson et al. 2003; Ustundag et al. 2000; Wang et al. 2006; Wirbelauer and

Pham 2004) Some studies have used OCT to examine donor corneas prior to transplantation, to assess whether they had undergone refractive surgery. (Priglinger et al. 2003; Wolf et al. 2004) None of the above studies however, discussed light backscatter differences between myopic and hyperopic LASIK ablation. In this study, light backscatter profiles of OCT images were analysed after LASIK, expecting the intensity of the flap interface to reduce with time. The intensity and width of the flap interface were measured and monitored throughout the six month study.

8.2.3 Study procedure

The cohort for this retrospective study was the same as that in the previous study (discussed above in Chapter 8.1). The data were obtained from the same twenty six subjects; [17 myopes (mean age ± SD 32.6 ± 8.9 years, range 21 – 48 years), and 9 hyperopes (mean age ± SD 47.0 ± 12.6 years, range 23 – 63 years)]. Data analysis was performed according to refractive error, since the laser ablation profile for myopes and hyperopes during LASIK is different.

Raw OCT scans of the central cornea were analysed using the custom OCT scan analysis software, to yield data for light backscatter intensity.

A peak in backscatter intensity was expected at the location of the flap interface (incision) in the backscatter plot. The interest was not only in the height of this incision peak, but in the slopes either side (see Figure 8.9 below). The ascending slope of the peak was classified to

represent the ‘pre-incision’ intensity, and the descending slope of the peak was classified as the ‘post-incision’ intensity. For each slope, the normalized intensity was recorded at the trough (‘A’ or ‘C’) and at the peak (‘B’), and each converted into a signal-to-noise (S:N) ratio.

Another interesting aspect of the incision interface was its width, defined as the band of light backscatter either side of the incision peak. Interface width was calculated as the distance (in microns) between troughs A and C (‘A-C’ in Figure 8.9), demonstrated in Figure 8.10, by the placement of cursors. In the example below, incision width was measured as 64μm.

Figure 8-9 Top: A normalized light backscatter intensity profile (average of 51 a-scans) of the central cornea one day after LASIK (from a random subject in the study). 'ABC' represents the flap interface, with A-B classifying the pre-incision intensity and B-C classifying the post-incision intensity. [F = first peak indicating anterior corneal surface, E = epithelial peak, and L = last peak indicating posterior corneal surface]. Bottom: The respective OCT image from which the backscatter profile was derived.

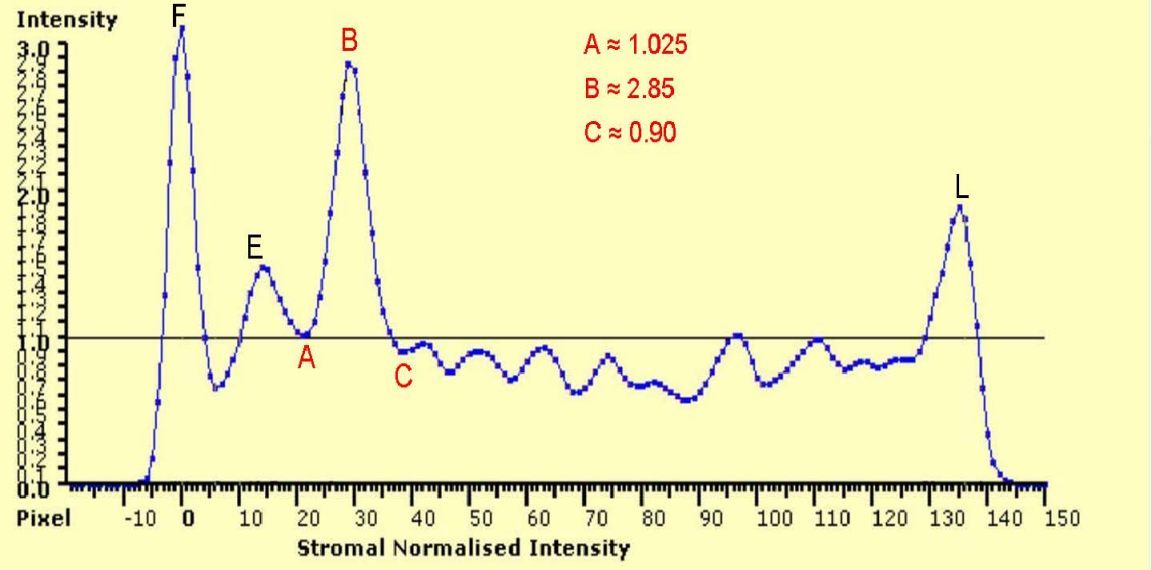

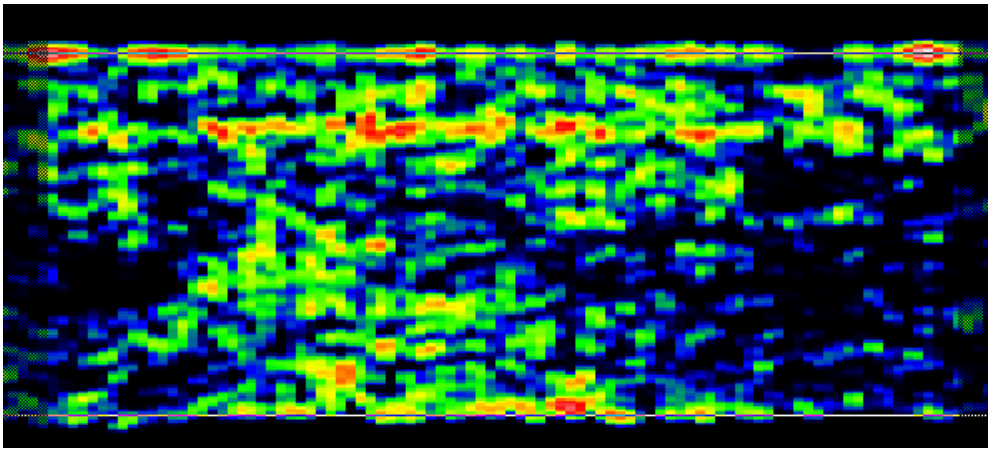

Figure 8-10 A light backscatter profile of the central cornea one day after LASIK, highlighting the measurement method for the width of the incision interface (A-C in Figure 8.9), as the distance between cursors IT1 and IT2 (IT = incision trough). The incision width in this example was calculated as (148µm – 84µm) = 64µm. [FP = first peak, at pixel 0, starting at 0µm. CO = corneal thickness of 544µm].

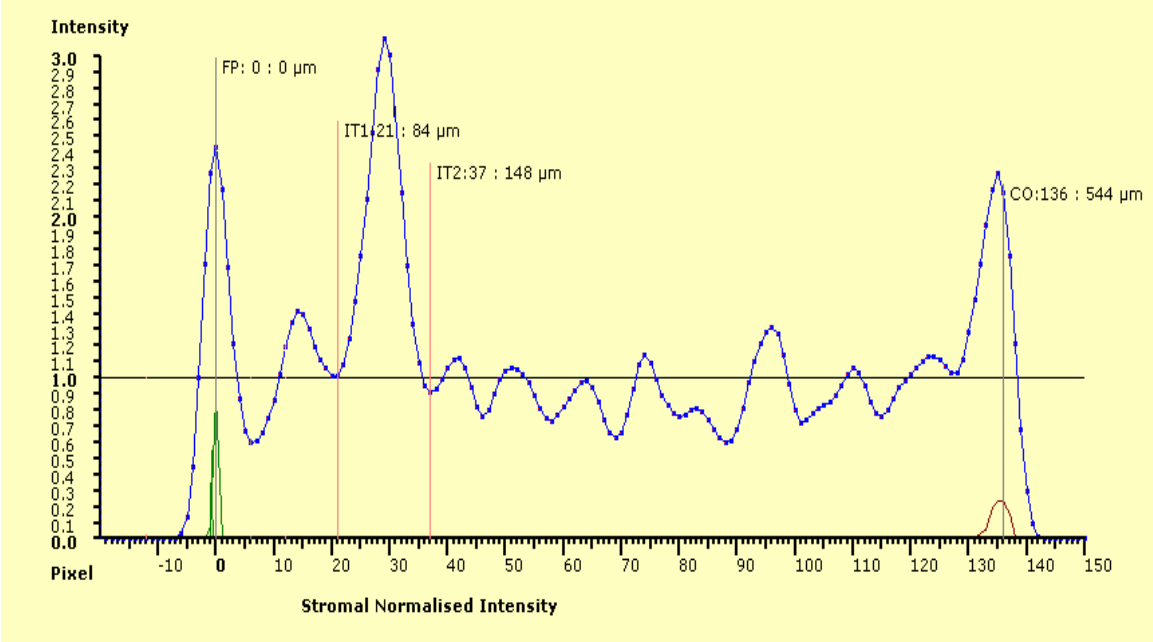

OCT scans of the central cornea obtained pre-operatively, at one day, one week, one month and six months following LASIK were analysed. Values for backscatter intensity of the incision peak, incision troughs and incision width were recorded, for each subject in the myopic and hyperopic groups that completed the full six month study. Statistical tests included Re-ANOVA and Tukey HSD post-hoc, with a significance level of $p<0.05$. Data analysis aimed to find differences between groups of subjects, in backscatter peak intensities

of the flap interface, comparing pre- and post-incision values, and also differences in the width of backscatter at the flap interface.

8.2.4 Results

One day post-operatively, the flap interface could be clearly seen on the OCT image in all eyes (as in Figure 8.11b), represented by a large intensity peak on the respective scan profile (as seen in Figures 8.9 and 8.10). However, to compare post-LASIK differences to baseline values, measurements were obtained from the baseline intensity profiles retrospectively, in a region estimated to be the location of the flap interface for that particular subject. Figures 8.11a-e show OCT images with their respective scatter profiles throughout the study. (All scans in Figure 8.11 were obtained from the same subject). At six months, the flap interface was not easily visible in the OCT images.

Figure 8-11 OCT scans of the central cornea obtained before LASIK (a), and at one day (b), one week (c), one month (d) and six months (e) after LASIK. Each scan is accompanied by its respective light backscatter profile.

a. Pre-Operative

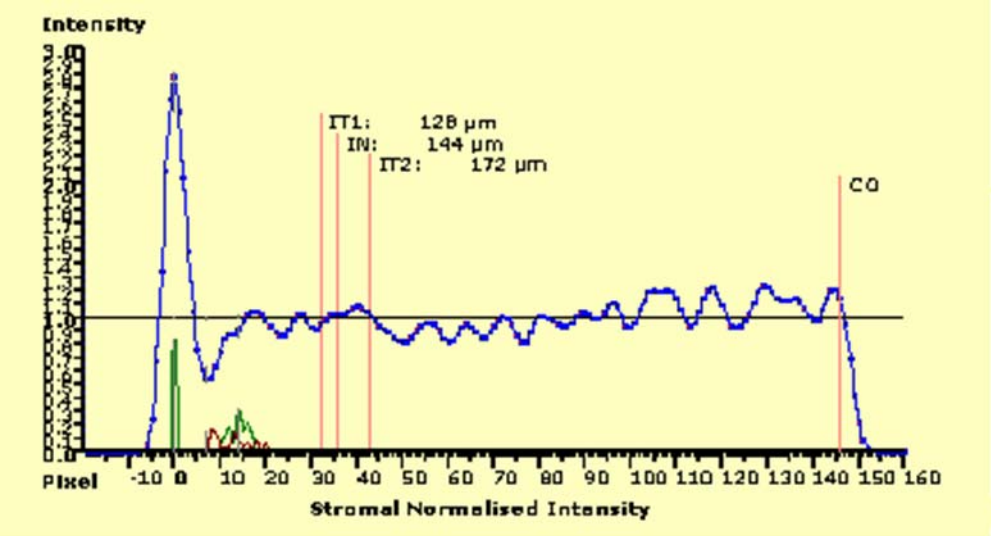

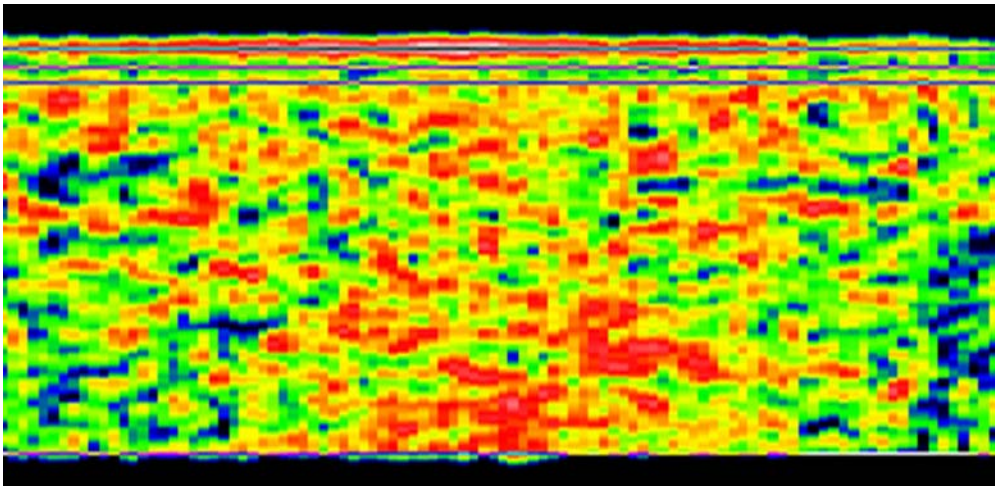

b. One day post-LASIK

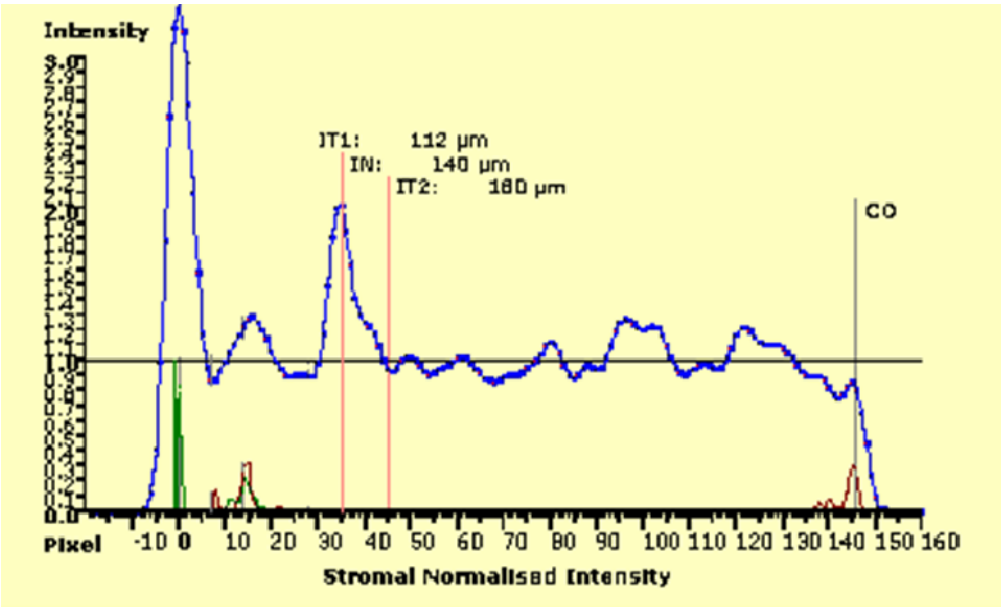

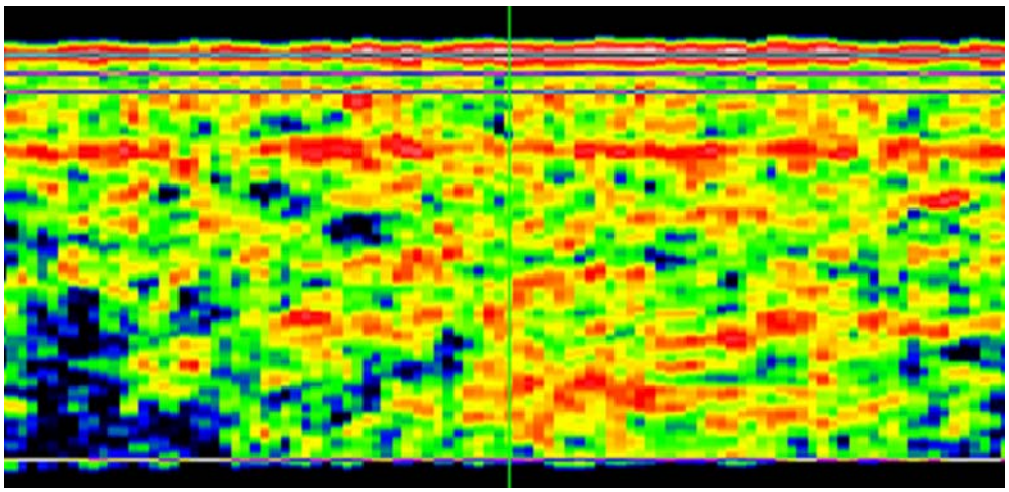

c. One week post-LASIK

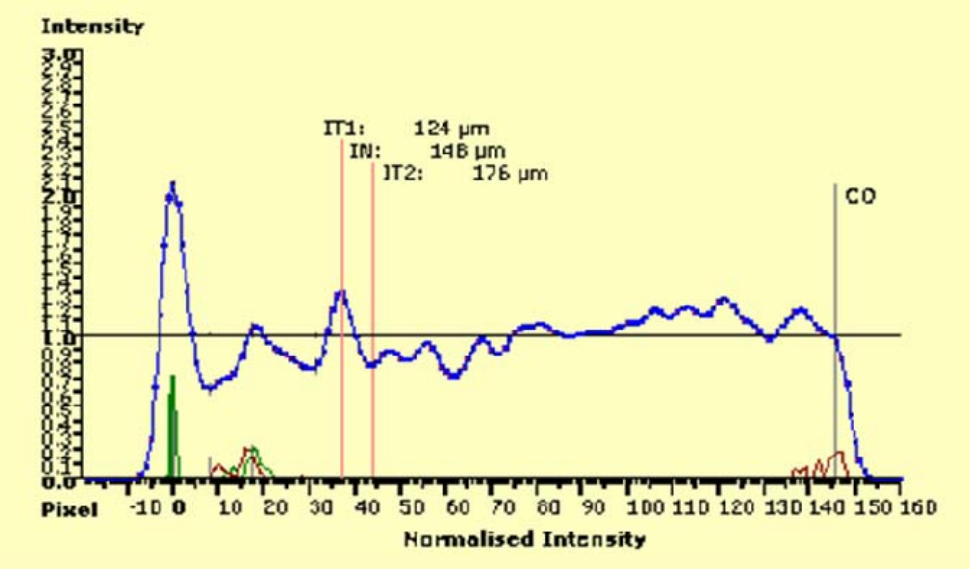

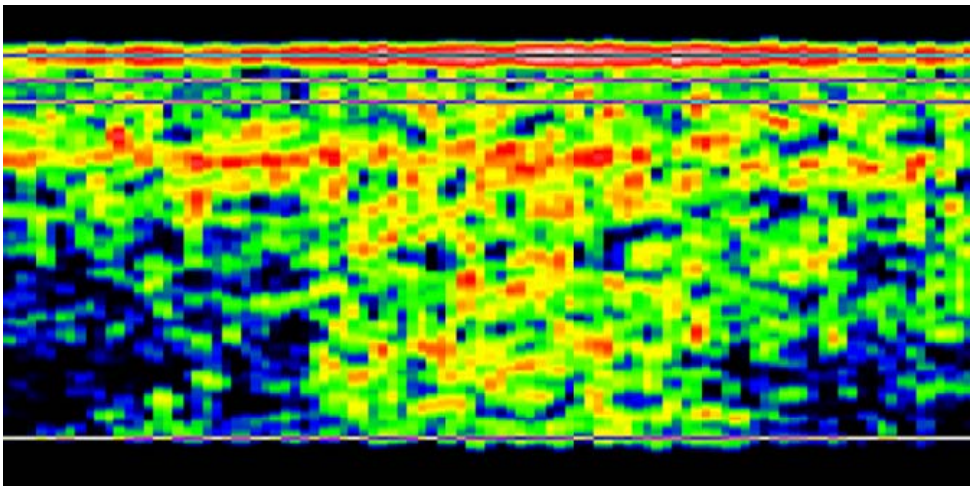

d. One month post-LASIK

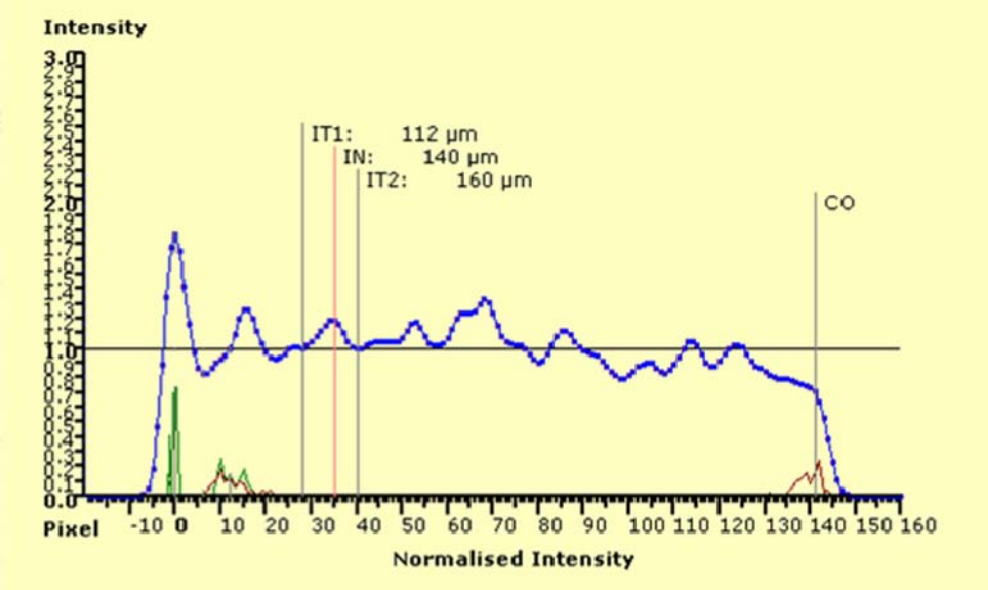

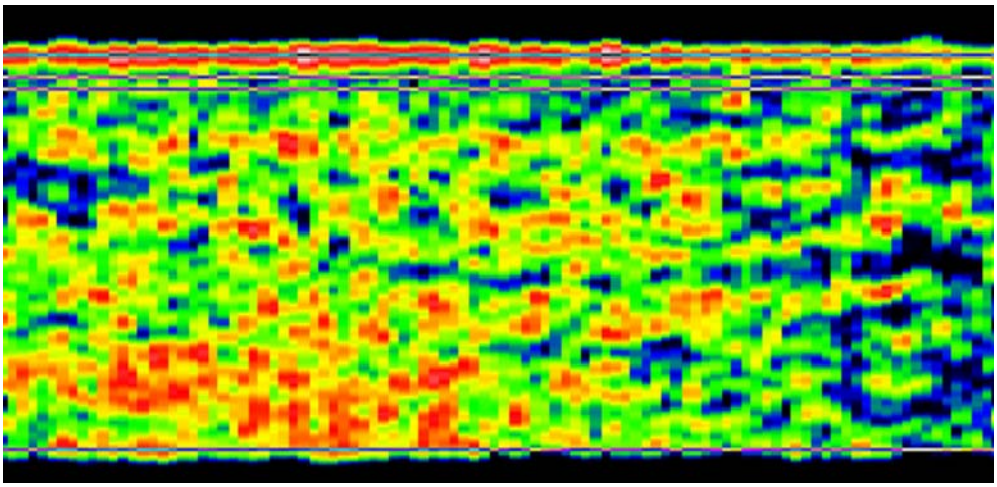

e. Six months post-LASIK

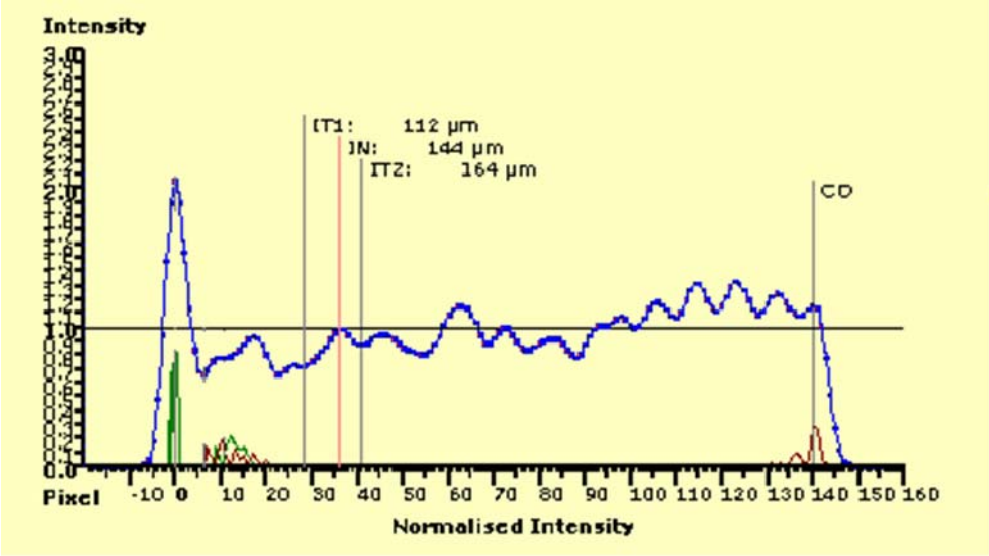

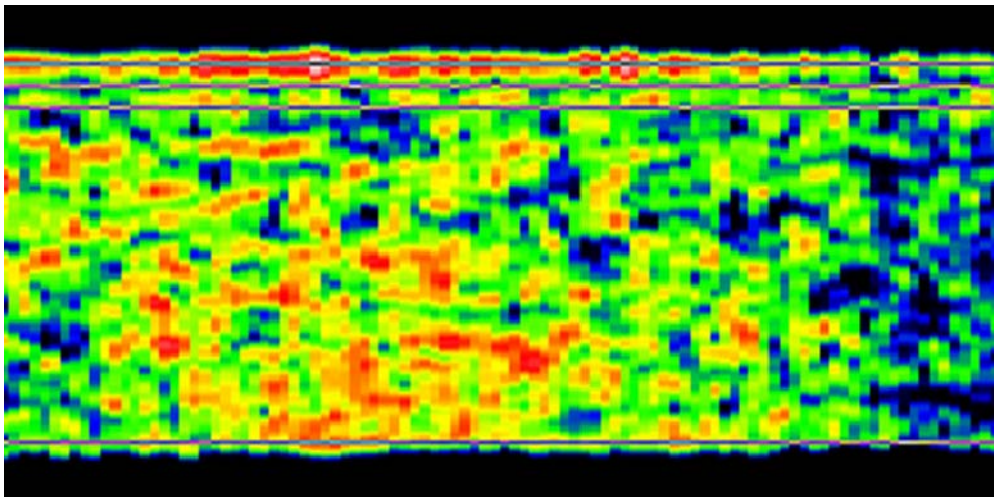

Mean (± SD) baseline values for backscatter intensity in the flap interface region, were estimated as 1.00 ± 0.12 for the myopic group and 1.05 ± 0.19 for the hyperopic group ($p>0.05$ compared to each other). Figure 8.12 shows the peak intensity in backscatter at the flap interface, for each group of subjects. In all subjects, incision peak intensity was significantly greater than baseline at one day after LASIK, measuring 1.39 ± 0.22 in myopes ($p<0.05$) and 1.57 ± 0.23 in hyperopes ($p<0.001$). At one week, peak intensity was still greater than baseline in both groups ($p<0.05$), and at one month a decrease in backscatter occurred in hyperopes eyes, to measure similar to myopic eyes. From one month onwards, there was no significant difference in backscatter compared to baseline ($p>0.05$). At no time in the study however, did the peak intensity at the interface differ statistically between myopes and hyperopes ($p>0.05$).

Figure 8-12 Peak intensity of the incision interface for each group of subjects, measured pre-operatively, and compared throughout the six month study period.

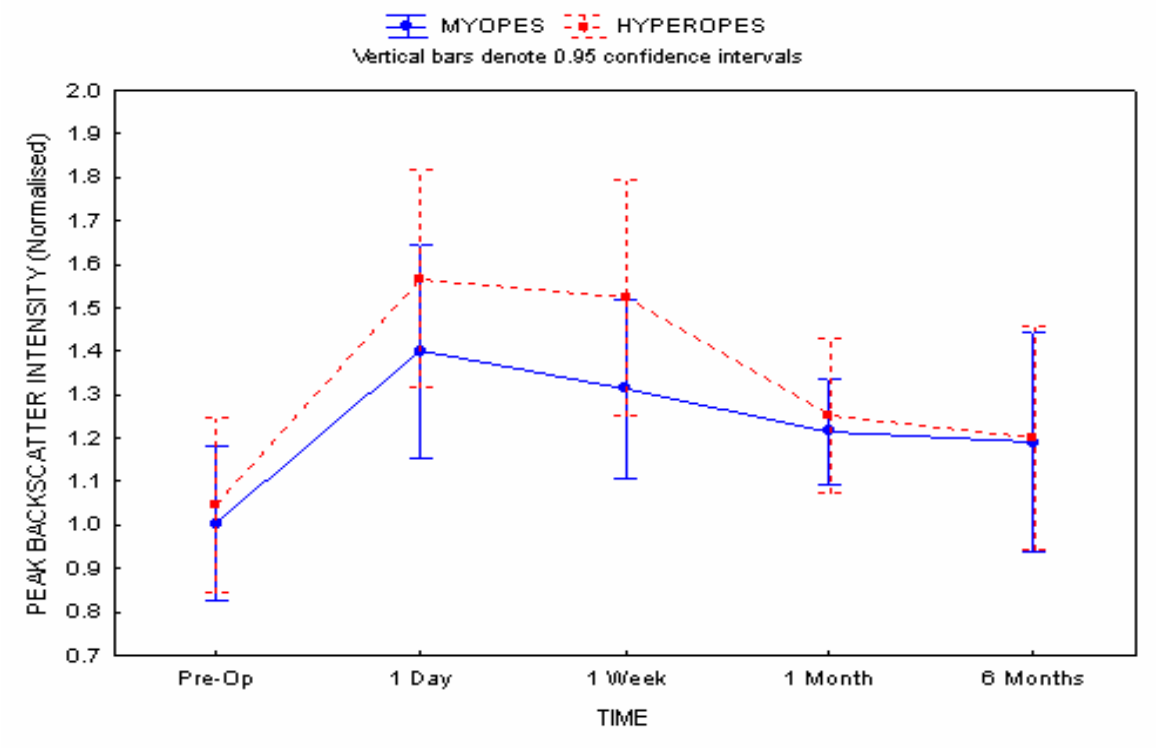

Figure 8.13 shows the signal-to-noise (S:N) ratio of the flap interface, comparing the anterior side closer to the epithelium (pre-incision) to the posterior side in the residual stromal bed (post-incision). Mean (± SD) baseline S:N ratio for the myopic group was 1.16 ± 0.05 and 1.15 ± 0.06 for the pre- and post-incision areas, respectively. These values for the hyperopic group were 1.18 ± 0.10 and 1.16 ± 0.09, respectively. One day after LASIK, pre- and post-incision S:N ratio was greater than baseline, in both groups of subjects (both $p<0.001$). Pre-incision intensity was significantly greater than post-incision, for myopes ($p<0.001$) and for hyperopes ($p<0.05$). At one week, there was a decrease in pre-incision S:N ratio towards baseline, more so in the myopic subjects, while there was an increase in post-incision S:N ratio in hyperopic eyes. Only at this time-point, was the pre- and post-incision S:N ratio

significantly different between myopic and hyperopic subjects ($p<0.05$). At six months, the post-incision intensity had recovered to baseline levels ($p>0.05$), but the pre-incision S:N ratio values remained significantly higher than baseline, in both myopes (1.52 ± 0.2) and hyperopes (1.45 ± 0.2; both $p<0.05$). Appendix CC displays the values of pre- and post-incision backscatter intensity at the LASIK flap interface (mean S:N ratio ± SD), for both myopes and hyperopes.

Figure 8-13 Pre- and post-incision intensity of the incision interface, in terms of signal-to-noise (S:N) ratio, for the myopic and hyperopic subjects.

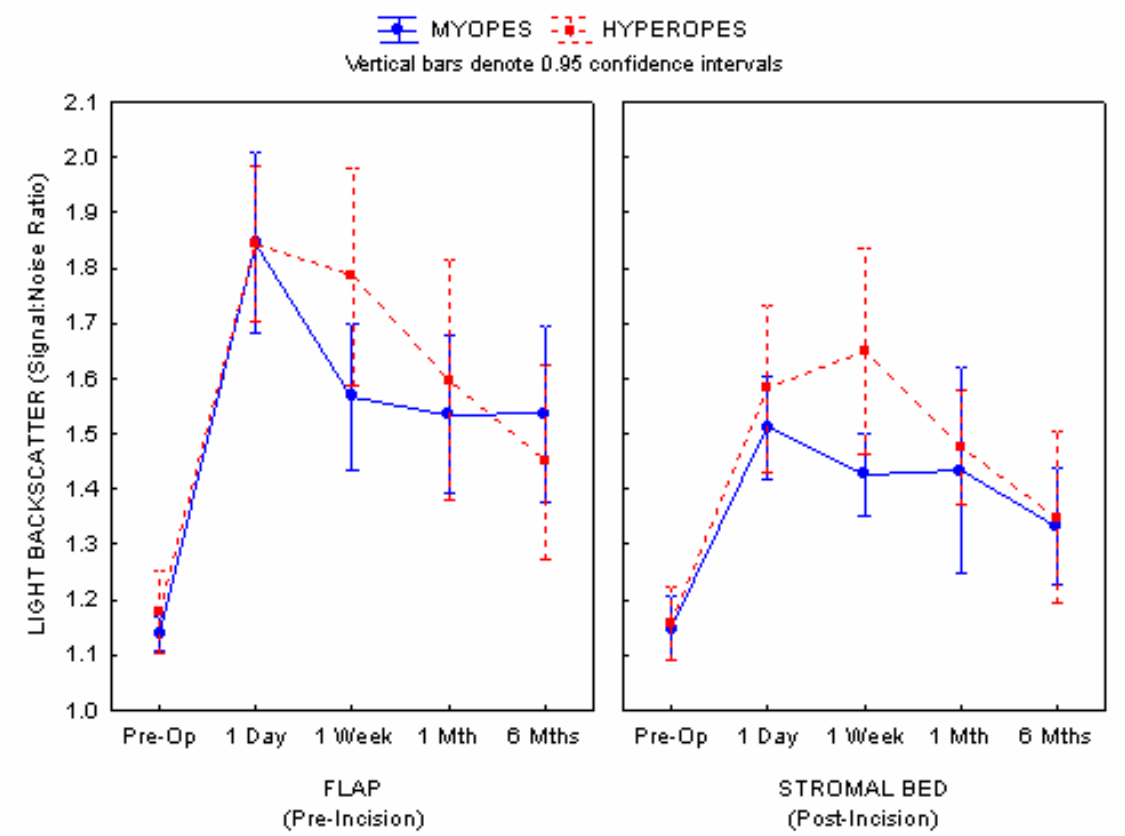

Figure 8.14 shows the width of the incision interface for each group of subjects. Since an incision peak was obviously not present on baseline scans, there were no pre-operative values for comparison. One day after LASIK, the incision width (mean ± SD) for myopes was 54.8 ± 11.4µm, and for hyperopes was 58.2 ± 8.9µm ($p>0.05$). The width was greatest at one week post-operatively for both myopes (57.8 ± 10.6µm) and hyperopes (64.2 ± 7.8µm), but neither change was significantly different from the day one values (both $p>0.05$). The six month values were not significantly different from the one day values, and at no point through the study was there any difference in the incision width between myopic and hyperopic subjects (all $p>0.05$).

Figure 8-14 Width of backscatter at the flap interface (in microns).

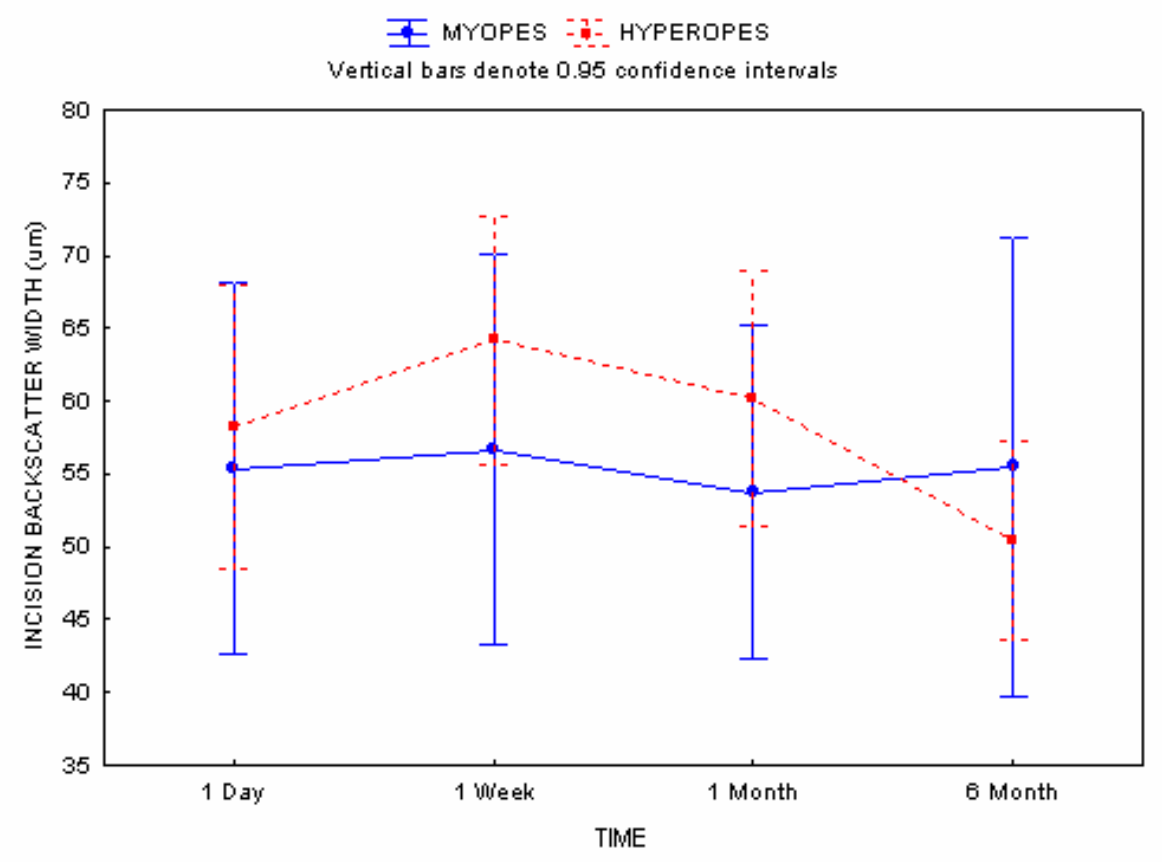

8.2.5 Discussion

This study used light backscatter profiles from OCT scans, to monitor the recovery of the flap interface, throughout six months following LASIK. To date, there have been no studies that have quantified light backscatter to monitor healing after LASIK, respective of refractive error. A novel aspect of this study was comparing the recovery of the flap interface between myopic and hyperopic eyes.

The day following LASIK surgery, the flap interface was easily located on the OCT scan. This remained the case in the one week and one month scans. At six months, the intensity peak representing the incision interface was still noticeable in the backscatter graphs, but was not as easily visible in the OCT images.

Re-treatment of the LASIK cornea is fairly common (Hersh et al. 2003; Kanellopoulos and Pe 2006; Lafond et al. 2004; Maldonado 2002; Zadok et al. 1999), and the easy relocation of the original flap position is desired. There are a lack of adhesions between the under-surface of the flap and the residual stromal bed, in terms of wound repair. (Ivarsen et al. 2003; Kato et al. 1999; Rumelt et al. 2001) Therefore, the separation of the existing flap is likely to be easier than creating a new one. (Rumelt et al. 2001) A non-contact, rapid imaging technique such as OCT may be beneficial in the surgeons consulting room, to locate the position of the flap interface prior to LASIK re-treatment. However, the flap interface is not always easily identifiable at six months after surgery, as found in this and in previous studies. (Priglinger et

al. 2006; Rumelt et al. 2001; Thompson et al. 2003) Maldonado et al. (Maldonado et al. 2000) used OCT backscatter profiles to assess the post-LASIK cornea, and found difficulty in detecting the intensity peak at the flap interface from as soon as three months after LASIK. Kato et al. (Kato et al. 1999) have reported that wound healing at the flap interface was still present nine months after LASIK.

Our particular model of OCT was unable to provide images that emphasize the flap interface region towards the end of the six month study. A recent study by Wang et al. (Wang et al. 2006) used a laboratory OCT set-up (scanning at 1310nm) to monitor the LASIK cornea using light backscatter measures, although only for a month. Similar to this study, the intensity of the flap interface was greatest at one day and one week following surgery. Although the authors do not provide OCT images of the cornea at one month, they mention that the detection of the flap interface reduces with time. Improving the sensitivity of OCT images (as discussed in detail in Chapter 3) may benefit the LASIK surgeon by highlighting the flap interface many months, or even years after surgery. (Helena et al. 1998; Lemley et al. 2000; Netto et al. 2006)

For the first time using OCT, this study found a greater increase in light backscatter on the anterior side of the flap interface (nearer the epithelium), compared to the posterior side (within the residual stromal bed), during the six months of healing after LASIK. This may be related to the higher keratocyte density in the anterior stroma, compared to the posterior stroma. (Hahnel et al. 2000; Moller-Pedersen and Ehlers 1995; Patel et al. 2001) Previous studies have found a higher keratocyte reaction in the anterior stroma following refractive

surgery. (Helena et al. 1998; Jester et al. 1999b; Wilson 1998, 2000, 2002; Wilson et al. 2001a) Following LASIK, there seems to be a greater reaction of activated keratocytes and myofibroblasts underlying the epithelium, rather than posterior to the incision. (Jester et al. 1999b; Wilson et al. 2001a) This may explain the greater level of light backscatter measured anterior to the flap incision in this study. The overall intensity and width of backscatter at the flap interface decreased with time, suggesting that the area of healing around the incision reduced throughout the six month study. A similar occurrence was found by Ivarsen et al. (Ivarsen et al. 2003).

The present study found that pre-incision interface backscatter was greater in the hyperopic subjects compared to the myopic subjects, after LASIK. Since there are no previous studies that measure light backscatter after LASIK according to refractive error, we cannot directly compare these results with previous work. Vesaluoma et al. (Vesaluoma et al. 2000) observed post-operative flap complications such as epithelial ingrowth and lamellar keratitis more frequently in those subjects who had undergone LASIK for hyperopia. However, it is of interest that a greater level of light backscatter was measured in the central cornea in hyperopes in the present study, even though a greater amount of laser ablation was performed in the central cornea during myopic LASIK.

The results of this study suggest that light backscatter at the interface, and the interface width may be used as indicators of healing following LASIK. OCT has the potential to become a useful device in monitoring LASIK subjects in the clinical setting.

Chapter 9

Summary

9.1 Summary of work

This project revolved around the use of optical coherence tomography, in the measurement and monitoring of clinical corneal conditions. Topographical corneal, stromal and epithelial thickness, as well as light backscatter was measured, following orthokeratology, LASIK and keratoconus.

The effect of orthokeratology is primarily based on the moulding of the epithelial layer, and yet many investigators choose to use instruments that do not measure epithelial changes to monitor the OK cornea. (Chan et al. 2006a; Fan et al. 1999; Nichols et al. 2000; Soni et al. 2004) OK changes are not restricted to the central epithelium, and so it is vitally important that measurements are obtained across the corneal surface and not just the centre. In the myopic OK studies mentioned throughout this project, either topographical corneal change was reported over a short period of time, or only central corneal changes were reported but over a longer follow-up time. Ideally, both of these factors need to be combined in the evaluation of the OK cornea.

If OK lenses are to be worn overnight for long periods of time without affecting the health of the cornea, the oxygen transmissibility of the lens material used must be improved. To prevent additional overnight oedema from lens wear, the lens material is advised to have a

Dk/t of at least 125 (Harvitt and Bonanno 1999) (as discussed in Chapter 5.3). Traditional open-eye contact lens wear has been found to lead to detrimental affects when worn for long periods, including epithelial thinning and stromal keratocyte apoptosis (which also leads to stromal thinning), among other complications. (Bourne 2001; Holden et al. 1985b; Holden et al. 1985c; Liesegang 2002; Sweeney 2003) The epithelium is the cornea's strongest barrier, and it has been found by many studies that this barrier's function is impaired by hypoxia, especially from overnight lens wear. (Bonanno and Polse 1987; Fonn and Holden 1988; Ichijima et al. 2000; Ichijima et al. 1993; Lin et al. 2002) In addition, it was reported in Chapter 7.3 that daily wear of traditional RGP lens wear alone may thin the epithelium. The two factors of overnight hypoxia and RGP lens wear combined, present an important case to carefully monitor the epithelium (and the rest of the cornea) during OK lens wear. Chapter 5.2 also reported that the amount of central epithelial thinning continues to decrease throughout a year of OK lens wear. The long-term effect (i.e. over many years) of OK lens wear on the epithelium remains unknown, and care needs to be taken to uphold the integrity of this protective barrier. Hence, the use of hyper oxygen transmissible lenses is essential for overnight OK lens wear.

The use of OCT to examine topographical changes in the keratoconic cornea was a novel chapter of this research, especially with regards the alteration of the epithelial layer across the entire cornea, and to associate the changes found with the length of diagnosis. To date, there have been no published studies investigating the keratoconic epithelium using OCT. An interesting finding in this study (Chapter 7.3) was the thinner epithelium found in the RGP lens wearing subjects. Since epithelial thinning occurs in keratoconus, and many

keratoconic subjects wear RGP lenses, extra care needs to be applied in the fitting of rigid keratoconic contact lenses, to not aggravate the thinning of the epithelium. The condition of keratoconus itself classically displays signs of epithelial and stromal degeneration, and to create a cascade of wound healing events due to micro-trauma of the epithelium from contact lens wear, may have potentially damaging consequences.

No published studies to date have measured the post-LASIK cornea from limbus to limbus using OCT, and monitored the changes throughout a period of six months. Previous studies using OCT have concentrated on epithelial and corneal flap thickness only centrally, and only for a short follow-up period. (Thompson et al. 2003; Wang et al. 2004) Particular areas of interest reported in Chapter 8 were the changes in epithelial thickness not only in the centre, but also at the margins of the corneal flap, and how these changes altered with healing. The resolution of OCT images needs to be improved, to be able to show the subtle healing changes within the flap interface after many months or years of surgery. This would assist refractive surgeons in the detection of the flap interface, should re-separation be necessary for additional ablation.

The construction of colour-coded, three-dimensional maps of corneal and epithelial thickness was a unique part of this project. The design and construction of an extended fixation target in this project aided in the measurement of the cornea in eight directions of gaze (Figure 3.9). However, it must be appreciated that each map shown in Chapter 7 was constructed from averaged data accounting for the whole study cohort (40 eyes per plot). Hence, the thickness

at one particular corneal location for one subject would not be identical for another. Nonetheless, individual maps for each subject were possible, if required.

9.2 Future considerations

To benefit the health care community, new technologies need to be transferred from their laboratories to the clinical setting. However, there are many hurdles in this process, including prototype development, clinical practicality, FDA approval, cost, time, and the interest in the technology from medical professionals. (Fujimoto 2003) The commercial release of the new Visante^{TM} OCT could prove beneficial in the routine monitoring of the cornea, especially in conditions such as orthokeratology, keratoconus and LASIK, where the cornea is likely to undergo constant change. Although this OCT instantly captures topographical corneal thickness maps, the production of epithelial maps is not mentioned by the manufacturer. This questions any great advantage of this instrument over the Orbscan II. An advantage of the Visante^{TM} OCT over the OCT2 is the automated analysis of the cornea, providing immediate thickness values. Instant data retrieval is necessary if OCT is to be used routinely in practice.

The experiments within this project did raise additional questions, to be answered in future studies. One is the use of OCT in the measurement of the abnormal cornea. Since OCT is an optical instrument, influenced by the refractive index of the structure being measured, we need to investigate how corneal oedema affects OCT thickness values, similar to the way it

affects Orbscan values. (Boscia et al. 2002; Fakhry et al. 2002; Lu et al. 2006a; Prisant et al. 2003) If so, we may need to apply a conversion factor to OCT values.

Another concern is the long-term wear of orthokeratology lenses. There are issues that have yet to be explored, that may the affect the normal functioning of the cornea after many years of lens wear. One complication may be keratocyte apoptosis. If the pressure of OK lens wear is great enough to re-distribute the epithelium, could it potentially encourage the loss of keratocytes, through the release of cytokines as part of a wound healing type response? The use of RGP lenses for visual correction in keratoconus has raised concern for many years, considering the effect of micro-trauma on the stroma. OK lens wear may inflict a similar action, leading to undesired stromal thinning over the long period. The effect of orthokeratology on keratocyte density may be investigated using clinical confocal microscopy.

Another unexplored complication of orthokeratology lens wear is the effect on corneal sensitivity. OK lens wear re-distributes the superficial epithelium, and so also has the potential to dislodge or alter the location of corneal nerve endings residing between the superficial epithelial cells. This may reduce the normal sensitivity of the cornea, which has been found in keratoconus (Simo Mannion et al. 2005), and following traditional contact lens wear. (Murphy et al. 2001; Patel et al. 2002)

Dry eye syndrome is one of the most common problems faced by eye care professionals today, presenting unbearable symptoms and severely affecting contact lens wear. (Lemp

1994; Lemp 1998) Yet no studies have been reported discussing the effect of dryness on epithelial thickness. This may be due to the lack of instruments readily available to measure the thickness of the epithelium in particular, this being a major advantage of OCT. LASIK refractive surgeons are also concerned about the effect of drying on epithelial thickness, especially during the surgical procedure (personal communication). Future studies should measure and monitor the topographical thickness of the epithelium in subjects clinically diagnosed with dry eye, to evaluate any deviation from the norm. The results may also assist pharmaceutical companies in the preparation of their dry eye treatment.

In conclusion, this project used optical coherence tomography to successfully measure and monitor corneal and epithelial thickness changes following orthokeratology, in keratoconus and after LASIK refractive surgery.

Appendices

Appendix A

Comparison of real lens thickness measured with digital callipers and lens thickness measured with OCT (in microns), obtained by three operators.

OPERATOR		SH				AM				YF			
Lens thickness		**T1**	**T2**	**AV**	**CF**	**T1**	**T2**	**AV**	**CF**	**T1**	**T2**	**AV**	**CF**
1	408	424	428	426	465	420	420	420	459	424	428	426	465
2	454	472	472	472	515	476	476	476	520	476	476	476	520
3	499	520	520	520	568	520	520	520	568	520	520	520	568
4	373	388	392	390	426	384	384	384	419	388	392	390	426
5	680	708	708	708	773	712	712	712	777	708	712	710	775
6	562	592	592	592	646	588	588	588	642	588	592	590	644
7	608	636	628	632	690	628	628	628	686	636	636	636	694
8	82	102	100	101	110	100	100	100	109	100	100	100	109
9	297	316	312	314	343	308	312	310	338	316	316	316	345
10	114	128	126	127	139	122	122	122	133	124	124	124	135

OCT operators: SH, AM and YF

T1 and T2: Thickness 1 and 2

AV: Average of T1 and T2

CF: Average thickness after conversion factor applied

Appendix B

Corneal thickness measurements (in microns) obtained by three OCT operators.

OPERATOR	SH			AM			YF		
Measurement	**C1**	**C2**	**AV**	**C1**	**C2**	**AV**	**C1**	**C2**	**AV**
PX									
1	494	491	493	487	498	492	496	494	495
2	487	496	491	494	499	496	496	487	491
3	517	521	519	503	505	504	523	530	526
4	528	525	527	525	520	522	525	521	523
5	493	491	492	491	498	494	494	486	490
6	511	513	512	510	503	507	511	517	514
7	560	560	560	560	560	560	560	560	560
8	524	526	525	514	524	519	519	524	521
9	465	464	465	462	461	462	466	468	467
10	486	490	488	485	487	486	486	490	488
MEAN	506.4	507.6	507.0	503.2	505.4	504.3	507.5	507.6	507.5
SD	27.1	26.9	26.9	26.5	25.7	26.0	26.1	27.3	26.6

OCT operators: SH, AM and YF

C1 and C2: Corneal thickness 1 and 2

AV: Average of C1 and C2

Appendix C

Epithelial thickness measurements (in microns) obtained by three OCT operators.

OPERATOR	SH			AM			YF		
Measurement	**E1**	**E2**	**AV**	**E1**	**E2**	**AV**	**E1**	**E2**	**AV**
PX									
1	51	53	52	50	51	50	54	51	53
2	48	50	49	48	52	50	52	56	54
3	53	54	53	54	51	52	54	48	51
4	48	47	48	50	48	49	48	51	49
5	54	56	55	52	55	54	53	52	53
6	51	49	50	52	51	51	51	52	51
7	54	50	52	56	55	56	52	51	51
8	50	51	51	52	47	50	48	54	51
9	52	52	52	51	53	52	49	52	50
10	52	49	51	49	50	50	48	54	51
MEAN	51.4	51.2	51.3	51.4	51.3	51.4	50.9	52.0	51.4
SD	2.2	2.7	2.1	2.4	2.6	2.1	2.5	2.2	1.4

OCT operators: SH, AM and YF

E1 and E2: Epithelial thickness 1 and 2

AV: Average of E1 and E2

Appendix D

Corneal thickness changes (mean % ± SD) during 4 weeks of myopic CRT™ lens wear.

DAY	TIME	LOCATION								
		-5.1	**-4.0**	**-2.2**	**-1.0**	**0.0**	**1.0**	**2.2**	**4.0**	**5.1**
1	Removal	3.1	7.0	6.9	6.5	4.9	6.5	5.1	5.9	3.9
		4.8	5.7	4.4	3.5	2.0	2.3	3.1	4.8	6.0
	HR 1	3.8	4.8	3.0	2.6	1.3	3.7	2.3	3.1	1.6
		4.8	4.4	2.1	1.7	1.5	1.7	3.5	4.4	3.8
	HR 3	0.2	1.7	0.8	0.8	-0.1	1.8	1.1	2.3	-0.7
		4.8	4.3	1.4	1.4	0.9	2.0	2.3	5.5	3.2
	HR 7	1.3	1.1	0.7	0.3	-0.7	1.0	0.8	2.0	-0.2
		5.6	3.4	1.5	1.1	1.0	1.6	2.8	6.7	4.9
	HR 14	1.9	0.9	-0.1	0.3	-0.8	0.8	0.1	0.7	-0.2
		4.8	3.7	1.3	1.3	1.2	1.9	2.8	5.9	5.4
4	Removal	5.5	5.8	6.1	5.0	3.1	6.6	6.3	7.3	3.6
		4.6	4.6	2.3	2.0	2.1	2.3	3.3	4.5	3.5
	HR 1	3.2	4.3	2.8	1.8	-0.2	2.7	3.3	3.1	1.7
		5.9	4.1	2.1	2.3	1.8	1.7	3.6	5.6	4.3
	HR 3	1.0	2.3	1.0	0.5	-1.4	1.3	1.3	2.1	-0.1
		5.7	3.8	2.0	1.4	1.2	1.6	3.1	5.8	3.9
	HR 7	0.2	1.3	0.3	0.2	-1.8	1.0	0.8	1.6	0.0
		6.6	3.5	1.8	1.5	1.3	1.8	2.9	5.9	3.4
	HR 14	3.5	1.3	0.2	-0.5	-2.1	0.5	0.4	0.8	1.1
		6.0	4.9	1.7	1.1	1.3	1.9	3.0	5.6	3.9
10	Removal	5.0	5.9	6.4	5.0	3.0	6.1	7.0	4.8	1.9
		6.2	4.1	3.2	2.8	2.8	3.3	3.1	7.0	6.4
	HR 1	3.7	2.9	2.1	1.3	-0.9	2.5	2.6	3.1	1.4
		5.6	3.7	3.8	1.7	1.6	1.6	2.9	5.6	3.7
	HR 3	2.2	1.1	1.4	0.1	-1.8	1.0	1.8	1.0	-0.4
		6.3	3.4	1.6	1.4	1.3	1.5	2.0	5.7	3.2
	HR 7	2.3	-0.6	0.8	0.0	-1.9	0.9	0.9	1.0	0.0
		6.8	3.9	1.8	1.7	1.2	1.8	2.2	6.1	2.9
	HR 14	3.4	0.3	0.3	-0.7	-2.5	-0.1	0.0	0.7	1.1
		6.0	4.5	1.4	1.3	1.2	1.2	3.0	7.3	2.9
28	Removal	3.7	4.3	6.9	5.0	3.2	6.1	5.4	2.3	0.7
		8.2	4.2	2.5	1.7	2.8	2.2	4.0	7.1	5.8
	HR 1	3.4	2.2	2.3	1.6	-0.9	2.6	2.4	3.5	0.0
		6.1	4.6	2.6	1.7	1.9	2.2	2.6	6.3	4.3
	HR 3	2.5	1.4	1.9	0.5	-1.9	1.6	1.5	1.7	-0.2
		4.8	4.1	1.4	1.3	1.4	2.1	2.9	5.5	4.7
	HR 7	1.8	0.9	0.3	-0.4	-2.3	0.9	1.2	2.6	0.7
		6.2	4.2	1.9	1.6	1.3	1.9	2.1	5.4	4.5
	HR 14	3.9	0.7	1.3	-0.5	-1.9	0.1	0.8	0.3	0.1
		7.7	3.0	1.7	1.4	1.7	1.7	2.9	7.6	3.5
72 hrs		2.6	1.0	0.8	0.1	0.2	1.1	1.4	2.4	-0.7
		7.6	4.6	1.6	2.4	4.5	2.2	2.3	6.6	4.0

Appendix E

Epithelial thickness changes (mean % ± SD) during 4 weeks of myopic CRT™.

DAY	TIME	LOCATION								
		-5.1	**-4.0**	**-2.2**	**-1.0**	**0.0**	**1.0**	**2.2**	**4.0**	**5.1**
1	Removal	-0.7	0.7	12.5	12.8	-7.3	13.5	13.1	1.2	0.5
		2.5	2.3	2.7	5.1	3.2	3.2	3.2	4.8	3.4
	HR 1	-3.2	-0.9	5.3	4.7	-7.2	9.1	10.4	3.3	4.1
		3.7	1.9	2.1	3.8	2.8	3.8	3.8	3.3	3.5
	HR 3	-0.8	0.0	3.1	0.9	-6.4	4.5	6.8	2.0	5.6
		3.4	3.7	3.8	2.9	2.7	4.0	4.8	4.9	4.1
	HR 7	-0.5	-1.8	3.5	-0.6	-6.4	2.8	6.3	1.2	5.6
		2.8	2.7	3.4	2.9	2.3	3.1	4.8	3.3	4.3
	HR 14	-1.3	-0.9	2.5	-0.3	-5.7	2.0	3.2	3.3	4.3
		3.1	2.2	2.3	3.5	2.2	3.0	4.1	3.2	3.5
4	Removal	-2.9	-1.0	12.1	6.5	-13.5	12.9	13.8	-0.2	-1.1
		3.2	2.6	3.1	4.3	2.0	4.3	4.3	3.5	2.1
	HR 1	-0.8	-0.7	9.5	0.1	-12.9	6.0	9.5	0.6	3.7
		3.1	2.1	3.0	4.0	2.3	3.5	3.7	3.8	3.9
	HR 3	-2.5	-0.3	2.8	-1.2	-14.2	1.6	12.2	4.0	3.8
		2.9	2.6	2.8	2.9	2.9	3.7	4.3	4.7	3.9
	HR 7	-3.0	-1.2	3.8	-1.8	-15.3	1.7	8.0	1.3	2.5
		3.3	2.8	2.7	2.8	2.4	3.2	4.1	4.0	3.5
	HR 14	-1.2	-1.8	1.6	-3.4	-15.0	2.9	2.5	1.2	7.7
		4.0	2.1	2.0	2.5	2.7	2.6	4.2	3.6	3.8
10	Removal	-1.2	0.0	10.8	4.8	-12.6	7.2	8.5	0.7	2.4
		2.4	2.9	3.9	4.0	1.7	4.5	2.8	3.2	3.5
	HR 1	-2.1	-1.5	9.6	1.3	-9.3	3.2	6.6	3.2	5.0
		3.1	2.4	3.7	3.4	3.6	3.0	2.9	4.3	3.4
	HR 3	-1.0	-1.7	5.8	-1.5	-12.9	2.8	4.8	3.2	2.3
		3.0	2.2	2.3	2.8	3.0	3.7	2.7	3.8	3.4
	HR 7	-1.5	-1.0	3.9	-1.8	-15.6	2.3	5.8	-0.1	3.5
		4.3	2.6	2.1	3.6	3.5	2.1	1.6	3.3	3.3
	HR 14	-2.4	-2.4	3.5	-3.8	-15.2	1.4	3.8	2.8	2.1
		3.0	2.2	1.9	2.8	3.5	2.7	2.4	3.8	3.4
28	Removal	-2.0	0.5	6.8	6.3	-11.4	5.6	9.8	2.6	0.5
		3.9	3.7	4.9	4.1	3.2	3.6	4.0	3.5	2.4
	HR 1	-2.4	0.5	6.9	1.9	-8.6	5.3	8.5	1.8	5.6
		3.1	2.2	2.8	3.5	2.8	2.8	2.8	3.7	4.7
	HR 3	-2.2	0.3	5.8	-1.6	-10.9	0.5	7.1	3.0	6.2
		3.3	2.3	2.3	3.5	3.7	2.5	2.0	3.0	4.5
	HR 7	-2.9	0.2	4.6	-0.5	-15.9	4.1	6.9	1.2	3.2
		3.8	2.0	2.7	4.0	3.6	3.3	2.7	2.8	4.2
	HR 14	-3.7	1.7	5.1	-2.2	-12.1	-0.5	8.2	-0.4	1.7
		2.9	4.0	2.2	2.1	2.5	2.1	2.6	2.2	3.8
72 hrs		-0.4	-1.8	3.6	-0.7	-4.1	2.5	4.0	-0.5	1.8
		2.6	2.3	1.6	3.0	2.5	2.5	2.3	2.1	2.1

Appendix F

Percentage changes (%) in topographical corneal thickness (mean ± SD) during 12 months of myopic CRT™ lens wear.

MONTH	LOCATION								
	-5.1	**-4.0**	**-2.2**	**-1.0**	**0.0**	**1.0**	**2.2**	**4.0**	**5.1**
1	2.1	1.4	2.0	0.4	-2.0	1.4	1.7	3.0	-0.9
	2.3	2.7	1.6	1.7	1.7	2.4	2.5	5.2	2.5
3	-1.6	2.7	1.8	0.3	-2.0	0.3	1.6	1.9	0.1
	6.9	4.8	1.9	2.1	2.6	2.6	3.7	4.7	4.2
6	-0.3	1.0	2.6	0.8	-1.5	0.6	2.6	2.9	-0.1
	6.8	5.1	3.5	2.5	1.9	3.3	2.9	3.5	2.6
9	-0.5	1.1	1.7	-0.4	-2.2	0.6	2.1	2.8	0.3
	2.1	3.5	2.3	2.1	1.8	2.8	2.6	4.4	1.8
12	-1.0	2.0	3.0	2.5	0.0	2.6	0.1	0.4	0.1
	2.4	2.5	3.2	3.2	6.0	5.9	3.3	7.3	4.8

Appendix G

Percentage changes (%) in topographical epithelial thickness (mean ± SD) during 12 months of myopic CRT™ lens wear.

MONTH	LOCATION								
	-5.1	**-4.0**	**-2.2**	**-1.0**	**0.0**	**1.0**	**2.2**	**4.0**	**5.1**
1	-5.3	0.1	7.4	1.0	-5.7	2.3	5.5	0.7	-2.3
	5.2	6.0	3.5	5.7	7.0	5.8	5.1	4.3	5.3
3	-3.5	0.8	4.8	-3.0	-12.5	-1.1	5.0	1.6	-3.6
	3.2	5.9	3.5	9.0	7.9	5.5	6.3	5.0	8.3
6	-5.5	-2.8	2.0	-3.9	-14.6	-2.7	3.0	-1.3	-3.7
	5.9	5.5	4.9	8.7	8.1	12.7	4.0	4.6	4.6
9	-1.8	-0.1	2.4	-3.4	-16.5	1.2	5.4	-2.4	-4.8
	8.7	6.9	4.0	9.3	8.8	9.4	3.6	6.8	7.6
12	-1.5	0.7	4.6	-2.0	-15.7	-3.3	5.8	-4.2	-3.6
	4.0	2.6	3.1	6.2	4.6	6.9	2.4	4.6	5.3

Appendix H

Percentage changes (%) in corneal thickness (mean ± SD) after myopic CRT™ lens wear using two different lens materials.

TIME	Menicon Z (Dk/t = 91)									Equalens II (Dk/t = 47)								
	LOCATION																	
	-5.1	**-4.0**	**-2.2**	**-1.0**	**0.0**	**1.0**	**2.2**	**4.0**	**5.1**	**-5.1**	**-4.0**	**-2.2**	**-1.0**	**0.0**	**1.0**	**2.2**	**4.0**	**5.1**
Removal	5.5	5.4	6.1	5.3	4.1	5.8	5.2	5.4	3.9	5.2	5.4	7.1	6.3	5.8	7.3	7.4	5.9	3.4
	4.3	3.4	2.2	2.6	2.0	2.7	2.2	3.2	2.5	3.3	2.8	2.2	2.3	2.6	2.7	3.3	2.6	3.3
Hr 1	2.5	2.8	3.0	2.1	1.0	2.7	2.8	1.5	2.0	3.9	2.8	3.0	2.3	1.8	2.9	3.5	3.0	1.8
	3.1	3.0	1.7	2.0	1.4	2.3	1.8	2.6	2.0	3.6	2.8	2.6	2.6	1.9	2.7	1.9	1.9	1.9
Hr 3	1.2	0.6	0.6	0.4	0.0	0.9	0.8	0.9	0.6	2.1	0.3	1.1	0.5	0.3	1.2	1.8	1.1	-0.1
	4.0	2.7	1.6	1.8	1.0	2.0	1.4	2.6	1.8	3.3	2.1	1.8	1.7	1.5	1.8	1.9	3.1	3.0
Hr 6	0.6	0.4	0.4	0.3	-0.5	0.3	0.2	-0.8	-0.5	0.9	0.1	0.5	0.6	0.4	1.2	0.5	0.6	-0.7
	3.4	2.5	1.8	1.8	1.1	1.7	2.3	2.4	2.2	3.1	2.7	1.6	2.1	1.1	1.5	1.3	2.5	2.4
Hr 12	1.0	0.6	0.5	0.8	-0.3	0.6	0.5	-1.1	0.9	1.2	0.3	0.5	0.3	0.3	1.1	1.4	0.3	0.0
	3.8	2.6	1.7	1.8	1.2	1.8	1.9	2.8	2.0	3.2	3.2	1.3	1.4	1.6	2.3	2.0	2.6	2.4

Appendix I

Percentage changes (%) in stromal thickness (mean ± SD) after myopic CRT™ lens wear using two different lens materials.

TIME	Menicon Z (Dk/t = 91)									Equalens II (Dk/t = 47)								
	LOCATION																	
	-5.1	**-4.0**	**-2.2**	**-1.0**	**0.0**	**1.0**	**2.2**	**4.0**	**5.1**	**-5.1**	**-4.0**	**-2.2**	**-1.0**	**0.0**	**1.0**	**2.2**	**4.0**	**5.1**
Removal	5.6	5.1	5.3	6.2	5.7	6.0	4.4	5.0	4.1	5.6	4.7	5.8	6.8	7.7	7.6	6.4	5.4	3.8
	4.8	4.0	2.8	3.1	2.2	3.1	2.9	3.5	3.0	3.6	3.5	2.3	2.8	3.1	2.9	3.7	2.8	3.6
Hr 1	2.8	2.5	2.6	2.5	2.2	3.1	1.9	0.8	2.1	4.2	2.2	1.7	2.1	3.1	2.9	3.0	2.4	1.7
	3.5	3.1	2.1	2.3	1.6	2.8	2.2	2.9	2.3	4.0	3.4	3.1	3.4	2.2	3.0	2.4	2.3	2.1
Hr 3	1.4	0.3	0.2	0.6	1.0	0.9	-0.2	0.0	0.6	2.2	-0.2	0.1	0.6	1.3	1.2	1.1	0.6	-0.2
	4.4	3.0	2.4	1.9	1.3	2.5	1.6	2.9	1.9	4.1	2.2	2.1	1.9	1.8	2.0	2.3	3.4	3.4
Hr 6	0.7	0.2	0.0	-0.1	0.2	0.3	-0.7	-1.4	-0.6	0.6	-0.3	-0.2	0.1	1.0	1.2	0.2	0.2	-0.7
	3.7	3.1	2.2	2.0	1.5	2.3	2.5	2.4	2.3	3.7	3.3	2.0	2.3	2.0	2.1	1.6	2.8	2.7
Hr 12	1.1	0.6	0.0	0.7	0.4	0.6	0.0	-1.7	0.7	0.7	-0.1	-0.3	0.2	0.8	1.3	0.6	-0.3	-0.1
	4.2	2.9	2.0	1.9	1.5	1.7	2.1	2.9	2.4	3.7	3.9	2.0	1.5	2.2	2.5	2.4	2.7	2.6

Appendix J

Percentage changes (%) in epithelial thickness (mean ± SD) after myopic CRT™ lens wear using two different lens materials.

TIME	Menicon Z (Dk/t = 91)									Equalens II (Dk/t = 47)								
	LOCATION																	
	-5.1	**-4.0**	**-2.2**	**-1.0**	**0.0**	**1.0**	**2.2**	**4.0**	**5.1**	**-5.1**	**-4.0**	**-2.2**	**-1.0**	**0.0**	**1.0**	**2.2**	**4.0**	**5.1**
Removal	5.0	9.1	13.4	-2.3	-10.0	3.7	13.5	9.0	1.7	1.5	11.9	19.4	3.1	-10.2	5.0	17.1	10.2	-0.2
	7.1	8.5	7.5	9.8	4.5	8.7	8.4	10.6	7.3	8.6	11.3	9.9	12.8	8.5	12.1	9.6	8.2	7.2
Hr 1	0.2	5.9	7.4	-0.6	-8.9	-0.6	10.9	8.4	0.9	1.4	8.4	15.5	5.2	-8.1	2.9	8.7	9.2	3.3
	8.6	6.3	10.3	10.8	6.5	7.7	6.8	7.7	5.9	5.3	8.7	9.9	10.8	9.0	10.3	10.5	8.8	11.2
Hr 3	0.3	3.9	4.2	-1.8	-8.5	0.7	10.2	9.5	1.1	1.7	5.4	11.3	-0.1	-7.4	1.5	8.5	6.5	0.6
	9.3	10.4	8.9	9.2	6.3	9.4	6.7	6.4	6.0	7.6	7.8	8.2	10.8	9.6	9.2	7.6	5.2	7.1
Hr 6	-0.7	3.4	3.9	3.4	-6.4	0.3	9.5	5.6	0.9	3.9	3.4	7.3	5.4	-4.6	1.0	3.1	4.2	-0.6
	8.3	8.3	8.3	6.8	5.9	9.8	9.0	9.2	6.2	7.2	8.7	6.8	10.9	10.4	8.3	7.6	10.9	7.0
Hr 12	0.4	1.8	5.2	1.7	-5.7	0.8	4.9	5.4	3.0	6.2	4.7	7.9	1.4	-3.3	-0.6	8.9	6.5	1.5
	8.2	7.6	10.2	8.5	6.5	8.1	8.8	5.8	7.0	6.0	7.1	9.2	9.2	9.2	9.6	8.2	6.6	6.5

Appendix K

Percentage changes (%) of the cornea (mean ± SD) following CRTH™ lens wear for hyperopia, comparing the experimental and control eyes.

TIME	CRTH™ eye									Control eye								
	LOCATION																	
	-5.1	**-4.0**	**-2.2**	**-1.0**	**0.0**	**1.0**	**2.2**	**4.0**	**5.1**	**-5.1**	**-4.0**	**-2.2**	**-1.0**	**0.0**	**1.0**	**2.2**	**4.0**	**5.1**
Removal	3.7	7.2	8.7	7.9	8.8	7.9	7.8	7.1	1.6	4.1	3.7	2.8	2.8	3.1	2.4	2.2	3.9	3.6
	7.3	4.4	3.7	3.0	2.2	3.3	3.5	4.4	5.3	4.0	4.1	2.3	2.0	1.6	1.3	2.3	5.3	4.1
Hr 1	0.7	2.8	3.5	3.0	4.1	3.9	3.9	3.3	-0.5	0.0	2.2	2.0	1.3	1.6	1.3	1.5	2.2	1.8
	4.4	3.3	1.9	1.9	2.1	2.7	3.4	3.2	3.0	8.0	4.2	3.2	2.1	1.4	1.8	2.4	4.0	3.5
Hr 3	-0.9	-0.1	0.7	0.2	1.3	1.1	0.7	0.9	-1.6	-0.5	0.6	0.9	0.3	0.5	-0.2	0.1	1.3	0.6
	4.9	4.1	3.9	3.4	2.0	1.4	3.0	3.3	4.0	4.9	4.0	1.7	1.8	1.6	2.0	3.1	4.9	2.8
Hr 6	-1.8	-0.4	0.8	0.5	1.0	0.9	1.0	0.8	-1.6	-1.1	-0.5	0.9	0.3	0.7	-0.4	-0.8	0.7	-1.3
	6.0	3.3	2.4	1.9	1.2	2.1	2.4	2.9	3.0	4.5	3.3	2.1	1.8	1.3	1.6	3.0	4.9	4.3
Hr 12	0.9	-1.1	0.0	0.1	1.2	1.0	0.6	1.3	-0.5	-0.1	0.1	0.3	-0.2	0.3	-0.3	-0.3	1.2	1.5
	5.4	3.6	3.0	2.1	2.9	1.7	2.5	4.5	5.8	4.5	3.0	2.3	1.3	1.8	1.6	2.2	4.9	5.5
28 Hrs	-1.4	0.3	1.0	0.4	1.0	0.5	0.4	1.0	-1.3	0.4	0.3	0.2	0.3	0.7	0.1	0.6	2.2	0.5
	4.1	3.9	3.1	2.2	1.0	1.6	4.2	4.3	5.7	4.5	3.7	2.2	1.4	0.9	1.8	2.9	6.0	4.5

Appendix L

Percentage changes (%) of the stroma (mean ± SD) following CRTH™ lens wear for hyperopia, comparing the experimental and control eyes.

TIME	CRTH™ eye									Control eye								
	LOCATION																	
	-5.1	**-4.0**	**-2.2**	**-1.0**	**0.0**	**1.0**	**2.2**	**4.0**	**5.1**	**-5.1**	**-4.0**	**-2.2**	**-1.0**	**0.0**	**1.0**	**2.2**	**4.0**	**5.1**
Removal	3.6	7.8	7.8	6.2	7.3	6.3	7.6	7.5	1.4	4.2	3.8	2.4	2.2	2.7	2.0	1.7	4.2	3.7
	8.1	4.7	4.1	3.5	2.6	4.1	4.5	5.0	6.0	4.5	4.4	2.7	2.0	1.7	1.6	2.4	5.9	4.4
Hr 1	1.2	3.3	3.3	1.8	2.7	2.6	3.4	3.4	-0.5	-0.1	2.5	2.0	1.1	1.4	1.0	1.2	2.5	1.7
	5.4	3.9	2.1	2.8	2.5	3.2	3.8	3.9	3.8	8.7	4.5	3.7	2.3	1.6	1.9	2.6	4.1	3.8
Hr 3	-0.8	0.3	0.7	-1.0	0.2	0.2	0.4	1.1	-1.8	-0.8	0.7	0.9	0.3	0.5	-0.4	-0.1	1.6	0.5
	5.6	4.6	4.5	3.8	2.4	1.9	3.2	3.9	4.6	5.4	4.3	1.8	2.3	1.9	2.2	3.6	5.2	3.1
Hr 6	-1.8	-0.6	0.9	-0.6	0.1	0.3	0.5	1.2	-2.2	-1.3	-0.4	0.9	0.2	0.7	-0.3	-1.2	0.8	-1.6
	6.8	3.3	2.6	2.5	1.6	2.5	3.2	3.5	3.5	5.2	3.7	2.4	2.1	1.5	1.8	3.4	5.1	4.5
Hr 12	0.9	-1.1	-0.2	-0.2	1.1	0.4	-0.1	1.1	-0.7	-0.5	0.3	0.2	-0.3	0.3	-0.4	-0.7	1.2	1.3
	6.2	4.0	3.8	2.6	3.2	2.1	3.1	4.9	6.5	4.9	3.4	2.5	1.7	2.2	1.7	2.6	5.1	6.1
28 Hrs	-1.7	0.1	1.1	-0.1	1.0	0.1	0.2	1.5	-1.5	0.4	0.7	0.1	0.1	0.4	0.0	0.6	2.6	0.4
	4.7	4.6	3.3	2.3	1.2	1.9	5.4	4.9	6.5	5.0	4.1	2.7	1.5	1.4	2.1	3.1	6.7	4.9

Appendix M

Percentage changes (%) of the epithelium (mean ± SD) following CRTH™ lens wear for hyperopia, comparing the experimental and control eyes.

TIME	CRTH™ eye									Control eye								
	LOCATION																	
	-5.1	**-4.0**	**-2.2**	**-1.0**	**0.0**	**1.0**	**2.2**	**4.0**	**5.1**	**-5.1**	**-4.0**	**-2.2**	**-1.0**	**0.0**	**1.0**	**2.2**	**4.0**	**5.1**
Removal	4.0	2.1	17.2	23.8	21.5	21.9	9.5	3.8	4.5	3.5	3.4	6.8	7.8	7.1	6.4	7.1	1.7	1.8
	9.9	9.9	9.6	10.9	8.6	12.3	9.7	10.0	13.7	8.9	7.6	7.0	7.3	6.0	5.3	8.3	5.5	5.5
Hr 1	-4.8	-0.6	5.3	14.1	16.3	16.0	8.1	3.2	0.8	2.1	-0.3	1.9	3.0	3.2	4.7	4.2	0.4	3.4
	9.9	13.3	6.7	11.4	6.2	11.9	12.9	10.9	13.6	6.3	7.5	6.3	6.1	5.9	7.3	5.0	8.3	6.2
Hr 3	-0.6	-3.6	1.5	11.0	10.8	8.5	4.0	-1.1	0.9	3.0	-0.1	1.2	0.9	0.4	1.1	2.1	-1.3	1.4
	7.5	8.3	8.0	8.6	10.6	10.7	7.8	8.4	10.2	6.4	7.3	5.0	5.6	5.7	7.8	5.9	8.2	6.1
Hr 6	-0.4	1.7	-0.1	10.2	9.7	7.0	5.0	-1.9	6.0	2.0	-1.5	1.4	1.0	1.5	-0.5	3.0	0.0	2.3
	8.4	8.0	7.6	9.8	8.6	10.5	8.8	13.1	11.6	8.2	8.1	7.9	6.3	6.2	8.6	6.5	8.1	6.8
Hr 12	1.5	-0.3	1.9	3.2	2.6	6.4	6.2	3.5	3.6	4.2	-1.8	0.8	0.3	0.3	0.2	3.7	1.2	3.9
	6.9	11.5	10.7	10.5	5.6	11.2	9.1	11.1	13.2	6.0	6.3	7.4	5.5	3.7	7.6	8.2	9.1	5.7
28 Hrs	2.5	3.3	0.1	4.6	1.5	4.6	2.8	-2.9	1.4	1.0	-3.0	0.6	2.8	3.7	1.3	1.5	-1.1	0.7
	6.5	9.5	6.8	5.3	5.9	7.0	9.9	9.3	10.6	4.7	6.5	6.1	4.1	6.6	6.1	4.0	7.1	4.8

Appendix N

Corneal thickness (mean ± SD) of the keratoconic and control corneas, measured with UP, ORB and OCT.

INST	Keratoconics				Controls		
	LOCATION						
	Temp	Centre	Apex	Nasal	Temp	Centre	Nasal
UP	574.3	494.2	439.8	570.8	607.6	530.5	611.3
	44.7	50.0	44.8	40.4	35.9	30.1	39.8
ORB	567.4	438.6	401.7	588.2	612.3	512.9	654.4
	38.7	47.7	47.9	36.1	59.8	44.0	53.7
OCT	574.7	433.5	398.1	561.7	613.1	496.0	611.9
	40.6	39.7	43.5	45.2	38.9	29.1	38.9

INST: Instrument

UP: Ultrasound pachymetry

ORB: Orbscan II

OCT: Optical coherence tomography

Appendix O

Thickness of the normal cornea (mean ± SD) at each measured point along 8 directions of gaze.

Direction	Location				
Centre	516.9 21.3				
	1	**2**	**3**	**4**	**5**
Temp	528.4 20.4	552.7 24.2	595.1 32.0	666.1 47.6	747.9 44.9
Nasal	547.0 21.0	585.5 28.3	639.7 33.9	698.2 35.8	
Sup	561.9 18.2	619.5 27.4	680.9 29.2	706.7 40.1	
Inf	519.1 23.0	545.4 25.3	582.8 30.3	629.7 30.8	690.0 40.7
SupTemp	547.4 19.5	591.8 24.3	659.4 31.0	719.4 43.0	
SupNasal	561.7 22.1	612.5 28.8	677.0 29.4	693.5 40.4	
InfTemp	518.7 22.9	538.8 25.9	578.0 32.8	631.2 37.4	698.8 43.3
InfNasal	529.8 22.3	557.7 25.9	606.0 32.9	666.4 42.5	699.0 31.8

Location 1 was closest to the central cornea

Location 5 closest to the limbus

Appendix P

Thickness of the normal stroma (mean ± SD) at each measured point along 8 directions of gaze.

Direction	Location				
Centre	463.4 21.1				
	1	**2**	**3**	**4**	**5**
Temp	473.9 20.4	496.9 23.6	537.3 31.2	606.0 46.2	683.3 45.0
Nasal	492.4 20.6	528.4 27.9	579.2 33.5	633.3 34.7	
Sup	507.7 18.0	562.9 26.6	621.1 30.0	638.7 38.0	
Inf	464.6 22.6	489.9 24.5	525.4 29.2	571.8 29.6	629.1 41.3
SupTemp	493.1 18.9	535.4 23.3	602.2 30.6	653.6 44.8	
SupNasal	507.4 21.5	555.4 29.5	617.9 28.9	627.7 40.9	
InfTemp	464.9 22.2	482.9 25.6	520.6 32.3	571.5 35.8	634.1 41.6
InfNasal	475.6 21.2	500.8 24.8	547.6 32.7	605.5 40.5	632.8 31.7

Location 1 was closest to the central cornea

Location 5 closest to the limbus

Appendix Q

Thickness of the normal epithelium (mean ± SD) at each measured point along 8 directions of gaze.

Direction	Location				
Centre	53.6 2.2				
	1	**2**	**3**	**4**	**5**
Temp	54.6 3.1	55.9 2.5	57.8 2.4	60.1 3.5	64.6 4.4
Nasal	54.7 3.2	57.2 2.6	60.5 2.6	64.9 4.7	
Sup	54.2 3.1	56.6 3.8	59.8 7.8	68.0 8.5	
Inf	54.5 2.6	55.6 2.7	57.5 3.7	58.0 4.3	60.8 9.3
SupTemp	54.3 2.6	56.5 3.1	57.3 3.5	65.8 6.1	
SupNasal	54.4 3.2	57.1 2.4	59.2 3.8	65.8 6.5	
InfTemp	53.8 3.3	55.9 3.4	57.4 3.6	59.7 3.3	64.7 6.6
InfNasal	54.2 3.0	57.0 3.7	58.4 3.5	60.9 3.8	66.2 3.9

Location 1 was closest to the central cornea

Location 5 closest to the limbus

Appendix R

Thickness of the RGP lens wearing cornea (mean ± SD) at each measured point along 8 directions of gaze.

Direction	Location				
Centre	517.8 31.5				
	1	**2**	**3**	**4**	**5**
Temp	531.5 29.8	559.7 29.7	604.4 28.8	689.8 48.7	741.4 14.6
Nasal	546.3 33.1	586.6 32.0	644.5 33.4	712.2 28.0	
Sup	561.6 33.5	616.8 34.1	671.7 33.0	675.8 27.1	
Inf	521.7 30.6	551.1 28.6	594.7 26.0	643.8 28.9	707.5 29.9
SupTemp	549.1 32.1	594.9 30.7	657.1 35.5	703.9 31.2	
SupNasal	559.5 33.8	606.7 33.4	665.2 30.3	678.6 24.3	
InfTemp	519.5 29.8	545.0 28.4	588.4 25.2	648.9 30.4	709.8 27.2
InfNasal	530.3 31.9	564.3 24.7	620.4 31.2	676.2 36.8	

Location 1 was closest to the central cornea

Location 5 closest to the limbus

Appendix S

Thickness of the keratoconic cornea (mean ± SD) at each measured point along 8 directions of gaze.

Direction	Location				
Centre	446.8 68.1				
	1	**2**	**3**	**4**	**5**
Temp	461.0 61.5	503.7 52.2	551.2 48.3	616.6 62.4	720.4 37.3
Nasal	508.4 40.1	536.9 44.1	581.5 46.2	677.4 57.0	
Sup	527.1 39.2	575.7 41.8	634.7 41.5	664.1 43.2	
Inf	425.1 66.2	459.5 58.9	523.1 50.1	578.9 46.8	660.2 37.9
SupTemp	511.7 43.1	556.8 42.1	611.0 47.1	674.9 40.9	
SupNasal	528.0 39.3	561.5 39.8	620.0 40.8	664.1 43.0	
InfTemp	420.5 71.1	451.9 58.8	516.7 47.9	577.7 51.0	670.9 44.0
InfNasal	469.7 54.4	512.7 42.9	564.8 43.2	630.6 40.2	678.1 32.5

Location 1 was closest to the central cornea

Location 5 closest to the limbus

Appendix T

Thickness of the RGP lens wearing stroma (mean ± SD) at each measured point along 8 directions of gaze.

Direction	Location				
Centre	467.9 31.5				
	1	**2**	**3**	**4**	**5**
Temp	480.0 30.3	505.4 29.5	546.5 28.4	627.6 45.9	674.0 14.1
Nasal	494.7 33.0	531.2 32.0	583.9 32.9	645.4 29.0	
Sup	510.7 32.8	561.6 33.5	613.0 33.6	608.1 30.3	
Inf	469.5 30.9	497.2 28.3	538.7 25.8	585.0 28.3	641.9 28.3
SupTemp	498.0 32.0	540.3 31.2	598.8 35.9	636.0 30.6	
SupNasal	506.8 33.0	550.1 32.6	607.0 31.2	612.3 25.8	
InfTemp	468.4 29.7	491.5 28.9	531.6 24.5	588.3 29.2	643.4 26.2
InfNasal	478.5 32.4	510.0 25.3	560.9 32.6	612.8 36.3	

Location 1 was closest to the central cornea

Location 5 closest to the limbus

Appendix U

Thickness of the keratoconic stroma (mean ± SD) at each measured point along 8 directions of gaze.

Direction	Location				
Centre	403.1 63.7				
	1	**2**	**3**	**4**	**5**
Temp	416.3 58.3	454.3 50.6	497.5 48.5	559.0 61.9	656.3 37.6
Nasal	460.0 39.9	485.1 44.5	526.5 46.4	614.7 56.6	
Sup	477.3 39.4	522.8 42.9	579.0 42.2	600.3 43.2	
Inf	382.3 64.0	415.1 56.2	472.8 48.7	523.7 46.7	600.7 36.9
SupTemp	463.8 42.3	504.2 42.2	555.3 48.0	613.6 39.9	
SupNasal	477.1 39.6	507.9 40.2	564.8 41.2	602.5 42.8	
InfTemp	378.2 68.9	407.7 56.7	466.9 47.1	522.2 52.0	609.4 44.2
InfNasal	424.1 52.9	462.6 43.1	509.7 44.2	571.3 40.6	644.7 17.6

Location 1 was closest to the central cornea

Location 5 closest to the limbus

Appendix V

Thickness of the RGP lens wearing epithelium (mean ± SD) at each measured point along 8 directions of gaze.

Direction	Location				
Centre	50.0 3.9				
	1	**2**	**3**	**4**	**5**
Temp	51.6 4.1	54.4 3.5	57.9 4.5	62.2 5.8	67.3 3.3
Nasal	51.6 4.1	55.4 3.8	60.7 4.5	66.8 5.7	
Sup	51.0 4.0	55.2 4.2	58.7 4.9	67.7 8.5	
Inf	52.3 3.1	53.9 2.9	56.0 2.0	58.7 3.7	65.6 8.9
SupTemp	51.2 3.7	54.6 4.0	58.3 4.5	67.9 7.8	
SupNasal	52.8 4.2	56.7 4.4	58.2 5.2	66.4 7.3	
InfTemp	51.2 3.8	53.5 3.0	56.9 2.9	60.6 3.9	66.3 5.6
InfNasal	51.9 3.2	54.3 2.8	59.5 5.4	63.4 5.0	

Location 1 was closest to the central cornea

Location 5 closest to the limbus

Appendix W

Thickness of the keratoconic epithelium (mean ± SD) at each measured point along 8 directions of gaze.

Direction	Location				
Centre	43.7 6.5				
	1	**2**	**3**	**4**	**5**
Temp	44.7 5.7	49.4 5.1	53.7 5.4	57.6 4.0	64.1 4.4
Nasal	48.4 4.0	51.8 4.8	54.9 4.5	62.7 6.2	
Sup	49.8 3.7	52.8 4.6	55.7 4.1	63.8 7.7	
Inf	42.7 6.0	44.4 5.8	50.3 5.8	55.1 5.0	59.5 4.5
SupTemp	47.9 4.2	52.6 3.4	55.7 4.4	61.3 5.1	
SupNasal	50.8 3.8	53.6 3.6	55.2 3.8	61.6 7.2	
InfTemp	42.3 5.2	44.2 6.2	49.7 6.1	55.5 4.9	61.4 4.7
InfNasal	45.6 5.5	50.2 4.6	55.0 4.7	59.2 4.5	66.8 2.1

Location 1 was closest to the central cornea

Location 5 closest to the limbus

Appendix X

Global epithelial thickness (mean ± SD) of the RGP lens wearing group, respective of length of lens wear.

Direction	**< 10 yrs**					**> 10 yrs**				
Centre	50.2 2.4					49.7 3.7				
	1	**2**	**3**	**4**	**5**	**1**	**2**	**3**	**4**	**5**
Temp	51.5 3.6	54.4 3.1	57.5 4.1	61.9 5.0	66.8 1.8	51.6 3.7	54.3 2.7	58.3 4.4	62.6 5.8	68.0 4.1
Nasal	52.1 3.3	55.7 2.6	60.7 3.8	66.7 5.4		51.0 4.1	55.0 2.9	60.6 4.2	66.9 5.1	
Sup	51.9 2.8	55.7 4.0	58.9 3.6	67.8 8.3		49.8 3.4	54.6 3.2	58.6 4.4	67.6 7.6	
Inf	51.7 2.6	52.6 2.2	56.2 1.7	58.8 2.3	67.3 6.7	52.9 2.3	55.4 1.8	55.8 1.2	58.6 3.4	63.4 4.4
SupTemp	51.1 2.9	54.7 3.4	58.5 4.2	68.5 5.4		51.2 3.5	54.4 3.1	58.1 3.6	67.2 7.7	
SupNasal	53.7 3.3	57.5 3.0	57.6 4.2	65.4 4.4		51.6 2.9	55.7 3.1	58.8 4.0	67.6 8.3	
InfTemp	51.0 2.7	53.5 2.1	56.6 2.3	60.2 3.4	65.9 3.4	51.3 1.9	53.6 2.4	57.1 2.9	61.1 3.6	66.9 4.1
InfNasal	52.0 1.9	54.2 2.0	58.8 3.6	63.4 3.7		51.7 3.2	54.4 2.7	60.3 5.9	63.4 4.2	

Location 1 was closest to the central cornea, location 5 was closest to the limbus.

Appendix Y

Changes in topographical stromal thickness (%) (mean ± SD) throughout 6 months, following LASIK for myopia.

TIME	LOCATION								
	-5.1	**-4.0**	**-2.2**	**-1.0**	**0.0**	**1.0**	**2.2**	**4.0**	**5.1**
1 Day	1.9	1.0	-2.9	-12.7	-15.1	-10.9	-3.0	-1.0	0.5
	4.0	5.2	6.0	4.3	4.3	3.0	2.7	3.1	2.4
1 Week	-0.4	-0.9	-5.8	-14.5	-17.3	-11.4	-4.3	-3.2	-0.1
	4.7	3.9	4.2	3.6	4.2	2.7	2.7	3.8	3.5
1 Mth	0.2	0.8	-3.8	-13.7	-16.8	-12.3	-5.4	-2.8	-0.8
	5.3	4.4	3.4	3.3	4.2	2.9	3.4	5.0	3.3
6 Mths	0.4	1.3	-3.7	-12.6	-13.9	-10.5	-4.7	-4.4	0.5
	5.2	5.6	5.1	4.0	4.8	4.0	5.9	5.1	4.3

Appendix Z

Changes in topographical stromal thickness (%) (mean ± SD) throughout 6 months, following LASIK for hyperopia.

TIME	LOCATION								
	-5.1	**-4.0**	**-2.2**	**-1.0**	**0.0**	**1.0**	**2.2**	**4.0**	**5.1**
1 Day	6.0	1.0	-2.4	-13.0	-1.0	-3.7	-2.9	-4.0	2.4
	5.5	4.3	2.7	2.3	1.9	2.9	3.5	7.8	6.6
1 Week	-0.9	0.8	-4.0	-14.6	-2.4	-4.0	-4.1	-4.4	-1.2
	4.4	2.7	3.1	2.8	1.2	3.1	3.7	7.3	3.8
1 Mth	2.5	1.2	-3.2	-14.2	-1.8	-3.6	-3.4	-5.4	-1.7
	3.9	1.9	3.1	2.7	1.6	3.1	4.9	7.9	2.9
6 Mths	0.5	0.9	-4.0	-13.7	-1.4	-3.6	-4.5	-7.1	-0.9
	4.0	2.7	2.6	2.8	1.8	2.9	3.5	6.8	3.3

Appendix AA

Changes in topographical epithelial thickness (%) (mean ± SD) throughout 6 months, following LASIK for myopia.

TIME	LOCATION								
	-5.1	**-4.0**	**-2.2**	**-1.0**	**0.0**	**1.0**	**2.2**	**4.0**	**5.1**
1 Day	-1.0	5.3	4.4	6.5	3.4	6.6	6.0	2.1	-5.7
	11.4	6.4	12.7	7.3	10.0	9.9	7.8	11.7	8.4
1 Week	-0.4	3.7	6.8	7.0	4.4	8.7	4.9	1.9	-5.1
	12.3	8.7	7.6	8.6	11.4	11.1	8.9	11.0	12.6
1 Mth	2.7	1.3	6.2	10.2	5.5	9.2	9.3	6.8	0.8
	12.9	8.7	9.4	8.7	10.0	7.3	4.2	12.4	11.3
6 Mths	2.5	6.0	8.7	9.9	2.0	8.1	5.5	1.4	1.1
	9.0	5.9	8.6	7.9	9.3	6.0	8.0	8.4	5.1

Appendix BB

Changes in topographical epithelial thickness (%) (mean ± SD) throughout 6 months, following LASIK for hyperopia.

TIME	LOCATION								
	-5.1	**-4.0**	**-2.2**	**-1.0**	**0.0**	**1.0**	**2.2**	**4.0**	**5.1**
1 Day	1.0	4.6	4.8	3.1	9.7	4.2	4.9	0.7	-7.8
	11.8	8.3	8.1	7.5	10.6	10.5	10.6	10.8	10.3
1 Week	6.4	3.7	7.7	6.5	11.1	9.4	11.4	1.0	-1.8
	11.7	5.6	9.9	11.5	12.1	10.9	11.9	7.1	7.0
1 Mth	3.3	2.1	9.4	1.4	2.6	7.8	6.2	2.4	4.5
	13.3	7.2	8.7	10.0	8.2	10.6	7.4	8.4	9.6
6 Mths	3.9	2.1	6.2	0.7	-1.1	4.1	5.3	-0.5	2.6
	10.4	8.3	7.2	5.5	6.5	6.5	7.1	10.9	10.8

Appendix CC

Pre- and post-incision backscatter intensity at the LASIK flap interface, in terms of signal-to-noise (S:N) ratio (mean ± SD), for the myopic and hyperopic subjects.

TIME	Myopes		Hyperopes	
	LOCATION			
	Flap (Pre-incision)	**Stromal bed (Post-incision)**	**Flap (Pre-incision)**	**Stromal bed (Post-incision)**
Pre-Op	1.16	1.15	1.18	1.16
	0.05	0.06	0.10	0.09
1 Day	1.79	1.52	1.84	1.58
	0.3	0.17	0.2	0.20
1 Week	1.57	1.43	1.78	1.65
	0.2	0.14	0.3	0.24
1 Month	1.51	1.36	1.60	1.48
	0.2	0.20	0.3	0.13
6 Mths	1.52	1.32	1.45	1.35
	0.2	0.10	0.2	0.20

Bibliography

Airiani S, Trokel SL, Lee SM, et al. (2006). Evaluating central corneal thickness measurements with non-contact optical low-coherence reflectometry and contact ultrasound pachymetry. Am J Ophthalmol 142(1): 164-5.

Aktekin M, Sargon MF, Cakar P, et al. (1998). Ultrastructure of the cornea epithelium in keratoconus. Okajimas Folia Anat Jpn 75(1): 45-53.

Alharbi A, La Hood D and Swarbrick HA (2005). Overnight orthokeratology lens wear can inhibit the central stromal edema response. Invest Ophthalmol Vis Sci 46(7): 2334-40.

Alharbi A and Swarbrick HA (2003). The effects of overnight orthokeratology lens wear on corneal thickness. Invest Ophthalmol Vis Sci 44(6): 2518-23.

Ambrosio R, Jr. and Wilson S (2003). LASIK vs LASEK vs PRK: advantages and indications. Semin Ophthalmol 18(1): 2-10.

Amm M, Wetzel W, Winter M, et al. (1996). Histopathological comparison of photorefractive keratectomy and laser in situ keratomileusis in rabbits. J Refract Surg 12(7): 758-66.

Anderson NJ, Beran RF and Schneider TL (2002a). Epi-LASEK for the correction of myopia and myopic astigmatism. J Cataract Refract Surg 28(8): 1343- 7.

Anderson NJ, Edelhauser HF, Sharara N, et al. (2002b). Histologic and ultrastructural findings in human corneas after successful laser in situ keratomileusis. Arch Ophthalmol 120(3): 288-93.

Andreassen TT, Simonsen AH and Oxlund H (1980). Biomechanical properties of keratoconus and normal corneas. Exp Eye Res 31(4): 435-41.

Arffa RC (1997). Physiology. Grayson's diseases of the cornea. Toronto, Mosby: 23-27.

Argento CJ and Cosentino MJ (1998). Laser in situ keratomileusis for hyperopia. J Cataract Refract Surg 24(8): 1050-8.

Armitage BS and Schoessler JP (1988). Overnight corneal swelling response in adapted and unadapted extended wear patients. Am J Optom Physiol Opt 65(3): 155-61.

Asano-Kato N, Toda I, Tsuruya T, et al. (2003). Diffuse lamellar keratitis and flap margin epithelial healing after laser in situ keratomileusis. J Refract Surg 19(1): 30-3.

Asbell PA (2004). Corneal refractive therapy and the corneal surface. Eye Contact Lens 30(4): 236-7; discussion 242-3.

Auffarth GU, Wang L and Volcker HE (2000). Keratoconus evaluation using the Orbscan Topography System. J Cataract Refract Surg 26(2): 222-8.

Avitabile T, Marano F, Uva MG, et al. (1997). Evaluation of central and peripheral corneal thickness with ultrasound biomicroscopy in normal and keratoconic eyes. Cornea 16(6): 639-44.

Avunduk AM, Senft CJ, Emerah S, et al. (2004). Corneal healing after uncomplicated LASIK and its relationship to refractive changes: a six-month prospective confocal study. Invest Ophthalmol Vis Sci 45(5): 1334-9.

Bansal AK and Veenashree MP (2001). Laser refractive surgery: technological advance and tissue response. Biosci Rep 21(4): 491-512.

Barkana Y, Gerber Y, Elbaz U, et al. (2005). Central corneal thickness measurement with the Pentacam Scheimpflug system, optical low-coherence reflectometry pachymeter, and ultrasound pachymetry. J Cataract Refract Surg 31(9): 1729-35.

Barker NH, Couper TA and Taylor HR (1999). Changes in corneal topography after laser in situ keratomileusis for myopia. J Refract Surg 15(1): 46-52.

Barr JT, Rah MJ, Meyers W, et al. (2004). Recovery of refractive error after corneal refractive therapy. Eye Contact Lens 30(4): 247-51; discussion 263-4.

Barr JT, Wilson BS, Gordon MO, et al. (2006). Estimation of the incidence and factors predictive of corneal scarring in the Collaborative Longitudinal Evaluation of Keratoconus (CLEK) Study. Cornea 25(1): 16-25.

Barr JT, Zadnik K, Wilson BS, et al. (2000). Factors associated with corneal scarring in the Collaborative Longitudinal Evaluation of Keratoconus (CLEK) Study. Cornea 19(4): 501-7.

Bechmann M, Thiel MJ, Neubauer AS, et al. (2001). Central corneal thickness measurement with a retinal optical coherence tomography device versus standard ultrasonic pachymetry. Cornea 20(1): 50-4.

Benjamin WJ and Cappelli QA (2002). Oxygen permeability (Dk) of thirty-seven rigid contact lens materials. Optom Vis Sci 79(2): 103-11.

Berlau J, Becker HH, Stave J, et al. (2002). Depth and age-dependent distribution of keratocytes in healthy human corneas: a study using scanning-slit confocal microscopy in vivo. J Cataract Refract Surg 28(4): 611-6.

Binder PS, May CH and Grant SC (1980). An evaluation of orthokeratology. Ophthalmology 87(8): 729-44.

Bizheva K, Povazay B, Hermann B, et al. (2003). Compact, broad-bandwidth fiber laser for sub-2-microm axial resolution optical coherence tomography in the 1300-nm wavelength region. Opt Lett 28(9): 707-9.

Bizheva K, Unterhuber A, Hermann B, et al. (2005). Imaging ex vivo healthy and pathological human brain tissue with ultra-high-resolution optical coherence tomography. J Biomed Opt 10(1): 11006.

Bohnke M, Chavanne P, Gianotti R, et al. (1998). Continuous non-contact corneal pachymetry with a high speed reflectometer. J Refract Surg 14(2): 140-6.

Bohnke M and Masters BR (1999). Confocal microscopy of the cornea. Prog Retin Eye Res 18(5): 553-628.

Bonanno JA and Polse KA (1985). Central and peripheral corneal swelling accompanying soft lens extended wear. Am J Optom Physiol Opt 62(2): 74-81.

Bonanno JA and Polse KA (1987). Effect of rigid contact lens oxygen transmissibility on stromal pH in the living human eye. Ophthalmology 94(10): 1305-9.

Boscia F, La Tegola MG, Alessio G, et al. (2002). Accuracy of Orbscan optical pachymetry in corneas with haze. J Cataract Refract Surg 28(2): 253-8.

Bourne WM (1998). Clinical estimation of corneal endothelial pump function. Trans Am Ophthalmol Soc 96: 229-39; discussion 239-42.

Bourne WM (2001). The effect of long-term contact lens wear on the cells of the cornea. Clao J 27(4): 225-30.

Braun DA and Anderson Penno EE (2003). Effect of contact lens wear on central corneal thickness measurements. J Cataract Refract Surg 29(7): 1319-22.

Brennan NA, Efron N and Carney LG (1987). Critical oxygen requirements to avoid oedema of the central and peripheral cornea. Acta Ophthalmol (Copenh) 65(5): 556-64.

Brookes NH, Loh IP, Clover GM, et al. (2003). Involvement of corneal nerves in the progression of keratoconus. Exp Eye Res 77(4): 515-24.

Bruce AS and Brennan NA (1993). Epithelial, stromal, and endothelial responses to hydrogel extended wear. Clao J 19(4): 211-6.

Buehl W, Stojanac D, Sacu S, et al. (2006). Comparison of three methods of measuring corneal thickness and anterior chamber depth. Am J Ophthalmol 141(1): 7-12.

Buzard KA and Fundingsland BR (1999). Excimer laser assisted in situ keratomileusis for hyperopia. J Cataract Refract Surg 25(2): 197-204.

Caldicott A and Charman WN (2002). Diffraction haloes resulting from corneal oedema and epithelial cell size. Ophthalmic Physiol Opt 22(3): 209-13.

Carones F, Vigo L and Scandola E (2003). Laser in situ keratomileusis for hyperopia and hyperopic and mixed astigmatism with LADARVision using 7 to 10-mm ablation diameters. J Refract Surg 19(5): 548-54.

Cavanagh HD (2003). The effects of low- and hyper-Dk contact lenses on corneal epithelial homeostasis. Ophthalmol Clin North Am 16(3): 311-25.

Cavanagh HD, El-Agha MS, Petroll WM, et al. (2000). Specular microscopy, confocal microscopy, and ultrasound biomicroscopy: diagnostic tools of the past quarter century. Cornea 19(5): 712-22.

Cavanagh HD, Jester JV, Essepian J, et al. (1990). Confocal microscopy of the living eye. Clao J 16(1): 65-73.

Cavanagh HD, Ladage PM, Li SL, et al. (2002). Effects of daily and overnight wear of a novel hyper oxygen-transmissible soft contact lens on bacterial binding and corneal epithelium: a 13-month clinical trial. Ophthalmology 109(11): 1957-69.

Chaidaroon W (2003). The comparison of corneal thickness measurement: ultrasound versus optical methods. J Med Assoc Thai 86(5): 462-6.

Chakrabarti HS, Craig JP, Brahma A, et al. (2001). Comparison of corneal thickness measurements using ultrasound and Orbscan slit-scanning topography in normal and post-LASIK eyes. J Cataract Refract Surg 27(11): 1823-8.

Chan B, Cho P and Cheung SW (2006a). Repeatability and agreement of two A-scan ultrasonic biometers and IOLMaster in non-orthokeratology subjects and post-orthokeratology children. Clin Exp Optom 89(3): 160-8.

Chan MC, Su YS, Lin CF, et al. (2006b). 2.2 microm axial resolution optical coherence tomography based on a 400 nm-bandwidth superluminescent diode. Scanning 28(1): 11-4.

Chang SW, Benson A and Azar DT (1998). Corneal light scattering with stromal reformation after laser in situ keratomileusis and photorefractive keratectomy. J Cataract Refract Surg 24(8): 1064-9.

Chayet AS, Assil KK, Montes M, et al. (1998a). Regression and its mechanisms after laser in situ keratomileusis in moderate and high myopia. Ophthalmology 105(7): 1194-9.

Chayet AS, Magallanes R, Montes M, et al. (1998b). Laser in situ keratomileusis for simple myopic, mixed, and simple hyperopic astigmatism. J Refract Surg 14(2 Suppl): S175-6.

Choo J, Caroline P and Harlin D (2004a). How does the cornea change under corneal reshaping contact lenses? Eye Contact Lens 30(4): 211-3; discussion 218.

Choo JD, Caroline P, Harlin D, et al. (2004b). Morphologic changes in cat epithelium following overnight lens wear with the Paragon CRT lens for corneal reshaping. Invest Ophthalmol Vis Sci 45: E-Abstract 1552.

Cobo-Soriano R, Llovet F, Gonzalez-Lopez F, et al. (2002). Factors that influence outcomes of hyperopic laser in situ keratomileusis. J Cataract Refract Surg 28(9): 1530-8.

Comaish IF and Lawless MA (2002). Progressive post-LASIK keratectasia: biomechanical instability or chronic disease process? J Cataract Refract Surg 28(12): 2206-13.

Cox I, Zantos S and Orsborn G (1990). The overnight corneal swelling response of non-lens wear, daily wear and extended wear soft lens patients. Int Contact Lens Clin 17(5/6): 134-137.

Crawford JB, Aldave AJ, McLeod S, et al. (2003). Histopathological analysis of the cornea after laser in situ keratomileusis. Arch Ophthalmol 121(6): 896-8.

Cristol SM, Edelhauser HF and Lynn MJ (1992). A comparison of corneal stromal edema induced from the anterior or the posterior surface. Refract Corneal Surg 8(3): 224-9.

Dave T and Ruston D (1998). Current trends in modern orthokeratology. Ophthalmic Physiol Opt 18(2): 224-33.

Davidorf JM, Eghbali F, Onclinx T, et al. (2001). Effect of varying the optical zone diameter on the results of hyperopic laser in situ keratomileusis. Ophthalmology 108(7): 1261-5.

Dawson DG, Edelhauser HF and Grossniklaus HE (2005a). Long-term histopathologic findings in human corneal wounds after refractive surgical procedures. Am J Ophthalmol 139(1): 168-78.

Dawson DG, Holley GP, Geroski DH, et al. (2005b). Ex vivo confocal microscopy of human LASIK corneas with histologic and ultrastructural correlation. Ophthalmology 112(4): 634-44.

Dawson DG, Kramer TR, Grossniklaus HE, et al. (2005c). Histologic, ultrastructural, and immunofluorescent evaluation of human laser-assisted in situ keratomileusis corneal wounds. Arch Ophthalmol 123(6): 741-56.

Dayhaw-Barker P (1995a). Corneal wound healing I: the players. Int Contact Lens Clin 22(May/June): 105-109.

Dayhaw-Barker P (1995b). Corneal wound healing II: the process. Int Contact Lens Clin 22(May/June): 110-115.

Dhaliwal DK and Mather R (2003). New developments in corneal and external disease--LASIK. Ophthalmol Clin North Am 16(1): 119-25.

Dierick HG and Missotten L (1992). Is the corneal contour influenced by a tension in the superficial epithelial cells? A new hypothesis. Refract Corneal Surg 8(1): 54-9; discussion 60.

Dillon EC, Eagle RC, Jr. and Laibson PR (1992). Compensatory epithelial hyperplasia in human corneal disease. Ophthalmic Surg 23(11): 729-32.

Diniz CM, Tzelikis PF, Rodrigues Junior A, et al. (2005). Unilateral keratoconus associated with continual eye rubbing due to nasolacrimal obstruction-case report. Arq Bras Oftalmol 68(1): 122-5.

Doughty MJ and Zaman ML (2000). Human corneal thickness and its impact on intraocular pressure measures: a review and meta-analysis approach. Surv Ophthalmol 44(5): 367-408.

Drexler W (2004). Ultrahigh-resolution optical coherence tomography. J Biomed Opt 9(1): 47-74.

Drexler W, Baumgartner A, Findl O, et al. (1997). Submicrometer precision biometry of the anterior segment of the human eye. Invest Ophthalmol Vis Sci 38(7): 1304-13.

Drexler W, Findl O, Menapace R, et al. (1998). Partial coherence interferometry: a novel approach to biometry in cataract surgery. Am J Ophthalmol 126(4): 524-34.

Drexler W, Morgner U, Ghanta RK, et al. (2001). Ultrahigh-resolution ophthalmic optical coherence tomography. Nat Med 7(4): 502-7.

du Toit R, Vega JA, Fonn D, et al. (2003). Diurnal variation of corneal sensitivity and thickness. Cornea 22(3): 205-9.

Dumbleton K (2002). Adverse events with silicone hydrogel continuous wear. Cont Lens Anterior Eye 25(3): 137-46.

Dupps WJ, Jr. and Wilson SE (2006). Biomechanics and wound healing in the cornea. Exp Eye Res(In Press): 1-12.

Durrie DS and Kezirian GM (2005). Femtosecond laser versus mechanical keratome flaps in wavefront-guided laser in situ keratomileusis: prospective contralateral eye study. J Cataract Refract Surg 31(1): 120-6.

Eckard A, Stave J and Guthoff RF (2006). In vivo investigations of the corneal epithelium with the confocal Rostock Laser Scanning Microscope (RLSM). Cornea 25(2): 127-31.

Edelhauser HF (2006). The balance between corneal transparency and edema: the Proctor Lecture. Invest Ophthalmol Vis Sci 47(5): 1754-67.

Edelhauser HF, Geroski DH and Ubels JL (1994). Physiology. The Cornea. G Smolin and RA Thoft. Toronto, Little, Brown and Company: 25-42.

Edelhauser HF and Ubels JL (2003). The Cornea and the Sclera. Adler's Physiology of the Eye: Clinical Application. PL Kaufman and A Alm. Toronto, Mosby: 47 - 114.

Edmund C (1987). Determination of the corneal thickness profile by optical pachometry. Acta Ophthalmol (Copenh) 65(2): 147-52.

Edrington TB, Zadnik K and Barr JT (1995). Keratoconus. Optom Clin 4(3): 65-73.

Efron N (1986). Intersubject variability in corneal swelling response to anoxia. Acta Ophthalmol (Copenh) 64(3): 302-5.

Efron N and Carney LG (1979). Oxygen levels beneath the closed eyelid. Invest Ophthalmol Vis Sci 18(1): 93-5.

Ehlers N and Hjortdal J (2004). Corneal thickness: measurement and implications. Exp Eye Res 78(3): 543-8.

Elliott DB, Mitchell S and Whitaker D (1991). Factors affecting light scatter in contact lens wearers. Optom Vis Sci 68(8): 629-33.

Erickson P, Comstock TL and Zantos SG (2002). Is the superior cornea continuously swollen? Clin Exp Optom 85(3): 168-71.

Erie JC, Hodge DO and Bourne WM (2004). Confocal microscopy evaluation of stromal ablation depth after myopic laser in situ keratomileusis and photorefractive keratectomy. J Cataract Refract Surg 30(2): 321-5.

Erie JC, Patel SV, McLaren JW, et al. (2002a). Keratocyte density in keratoconus. A confocal microscopy study. Am J Ophthalmol 134(5): 689-95.

Erie JC, Patel SV, McLaren JW, et al. (2002b). Effect of myopic laser in situ keratomileusis on epithelial and stromal thickness: a confocal microscopy study. Ophthalmology 109(8): 1447-52.

Essex-Sorlie D (1995). Medical Biostatistics and Epidemiology - Examination and Board Review. London, England, Appleton and Lange.

Fakhry MA, Artola A, Belda JI, et al. (2002). Comparison of corneal pachymetry using ultrasound and Orbscan II. J Cataract Refract Surg 28(2): 248-52.

Fan L, Jun J, Jia Q, et al. (1999). Clinical study of orthokeratology in young myopic adolescents. Int. Contact Lens Clin. 26(5): 113-116.

Feng Y and Simpson TL (2005). Comparison of human central cornea and limbus in vivo using optical coherence tomography. Optom Vis Sci 82(5): 416-9.

Feng Y, Varikooty J and Simpson TL (2001). Diurnal variation of corneal and corneal epithelial thickness measured using optical coherence tomography. Cornea 20(5): 480-3.

Fleiszig SM, Efron N and Pier GB (1992). Extended contact lens wear enhances Pseudomonas aeruginosa adherence to human corneal epithelium. Invest Ophthalmol Vis Sci 33(10): 2908-16.

Fonn D and Bruce AS (2005). A review of the Holden-Mertz criteria for critical oxygen transmission. Eye Contact Lens 31(6): 247-51.

Fonn D, du Toit R, Simpson TL, et al. (1999). Sympathetic swelling response of the control eye to soft lenses in the other eye. Invest Ophthalmol Vis Sci 40(13): 3116-21.

Fonn D and Holden BA (1988). Rigid gas-permeable vs. hydrogel contact lenses for extended wear. Am J Optom Physiol Opt 65(7): 536-44.

Fonn D, Holden BA, Roth P, et al. (1984). Comparative physiologic performance of polymethyl methacrylate and gas-permeable contact lenses. Arch Ophthalmol 102(5): 760-4.

Fonn D, Sweeney D, Holden BA, et al. (2005). Corneal oxygen deficiency. Eye Contact Lens 31(1): 23-7.

Foster FS, Pavlin CJ, Harasiewicz KA, et al. (2000). Advances in ultrasound biomicroscopy. Ultrasound Med Biol 26(1): 1-27.

Fujimoto J (2001). Optical and acoustical imaging of biological media: Optical Coherence Tomography. C.R.Acad.Sci.Paris 2(4): 1099-1111.

Fujimoto JG (2003). Optical coherence tomography for ultrahigh resolution in vivo imaging. Nat Biotechnol 21(11): 1361-7.

Fujimoto JG, Bouma B, Tearney GJ, et al. (1998). New technology for high-speed and high-resolution optical coherence tomography. Ann N Y Acad Sci 838: 95-107.

Fujimoto JG, Brezinski ME, Tearney GJ, et al. (1995). Optical biopsy and imaging using optical coherence tomography. Nat Med 1(9): 970-2.

Fujimoto JG, Drexler W, Morgner U, et al. (2000a). Optical coherence tomography: high resolution imaging using echoes of light. Optics & Photonics News(Jan): 24-31.

Fujimoto JG, Pitris C, Boppart SA, et al. (2000b). Optical coherence tomography: an emerging technology for biomedical imaging and optical biopsy. Neoplasia 2(1-2): 9-25.

Gambichler T, Moussa G, Sand M, et al. (2005). Applications of optical coherence tomography in dermatology. J Dermatol Sci 40(2): 85-94.

Gatlin J, Melkus MW, Padgett A, et al. (2003). In vivo fluorescent labeling of corneal wound healing fibroblasts. Exp Eye Res 76(3): 361-71.

Gauthier CA, Fagerholm P, Epstein D, et al. (1996). Failure of mechanical epithelial removal to reverse persistent hyperopia after photorefractive keratectomy. J Refract Surg 12(5): 601-6.

Gauthier CA, Holden BA, Epstein D, et al. (1997). Factors affecting epithelial hyperplasia after photorefractive keratectomy. J Cataract Refract Surg 23(7): 1042-50.

Genth U, Mrochen M, Walti R, et al. (2002). Optical low coherence reflectometry for noncontact measurements of flap thickness during laser in situ keratomileusis. Ophthalmology 109(5): 973-8.

Gherghel D, Hosking SL, Mantry S, et al. (2004). Corneal pachymetry in normal and keratoconic eyes: Orbscan II versus ultrasound. J Cataract Refract Surg 30(6): 1272-7.

Gillis A and Zeyen T (2004). Comparison of optical coherence reflectometry and ultrasound central corneal pachymetry. Bull Soc Belge Ophtalmol(292): 71-5.

Giraldez Fernandez MJ, Diaz Rey A, Cervino A, et al. (2002). A comparison of two pachymetric systems: slit-scanning and ultrasonic. CLAO J 28(4): 221-3.

Gokmen F, Jester JV, Petroll WM, et al. (2002). In vivo confocal microscopy through-focusing to measure corneal flap thickness after laser in situ keratomileusis. J Cataract Refract Surg 28(6): 962-70.

Gonzalez-Meijome JM, Cervino A, Yebra-Pimentel E, et al. (2003). Central and peripheral corneal thickness measurement with Orbscan II and topographical ultrasound pachymetry. J Cataract Refract Surg 29(1): 125-132.

Graham AD, Fusaro RE, Polse KA, et al. (2001). Predicting extended wear complications from overnight corneal swelling. Invest Ophthalmol Vis Sci 42(13): 3150-7.

Greenberg MH and Hill RM (1973). The physiology of contact lens imprints. Am J Optom Arch Am Acad Optom 50(9): 699-702.

Griffiths SN, Drasdo N, Barnes DA, et al. (1986). Effect of epithelial and stromal edema on the light scattering properties of the cornea. Am J Optom Physiol Opt 63(11): 888-94.

Gromacki SJ and Barr JT (1994). Central and peripheral corneal thickness in keratoconus and normal patient groups. Optom Vis Sci 71(7): 437-41.

Guell JL, Lohmann CP, Malecaze FA, et al. (1999). Intraepithelial photorefractive keratectomy for regression after laser in situ keratomileusis. J Cataract Refract Surg 25(5): 670-4.

Gurdal C, Aydin S, Kirimlioglu H, et al. (2003). Effects of extended-wear soft contact lenses on the ocular surface and central corneal thickness. Ophthalmologica 217(5): 329-36.

Guzey M, Satici A, Kilic A, et al. (2002). Oedematous corneal response of the fellow control eye to lotrafilcon a and vifilcon a hydrogel contact lenses in the rabbit. Ophthalmologica 216(2): 139-43.

Hahnel C, Somodi S, Weiss DG, et al. (2000). The keratocyte network of human cornea: a three-dimensional study using confocal laser scanning fluorescence microscopy. Cornea 19(2): 185-93.

Hamano H, Hori M, Hamano T, et al. (1983). Effects of contact lens wear on mitosis of corneal epithelium and lactate content in aqueous humor of rabbit. Jpn J Ophthalmol 27(3): 451-8.

Harper CL, Boulton ME, Bennett D, et al. (1996). Diurnal variations in human corneal thickness. Br J Ophthalmol 80(12): 1068-72.

Harvitt DM and Bonanno JA (1999). Re-evaluation of the oxygen diffusion model for predicting minimum contact lens Dk/t values needed to avoid corneal anoxia. Optom Vis Sci 76(10): 712-9.

Haun A, Gunvant P, Baskaran M, et al. (2004). Central corneal thickness measurement using a pachometer: mean or lowest values? Invest Ophthalmol Vis Sci 45: E-abstract 137.

Hee MR, Izatt JA, Swanson EA, et al. (1995). Optical coherence tomography of the human retina. Arch Ophthalmol 113(3): 325-32.

Helena MC, Baerveldt F, Kim WJ, et al. (1998). Keratocyte apoptosis after corneal surgery. Invest Ophthalmol Vis Sci 39(2): 276-83.

Hermann B, Fernandez EJ, Unterhuber A, et al. (2004). Adaptive-optics ultrahigh-resolution optical coherence tomography. Opt Lett 29(18): 2142-4.

Hersh PS, Fry KL and Bishop DS (2003). Incidence and associations of retreatment after LASIK. Ophthalmology 110(4): 748-54.

Hirano K, Ito Y, Suzuki T, et al. (2001). Optical coherence tomography for the noninvasive evaluation of the cornea. Cornea 20(3): 281-9.

Hirji NK and Larke JR (1979). Corneal thickness in extended wear of soft contact lenses. Br J Ophthalmol 63(4): 274-6.

Hjortdal JO, Moller-Pedersen T, Ivarsen A, et al. (2005). Corneal power, thickness, and stiffness: results of a prospective randomized controlled trial of PRK and LASIK for myopia. J Cataract Refract Surg 31(1): 21-9.

Holden BA, McNally JJ and Egan P (1988a). Limited lateral spread of stromal edema in the human cornea fitted with a ('donut') contact lens with a large central aperture. Curr Eye Res 7(6): 601-5.

Holden BA, McNally JJ, Mertz GW, et al. (1985a). Topographical corneal oedema. Acta Ophthalmol (Copenh) 63(6): 684-91.

Holden BA and Mertz GW (1984). Critical oxygen levels to avoid corneal edema for daily and extended wear contact lenses. Invest Ophthalmol Vis Sci 25(10): 1161-7.

Holden BA, Mertz GW and McNally JJ (1983). Corneal swelling response to contact lenses worn under extended wear conditions. Invest Ophthalmol Vis Sci 24(2): 218-26.

Holden BA, Sweeney DF, La Hood D, et al. (1988b). Corneal deswelling following overnight wear of rigid and hydrogel contact lenses. Curr Eye Res 7(1): 49-53.

Holden BA, Sweeney DF and Sanderson G (1984). The minimum precorneal oxygen tension to avoid corneal edema. Invest Ophthalmol Vis Sci 25(4): 476-80.

Holden BA, Sweeney DF, Vannas A, et al. (1985b). Effects of long-term extended contact lens wear on the human cornea. Invest Ophthalmol Vis Sci 26(11): 1489-501.

Holden BA, Vannas A, Nilsson K, et al. (1985c). Epithelial and endothelial effects from the extended wear of contact lenses. Curr Eye Res 4(6): 739-42.

Hollingsworth JG, Bonshek RE and Efron N (2005a). Correlation of the appearance of the keratoconic cornea in vivo by confocal microscopy and in vitro by light microscopy. Cornea 24(4): 397-405.

Hollingsworth JG and Efron N (2004). Confocal microscopy of the corneas of long-term rigid contact lens wearers. Cont Lens Anterior Eye 27(2): 57-64.

Hollingsworth JG, Efron N and Tullo AB (2005b). In vivo corneal confocal microscopy in keratoconus. Ophthalmic Physiol Opt 25(3): 254-60.

Holzer MP, Rabsilber TM and Auffarth GU (2006). Femtosecond laser-assisted corneal flap cuts: morphology, accuracy, and histopathology. Invest Ophthalmol Vis Sci 47(7): 2828-31.

Hori-Komai Y, Toda I, Asano-Kato N, et al. (2002). Reasons for not performing refractive surgery. J Cataract Refract Surg 28(5): 795-7.

Hrynchak P and Simpson T (2000). Optical coherence tomography: an introduction to the technique and its use. Optom Vis Sci 77(7): 347-56.

Huang D, Swanson EA, Lin CP, et al. (1991). Optical coherence tomography. Science 254(5035): 1178-81.

Huang D, Tang M and Shekhar R (2003). Mathematical model of corneal surface smoothing after laser refractive surgery. Am J Ophthalmol 135(3): 267-78.

Humphrey Z (2001). OCT2 User Manual. Dublin, CA**:** 1-2.

Ichijima H, Imayasu M, Tanaka H, et al. (2000). Effects of RGP lens extended wear on glucose-lactate metabolism and stromal swelling in the rabbit cornea. Clao J 26(1): 30-6.

Ichijima H, Jester JV, Petroll WM, et al. (1994). Laser and tandem scanning confocal microscopic studies of rabbit corneal wound healing. Scanning 16(5): 263-8.

Ichijima H, Ohashi J, Petroll WM, et al. (1993). Morphological and biochemical evaluation for rigid gas permeable contact lens extended wear on rabbit corneal epithelium. Clao J 19(2): 121-8.

Ichikawa H, Kozai A, MacKeen DL, et al. (1989). Corneal swelling responses with extended wear in naive and adapted subjects with menicon RGP contact lenses. CLAO J 15(3): 192-4.

Imanishi J, Kamiyama K, Iguchi I, et al. (2000). Growth factors: importance in wound healing and maintenance of transparency of the cornea. Prog Retin Eye Res 19(1): 113-29.

Imayasu M, Petroll WM, Jester JV, et al. (1994). The relation between contact lens oxygen transmissibility and binding of Pseudomonas aeruginosa to the cornea after overnight wear. Ophthalmology 101(2): 371-88.

Ioannidis AS, Speedwell L and Nischal KK (2005). Unilateral keratoconus in a child with chronic and persistent eye rubbing. Am J Ophthalmol 139(2): 356-7.

Iskander NG, Anderson Penno E, Peters NT, et al. (2001). Accuracy of Orbscan pachymetry measurements and DHG ultrasound pachymetry in primary laser in situ keratomileusis and LASIK enhancement procedures. J Cataract Refract Surg 27(5): 681-5.

Ivarsen A, Laurberg T and Moller-Pedersen T (2003). Characterisation of corneal fibrotic wound repair at the LASIK flap margin. Br J Ophthalmol 87(10): 1272-8.

Ivarsen A, Laurberg T and Moller-Pedersen T (2004). Role of keratocyte loss on corneal wound repair after LASIK. Invest Ophthalmol Vis Sci 45(10): 3499-506.

Izatt JA, Hee MR, Swanson EA, et al. (1994). Micrometer-scale resolution imaging of the anterior eye in vivo with optical coherence tomography. Arch Ophthalmol 112(12): 1584-9.

Javaloy J, Vidal MT, Villada JR, et al. (2004). Comparison of four corneal pachymetry techniques in corneal refractive surgery. J Refract Surg 20(1): 29-34.

Jayakumar J and Swarbrick HA (2005). The effect of age on short-term orthokeratology. Optom Vis Sci 82(6): 505-11.

Jaycock PD, O'Brart DP, Rajan MS, et al. (2005). 5-year follow-up of LASIK for hyperopia. Ophthalmology 112(2): 191-9.

Jester JV, Moller-Pedersen T, Huang J, et al. (1999a). The cellular basis of corneal transparency: evidence for 'corneal crystallins'. J Cell Sci 112 (Pt 5): 613-22.

Jester JV, Petroll WM and Cavanagh HD (1999b). Corneal stromal wound healing in refractive surgery: the role of myofibroblasts. Prog Retin Eye Res 18(3): 311-56.

Jin GJ, Lyle WA and Merkley KH (2005). Laser in situ keratomileusis for primary hyperopia. J Cataract Refract Surg 31(4): 776-84.

Johnson ME and Murphy PJ (2005). The agreement and repeatability of tear meniscus height measurement methods. Optom Vis Sci 82(12): 1030-7.

Johnson MH, Boltz RL and Godio LB (1985). Deswelling of the cornea after hypoxia. Am J Optom Physiol Opt 62(11): 768-73.

Jones L, Leech R, Rahman S, et al. (2003). Determination of tear meniscus height using a novel method based upon Optical Coherence Tomography. Invest Ophthalmol Vis Sci 44: E-abstract 2461.

Kallinikos P and Efron N (2004). On the etiology of keratocyte loss during contact lens wear. Invest Ophthalmol Vis Sci 45(9): 3011-20.

Kallinikos P, Morgan P and Efron N (2006). Assessment of stromal keratocytes and tear film inflammatory mediators during extended wear of contact lenses. Cornea 25(1): 1-10.

Kanellopoulos AJ and Pe LH (2006). Wavefront-guided enhancements using the wavelight excimer laser in symptomatic eyes previously treated with LASIK. J Refract Surg 22(4): 345-9.

Kangas TA, Edelhauser HF, Twining SS, et al. (1990). Loss of stromal glycosaminoglycans during corneal edema. Invest Ophthalmol Vis Sci 31(10): 1994-2002.

Kato T, Nakayasu K, Hosoda Y, et al. (1999). Corneal wound healing following laser in situ keratomileusis (LASIK): a histopathological study in rabbits. Br J Ophthalmol 83(11): 1302-5.

Kaufman HE, Barron BA and McDonald MB (1998). The Cornea. The Cornea. Boston, Butterworth-Heinemann: 28-43.

Kawana K, Miyata K, Tokunaga T, et al. (2005). Central corneal thickness measurements using Orbscan II scanning slit topography, noncontact specular microscopy, and ultrasonic pachymetry in eyes with keratoconus. Cornea 24(8): 967-71.

Kawana K, Tokunaga T, Miyata K, et al. (2004). Comparison of corneal thickness measurements using Orbscan II, non-contact specular microscopy, and ultrasonic pachymetry in eyes after laser in situ keratomileusis. Br J Ophthalmol 88(4): 466-8.

Kerns RL (1976). Research in orthokeratology. Part I: Introduction and background. J Am Optom Assoc 47(8): 1047-51.

Kerns RL (1978). Research in orthokeratology. Part VIII: results, conclusions and discussion of techniques. J Am Optom Assoc 49(3): 308-14.

Kezirian GM and Stonecipher KG (2004). Comparison of the IntraLase femtosecond laser and mechanical keratomes for laser in situ keratomileusis. J Cataract Refract Surg 30(4): 804-11.

Kiely PM, Carney LG and Smith G (1982). Diurnal variations of corneal topography and thickness. Am J Optom Physiol Opt 59(12): 976-82.

Kim JK, Kim SS, Lee HK, et al. (2004). Laser in situ keratomileusis versus laser-assisted subepithelial keratectomy for the correction of high myopia. J Cataract Refract Surg 30(7): 1405-11.

Kim JY, Kim MJ, Kim TI, et al. (2006). A femtosecond laser creates a stronger flap than a mechanical microkeratome. Invest Ophthalmol Vis Sci 47(2): 599-604.

Kim WJ, Helena MC, Mohan RR, et al. (1999). Changes in corneal morphology associated with chronic epithelial injury. Invest Ophthalmol Vis Sci 40(1): 35-42.

King-Smith PE, Fink BA, Fogt N, et al. (2000). The thickness of the human precorneal tear film: evidence from reflection spectra. Invest Ophthalmol Vis Sci 41(11): 3348-59.

King-Smith PE, Fink BA, Hill RM, et al. (2004). The thickness of the tear film. Curr Eye Res 29(4-5): 357-68.

Kitagawa K, Sakamoto Y, Sasaki K, et al. (1996). Evaluation of transparency and barrier function of the cornea by Scheimpflug images. Ophthalmic Res 28 Suppl 2: 72-7.

Kobayashi A, Yoshita T and Sugiyama K (2005). In vivo findings of the bulbar/palpebral conjunctiva and presumed meibomian glands by laser scanning confocal microscopy. Cornea 24(8): 985-8.

Komai Y and Ushiki T (1991). The three-dimensional organization of collagen fibrils in the human cornea and sclera. Invest Ophthalmol Vis Sci 32(8): 2244-58.

Kozak I, Hornak M, Juhas T, et al. (2003). Changes in central corneal thickness after laser in situ keratomileusis and photorefractive keratectomy. J Refract Surg 19(2): 149-53.

Krueger RR, Juhasz T, Gualano A, et al. (1998). The picosecond laser for nonmechanical laser in situ keratomileusis. J Refract Surg 14(4): 467-9.

Kuo IC, Ou R and Hwang DG (2001). Flap haze after epithelial debridement and flap hydration for treatment of post-laser in situ keratomileusis striae. Cornea 20(3): 339-41.

La Hood D, Sweeney DF and Holden BA (1988). Overnight corneal edema with hydrogel, rigid gas-permeable and silicone elastomer contact lenses. Int Contact Lens Clin 15: 149-152.

Lackner B, Schmidinger G, Pieh S, et al. (2005a). Repeatability and reproducibility of central corneal thickness measurement with Pentacam, Orbscan, and ultrasound. Optom Vis Sci 82(10): 892-9.

Lackner B, Schmidinger G and Skorpik C (2005b). Validity and repeatability of anterior chamber depth measurements with Pentacam and Orbscan. Optom Vis Sci 82(9): 858-61.

Ladage PM (2004). What does overnight lens wear do to the corneal epithelium? is corneal refractive therapy different? Eye Contact Lens 30(4): 194-7; discussion 205-6.

Ladage PM, Jester JV, Petroll WM, et al. (2003a). Role of oxygen in corneal epithelial homeostasis during extended contact lens wear. Eye Contact Lens 29(1 Suppl): S2-6; discussion S26-9, S192-4.

Ladage PM, Jester JV, Petroll WM, et al. (2003b). Vertical movement of epithelial basal cells toward the corneal surface during use of extended-wear contact lenses. Invest Ophthalmol Vis Sci 44(3): 1056-63.

Ladage PM, Ren DH, Petroll WM, et al. (2003c). Effects of eyelid closure and disposable and silicone hydrogel extended contact lens wear on rabbit corneal epithelial proliferation. Invest Ophthalmol Vis Sci 44(5): 1843-9.

Ladage PM, Yamamoto K, Li L, et al. (2002a). Corneal epithelial homeostasis following daily and overnight contact lens wear. Cont Lens Anterior Eye 25(1): 11-21.

Ladage PM, Yamamoto K, Li L, et al. (2002b). Effects of O2 transmissibility on corneal epithelium after daily and extended contact lens wear in rabbit and man. Adv Exp Med Biol 506(Pt B): 885-93.

Ladage PM, Yamamoto K, Ren DH, et al. (2003d). Recovery time of corneal epithelial proliferation in the rabbit following rigid gas-permeable extended contact-lens wear. Eye Contact Lens 29(2): 61-4.

Ladage PM, Yamamoto K, Ren DH, et al. (2001a). Proliferation rate of rabbit corneal epithelium during overnight rigid contact lens wear. Invest Ophthalmol Vis Sci 42(12): 2804-12.

Ladage PM, Yamamoto K, Ren DH, et al. (2001b). Effects of rigid and soft contact lens daily wear on corneal epithelium, tear lactate dehydrogenase, and bacterial binding to exfoliated epithelial cells. Ophthalmology 108(7): 1279-88.

Ladage PM, Yamamoto N, Robertson DM, et al. (2004). Pseudomonas aeruginosa corneal binding after 24-hour orthokeratology lens wear. Eye Contact Lens 30(3): 173-8.

Lafond G, Solomon L and Bonnet S (2004). Retreatment to enlarge small excimer laser optical zones using combined myopic and hyperopic ablations. J Refract Surg 20(1): 46-52.

Lambert SR and Klyce SD (1981). The origins of Sattler's veil. Am J Ophthalmol 91(1): 51-6.

Lang J and Rah MJ (2004). Adverse corneal events associated with corneal reshaping: a case series. Eye Contact Lens 30(4): 231-3; discussion 242-3.

Lee HK, Lee KS, Kim JK, et al. (2005). Epithelial healing and clinical outcomes in excimer laser photorefractive surgery following three epithelial removal techniques: mechanical, alcohol, and excimer laser. Am J Ophthalmol 139(1): 56-63.

Leibowitz H and Waring G (1998). The normal cornea. Corneal disorders: clinical diagnosis and management. Philadelphia, Saunders: 10-26.

Lemley HL, Chodosh J, Wolf TC, et al. (2000). Partial dislocation of laser in situ keratomileusis flap by air bag injury. J Refract Surg 16(3): 373-4.

Lemp MA (1994). Dry eye syndromes: treatment and clinical trials. Adv Exp Med Biol 350: 553-9.

Lemp MA (1998). Epidemiology and classification of dry eye. Adv Exp Med Biol 438: 791-803.

Leung CK, Chan WM, Ko CY, et al. (2005). Visualization of anterior chamber angle dynamics using optical coherence tomography. Ophthalmology 112(6): 980-4.

Li HF, Petroll WM, Moller-Pedersen T, et al. (1997). Epithelial and corneal thickness measurements by in vivo confocal microscopy through focusing (CMTF). Curr Eye Res 16(3): 214-21.

Li X, Liu L and Qiu L (2002). Early diagnosis of keratoconus with Orbscan-II anterior system. J Huazhong Univ Sci Technolog Med Sci 22(4): 369-70.

Li Y, Shekhar R and Huang D (2006). Corneal pachymetry mapping with high-speed optical coherence tomography. Ophthalmology 113(5): 799 e1-2.

Liesegang TJ (2002). Physiologic changes of the cornea with contact lens wear. CLAO J 28(1): 12-27.

Lim H, Jiang Y, Wang Y, et al. (2005). Ultrahigh-resolution optical coherence tomography with a fiber laser source at 1 microm. Opt Lett 30(10): 1171-3.

Lim T, Yang S, Kim M, et al. (2006). Comparison of the IntraLase femtosecond laser and mechanical microkeratome for laser in situ keratomileusis. Am J Ophthalmol 141(5): 833-9.

Lin MC, Graham AD, Fusaro RE, et al. (2002). Impact of rigid gas-permeable contact lens extended wear on corneal epithelial barrier function. Invest Ophthalmol Vis Sci 43(4): 1019-24.

Linnola RJ, Findl O, Hermann B, et al. (2005). Intraocular lens-capsular bag imaging with ultrahigh-resolution optical coherence tomography Pseudophakic human autopsy eyes. J Cataract Refract Surg 31(4): 818-23.

Liu Z, Huang AJ and Pflugfelder SC (1999). Evaluation of corneal thickness and topography in normal eyes using the Orbscan corneal topography system. Br J Ophthalmol 83(7): 774-8.

Liu Z and Pflugfelder SC (2000). The effects of long-term contact lens wear on corneal thickness, curvature, and surface regularity. Ophthalmology 107(1): 105-11.

Liu Z, Zhang M, Chen J, et al. (2002). Corneal topography and thickness in keratoconus. Zhonghua Yan Ke Za Zhi 38(12): 740-3.

Lohman LE, Rao GN and Aquavella JV (1982a). In vivo microscopic observations of human corneal epithelial abnormalities. Am J Ophthalmol 93(2): 210-7.

Lohman LE, Rao GN, Tripathi RC, et al. (1982b). In vivo specular microscopy of edematous human corneal epithelium with light and scanning electron microscopic correlation. Ophthalmology 89(6): 621-9.

Lohmann CP and Guell JL (1998). Regression after LASIK for the treatment of myopia: the role of the corneal epithelium. Semin Ophthalmol 13(2): 79-82.

Lohmann CP, Patmore A, O'Brart D, et al. (1997). Regression and wound healing after excimer laser PRK: a histopathological study on human corneas. Eur J Ophthalmol 7(2): 130-8.

Lohmann CP, Reischl U and Marshall J (1999). Regression and epithelial hyperplasia after myopic photorefractive keratectomy in a human cornea. J Cataract Refract Surg 25(5): 712-5.

Lowther GE and Hill RM (1973). Recovery of the corneal epithelium after a period of anoxia. Am J Optom Arch Am Acad Optom 50(3): 234-41.

Lowther GE and Hill RM (1974). Corneal epithelium. Arch Ophthalmol 92(3): 231-4.

Lu F, Simpson T, Fonn D, et al. (2006a). Validity of pachymetric measurements by manipulating the acoustic factor of Orbscan II. Eye Contact Lens 32(2): 78-83.

Lu F, Simpson T, Sorbara L, et al. (2006b). Moldability of the ocular surface in response to local mechanical stress. Invest Ophthalmol Vis Sci 47: E-abstract 2390.

Lu L, Reinach PS and Kao WW (2001). Corneal epithelial wound healing. Exp Biol Med (Maywood) 226(7): 653-64.

Lum E and Swarbrick H (2006). Lens Dk/t influences the clinical response in overnight orthokeratology. Invest Ophthalmol Vis Sci(47): E-abstract 110.

Maatta M, Vaisanen T, Vaisanen MR, et al. (2006). Altered expression of type XIII collagen in keratoconus and scarred human cornea: Increased expression in scarred cornea is associated with myofibroblast transformation. Cornea 25(4): 448-53.

MacDougall N, Situ P, Chan A, et al. (2002). Single site 6 month clinical outcomes for Custom LASIK. Optom Vis Sci 79(12s): 264.

MacDougall N, Situ P, Chan A, et al. (2003). Low contrast acuity, contrast sensitivity and higher-order aberration outcomes following Custom LASIK. Invest Ophthalmol Vis Sci 44: E-abstract 2629.

Magallanes R, Shah S, Zadok D, et al. (2001). Stability after laser in situ keratomileusis in moderately and extremely myopic eyes. J Cataract Refract Surg 27(7): 1007-12.

Maldonado MJ (2002). Undersurface ablation of the flap for laser in situ keratomileusis retreatment. Ophthalmology 109(8): 1453-64.

Maldonado MJ, Ruiz-Oblitas L, Munuera JM, et al. (2000). Optical coherence tomography evaluation of the corneal cap and stromal bed features after laser in situ keratomileusis for high myopia and astigmatism. Ophthalmology 107(1): 81-7; discussion 88.

Marsich MW and Bullimore MA (2000). The repeatability of corneal thickness measures. Cornea 19(6): 792-5.

Masters BR and Bohnke M (1999). Video-rate, scanning slit confocal microscopy of living human cornea in vivo: three-dimensional confocal microscopy of the eye. Methods Enzymol 307: 536-63.

Masters BR and Bohnke M (2001). Three-dimensional confocal microscopy of the human cornea in vivo. Ophthalmic Res 33(3): 125-35.

Masters BR and Bohnke M (2002). Three-dimensional confocal microscopy of the living human eye. Annu Rev Biomed Eng 4: 69-91.

Matilla T, Douthwaite W and Hurst M (1995). Forward and backward light scatter measurements in the assessment of corneal oedema. British Congress of Optometry and Vision Science, Bradford University, Bradford, UK, Ophthal. Physiol. Opt.

Matsubara M, Kamei Y, Takeda S, et al. (2004). Histologic and histochemical changes in rabbit cornea produced by an orthokeratology lens. Eye Contact Lens 30(4): 198-204; discussion 205-6.

Maurice DM (1957). The structure and transparency of the cornea. J Physiol 136(2): 263-86.

Maurice DM (1987). The biology of wound healing in the corneal stroma. Castroviejo lecture. Cornea 6(3): 162-8.

May CA, Priglinger SG, Neubauer AS, et al. (2004). Laser in situ keratomileusis in human corneas: new organ culture model. J Cataract Refract Surg 30(1): 179-86.

McLaren JW, Nau CB, Erie JC, et al. (2004). Corneal thickness measurement by confocal microscopy, ultrasound, and scanning slit methods. Am J Ophthalmol 137(6): 1011-20.

McMonnies CW (2005). The biomechanics of keratoconus and rigid contact lenses. Eye Contact Lens 31(2): 80-92.

McMonnies CW and Boneham GC (2003). Keratoconus, allergy, itch, eye-rubbing and hand-dominance. Clin Exp Optom 86(6): 376-84.

Meek KM, Blamires T, Elliott GF, et al. (1987). The organisation of collagen fibrils in the human corneal stroma: a synchrotron X-ray diffraction study. Curr Eye Res 6(7): 841-6.

Meek KM, Dennis S and Khan S (2003a). Changes in the refractive index of the stroma and its extrafibrillar matrix when the cornea swells. Biophys J 85(4): 2205-12.

Meek KM, Leonard DW, Connon CJ, et al. (2003b). Transparency, swelling and scarring in the corneal stroma. Eye 17(8): 927-36.

Meek KM and Newton RH (1999). Organization of collagen fibrils in the corneal stroma in relation to mechanical properties and surgical practice. J Refract Surg 15(6): 695-9.

Meek KM, Tuft SJ, Huang Y, et al. (2005). Changes in collagen orientation and distribution in keratoconus corneas. Invest Ophthalmol Vis Sci 46(6): 1948-56.

Meinhardt B, Stachs O, Stave J, et al. (2006). Evaluation of biometric methods for measuring the anterior chamber depth in the non-contact mode. Graefes Arch Clin Exp Ophthalmol 244(5): 559-64.

Meissner OA, Rieber J, Babaryka G, et al. (2006). Intravascular optical coherence tomography: comparison with histopathology in atherosclerotic peripheral artery specimens. J Vasc Interv Radiol 17(2 Pt 1): 343-9.

Mertz GW (1980). Overnight swelling of the living human cornea. J Am Optom Assoc 51(3): 211-4.

Miglior S, Albe E, Guareschi M, et al. (2004). Intraobserver and interobserver reproducibility in the evaluation of ultrasonic pachymetry measurements of central corneal thickness. Br J Ophthalmol 88(2): 174-7.

Miller AE, McCulley JP, Bowman RW, et al. (2001). Patient satisfaction after LASIK for myopia. Clao J 27(2): 84-8.

Modis L, Jr., Langenbucher A and Seitz B (2001a). Corneal thickness measurements with contact and noncontact specular microscopic and ultrasonic pachymetry. Am J Ophthalmol 132(4): 517-21.

Modis L, Jr., Langenbucher A and Seitz B (2001b). Scanning-slit and specular microscopic pachymetry in comparison with ultrasonic determination of corneal thickness. Cornea 20(7): 711-4.

Moezzi AM, Fonn D, Simpson TL, et al. (2004). Contact lens-induced corneal swelling and surface changes measured with the Orbscan II corneal topographer. Optom Vis Sci 81(3): 189-93.

Mohan RR, Hutcheon AE, Choi R, et al. (2003). Apoptosis, necrosis, proliferation, and myofibroblast generation in the stroma following LASIK and PRK. Exp Eye Res 76(1): 71-87.

Moller-Pedersen T (2004). Keratocyte reflectivity and corneal haze. Exp Eye Res 78(3): 553-60.

Moller-Pedersen T, Cavanagh HD, Petroll WM, et al. (2000). Stromal wound healing explains refractive instability and haze development after photorefractive keratectomy: a 1-year confocal microscopic study. Ophthalmology 107(7): 1235-45.

Moller-Pedersen T and Ehlers N (1995). A three-dimensional study of the human corneal keratocyte density. Curr Eye Res 14(6): 459-64.

Moller-Pedersen T, Vogel M, Li HF, et al. (1997). Quantification of stromal thinning, epithelial thickness, and corneal haze after photorefractive keratectomy using in vivo confocal microscopy. Ophthalmology 104(3): 360-8.

Montes M, Chayet A, Gomez L, et al. (1999). Laser in situ keratomileusis for myopia of -1.50 to -6.00 diopters. J Refract Surg 15(2): 106-10.

Moon JW, Shin KC, Lee HJ, et al. (2006). The effect of contact lens wear on the ocular surface changes in keratoconus. Eye Contact Lens 32(2): 96-101.

Mountford J (1997a). An analysis of the changes in corneal shape and refractive error induced by accelerated orthokeratology. Int Contact Lens Clin(24): 128-43.

Mountford J (1997b). Orthokeratology. Contact Lenses. A Phillips and L Speedwell. Oxford, Butterworth-Heinemann: 653-692.

Muallem MS, Yoo SH, Romano AC, et al. (2004). Flap and stromal bed thickness in laser in situ keratomileusis enhancement. J Cataract Refract Surg 30(11): 2295-302.

Murphy PJ, Patel S and Marshall J (2001). The effect of long-term, daily contact lens wear on corneal sensitivity. Cornea 20(3): 264-9.

Muscat S, McKay N, Parks S, et al. (2002). Repeatability and reproducibility of corneal thickness measurements by optical coherence tomography. Invest Ophthalmol Vis Sci 43(6): 1791-5.

Myrowitz EH, Melia M and O'Brien TP (2002). The relationship between long-term contact lens wear and corneal thickness. Clao J 28(4): 217-20.

Nakagawa T, Maeda N, Okazaki N, et al. (2006). Ultrasound biomicroscopic examination of acute hydrops in patients with keratoconus. Am J Ophthalmol 141(6): 1134-6.

Nakamura K, Kurosaka D, Bissen-Miyajima H, et al. (2001a). Intact corneal epithelium is essential for the prevention of stromal haze after laser assisted in situ keratomileusis. Br J Ophthalmol 85(2): 209-13.

Nakamura Y, Sotozono C and Kinoshita S (2001b). The epidermal growth factor receptor (EGFR): role in corneal wound healing and homeostasis. Exp Eye Res 72(5): 511-7.

Nanba A, Amano S, Oshika T, et al. (2005). Corneal higher order wavefront aberrations after hyperopic laser in situ keratomileusis. J Refract Surg 21(1): 46-51.

Naoumidi I, Papadaki T, Zacharopoulos I, et al. (2003). Epithelial ingrowth after laser in situ keratomileusis: a histopathologic study in human corneas. Arch Ophthalmol 121(7): 950-5.

Nau CB, Erie JC, Hodge DO, et al. (2005). Central, epithelial and stromal thickness 5 years after LASIK and PRK. Invest Ophthalmol Vis Sci 46: E-abstract 4387.

Nauheim JS and Perry HD (1985). A clinicopathologic study of contact-lens-related keratoconus. Am J Ophthalmol 100(4): 543-6.

Nejima R, Miyata K, Tanabe T, et al. (2005). Corneal barrier function, tear film stability, and corneal sensation after photorefractive keratectomy and laser in situ keratomileusis. Am J Ophthalmol 139(1): 64-71.

Nepomuceno RL, Boxer BS, Wachler, et al. (2004). Laser in situ keratomileusis for hyperopia with the LADARVision 4000 with centration on the coaxially sighted corneal light reflex. J Cataract Refract Surg 30(6): 1281-6.

Netto MV, Ambrosio R, Jr., Chalita MR, et al. (2005a). Corneal wound healing response following different modalities of refractive surgical procedures. Arq Bras Oftalmol 68(1): 140-9.

Netto MV, Mohan RR, Ambrosio R, Jr., et al. (2005b). Wound healing in the cornea: a review of refractive surgery complications and new prospects for therapy. Cornea 24(5): 509-22.

Netto MV, Mohan RR, Sinha S, et al. (2006). Stromal haze, myofibroblasts, and surface irregularity after PRK. Exp Eye Res 82(5): 788-97.

Nichols JJ and King-Smith PE (2003). Thickness of the pre- and post-contact lens tear film measured in vivo by interferometry. Invest Ophthalmol Vis Sci 44(1): 68-77.

Nichols JJ, Marsich MM, Nguyen M, et al. (2000). Overnight orthokeratology. Optom Vis Sci 77(5): 252-9.

Nielsen K, Vorum H, Fagerholm P, et al. (2006). Proteome profiling of corneal epithelium and identification of marker proteins for keratoconus, a pilot study. Exp Eye Res 82(2): 201-9.

Noda-Tsuruya T, Toda I, Asano-Kato N, et al. (2004). Risk factors for development of diffuse lamellar keratitis after laser in situ keratomileusis. J Refract Surg 20(1): 72-5.

Nordan LT, Slade SG, Baker RN, et al. (2003). Femtosecond laser flap creation for laser in situ keratomileusis: six-month follow-up of initial U.S. clinical series. J Refract Surg 19(1): 8-14.

O'Donnell C and Maldonado-Codina C (2005). Agreement and repeatability of central thickness measurement in normal corneas using ultrasound pachymetry and the OCULUS Pentacam. Cornea 24(8): 920-4.

O'Leary DJ, Wilson G and Henson DB (1981). The effect of anoxia on the human corneal epithelium. Am J Optom Physiol Opt 58(6): 472-6.

O'Neal MR and Polse KA (1985). In vivo assessment of mechanisms controlling corneal hydration. Invest Ophthalmol Vis Sci 26(6): 849-56.

Odenthal MT, Nieuwendaal CP, Venema HW, et al. (1999). In vivo human corneal hydration control dynamics: a new model. Invest Ophthalmol Vis Sci 40(2): 312-9.

Oliva MS, Ambrosio Junior R and Wilson SE (2004). Influence of intraoperative epithelial defects on outcomes in LASIK for myopia. Am J Ophthalmol 137(2): 244-9.

Oqbuehi KC and Almubrad TM (2005). Limits of agreement between the optical pachymeter and a non-contact specular microscope. Cornea 24(5): 545-9.

Owens H and Watters GA (1996). An evaluation of the keratoconic cornea using computerised corneal mapping and ultrasonic measurements of corneal thickness. Ophthalmic Physiol Opt 16(2): 115-23.

Oyster C (1999). The Cornea and the Sclera. The Human Eye: Structure and Function. Sunderland, Massachusetts, Sinauer Associates, Inc.: 325 - 378.

Pallikaris IG, Papatzanaki ME, Stathi EZ, et al. (1990). Laser in situ keratomileusis. Lasers Surg Med 10(5): 463-8.

Pallikaris IG and Siganos DS (1994). Excimer laser in situ keratomileusis and photorefractive keratectomy for correction of high myopia. J Refract Corneal Surg 10(5): 498-510.

Pallikaris IG and Siganos DS (1997). Laser in situ keratomileusis to treat myopia: early experience. J Cataract Refract Surg 23(1): 39-49.

Park CK and Kim JH (1999). Comparison of wound healing after photorefractive keratectomy and laser in situ keratomileusis in rabbits. J Cataract Refract Surg 25(6): 842-50.

Patel DV and McGhee CN (2006). Mapping the corneal sub-basal nerve plexus in keratoconus by in vivo laser scanning confocal microscopy. Invest Ophthalmol Vis Sci 47(4): 1348-51.

Patel S, McLaren J, Hodge D, et al. (2001). Normal human keratocyte density and corneal thickness measurement by using confocal microscopy in vivo. Invest Ophthalmol Vis Sci 42(2): 333-9.

Patel SV, McLaren JW, Hodge DO, et al. (2002). Confocal microscopy in vivo in corneas of long-term contact lens wearers. Invest Ophthalmol Vis Sci 43(4): 995-1003.

Pavlin CJ and Foster FS (1998). Ultrasound biomicroscopy. High-frequency ultrasound imaging of the eye at microscopic resolution. Radiol Clin North Am 36(6): 1047-58.

Pavlin CJ, Harasiewicz K, Sherar MD, et al. (1991). Clinical use of ultrasound biomicroscopy. Ophthalmology 98(3): 287-95.

Perez JG, Meijome JM, Jalbert I, et al. (2003). Corneal epithelial thinning profile induced by long-term wear of hydrogel lenses. Cornea 22(4): 304-7.

Perez-Santonja JJ, Linna TU, Tervo KM, et al. (1998). Corneal wound healing after laser in situ keratomileusis in rabbits. J Refract Surg 14(6): 602-9.

Pfister RR and Burstein NL (1977). The normal and abnormal human corneal epithelial surface: a scanning electron microscope study. Invest Ophthalmol Vis Sci 16(7): 614-22.

Pflugfelder SC, Liu Z, Feuer W, et al. (2002). Corneal thickness indices discriminate between keratoconus and contact lens-induced corneal thinning. Ophthalmology 109(12): 2336-41.

Philipp WE, Speicher L and Gottinger W (2003). Histological and immunohistochemical findings after laser in situ keratomileusis in human corneas. J Cataract Refract Surg 29(4): 808-20.

Phillips AJ (2003). Can true monocular keratoconus occur? Clin Exp Optom 86(6): 399-402.

Phillips CI (1990). Contact lenses and corneal deformation: cause, correlate or co-incidence? Acta Ophthalmol (Copenh) 68(6): 661-8.

Polse KA (1977). Orthokeratology as a clinical procedure. Am J Optom Physiol Opt 54(6): 345-6.

Polse KA, Brand RJ, Cohen SR, et al. (1990). Hypoxic effects on corneal morphology and function. Invest Ophthalmol Vis Sci 31(8): 1542-54.

Polse KA, Brand RJ, Schwalbe JS, et al. (1983a). The Berkeley Orthokeratology Study, Part II: Efficacy and duration. Am J Optom Physiol Opt 60(3): 187-98.

Polse KA, Brand RJ, Vastine DW, et al. (1983b). Corneal change accompanying orthokeratology. Plastic or elastic? Results of a randomized controlled clinical trial. Arch Ophthalmol 101(12): 1873-8.

Price FW, Jr., Koller DL and Price MO (1999). Central corneal pachymetry in patients undergoing laser in situ keratomileusis. Ophthalmology 106(11): 2216-20.

Priglinger SG, May CA, Alge CS, et al. (2006). Immunohistochemical findings after LASIK confirm in vitro LASIK model. Cornea 25(3): 331-5.

Priglinger SG, Neubauer AS, May CA, et al. (2003). Optical coherence tomography for the detection of laser in situ keratomileusis in donor corneas. Cornea 22(1): 46-50.

Prisant O, Calderon N, Chastang P, et al. (2003). Reliability of pachymetric measurements using orbscan after excimer refractive surgery. Ophthalmology 110(3): 511-5.

Puliafito CA, Hee MR, Lin CP, et al. (1995). Imaging of macular diseases with optical coherence tomography. Ophthalmology 102(2): 217-29.

Qazi MA, Roberts CJ, Mahmoud AM, et al. (2005). Topographic and biomechanical differences between hyperopic and myopic laser in situ keratomileusis. J Cataract Refract Surg 31(1): 48-60.

Rabinowitz YS (1998). Keratoconus. Surv Ophthalmol 42(4): 297-319.

Rabinowitz YS, Rasheed K, Yang H, et al. (1998). Accuracy of ultrasonic pachymetry and videokeratography in detecting keratoconus. J Cataract Refract Surg 24(2): 196-201.

Rabsilber TM, Khoramnia R and Auffarth GU (2006). Anterior chamber measurements using Pentacam rotating Scheimpflug camera. J Cataract Refract Surg 32(3): 456-9.

Radford SW, Lim R and Salmon JF (2004). Comparison of Orbscan and ultrasound pachymetry in the measurement of central corneal thickness. Eye 18(4): 434-6.

Radhakrishnan S, Rollins AM, Roth JE, et al. (2001). Real-time optical coherence tomography of the anterior segment at 1310 nm. Arch Ophthalmol 119(8): 1179-85.

Rah MJ, Barr JT and Bailey MD (2002a). Corneal pigmentation in overnight orthokeratology: a case series. Optometry 73(7): 425-34.

Rah MJ, Jackson JM, Jones LA, et al. (2002b). Overnight orthokeratology: preliminary results of the Lenses and Overnight Orthokeratology (LOOK) study. Optom Vis Sci 79(9): 598-605.

Rainer G, Findl O, Petternel V, et al. (2004). Central corneal thickness measurements with partial coherence interferometry, ultrasound, and the Orbscan system. Ophthalmology 111(5): 875-9.

Rainer G, Petternel V, Findl O, et al. (2002). Comparison of ultrasound pachymetry and partial coherence interferometry in the measurement of central corneal thickness. J Cataract Refract Surg 28(12): 2142-5.

Rajan MS, Watters W, Patmore A, et al. (2005). In vitro human corneal model to investigate stromal epithelial interactions following refractive surgery. J Cataract Refract Surg 31(9): 1789-801.

Rapuano CJ, Fishbaugh JA and Strike DJ (1993). Nine point corneal thickness measurements and keratometry readings in normal corneas using ultrasound pachymetry. Insight 18(4): 16-22.

Ratkay-Traub I, Juhasz T, Horvath C, et al. (2001). Ultra-short pulse (femtosecond) laser surgery: initial use in LASIK flap creation. Ophthalmol Clin North Am 14(2): 347-55, viii-ix.

Realini T and Lovelace K (2003). Measuring central corneal thickness with ultrasound pachymetry. Optom Vis Sci 80(6): 437-9.

Reinstein DZ, Ameline B, Puech M, et al. (2005). VHF digital ultrasound three-dimensional scanning in the diagnosis of myopic regression after corneal refractive surgery. J Refract Surg 21(5): 480-4.

Reinstein DZ, Silverman RH and Coleman DJ (1993). High-frequency ultrasound measurement of the thickness of the corneal epithelium. Refract Corneal Surg 9(5): 385-7.

Reinstein DZ, Silverman RH, Raevsky T, et al. (2000). Arc-scanning very high-frequency digital ultrasound for 3D pachymetric mapping of the corneal epithelium and stroma in laser in situ keratomileusis. J Refract Surg 16(4): 414-30.

Reinstein DZ, Silverman RH, Rondeau MJ, et al. (1994a). Epithelial and corneal thickness measurements by high-frequency ultrasound digital signal processing. Ophthalmology 101(1): 140-6.

Reinstein DZ, Silverman RH, Sutton HF, et al. (1999). Very high-frequency ultrasound corneal analysis identifies anatomic correlates of optical complications of lamellar refractive surgery: anatomic diagnosis in lamellar surgery. Ophthalmology 106(3): 474-82.

Reinstein DZ, Silverman RH, Trokel SL, et al. (1994b). Corneal pachymetric topography. Ophthalmology 101(3): 432-8.

Reinstein DZ, Srivannaboon S and Holland SP (2001). Epithelial and stromal changes induced by intacs examined by three-dimensional very high-frequency digital ultrasound. J Refract Surg 17(3): 310-8.

Reinstein DZ, Sutton HF, Srivannaboon S, et al. (2006). Evaluating microkeratome efficacy by 3D corneal lamellar flap thickness accuracy and reproducibility using Artemis VHF digital ultrasound arc-scanning. J Refract Surg 22(5): 431-40.

Ren DH, Petroll WM, Jester JV, et al. (1999a). The effect of rigid gas permeable contact lens wear on proliferation of rabbit corneal and conjunctival epithelial cells. Clao J 25(3): 136-41.

Ren DH, Petroll WM, Jester JV, et al. (1999b). The relationship between contact lens oxygen permeability and binding of Pseudomonas aeruginosa to human corneal epithelial cells after overnight and extended wear. Clao J 25(2): 80-100.

Ren DH, Yamamoto K, Ladage PM, et al. (2002). Adaptive effects of 30-night wear of hyper-O(2) transmissible contact lenses on bacterial binding and corneal epithelium: a 1-year clinical trial. Ophthalmology 109(1): 27-39; discussion 39-40.

Ren H, Petroll WM, Jester JV, et al. (1997). Adherence of Pseudomonas aeruginosa to shed rabbit corneal epithelial cells after overnight wear of contact lenses. Clao J 23(1): 63-8.

Roman Guindo JM, Teus Guezala MA, Sanchez Pina JM, et al. (2005). [Evaluation of the efficacy of long term topical steroid treatment to prevent regression after hyperopic LASIK]. Arch Soc Esp Oftalmol 80(1): 13-8.

Rosa DS and Febbraro JL (1999). Laser in situ keratomileusis for hyperopia. J Refract Surg 15(2 Suppl): S212-5.

Ruberti JW and Klyce SD (2003). NaCl osmotic perturbation can modulate hydration control in rabbit cornea. Exp Eye Res 76(3): 349-59.

Rumelt S, Cohen I, Skandarani P, et al. (2001). Ultrastructure of the lamellar corneal wound after laser in situ keratomileusis in human eye. J Cataract Refract Surg 27(8): 1323-7.

Ruskell GL (1997). Anatomy and physiology of the cornea and related structures. Contact Lenses. AJ Phillips and L Speedwell. Boston, Butterworth-Heinemann: 17-49.

Sachdev N, McGhee CN, Craig JP, et al. (2002). Epithelial defect, diffuse lamellar keratitis, and epithelial ingrowth following post-LASIK epithelial toxicity. J Cataract Refract Surg 28(8): 1463-6.

Sacu S, Findl O, Buehl W, et al. (2005). Optical biometry of the anterior eye segment: interexaminer and intraexaminer reliability of ACMaster. J Cataract Refract Surg 31(12): 2334-9.

Sakamoto R, Miyanaga Y and Hamano H (1991). Soft and RGP lens corneal swelling and deswelling with overnight wear. Int Contact Lens Clin 18(Nov/Dec): 214-217.

Sakamoto R and Sugimoto K (2004). Will higher-Dk materials give better corneal refractive therapy results and fewer complications? Eye Contact Lens 30(4): 252-3; discussion 263-4.

Sallet G (2001). Comparison of optical and ultrasound central corneal pachymetry. Bull Soc Belge Ophtalmol(281): 35-8.

Sanchis-Gimeno JA, Herrera M, Lleo-Perez A, et al. (2006). Quantitative anatomical differences in central corneal thickness values determined with scanning-slit corneal topography and noncontact specular microscopy. Cornea 25(2): 203-5.

Schmid GF, Petrig BL, Riva CE, et al. (2001). Measurement of eye length and eye shape by optical low coherence reflectometry. Int Ophthalmol 23(4-6): 317-20.

Schoessler JP and Barr JT (1980). Corneal thickness changes with extended contact lens wear. Am J Optom Physiol Opt 57(10): 729-33.

Schuman JS, Puliafito CA and Fujimoto JG (2004). Optical Coherence Tomography of Ocular Diseases. Boston, Massachusetts, Slack Incorporated.

Seiler T, Koufala K and Richter G (1998). Iatrogenic keratectasia after laser in situ keratomileusis. J Refract Surg 14(3): 312-7.

Sharp PF, Manivannan A, Xu H, et al. (2004). The scanning laser ophthalmoscope--a review of its role in bioscience and medicine. Phys Med Biol 49(7): 1085-96.

Shin YJ, Kim MK, Wee WR, et al. (2005). Change of proliferation rate of corneal epithelium in the rabbit with orthokeratology lens. Ophthalmic Res 37(2): 94-103.

Simo Mannion L, Tromans C and O'Donnell C (2005). An evaluation of corneal nerve morphology and function in moderate keratoconus. Cont Lens Anterior Eye 28(4): 185-92.

Sin S and Simpson TL (2006). The repeatability of corneal and corneal epithelial thickness measurements using optical coherence tomography. Optom Vis Sci 83(6): 360-5.

Skavenski AA, Hansen RM, Steinman RM, et al. (1979). Quality of retinal image stabilization during small natural and artificial body rotation in man. Vision Research 19: 675-83.

Smith GT, Brown NA and Shun-Shin GA (1990). Light scatter from the central human cornea. Eye 4 (Pt 4): 584-8.

Somodi S, Hahnel C, Slowik C, et al. (1996). Confocal in vivo microscopy and confocal laser-scanning fluorescence microscopy in keratoconus. Ger J Ophthalmol 5(6): 518-25.

Soni PS and Nguyen TT (2006). Overnight Orthokeratology Experience With XO Material. Eye Contact Lens 32(1): 39-45.

Soni PS, Nguyen TT and Bonanno JA (2003). Overnight orthokeratology: visual and corneal changes. Eye Contact Lens 29(3): 137-45.

Soni PS, Nguyen TT and Bonanno JA (2004). Overnight orthokeratology: refractive and corneal recovery after discontinuation of reverse-geometry lenses. Eye Contact Lens 30(4): 254-62; discussion 263-4.

Sonigo B, Iordanidou V, Chong-Sit D, et al. (2006). In vivo corneal confocal microscopy comparison of intralase femtosecond laser and mechanical microkeratome for laser in situ keratomileusis. Invest Ophthalmol Vis Sci 47(7): 2803-11.

Sorbara L, Fonn D, Simpson T, et al. (2005a). Reduction of myopia from corneal refractive therapy. Optom Vis Sci 82(6): 512-8.

Sorbara L, Lu F, Fonn D, et al. (2004). Refractive and keratometric effects of corneal refractive therapy for hyperopia after one night of lens wear. Optom Vis Sci 46: E-abstract.

Sorbara L, Lu F, Fonn D, et al. (2005b). Topographic keratometric effects of corneal refractive therapy for hyperopia after one night of lens wear. Invest Ophthalmol Vis Sci: E-abstract 2061.

Spadea L, Fasciani R, Necozione S, et al. (2000). Role of the corneal epithelium in refractive changes following laser in situ keratomileusis for high myopia. J Refract Surg 16(2): 133-9.

Spadea L, Sabetti L, D'Alessandri L, et al. (2006). Photorefractive keratectomy and LASIK for the correction of hyperopia: 2-year follow-up. J Refract Surg 22(2): 131-6.

Sridharan R and Swarbrick H (2003). Corneal response to short-term orthokeratology lens wear. Optom Vis Sci 80(3): 200-6.

Stave J and Guthoff R (1998). Imaging the tear film and in vivo cornea. Initial results with a modified confocal laser scanning ophthalmoscope. Ophthalmologe 95(2): 104-9.

Stonecipher KG, Dishler JG, Ignacio TS, et al. (2006). Transient light sensitivity after femtosecond laser flap creation: clinical findings and management. J Cataract Refract Surg 32(1): 91-4.

Sugar A (2002). Ultrafast (femtosecond) laser refractive surgery. Curr Opin Ophthalmol 13(4): 246-9.

Swarbrick H, Jayakumar J, Co W, et al. (2005). Overnight corneal edema can modulate the short-term clinical response to orthokeratology lens wear. Invest Ophthalmol Vis Sci 46: E-abstract 2056.

Swarbrick HA (2004). Orthokeratology (corneal refractive therapy): what is it and how does it work? Eye Contact Lens 30(4): 181-5; discussion 205-6.

Swarbrick HA (2006). Orthokeratology review and update. Clin Exp Optom 89(3): 124-43.

Swarbrick HA, Hiew R, Kee AV, et al. (2004). Apical clearance rigid contact lenses induce corneal steepening. Optom Vis Sci 81(6): 427-35.

Swarbrick HA, Wong G and O'Leary DJ (1998). Corneal response to orthokeratology. Optom Vis Sci 75(11): 791-9.

Sweeney DF (2003). Clinical signs of hypoxia with high-Dk soft lens extended wear: is the cornea convinced? Eye Contact Lens 29(1 Suppl): S22-5; discussion S26-9, S192-4.

Tahhan N, Du Toit R, Papas E, et al. (2003). Comparison of reverse-geometry lens designs for overnight orthokeratology. Optom Vis Sci 80(12): 796-804.

Tahzib NG, Bootsma SJ, Eggink FA, et al. (2005). Functional outcomes and patient satisfaction after laser in situ keratomileusis for correction of myopia. J Cataract Refract Surg 31(10): 1943-51.

Tam ES and Rootman DS (2003). Comparison of central corneal thickness measurements by specular microscopy, ultrasound pachymetry, and ultrasound biomicroscopy. J Cataract Refract Surg 29(6): 1179-84.

Tanaka T (2000). Comparison of stromal remodeling and keratocyte response after corneal incision and photorefractive keratectomy. Jpn J Ophthalmol 44(6): 579-90.

Taneri S, Zieske JD and Azar DT (2004). Evolution, techniques, clinical outcomes, and pathophysiology of LASEK: review of the literature. Surv Ophthalmol 49(6): 576-602.

Tervo T and Moilanen J (2003). In vivo confocal microscopy for evaluation of wound healing following corneal refractive surgery. Prog Retin Eye Res 22(3): 339-58.

Thomas J, Wang J, Cox I, et al. (2003). Central corneal, epithelial, and flap thickness after LASIK measured with Optical Coherence Tomography (OCT) at 1310nm. Invest Ophthalmol Vis Sci 44: E-abstract 2639.

Thompson RW, Jr., Choi DM, Price MO, et al. (2003). Noncontact optical coherence tomography for measurement of corneal flap and residual stromal bed thickness after laser in situ keratomileusis. J Refract Surg 19(5): 507-15.

Thota S, Miller WL and Bergmanson JP (2006). Acute corneal hydrops: a case report including confocal and histopathological considerations. Cont Lens Anterior Eye 29(2): 69-73.

Touboul D, Salin F, Mortemousque B, et al. (2005). [Advantages and disadvantages of the femtosecond laser microkeratome]. J Fr Ophtalmol 28(5): 535-46.

Tran DB, Sarayba MA, Bor Z, et al. (2005). Randomized prospective clinical study comparing induced aberrations with IntraLase and Hansatome flap creation in fellow eyes: potential impact on wavefront-guided laser in situ keratomileusis. J Cataract Refract Surg 31(1): 97-105.

Tsubota K, Mashima Y, Murata H, et al. (1995). Corneal epithelium in keratoconus. Cornea 14(1): 77-83.

Tuan KM (2006). Visual experience and patient satisfaction with wavefront-guided laser in situ keratomileusis. J Cataract Refract Surg 32(4): 577-83.

Ucakhan OO, Ozkan M and Kanpolat A (2006). Corneal thickness measurements in normal and keratoconic eyes: Pentacam comprehensive eye scanner versus noncontact specular microscopy and ultrasound pachymetry. J Cataract Refract Surg 32(6): 970-7.

Ucakhan OO, Tello C, Liebmann JM, et al. (2001). Optical coherence tomography of Intacs. J Cataract Refract Surg 27(10): 1535.

Uniacke CA, Augsburger A and Hill RM (1971). Epithelial swelling with oxygen insufficiency. Am J Optom Arch Am Acad Optom 48(7): 565-8.

Unterhuber A, Povazay B, Bizheva K, et al. (2004). Advances in broad bandwidth light sources for ultrahigh resolution optical coherence tomography. Phys Med Biol 49(7): 1235-46.

Unterhuber A, Povazay B, Hermann B, et al. (2003). Compact, low-cost Ti:Al2O3 laser for in vivo ultrahigh-resolution optical coherence tomography. Opt Lett 28(11): 905-7.

Ustundag C, Bahcecioglu H, Ozdamar A, et al. (2000). Optical coherence tomography for evaluation of anatomical changes in the cornea after laser in situ keratomileusis. J Cataract Refract Surg 26(10): 1458-62.

Vesaluoma MH, Petroll WM, Perez-Santonja JJ, et al. (2000). Laser in situ keratomileusis flap margin: wound healing and complications imaged by in vivo confocal microscopy. Am J Ophthalmol 130(5): 564-73.

Vogel A, Dick HB and Krummenauer F (2001). Reproducibility of optical biometry using partial coherence interferometry: intraobserver and interobserver reliability. J Cataract Refract Surg 27(12): 1961-8.

Voo I, Mavrofrides EC and Puliafito CA (2004). Clinical applications of optical coherence tomography for the diagnosis and management of macular diseases. Ophthalmol Clin North Am 17(1): 21-31.

Wallis NE (1969). Recovery time course of corneal edema as determined by light scatter. J Am Optom Assoc 40(3): 276-9.

Wang J, Fonn D and Simpson TL (2003a). Topographical thickness of the epithelium and total cornea after hydrogel and PMMA contact lens wear with eye closure. Invest Ophthalmol Vis Sci 44(3): 1070-4.

Wang J, Fonn D, Simpson TL, et al. (2002a). The measurement of corneal epithelial thickness in response to hypoxia using optical coherence tomography. Am J Ophthalmol 133(3): 315-9.

Wang J, Fonn D, Simpson TL, et al. (2002b). Relation between optical coherence tomography and optical pachymetry measurements of corneal swelling induced by hypoxia. Am J Ophthalmol 134(1): 93-8.

Wang J, Fonn D, Simpson TL, et al. (2003b). Precorneal and pre- and postlens tear film thickness measured indirectly with optical coherence tomography. Invest Ophthalmol Vis Sci 44(6): 2524-8.

Wang J, Fonn D, Simpson TL, et al. (2003c). Topographical thickness of the epithelium and total cornea after overnight wear of reverse-geometry rigid contact lenses for myopia reduction. Invest Ophthalmol Vis Sci 44(11): 4742-6.

Wang J, Simpson T and Fonn D (2003d). Objective measurements of corneal light backscatter during corneal swelling using optical coherence tomography. ARVO, Fort Lauderdale, FL, Invest Ophthalmol Vis Sci.

Wang J, Thomas J and Cox I (2006). Corneal light backscatter measured by optical coherence tomography after LASIK. J Ref Surg 22: 604-610.

Wang J, Thomas J, Cox I, et al. (2004). Noncontact measurements of central corneal epithelial and flap thickness after laser in situ keratomileusis. Invest Ophthalmol Vis Sci 45(6): 1812-6.

Weed KH and McGhee CN (1998). Referral patterns, treatment management and visual outcome in keratoconus. Eye 12 (Pt 4): 663-8.

Welzel J, Lankenau E, Birngruber R, et al. (1997). Optical coherence tomography of the human skin. J Am Acad Dermatol 37(6): 958-63.

Wilson G and Fatt I (1980). Thickness of the corneal epithelium during anoxia. Am J Optom Physiol Opt 57(7): 409-12.

Wilson SE (1998). Everett Kinsey Lecture. Keratocyte apoptosis in refractive surgery. Clao J 24(3): 181-5.

Wilson SE (2000). Role of apoptosis in wound healing in the cornea. Cornea 19(3 Suppl): S7-12.

Wilson SE (2002). Analysis of the keratocyte apoptosis, keratocyte proliferation, and myofibroblast transformation responses after photorefractive keratectomy and laser in situ keratomileusis. Trans Am Ophthalmol Soc 100: 411-33.

Wilson SE and Ambrosio R, Jr. (2002). Sporadic diffuse lamellar keratitis (DLK) after LASIK. Cornea 21(6): 560-3.

Wilson SE, Chen L, Mohan RR, et al. (1999a). Expression of HGF, KGF, EGF and receptor messenger RNAs following corneal epithelial wounding. Exp Eye Res 68(4): 377-97.

Wilson SE, He YG, Weng J, et al. (1996). Epithelial injury induces keratocyte apoptosis: hypothesized role for the interleukin-1 system in the modulation of corneal tissue organization and wound healing. Exp Eye Res 62(4): 325-7.

Wilson SE and Kim WJ (1998). Keratocyte apoptosis: implications on corneal wound healing, tissue organization, and disease. Invest Ophthalmol Vis Sci 39(2): 220-6.

Wilson SE, Liang Q and Kim WJ (1999b). Lacrimal gland HGF, KGF, and EGF mRNA levels increase after corneal epithelial wounding. Invest Ophthalmol Vis Sci 40(10): 2185-90.

Wilson SE, Mohan RR, Ambrosio R, et al. (2003a). Corneal injury. A relatively pure model of stromal-epithelial interactions in wound healing. Methods Mol Med 78: 67-81.

Wilson SE, Mohan RR, Hong J, et al. (2002). Apoptosis in the cornea in response to epithelial injury: significance to wound healing and dry eye. Adv Exp Med Biol 506(Pt B): 821-6.

Wilson SE, Mohan RR, Hong JW, et al. (2001a). The wound healing response after laser in situ keratomileusis and photorefractive keratectomy: elusive control of biological variability and effect on custom laser vision correction. Arch Ophthalmol 119(6): 889-96.

Wilson SE, Mohan RR, Hutcheon AE, et al. (2003b). Effect of ectopic epithelial tissue within the stroma on keratocyte apoptosis, mitosis, and myofibroblast transformation. Exp Eye Res 76(2): 193-201.

Wilson SE, Mohan RR, Mohan RR, et al. (2001b). The corneal wound healing response: cytokine-mediated interaction of the epithelium, stroma, and inflammatory cells. Prog Retin Eye Res 20(5): 625-37.

Wilson SE, Netto M and Ambrosio R, Jr. (2003c). Corneal cells: chatty in development, homeostasis, wound healing, and disease. Am J Ophthalmol 136(3): 530-6.

Wirbelauer C, Gochmann R and Pham DT (2005). Imaging of the anterior eye chamber with optical coherence tomography. Klin Monatsbl Augenheilkd 222(11): 856-62.

Wirbelauer C and Pham DT (2004). Monitoring corneal structures with slitlamp-adapted optical coherence tomography in laser in situ keratomileusis. J Cataract Refract Surg 30(9): 1851-60.

Wirbelauer C, Scholz C, Haberle H, et al. (2002a). Corneal optical coherence tomography before and after phototherapeutic keratectomy for recurrent epithelial erosions(2). J Cataract Refract Surg 28(9): 1629-35.

Wirbelauer C, Scholz C, Hoerauf H, et al. (2001). Examination of the cornea using optical coherence tomography. Ophthalmologe 98(2): 151-6.

Wirbelauer C, Scholz C, Hoerauf H, et al. (2000). Corneal optical coherence tomography before and immediately after excimer laser photorefractive keratectomy. Am J Ophthalmol 130(6): 693-9.

Wirbelauer C, Scholz C, Hoerauf H, et al. (2002b). Noncontact corneal pachymetry with slit lamp-adapted optical coherence tomography. Am J Ophthalmol 133(4): 444-50.

Wirbelauer C, Winkler J, Bastian GO, et al. (2002c). Histopathological correlation of corneal diseases with optical coherence tomography. Graefes Arch Clin Exp Ophthalmol 240(9): 727-34.

Wojtkowski M, Srinivasan V, Fujimoto JG, et al. (2005). Three-dimensional retinal imaging with high-speed ultrahigh-resolution optical coherence tomography. Ophthalmology 112(10): 1734-46.

Wolf AH, Neubauer AS, Priglinger SG, et al. (2004). Detection of laser in situ keratomileusis in a postmortem eye using optical coherence tomography. J Cataract Refract Surg 30(2): 491-5.

Wollstein G, Paunescu LA, Ko TH, et al. (2005). Ultrahigh-resolution optical coherence tomography in glaucoma. Ophthalmology 112(2): 229-37.

Wong AC, Wong CC, Yuen NS, et al. (2002). Correlational study of central corneal thickness measurements on Hong Kong Chinese using optical coherence tomography, Orbscan and ultrasound pachymetry. Eye 16(6): 715-21.

Yabushita H, Bouma BE, Houser SL, et al. (2002). Characterization of human atherosclerosis by optical coherence tomography. Circulation 106(13): 1640-5.

Yamamoto K, Ladage PM, Ren DH, et al. (2002). Effect of eyelid closure and overnight contact lens wear on viability of surface epithelial cells in rabbit cornea. Cornea 21(1): 85-90.

Yaylali V, Kaufman SC and Thompson HW (1997). Corneal thickness measurements with the Orbscan Topography System and ultrasonic pachymetry. J Cataract Refract Surg 23(9): 1345-50.

Young C, Leach N, Gondo M, et al. (2004). Thickness measurements of rabbit cornea using ultrasound and histology: do they compare? Optom Vis Sci 81(12s): E-abstract.

Young MD and Benjamin WJ (2003). Oxygen permeability of the hypertransmissible contact lenses. Eye Contact Lens 29(1 Suppl): S17-21; discussion S26-9, S192-4.

Zadnik K, Barr JT, Gordon MO, et al. (1996). Biomicroscopic signs and disease severity in keratoconus. Collaborative Longitudinal Evaluation of Keratoconus (CLEK) Study Group. Cornea 15(2): 139-46.

Zadok D, Maskaleris G, Garcia V, et al. (1999). Outcomes of retreatment after laser in situ keratomileusis. Ophthalmology 106(12): 2391-4.

Zadok D, Maskaleris G, Montes M, et al. (2000). Hyperopic laser in situ keratomileusis with the Nidek EC-5000 excimer laser. Ophthalmology 107(6): 1132-7.

Zadok D, Raifkup F, Landau D, et al. (2003). Long-term evaluation of hyperopic laser in situ keratomileusis. J Cataract Refract Surg 29(11): 2181-8.

Zaldivar R, Oscherow S and Bains HS (2005). Five techniques for improving outcomes of hyperopic LASIK. J Refract Surg 21(5 Suppl): S628-32.